Broken Symmetries and Transport in Holography

Memoria de Tesis Doctoral realizada por

Amadeo Jiménez

presentada ante el Departamento de Física Teórica
de la Universidad Autónoma de Madrid
para optar al Título de Doctor en Física Teórica

Tesis Doctoral dirigida por **Karl Landsteiner,**
Investigador del Instituto de Física Teórica UAM/CSIC

Departamento de Física Teórica
Universidad Autónoma de Madrid

Instituto de Física Teórica
UAM/CSIC

Marzo de 2015

Agradecimientos

Por suerte tengo mucho que agradecer.

En primer lugar quiero expresar mi gratitud a Karl, que ha iluminado mi odisea a través de la ocuridad holográfica. Por su infinita paciencia y su buen humor. Por estar siempre dispuesto a discutir y ayudarme a comprender. Realmente ha sido un placer y un honor. Gracias por ponerme en el camino en el que estoy.

He tenido la suerte de coincidir con Luis, mi "hermano" de tesis, a lo largo de este viaje. Gracias por explicarme tantas cosas. Estoy convencido de que no hubiera llegado hasta aquí sin tu ayuda.

No olvidaré las conversaciones de física y de no física con Dani, Diego, Javi, João, Mateo y Pablo día tras día. Ojalá se repitan.

Querría tambien mencionar a algunos profesores con los que he tenido la oportunidad de conversar y que me han iluminado e inspirado especialmente: Ho-Ung, Ioannis y Pepe.

No me olvido de mis amigos de siempre: Badía, Blanco, Charlie, Hector, Jaime, Juan y Tupi. Con vosotros la vida es mejor.

Hay un lugar especial aquí para Irene, el gusano que me ha acompañado y soportado en esta maravillosa etapa de mi vida. Gracias por enseñarme lo bueno que puede ser el mundo.

Por último agradecer a mis incondicionales, mis padres Amadeo y Susana y mi hermano Víctor. Soy vuestro.

Contents

1
Introducción

Los tres pilares principales de esta tesis se encuentran en el título. El primer concepto que en él encontramos es el de simetrías o, más concretamente, el de simetrías rotas. En física, la siemtría ha sido una herramienta de gran utilidad desde tiempos inmemoriales. La definición matemática de simetría es "invariancia bajo una transformación". Esta idea aparentemente simple esconde una vasta cantidad de profundas implicaciones en nuestra manera de entender la naturaleza. Tal es así que el teorema de Noether (que establece la existencia de corrientes conservadas en base al contenido de simetrías de la teoría) se conoce como el teorema principal de la física teórica. Sin embargo, en esta tesis, no son exactamente las simetrías sino sus versiones rotas lo que nos interesa. No solo en física, la idea de simetría rota hace referencia a una simetría que había antes y que de algún modo ya no hay. Sin embargo se entiende que debe haber cierta memoria, cierto remanente de dicha simetría ausente: una simetría rota no es lo mismo que la ausencia total de simetría. Para nosotros los restos de una simetría pueden ser de igual o más valor que la propa simetría en si misma. En este sentido los físicos somos más afortunados que otros.

La segunda noción básica de este trabajo es la de transporte. De nuevo, el significado que tiene esta palabra para la física no dista mucho del que tiene para todo el mundo: transportar algo significa moverlo de un sitio a otro. A pesar de que los seres humanos han transportado cosas durante miles de aos, la importancia de este concepto aumentó dramáticamente con la revolución industrial y el desarrollo de la termodinámica: la necesidad de un a descripcion concisa de sistemas de muchos cuerpos dio lugar a los conceptos de transporte de energía, partículas etc... A pesar de lo antiguo de estos conceptos, aun queda mucho por descubrir. Cada día se descubren nuevos materiales con propiedades fascinantes: Los superconductores de alta temperatura siguen siendo un misterio desde el punto de vista teórico. EL grafeno promete revolucionar nuestras vidas con sus extremas propiedades. Los fenómenos de transporte no disipativos esperan a la vuelta de la esquina. Sin duda, es una época interesante en lo que se refiere a los fenómenos de transporte. A pesar de esto, una tesis sobre la relación entre transporte y simetría sería más propia de mediados del siglo XX. Es precisamente el tercer (y más exótico) concepto que aparece en el título el que nos trae de vuelta al siglo XXI.

Holografía, la dualidad gauge/gravedad o simplemente AdS/CFT es una idea surgida hace menos de veinte aos y que ha abierto un puerta de gran interés y profundidad para la física teórica. Esta dualidad relaciona teorías gauge en acoplo fuerte con teorías de gravedad en acoplo débil y viceversa. Su descubriemiento tuvo y sigue teniendo un fuerte impacto en la comunidad científica. Por un lado, la conexión entre teorías de gravedad

y teorías gauge es una de las más impresionantes y sugestivas que uno pueda imaginar dentro del campo de la física teórica. Lo que este inesperado matrimonio intenta decirnos no ha sido comprendido completamente aún. Por otro lado, la dualidad nos brinda una oportunidad única para desarrollar las herrmaientas adecuadas para estudiar sistemas en acoplo fuerte, uno de los problemas abiertos en la física de las últimas décadas.

Obtener una comprensión más profunda sobre la relación de estos conceptos es el objetivo de esta tesis. A lo largo de los siguientes capítulos se presenta un estudio de varios modelos, con énfasis en sus fenómenos de transporte desde el punto de vista holográfico. Para ello el concepto de simetría será nuestra herrmienta principal e indispensable. Por ello, comprender cómo esta se manifiesta en la dualidad es de vital importancia.

La tesis está organizada del siguiente modo. En la primera parte revisamos los conceptos anteriormente mencionados: Ruptura de simetía en las seciones 2-3, transporte en la sección 4 y holografía en la sección 5. Estos repasos se hacen con el fin de servir como recordatorio de los conceptos más básicos, haciendo énfaiss en las ideas que aparecen en nuestros modelos holográficos.

En el capítulo 2 introducimos el concepto de ruptura espontánea de simetría. En la sección 2.2 presentamos el teorema de Goldstone y sus extensiones. Este capítulo está basado en [1, 2].

En el capítulo 2 revisamos la idea de anomalías, invluyendo la derivación de integral de camino, el teorema de no renormalización y algunos apuntes sobre las definiciones covariante y consistente de las anomalías. Además se incluye una introducción a los fenómenos de transporte anómalos, haciendo incapié en el efecto magnético quiral. Este capítulo está basado en [3–7].

El capítulo4 esta dedicado al estudio del transporte y la hidrodinámica. Se presenta una introducción a los conceptos necesarios para comprender la seguna parte de la tesis: hidrodinámica, respuesta lineal y transiciones de fase, todo ello conectado con el concepto de ruptura de simetría. Este capítulo esta basado en [8–12]. En el capítulo5 revisamos los aspectos básicos de la correspondencia AdS/CFT. Se exponen la ideas de la formula GKPW y el paperl de las expansiones asintóticas. Se hace una detallada revisión del procedimiento de renormalización holográfica con el método de Hamilton-Jacobi. Finalmente se exploran las consecuencias que tiene la presencia de agujeros negros en la dualidad. Este capítulo esta basado en [13–17].

La segunda parte de esta tesis está dedicada a la investigación original realizada por el autor en colaboración con Daniel Arean, Irene Amado, Karl Landsteiner, Luis Melgar and Ignacio Salazar-Landea. El capítulo 6, está enfocado al mecanismo de ruptura espontánea de simetría y sus consecuenccias en los fenómenos de transporte. Concretamente, se presenta una extensíon no abeliana del superconductor holográfico. Esta extensión contiene bosones de Nambu-Goldstone exóticos. Con este modelo es posible estudiar los teoremas de contaje modernos introducidos al comienzo del capítulo. Además, se exploran las implicaciones que la ruptura espontánea de una simetría global en el lado gravitatorio. Hasta donde llega nuestro conocimiento esta es la primera vez que se realiza dicho estudio. También estudiamos el espectro de excitaciones, sus relaciones de dispersión y el comportamiento de las conductividades del sistema. Este capítulo está basado en [18].

En el capítulo 7 se hace una extensión del análisis anterior, incoroporando velocidad finita de la componente superfluida del sistema. Se estudian las restricciones que dicha velocidad impone en la estabilidad del sistema basándonos en el criterio de Landau. Se

comparan estos resultados con los obtenidos en estudios basados en la energía libre. De este modo se encuetra una inestabilidad previamente desconocida en el diagrama de fases del superconductor holográfico. Este capítulo está basado en [19].

En el capitulo8 se presenta el primer modelo de superconductor holográfico tipo s+p. Dicha fase aparece en cierta zona del diagrama de fases del modelo estudiado en el capítulo 6. Se estudian la relación entre las fases s y p y se encuentra que para ciertos valores de las variables termodinámocas la fase favorecida es aquella en la que ambos condensados coexisten. Este capítulo está basado en [20].

En el capítulo 9 pasamos a estudiar la ruptura de simtrías abelianas via anomalías y los fenómenos de transporte relacionados con estas. Concretamente se estudia el efecto que tienen los procesos de rescattering de grados de libertad gauge internos. Con el fin de implementar dichos efectos de manera efectiva se le da masa al fotón utilizando el mecanismo de Stueckelberg en el bulk. Este capítulo está basado en [21].

En el capítulo 10 se estudia la relación entre anomalías y simetrías espontáneamente rotas en holografía. Para ellos se estudia el efecto que la presendia de un superfluido tiene en las conductividades anómalas. Se propone una formula de Kubo para el efecto eléctrico quiral y se estudia su comportamiento en dos modelos distintos. De manera adicional, se identifica un efecto que se había pasado por alto en la literatura "efecto de generación de carga quiral". Nuestros resultados confirman la conjetura de universalidad de la conductividad quiral magnética a temperatura cero en superfluidos quirales hecha en [22]. Este capítulo está basado en [23]. Finalmente en 11 se presentan las conclusiones.

TRANSPORT

The study of transport, or transport phenomena, is concerned with the exchange of certain quantities along/between many body systems. Traditionally the quantities under consideration were mass, electric charge, energy and momentum. From now on we will refer to these, and other non-traditionally studied quantities, as charges. Transport does not only happen in fluids, of course. However along this thesis we will focus on the hydrodynamic regime of several theoretical systems. Therefore we will always refer to hydrodynamic transport. Hydrodynamic transport phenomena are characterized by certain coefficients in the constitutive relations: transport coefficients. Within hydrodynamics there are two key concepts to consider: transport coefficients and hydrodynamic modes. These two are closely related and a great part of our research will focus on this relation. As any other macroscopical description of nature, we can [1] express hydrodynamics as an effective version of an underlying consistent and complete Quantum Field Theory (QFT). One says that hydrodynamics can be viewed as a coarse grained version of an underlying QFT. As any effective theory, this is accomplished by removing (integrating out) massive degrees of freedom (d.o.f.) from the spectrum. In the case of hydrodynamics one is only left to the massless degrees of freedom and calls them hydrodynamic modes. From the QFT point of view these modes are still nothing else that poles in certain correlators. In this sense, since hydrodynamic modes and hydrodynamic transport phenomena are so closely related, it should not come as a surprise that transport coefficients are related to certain correlators too. Such a relation is accomplished by means of the Kubo-Martin relations. This relations appear within linear response theory: the formalism that allows us to study the response to slight perturbations of systems.

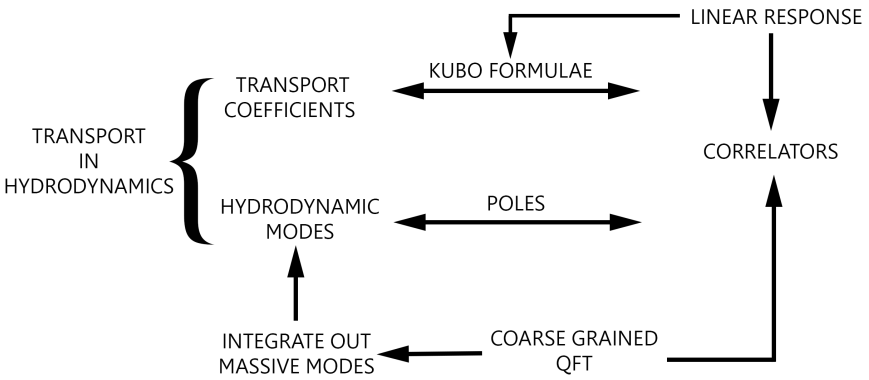

SYMMETRY BREAKING

Symmetries are a major concept in theoretical physics. Symmetry considerations allow us to obtain information that would be very difficult to get by other means. Since the world around us is highly non-symmetric, how to break symmetries and the consequences of doing so are very active and fruitful areas of research. Several ways to accomplish the breakdown of a symmetry are known within QFT: explicit symmetry breaking, spontaneous symmetry breaking and anomalous symmetry breaking or just anomalies. The case

[1] For some cases this "can should be substituted by "expect to be able to".

of spontaneous symmetry breaking is probably the best known one. Specially after the discovery of the Higgs boson in 2014. But the crucial signature of spontaneous symmetry breaking: Nambu-Goldstone modes do not only affect the vacuum. Actually it was in the context of condensed matter where this concepts where born. Regarding transport, a special role was played by the physicist Lev Landau. He gave a clear interpretation of the relation between symmetry breaking and (certain) phase transitions. Something we expect is that new phases of matter behave in a different manner. This naturally affects the transport phenomena, allowing us to make a link to the diagram for transport. We could just add (spontaneous symmetry breaking) before every concept there. Hydrodynamics are affected by spontaneous symmetry breaking. This leads to new hydrodynamic modes and new transport coefficients. There are obvious good phenomenological reasons to expect that hydrodynamics of different phases should be different. However this is not the only path one may take to reach such idea. Hydrodynamics can be viewed as an effective field theory. Since the Nambu-Goldstone modes are massless, they should survive the process of coarse graining. It cannot be surprising that new hydrodynamic modes and new transport coefficients arise. As stated before, these can be related to certain correlators. Some of these correlators will now show some new poles: the NG modes.
One can play an analogous game in the presence of anomalies. Rather recently it was discovered that anomalies can give rise to new transport phenomena under certain circumstances (see section 3.4). So we can in principle go through figure in the revious page adding "anomalous" or "in presence of anomalies" next to every concept. One can consider how hydrodynamics gets modified by the presence of anomalies [24]. Not surprisingly there are anomalous transport coefficients. Anomalies do not give rise to massless modes in the spectrum of a QFT. Despite of this, as we will see, new massless modes have been shown to appear in the hydrodynamic regime.

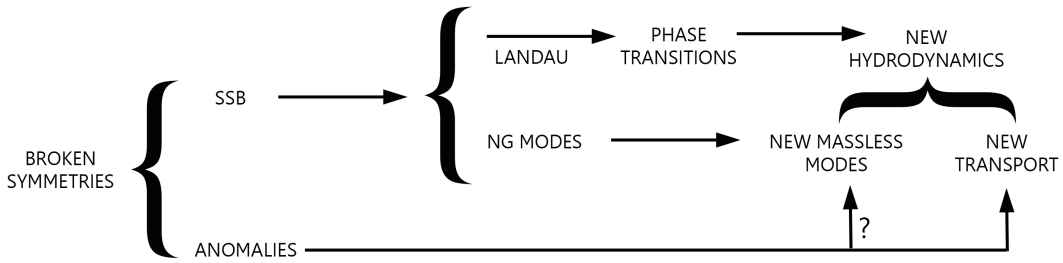

HOLOGRAPHY

Holography relates gauge theories and gravity theories[2] in an amazingly convenient way: the coupling in one side is, roughly, the inverse of the coupling in the other side. In principle one may take advantage of this in both directions. Nevertheless, we will focus on the perspective depicted in the diagram above: obtaining information of the strongly coupled gauge theory from the gravitational side. Exploring the previous diagrams (transport and symmetry) in the strongly coupled regime is the basic idea of this work. In order to do so we need to understand how the concepts of symmetry, symmetry breaking, correlators, thermodynamic variables... etc are translated to the weakly coupled side. This is accomplished by means of the so called holographic "dictionary". Understanding and expanding the dictionary within this topics is one of the main objectives of this thesis. Another important aim of the current work is to give concrete solutions of how to compute and obtain the desired quantities. Last but not least, we are interested in the concrete quantities that we will obtain from a phenomenological point fo view. Although the duals to our systems are extremely idealized systems, we are able to obtain significative results about the (broken symmetry related) transport phenomena in strongly coupled systems.

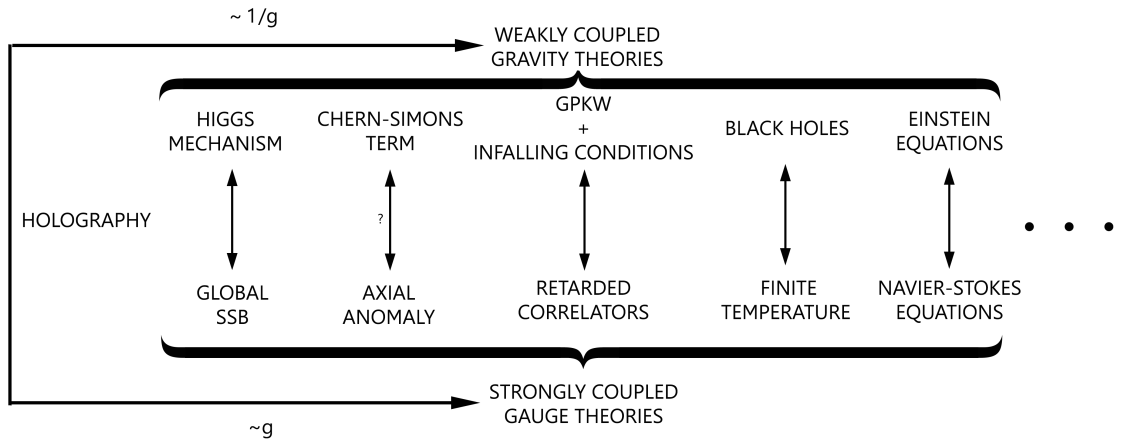

[2]With gauge theories we mean theories with gauge fields of spin< 2.

2

Breaking Symmetries with the Vacuum

2.1 Spontaneous Symmetry Breaking

When we say that a theory is invariant or symmetric under certain transformation we usually mean that the dynamics of the theory respect that symmetry AND that there are observables which are invariant under those transformations too. However it is possible that a symmetry is only respected at the level of the dynamics, with no realization from the observables point of view. In this case one says that the theory is symmetric but the vacuum breaks the symmetry: this phenomenon is known as Spontaneous Symmetry Breaking . The idea is that of the existence of a continuum (we will just focus on the case of continuous symmetries) of degenerate vacua, all connected by some transformation, the " broken" symmetry transformation. Despite of the degeneracy of the vacua, the actual physical system chooses one point in the orbit of the transformation. A more rigorous way to characterize this is to say that a symmetry is spontaneously broken if there exists an operator $\hat{\psi}$ such that

$$\langle 0|\hat{\Psi}|0\rangle \equiv \langle 0|[\hat{\mathcal{Q}}, \hat{\psi}]|0\rangle \neq 0\,. \tag{2.1}$$

The operator Ψ is called the order parameter, in clear connection with the concept of phase transitions. The more prominent physical consequences of spontaneous symmetry breaking are

- Some operator(s) acquire a non-zero vev: The order parameter
- Appearance of massless modes in the spectrum: Nambu-Goldstone modes
- The symmetry affects only the dynamics: No multiplets in the spectrum

Let us review the most common example in classical field theory: U(1) spontaneous symmetry breaking in $\lambda\phi^4$. Consider the following U(1) symmetric Lagrangian for a complex scalar

$$\mathcal{L} = -\partial_\mu \phi^\dagger \partial^\mu \phi - m^2\phi^2 - \frac{1}{4}\lambda(\phi^\dagger\phi)^2\,. \tag{2.2}$$

If $m^2 < 0$ the potential takes a mexican-hat shape and it has therefore a continuum of degenerate vacua given by

$$\phi = \frac{v}{\sqrt{2}}e^{-i\theta} = \frac{\sqrt{2}|m|}{\sqrt{\lambda}}e^{-i\theta}\,. \tag{2.3}$$

Where theta is the phase that parametrizes the position in the flat direction. To see how the spectrum is affected let us study perturbations on top of one of these backgrounds.

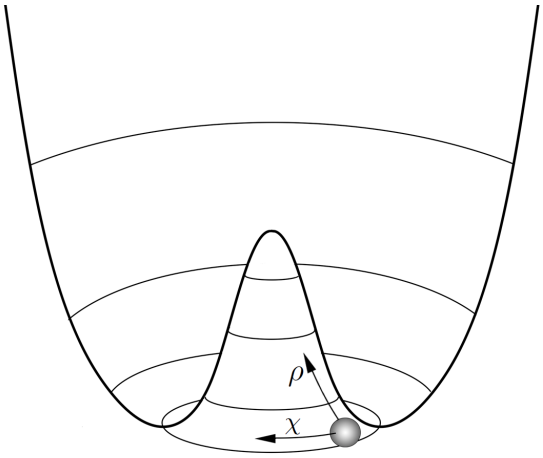

Figure 2.1: Pictorial representation of a spontaneous symmetry breaking potential "the mexican hat". The flat direction in field space gives rise to the massless mode. The radial direction has a usual U shaped "massive potential" and gives rise to a gapped mode.

For simplicity we choose $\theta = 0$ and

$$\phi(x) = \frac{1}{\sqrt{2}}(v + \rho(x))e^{-i\chi(x)/v}\,. \tag{2.4}$$

Then the Lagrangian looks

$$\mathcal{L} = -\frac{1}{2}\partial_\mu\rho\partial^\mu\rho - \frac{1}{2}\left(1+\frac{\rho}{v}\right)^2\partial_\mu\chi\partial^\mu\chi + m^2\rho^2 - \frac{\sqrt{\lambda}}{2}|m|\rho^3 - \frac{1}{16}\lambda\rho^4\,. \tag{2.5}$$

Which describes a massless excitation parametrized by the perturbation of the phase χ and a massive mode described by the perturbation of the modulus ρ. In the mexican hat picture these correspond to a ball moving in the angular (flat, massless) and in the radial (U shape, massive) directions. This extends naturally to the non-abelian case. Moreover, the effects of the quantization do not affect the main results, as the masslessness of the NG-mode.
A subtle concept is that of spontaneous symmetry breaking of gauge symmetries, nowadays termed the Higgs mechanism. An analogous model to the previous one can be implemented if the symmetry is promoted to a local symmetry. However, due to the fact that local symmetries are actually redundancies, these cannot be broken (Elitzur's theorem). A broken local symmetry leads to inconsistencies in the theory. So spontaneous symmetry breaking of gauge symmetries is a bit of a misnomer. In reality this mechanism is a combination of spontaneous symmetry breaking of the **global** part of the symmetry and gauge fixing. The apparent breakdown of the local symmetry is actually due to the gauge fixing; it is not trivial to see that the theory is still gauge invariant once a particular gauge has been chosen.

Let us see how this works in the simplest model a U(1) gauge field coupled to a complex scalar with the appropriate potential

$$\mathcal{L} = -(D_\mu\phi)^\dagger D^\mu\phi - \frac{1}{4}\lambda(\phi^\dagger\phi - \frac{1}{2}v^2)^2 - \frac{1}{4}F^{\mu\nu}F_{\mu\nu}\,. \tag{2.6}$$

This potential is minimized for a non-zero vev of the scalar field, that we can parametrize as vev + perturbations

$$\phi(x) = \frac{1}{\sqrt{2}}(v + \rho(x))e^{i(\theta - \chi(x))} \,. \tag{2.7}$$

As in the global case we can use the global part of the symmetry to set $\theta = 0$. The Lagrangian now looks

$$\mathcal{L} = -\frac{1}{4}F^{\mu\nu}F_{\mu\nu} + \partial_\mu\rho(x)\partial^\mu\rho(x) + \frac{1}{4}\lambda v^2\rho(x)^2 + \frac{(v+\rho(x))^2}{v^2}\left(\partial^\mu\chi + vA^\mu\right)\left(\partial_\mu\chi + vA_\mu\right) \,. \tag{2.8}$$

This Lagrangian is explicitly gauge invariant. However, we can now use a gauge transformation[1] to set $\chi(x) = 0$. This is a concrete gauge, called unitary gauge. Of course, if we now look at the lagrangian

$$\mathcal{L} = -\frac{1}{4}F^{\mu\nu}F_{\mu\nu} + \partial_\mu\rho(x)\partial^\mu\rho(x) + \frac{1}{4}\lambda v^2\rho(x)^2 + (v+\rho(x))^2 A^\mu A_\mu \,. \tag{2.9}$$

we see that it is not gauge invariant anymore. This should not be a surprise since we have chosen a particular gauge. In addition we see (this was clear before gauge fixing too) that the photon has acquired a mass. So we see that the (apparent) Nambu-Goldstone boson was non-physical in this case, since it could be removed by the appropriate choice of gauge. The number of d.o.f. however remains unaltered compared to the global spontaneous symmetry breaking case, since now the photon has a mass and therefore an extra polarization mode. The massive mode ρ remains there and cannot be removed by gauge transformations: this is the Higgs mode.
Let us go back to the Lagrangian (2.10). We can think of λ being very big and integrate out the Higgs mode

$$\mathcal{L} = -\frac{1}{4}F^{\mu\nu}F_{\mu\nu} + \left(\partial^\mu\chi + vA^\mu\right)\left(\partial_\mu\chi + vA_\mu\right) \,, \tag{2.10}$$

and arrive to the Stueckelberg action. This model was proposed by Stueckelberg as a gauge invariant way to give mass to the photon. In his approach he just imposed the appropriated symmetry transformation to the "Stueckelberg field" χ such that the mass term remained invariant. Here we have seen that the Stueckelberg and the Higgs mechanisms are not independent, since the former is a truncation of the latter. Nevertheless, there are further differences. Although both the global spontaneous symmetry breaking and the gauge spontaneous symmetry breaking mechanisms can be extended to non-abelian symmetries, the Stueckelberg mechanism gives rise to non renormalizable theories in this case. In chapter 9 we will see how these ideas are implemented in AdS space.
A central piece in the study of spontaneous symmetry breaking is the Nambu-Goldstone theorem, that shows that massless modes must always appear in the spectrum after spontaneous symmetry breaking. Moreover in certain cases it is possible to determine how many of these modes must appear.

[1] This is a "true" gauge transformation: it vanishes at infinity.

2.2 Counting Nambu-Goldstone Bosons

Let us review the state of art of the theorems on Goldstone bosons. First we have of course the actual **Goldstone theorem**. Its proof assumes the existence of a conserved current j^μ such that the broken charge is $Q = \int d^d x j^0$ (with d spatial dimensions). The theorem then states that spontaneous breaking of a continuous global symmetry implies the existence of a mode whose energy fulfills

$$\lim_{k\to 0} \omega(k) = 0\,. \tag{2.11}$$

The theorem by itself does not make any statement about the number of these modes, nor does it fix the k-dependence of the frequency. In the presence of Poincaré symmetry one can make however a stronger statement, namely that the dispersion relation of the Goldstone mode has to be linear and that the number of Goldstone bosons equals the number of broken generators.

Lorentz symmetry might be absent however for various reasons: the theory might be non-relativistic or the system under consideration might be in a Lorentz symmetry breaking state, at finite density for example. In these cases another theorem classifies **Goldstone bosons** as **type I** if their dispersion relation depends on a **odd power** of the momentum or as **type II** if their energy goes as an **even power** of the momentum, both in the low momentum limit. The number of type I and type II Goldstone bosons has to fulfill then

$$n_I + 2n_{II} \geq N_{BG}\,, \tag{2.12}$$

where N_{BG} is the number of broken generators [25]. The number of type I and type II Goldstone bosons can be further constrained. Upon assuming that the broken symmetry generators obey $\langle [Q_a, Q_b] \rangle = B_{ab}$ the number of Goldstone bosons has to fulfill [26–28] (see also [2, 29, 30] for more on counting rules of Goldstone bosons).

$$n_I + n_{II} = N_{BG} - \frac{1}{2}\mathrm{rank}(B)\,. \tag{2.13}$$

This counting rule was proven in [27]. In the same paper where the proof was given, a new classification for the NG modes was introduced. Within this classification the massless modes appearing after spontaneous symmetry breaking can be identified as type A and type B. The difference relies on whether the polarization vector of the gapless modes is in the kernel of the previously defined matrix B. This matrix can be obtained from the effective action [29] after linearization of the terms with just one time derivative in the action. In this language the counting rule reads

$$n_A = N_{BG} - \mathrm{rank}(B) \qquad\qquad n_B = \frac{1}{2}\mathrm{rank}(B)\,. \tag{2.14}$$

Generically type A NG modes are type I whereas type B are type II. In this case the above counting rule confirms (2.13). However, one may fine tune the effective action in order to have type A NG modes with quadratic dispersion relations, etc... which ultimately implies that (2.14) si more general. There is a simple way to understand how this can happen. In order to have non-linear dispersion relations it is needed that the time and space derivatives have different powers. The origin of such difference, however, may arise in different ways. One possible example is that of Lifshitz scaling. In this case one imposes

the anisotropic behaviour by hand, setting $|\nabla\phi|^{2z}$ where z is the Lifshitz parameter and $z = 1$ corresponds to the isotropic case. Another possiblity is to add a chemical potential $A_0 = \mu$, which gives rise to a term linear in time derivatives $\sim \mu(\phi\partial_t\bar{\phi} - \bar{\phi}\partial_t\phi$. The fact that these two possibilities may give the same dispersion relation (for z=2) does not imply, however, that the counting rules are the same. Concretely the Lifshitz case corresponds to Type A whereas the chemical potential option gives rise to Type B NG bosons. The latter is reviewed in section 6.2, where the model of [31], which shows type II (B) NG bosons in the spectrum, is reproduced. It is placed in chapter 6 for it was the motivation for our holographic model. The cases we consider there are of generic nature in the sense explained before, therefore we will adopt the language of type I and type II NG bosons.

3

Breaking symmetries with $\hbar$

3.1 Anomalies

Anomalies in the quantum theories of chiral fermions belong to the most emblematic properties of relativistic quantum field theory. They provide stringent consistency conditions on possible gauge interactions and also predict physical processes that would be otherwise highly suppressed such as the decay of the neutral pion into two photons.
Anomalies are not only important for the phenomenology of particle physics but they also are of utmost importance to the theory of quantum many body systems containing chiral fermions. Anomaly cancellation plays a crucial role in the field theoretic understanding of the electro response of quantum hall fluids for example. Chiral fermions appear as edge states and the associated anomalies have to be canceled by appropriate anomaly inflow from a gapped bulk reservoir of charge. From the point of view of symmetry breaking, anomalies signal the failure of classical symmetry to survive the process of quantization and regularization. The existence of anomalies was discovered due to the tension between the measured neutral Pion decay into two photons and the symmetry based theorem by Veltman and Sutherland that forbade this decay. The solution to this problem was found by Adler, Bell and Jackiw [32, 33]: a symmetry of the (classical) Lagrangian can be broken after quantizing the theory. When this happens, loop corrections modify the Ward identity for the classically conserved current:

$$\partial_\mu J^{\mu 5} = 2imP \qquad \longrightarrow \qquad \partial_\mu J^{\mu 5} = 2imP + \frac{e^2}{16\pi^2}\epsilon^{\mu\nu\alpha\beta}F_{\mu\nu}F_{\alpha\beta}\,. \tag{3.1}$$

Where $P = \bar{\psi}\gamma_5\psi$. This symmetry breaking mechanism is completely different from spontaneous symmetry breaking. Spontaneous symmetry breaking happens at the classical level. In addition, the dynamics of the theory in the spontaneous symmetry breaking case remain symmetric, it is the vacuum that breaks the symmetry. Anomalies, however, do break the symmetry at the level of the (quantum) dynamics. A big difference between both mechanisms is that spontaneous symmetry breaking can be switched off by conveniently tuning the value of some parameter (the negative mass in the concrete case of the previous chapter). Since anomalies appear when $\sim \hbar$ effects are taken into account this is more complicated; switching off Plank's constant is not a good solution. However, in the large N limit it is possible to study how anomaly related effect arise [34]. This is due to the suppresion of the anomaly coefficient in the large N_c expansion. On the other hand, as it happened with spontaneous symmetry breaking, only global symmetries are allowed to be anomalous in a consistent theory. The breakdown of a gauge symmetry leads to an unavoidable breakdown of unitarity. Let us remark that all kinds of classical symmetries

are potentially affected by anomalies. The most studied examples are the axial anomaly, the conformal anomaly and the gravitational and mixed chiral-gravitational anomalies. In chapter 9 we study implications of the axial anomaly on transport from the holographic point of view. More concretely, we focus on situations in which the matrix elements of the divergence of the current do receive radiative corrections beyond 1-loop. This might seem contrary to the Adler-Bardeen non-renormalization theorem.However, it was actually Adler who realized this in the first place. Let us first review the basics of the axial anomaly and then introduce the ideas the non-renormalization theorem.

The axial anomaly appears in theories of massless fermions[1], which are invariant under a global $U(1)_A$ transformation. There are several ways to compute the anomaly. Here we will follow the path integral derivation first elucidated by Fujikawa.
From the classical point of view a symmetry exists if the Lagrangian is invariant under the corresponding transformation (without spontaneous symmetry breaking). One possibility to check wether a symmetry remains conserved after quantization is to compute the ward identities for the divergence of the current. This is related to the usual triangle diagram computation of the anomaly. This is however not the only way that symmetries can be tested in a quantum theory. If the symmetry is respected at the quantum level then the generating functional (quantum action) must be invariant under the (classical) symmetry transformation. It can happen that a quantum action does not respect an invariance of the Lagrangian. The theory is anomalous. One can therefore directly study the generating functional with no need to compute current correlators. Let us consider massless fermions minimally coupled to a photon. The expression for the generating functional

$$e^{W_{eff}[A_\mu]} \equiv \int \mathcal{D}\Psi\mathcal{D}\bar{\Psi} e^{\mathcal{S}[\Psi,A_\mu]}\,. \tag{3.2}$$

We have only integrated over fermion configurations since A_μ is not a dynamical d.o.f. of this theory. The theory is invariant under a certain transformation "g" if

$$\delta_g W_{eff} = 0\,. \tag{3.3}$$

Since $\delta_g\mathcal{L} = 0$ the only possible origin of the non-conservation is the measure of the path integral in3.2.

$$e^{\delta W_{eff}[A_\mu]} = \delta \int \mathcal{D}\Psi\mathcal{D}\bar{\Psi} e^{\mathcal{S}[\Psi,A_\mu]} = \int \delta(\mathcal{D}\Psi\mathcal{D}\bar{\Psi}) e^{\mathcal{S}[\Psi,A_\mu]}\,. \tag{3.4}$$

Where $\mathcal{L} = \bar{\Psi}\not{D}\Psi$. In order to compute the variation of the measure we first decompose the spinors in orthonormal eigenfunctions of the Dirac operator $\not{D}\phi_n = \lambda_n\phi_n$ and Grassmann variables

$$\Psi(x) = \sum a_n\phi_n(x) = \sum a_n\langle x|n\rangle\,. \tag{3.5}$$

Then

$$\mathcal{D}\Psi\mathcal{D}\bar{\Psi} = \prod_n da_n d\bar{b}_n\,. \tag{3.6}$$

Where $\bar{b}_n$ are the Grassman coefficients in the decomposition of $\bar{\Psi}$. We can now perform the axial transformation to the measure

$$\Psi' = (\mathbb{1} + i\beta(x)\gamma_5)\Psi = (\mathbb{1} + i\beta(x)\gamma_5)\sum_m a_m\phi_m = \sum_n a'_n\phi_n\,. \tag{3.7}$$

[1]Anomalies depend on the number of space-time dimensions. In this chapter we will implicitly always refer to 3+1 space times

So we have

$$a'_n = \sum_m C_{nm} a_m \,. \tag{3.8}$$

with

$$C_n m = \delta_{nm} + i \int d^4x \beta(x) \phi_n^\dagger(x) \gamma_5 \phi_m(x) \,. \tag{3.9}$$

So one can finally write

$$\delta(\mathcal{D}\Psi\mathcal{D}\bar{\Psi}) = (\det C)^{-2} \mathcal{D}\Psi\mathcal{D}\bar{\Psi} \,. \tag{3.10}$$

Only if $(\det C)^2 = 1$ the theory will remain invariant under the symmetry transformation at the quantum level. Using $\det C = e^{\mathrm{Tr}\,\log C}$

$$(\det C)^{-2} = e^{-2i \int d^4x \beta(x) \sum_n \phi_n^\dagger \gamma_5 \phi_n} \,. \tag{3.11}$$

The sum in last expression is not well defined and must be regularized. Several regularization schemes can be chosen now. However we can divide them in two groups: gauge (recall the field A_μ is associated with a vector symmetry) invariant schemes and others. All possible schemes in the first group give rise to the same answer

$$(\det C) {-} 2 = e^{-\int d^4x \beta(x) \frac{-i}{16\pi^2} F \wedge F} \,. \tag{3.12}$$

Where F is the field strength of the external vector field. This is the case of Fujikawas gaussian regularization scheme

$$\sum_n \phi_n^\dagger \gamma_5 \phi_n = \lim_{M\to\infty} \sum_n \phi_n^\dagger \gamma_5 \phi_n e^{-\frac{\lambda_n^2}{M^2}} \,. \tag{3.13}$$

Nevertheless, there are schemes, those contained in the second group, that give rise to a different answer. One can even choose a scheme in which $\sum_n \phi_n^\dagger \gamma_5 \phi_n = 0$. But this does not mean that the anomaly has been cancelled. In order to get a different result in (3.12) one has to choose a scheme which does not respect vector invariance. In order to "save" the axial symmetry one has to spoil the vector symmetry. In the case of massless QED this is unacceptable since it gives rise to negative norm states. When none of the symmetries is gauged there is however an ambiguity, one can choose where the anomaly can be located. In this sense it is said that the anomaly appears from the tension between two different symmetries in the process of quantization. Fujikawa proposed an uncertainty principle to illustrate this. He found that this tension can be expressed from the non-commutativity of the Dirac operator (which vector gauge field) and γ_5

$$\langle \bar{\Psi} | [\not{D}, \gamma_5] | \Psi \rangle = \frac{-i}{16\pi^2} F \wedge F \,. \tag{3.14}$$

The previously commented ambiguity is not only visible from the path integral formalism. When computing the triangle diagrams an ambiguity in the regularization of a linearly divergent integral appears. The concrete choice made alters the expectation value of the divergence of the current.

The axial and vector Ward identities can be expressed as

$$\langle \partial_\mu J^\mu_{axial} \rangle = 0 \to (k_1^\lambda + k_2^\lambda) T_{\mu\nu\lambda} = 0 \,, \tag{3.15}$$

$$\langle \partial_\mu J^\mu_{vector} \rangle = 0 \to (k_1^\lambda) T_{\mu\nu\lambda} = 0 \,. \tag{3.16}$$

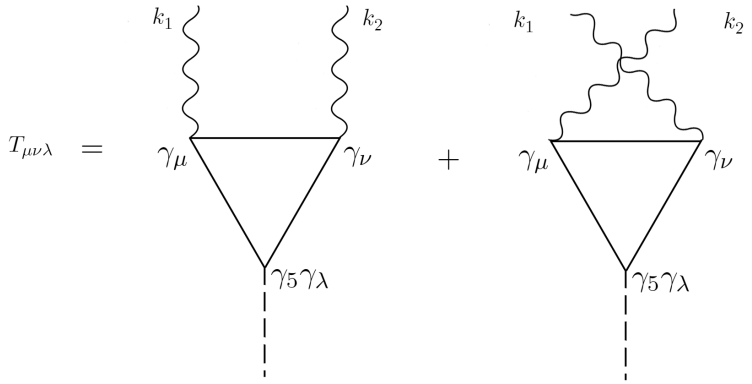

Figure 3.1: Triangle diagrams give rise to the anomalous conservation of the current.

when computing the triangle diagram in momentum space. $T_{\mu\nu\lambda}$ is the (one loop) axial current to two vector currents amplitude as depicted in figure 3.1. The ambiguity in the computation of the triangle can be parametrized, and gives rise to the following expressions

$$(k_1^\lambda + k_2^\lambda)T_{\mu\nu\lambda} = \frac{\beta - 1}{4\pi^2}\epsilon_{\mu\nu\alpha\beta}k_1^\alpha k_2^\beta \,, \tag{3.17}$$

$$(k_1^\lambda)T_{\mu\nu\lambda} = \frac{\beta + 1}{8\pi^2}\epsilon_{\mu\nu\alpha\beta}k_1^\alpha k_2^\beta \,. \tag{3.18}$$

Where β is the parameter that controls the specific shift made in the regularization of the divergent integral. Here one can see more clearly how the tension among symmetries occur: there is no value of β that cancels both contributions. Either one or both currents are not conserved due to 1-loop corrections.
Once we have introduced the basic ideas related to the axial anomaly we are ready to comment on two related concepts that will appear in our holographic studies: the non-renormalization theorem and the distinction between consistent and covariant anomalies/currents.

3.2 Adler-Bardeen theorem

The Adler-Bardeen theorem [5] is one of the features that make anomalies so special and useful. The standard assertion based on this theorem is that "the anomaly is 1-loop exact". However such affirmation is not very concrete, and may give rise to the wrong assumption that any anomaly related quantity is 1-loop exact. In the original paper, Adler and Bardeen show that in spinor electrodynamics the **operator** equation

$$\partial_\mu J_5^\mu = 2im_0 J_5 + \frac{\alpha}{4\pi}\epsilon^{\alpha\beta\gamma\eta}F_{\alpha\beta}F_{\gamma\eta} \,. \tag{3.19}$$

is exact at 1-loop. This means that the coefficients appearing in the previous equation are not modified by higher loop corrections. In [5] they considered a process $J_5^\mu \to n_{fermions} + m_{bosons}$.

They found that only diagrams with a triangle loop of virtual fermions attached to the axial current could give rise to the anomalous term. Moreover any internal photon/meson line in the triangle lowers the degree of divergence, thus not allowing for ambi-

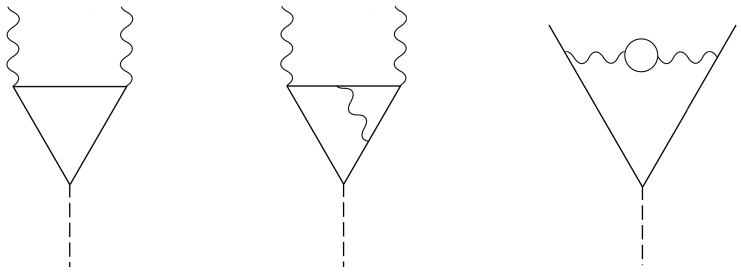

Figure 3.2: Possible diagrams mediating $J_5^\mu \to$ something. Only the left diagram gives rise to an anomaly proportional term. Linear divergences in the loop integrals are absent if the current is not attached to a closed triangle fermion loop (right) or radiative corrections are included in it (center).

guities in the regularization scheme[2]. In their own words *The coefficient of the anomalous term is exactly $\alpha/4\pi$ and does not involve an unknown power series in the coupling constant coming from higher orders int he perturbation theory*
This does not mean, however, that the divergence of the axial current does not renormalize! If one considers the photons as dynamic degrees fo freedom (in contrast to external fields) then the operator $\sim F \wedge F$ may, and does, renormalize. Among others this gives rise to an anomalous dimension for the axial current J_5. Therefore, it is NOT enough to just compute the triangle diagram to obtain an amplitude proportional to the anomaly. The photon rescattering process in figure 3.3

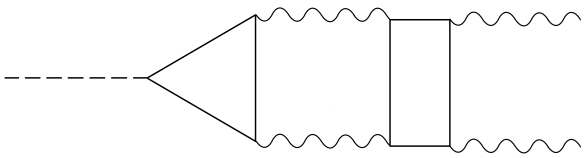

Figure 3.3: Rescattering processes can modify the expectation value of the axial current divergence

is an example of this.

Despite of this, Adler and Bardeen were able to show that **certain** anomaly proportional amplitudes where 1 loop exact in a special kinematic regime. More concretely, they showed that the expectation value of the "naive (classical) divergence"

$$\langle 2im_0 J_5 \rangle = \frac{-2\pi}{\alpha}\,. \tag{3.20}$$

is exact to all orders in the perturbation theory. This, however only holds to leading order in the energy expansion ($k_1, k_2 << m_0$) and for $k_1 \cdot k_2 = 0$. It is pretty clear that such result cannot hold in massless QED. Moreover, when considering strongly coupled theories the radiative corrections to anomaly related quantities can be of great importance. We explore further in this direction in chapter 9.

[2] As commented in by the end of the previous chapter, the anomaly arises form the ambiguity in the regularization of a linearly divergent integral that appears in the triangle diagram

3.3 Covariant and consistent currents

In 3.17 we wrote down the modified Ward identities for the axial and vector currents due to the existence of the anomaly. In the Fujikawa computation of the anomaly, we saw that only those regularizations that respected gauge (vector) invariance gave rise to a conserved vector current and an anomalous axial current. These currents are called consistent currents, for the non-divergence found in the axial current, i.e. the anomaly, fulfils the Wess-Zumino consistency condition. Nevertheless the consistent currents are not covariant under the anomalous symmetry. This is an unavoidable effect of the anomaly. In order to get a covariant version of the currents one has to modify the definition of them, by adding a Bardeen-Zumino term to the currents. By doing so the gauge covariance of the currents is reinstored. These are called the covariant currents. The definition of the current is frequently chosen when dealing with anomalous hydrodynamics. In the case of the abelian axial anomaly, and with the choice $\partial_\mu J^\mu = 0$ in presence of external axial and vector fields the concrete BZ terms are

$$J^\mu_{A\,cov} = J^\mu_{A\,cons} + \frac{1}{12\pi^2}\epsilon^{\mu\nu\rho\sigma}A_\nu F^V_{\rho\sigma}\,, \tag{3.21}$$

$$J^\mu_{V\,cov} = J^\mu_{V\,cons} + \frac{1}{4\pi^2}\epsilon^{\mu\nu\rho\sigma}A_\nu F^A_{\rho\sigma}\,. \tag{3.22}$$

Let us remark that the covariant currents cannot be obtained from the variation of a vacuum functional. In addition neither the axial nor the vector covariant currents are conserved in presence of axial and vector external fields.

$$\partial_\mu J^\mu_{A\,cov} = 2imP + \frac{e^2}{16\pi^2}\epsilon^{\mu\nu\alpha\beta}\left(F^V_{\mu\nu}F^V_{\alpha\beta} + F^A_{\mu\nu}F^A_{\alpha\beta}\right)\,, \tag{3.23}$$

$$\partial_\mu J^\mu_{V\,cov} = -\frac{1}{8\pi^2}\epsilon^{\mu\nu\alpha\beta}F^A_{\mu\nu}F^V_{\alpha\beta}\,. \tag{3.24}$$

This cannot be changed by changing the regularizations scheme: they are unambiguously determined. The Wess-Zumino consistency condition provides an elegant way to understand why the consistent anomaly is not unique. Let us briefly review this.
Define the (BRS) operator s

$$sA_\mu = D_\mu c \qquad sc = -ic^2\,, \tag{3.25}$$

where c is a Faddeev-Popov ghost. The s operator generatres the BRST symmetry that leaves invariant a Lagrangian **after** gauge fixing by means of the ghost fields. Since it acts on the gauge fields as a gague transformation, the anomaly can be obtained by acting with s on the generating functional

$$sW_{eff}[A_\mu] = \mathcal{A}\,. \tag{3.26}$$

Where $\mathcal{A}$ is the anomaly. Since s is nilpotent, it is clear that $s\mathcal{A} = 0$. This is the Wess-Zumino consistency condition. Now, an anomaly exists in the theory if the Wess-Zumino condition is non-trivially satisfied, i.e. if $\mathcal{A} \neq sB[A_\mu]$ where B is any local functional. Moreover, it is clear that by adding $B[A_\mu]$ terms to the generating funtional the anomaly as defined in (3.26) is still consistent

$$\tilde{W}[a_\mu] \equiv W[A_\mu] + B[A_\mu] \qquad \rightarrow \qquad \tilde{\mathcal{A}} = \tilde{W}[a_\mu] = \mathcal{A} + sB[A_\mu]\,. \tag{3.27}$$

The local functional B corresponds to the Bardeen counterterms that allow us to "place" the consistent anomaly in the current (think here of the U(1)xU(1) case) we choose.

3.4 Anomalous transport

Anomalies are a central piece of QFT and have played a major role since they were discovered in 1969. In recent years some effects that link anomalies to transport coefficients have been proposed: The Chiral Magnetic Effect (CME), the Chiral Separation Effect (CSE) and the Chiral Vortical Effect (CVE). The CME describes the generation of an electric current parallel to a magnetic field in presence of a non-zero chiral imbalance. On the other hand the CSE describes the generation of an axial current parallel to a magnetic field in presence of a non-zero electric charge. The CVE is an analogous effect in which the current generated is parallel to a vertex instead of a magnetic field. It has been argued that these may be observed in Heavy Ion Collisions and therefore present a unique opportunity for the study of the theory. From this point of view the fact that anomalous transport coefficients have gained much attention within the last years should not be surprising at all; anomalies are a very deep and subtle property of QFT and their manifestations have a great interest. It is an important task for both theoretical and experimental physicists to find macroscopic and (possibly) measurable! effects that may be, not only related, but unambiguously determined by anomalies. Let us review the most prominent of these effects: the Chiral Magnetic Effect (CME).

The Chiral Magnetic Effect [6,35,36] is a mechanism by which an anomaly mediated chiral excess in presence of a magnetic field produces an electromagnetic current parallel to the magnetic field.

$$J^i = \sigma_{CME} B^i \,. \tag{3.28}$$

The concrete theoretical value for the Chiral Magnetic Conductivity (σ_{CME}) has been computed in several different ways both at weak and strong (AdS/CFT) coupling. Let us sketch the weak coupling computation based on the Kubo formula for σ_{CME}:

$$\sigma_{CME} = \lim_{\omega\to 0}\lim_{k\to 0} \frac{i}{k_i}\langle J_j J_k\rangle \,. \tag{3.29}$$

For some time there was the puzzle regarding the order of the limits. Calculations at weak coupling were order dependent while strong coupling results were not. It was argued in [37] that the order of the limits should be unimportant and that the non-commutativity of some computations was an artifact of the free theory: adding interactions solves the puzzle [3]. The diagram for the current current two point function is

The well known final result is

$$\sigma_{CME} = \frac{e^2 \mu_A}{4\pi^2} \,. \tag{3.30}$$

Where μ_A is the chemical potential associated to the axial charge. In figure 3.5 a pictorial representation of the effect is shown. In presence of equal lefthanded and righthanded carriers the current cancels. However, if we managed to have more d.o.f. of one chirality the current could be observed. This is a key piece of the CME: in order for the current to appear there must be an imbalance of axial charge i.e. more right/left movers. This is in principle a great inconvenience for the experiment since axial symmetry is not a true symmetry in any sector of the Standard Model.

[3] This is yet another example of the potentially problematic assumption of free charges when computing conductivities: The usual electric conductivity diverges if free charge carriers propagators are considered.

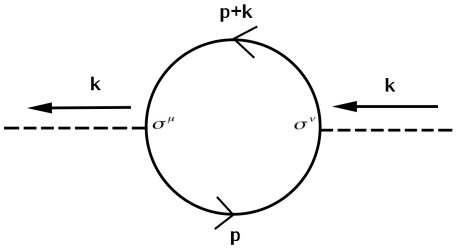

Figure 3.4: Diagram for the retarded current-current correlator for Weyl fermions in the Kubo formula for the CME. Radiative corrections are not needed for the frequency independent conductivity [37]

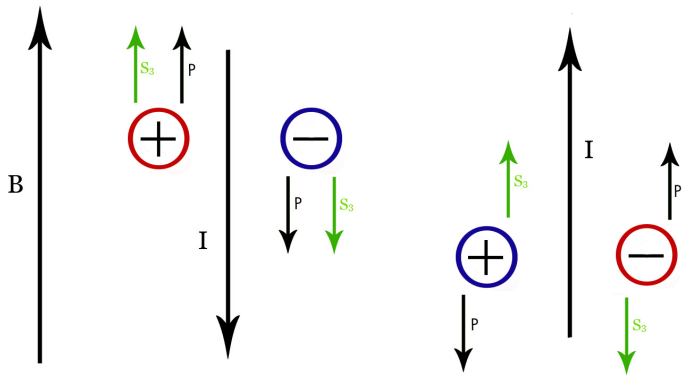

Figure 3.5: Pictorial representation of the effect. Red and blue stand for the chirality of the field. Each field includes the information of particles (+) and antiparticles (-). The helicity is determined by the relative orientation of spin and momentum. An excess of right chirality (more quantity of the first two particles) implies a total non-zero current.

In [6] it was argued that Heavy Ion Collisions and the QGP might be the correct ground to test this effect. At high temperatures chiral symmetry is restored. In addition, event by event there might be an effective generation of axial imbalance. An heuristic explanation goes as follow: non-trivial topological gluon configurations are produced with a probability suppressed with the inverse of temperature (tunneling process). Nevertheless, at high temperatures these states may be effectively produced via a different mechanism: sphalerons. The topological term (winding number) associated to these configurations

$$n_W = -\frac{g^2 N_f}{16\pi^2}\int d^3x\, F_a^{\mu\nu}\tilde{F}^a_{\mu\nu}\,, \tag{3.31}$$

has the same expression as the spatial integration of the chiral anomaly:

$$\partial_\mu J_5^\mu = -\frac{g^2 N_f}{16\pi^2} F_a^{\mu\nu}\tilde{F}^a_{\mu\nu}\,, \tag{3.32}$$

so the production of net topological charge would render net chirality in the system:

$$\frac{d(N_R - N_L)}{dt} \;\alpha\; n_W\,. \tag{3.33}$$

When producing these nontrivial states one expects the **mean** net topological charge to vanish. This however is what we expect for many collisions, for just one event one may produce net charge and therefore net chirality. This situation would tend to dissipate in thermal equilibrium, so still stands the question of whether this dissipation rate is slow enough compared with the typical time of HIC to let us measure the effect. Since N_R is the number of particles minus antiparticles related to a righthanded field (here righthanded stands for the chirality), having positive net chirality would imply that the sum of particles from a righthanded field and antiparticles from a lefthanded field is bigger than the sum of particles in a lefthanded filed and antiparticles in a righthanded field. Finally, the presence of the generated current at any stage of the QGP could in principle be measured as a charge asymmetry in final states [38]. This imbalance has been found already at RHIC [39–41]. Although it is difficult to make quantitative predictions, this points in the direction of the CME happening in HIC [42, 43].

On the other hand there is an increasing interest in the study of anomalous transport in condensed matter systems: Dirac and Weyl Semimetals. These have a very particular band structure that allows to describe the charge carrier d.o.f. as relativistic chiral fermions in vacuum. Therefore they should be sensible to the axial anomaly and may give a more controlable system to study anomalous transport. Indirect measurements, based of the magnetoresponse of Dirac semimetals, have been already performed with positive results [44]. As a last remark let us comment on the importance of the definition of the currents introduced in the previous chapter. One can compute the current generated paralel to a magnetic field using either the consistent or the covariant definitions of the current. If one introduces the chemical potential as the value of the temporal component of the gauge field [4] then

$$J^i_{cons} = 0 \qquad\qquad J^i_{cov} = \frac{N_c}{2\pi} B^i \,, \tag{3.34}$$

which clearly shows how important it can be to correctly identify the current to compute.

Another important concept regarding anomalous transport is the Chiral Magnetic Wave (CMW) [46]. The CMW is a gapless mode that arises in presence of a magnetic field and triangle anomalies. It describes a (both axial and vector) charge density wave with velocity

$$v_\chi = \frac{N_c e B}{4\pi^2} \left(\frac{\partial \mu_{R/L}}{\partial \rho_{R/L}} \right) . \tag{3.35}$$

Where $\frac{\partial \mu_{R/L}}{\partial \rho_{R/L}}$ are the susceptibilities for right/left handed fermions. The CMW can be thought of as a combination of the CME and the CSE: oscillations in electric/axial charge generate axial/electric currents. This coupling gives rise to the massless mode. Remarkably the existence of this mode does not rely on any net chemical potential; it appears in neutral (electric and axial) systems as long as both charges are free to oscillate. From the phenomenological point of view the CMW has interesting consequences. First, the fact that it does not require a finite axial chemical potential is a great advantage for both HIC and condensed matter experiments. It was argued in [47] that the CMW should induce an electric quadrupole moment in the QGP. This moment affects the elliptic flow of the late time QGP and could be observable in the experiment. We will come back to this mode in section 9.3.3.

[4] See [45] a more complete discussion of this.

4 Transport

4.1 Hydrodynamics

Hydrodynamics is an effective description of a many body, locally thermalized system in the long wavelength limit. More concretely, the spatial variations of the relevant quantities in hydrodynamics must be smaller than the mean free path of the underlying microscopic constituents of the system. The ingredients for this description are the thermodynamic variables temperature (T), pressure (p), chemical potential (μ)... and the (conserved) currents of the system. In the hydrodynamic approximation these currents are expressed as functions of the thermodynamic variables. It is concretely in these expressions where the approximation of hydrodynamics enters. Currents are functions of the thermodynamic variables and we have assumed that these must have a rate of change that is small compared to some length. Therefore we perform a gradient expansion in the explicit expression for the currents. These are called constitutive relations and the possible terms appearing in them can be constrained by symmetry considerations.
The equations of hydrodynamics are the conservation laws for the different currents expressed by means of their constitutive relations and the thermodynamic equation of state that describes the equilibrium of the system. As an example let us consider non-relativistic ideal hydrodynamics of a neutral system. In this context "ideal" means to zeroth order in the gradient expansion. The conserved quantities in this setup are the mass, the momentum and the energy. Their conservation laws are given by the following equations

$$\partial_t \rho + \partial_i(\rho v_i) = 0\,, \tag{4.1}$$

$$\partial_t(\rho v_i) + \partial_j \Pi_{ij} = 0\,, \tag{4.2}$$

$$\partial_t \left(\epsilon + \frac{\rho v^2}{2}\right) + \partial_i j_i^\epsilon = 0\,. \tag{4.3}$$

Where Π_{ij} is the stress tensor and j_i^ϵ is the energy current. To leading order in the gradient expansion the constitutive relations are

$$\Pi_{ij} = p\delta_{ij} + \rho v_i v_j\,, \tag{4.4}$$

$$j_i^\epsilon = \left(\epsilon + p + \frac{\rho v^2}{2}\right) v_i\,. \tag{4.5}$$

The five conservation equations together with the the equation of state render a definite system for the six unknown variables ρ, v_i, ϵ, p. The next logical step is to consider hydrodynamic fluctuations. Linearizing the hydrodynamic equations for perturbations on top of equilibrium one can study the dynamics of these modes. Hydrodynamic modes are in

general gapless [1]. In order to have a consistent approximation, the amplitude of these modes must be small enough, such that the hypothesis of local equilibrium is not violated. One of the best known examples of hydrodynamic modes is the sound mode $\omega \sim v_s k$. Let's see how it can be obtained.

Consider the reference frame in which the velocity of the fluid is zero. Then we have $v_i = \delta v_i$, $\rho = \bar{\rho} + \delta\rho$, $\epsilon = \bar{\epsilon} + \delta\epsilon$. The linearized equations read

$$\partial_t \delta\rho + \bar{\rho}\partial_i \delta v_i = 0\,, \tag{4.6}$$

$$\rho\partial_t \delta v_i + \partial_i \delta p = 0\,, \tag{4.7}$$

$$\partial_t \delta\epsilon + (\epsilon + p)\partial_i \delta v_i = 0\,. \tag{4.8}$$

We can take all variables to be proportional to $e^{i\mathbf{k}\cdot\mathbf{x}}$ since we are in an infinite homogeneous background. If we consider that the process is adiabatic we can write $\partial_i \delta p = \left(\frac{\partial p}{\partial \rho}\right)_\epsilon \partial_i \delta\rho$. Choosing $\mathbf{k} = k_z$ and taking derivatives of the equations (4.6, 4.7)

$$\partial_t^2 \delta p + k^2 \left(\frac{\partial p}{\partial \rho}\right)_\epsilon \delta p = 0\,. \tag{4.9}$$

This is a wave equation for pressure: it is a longitudinal [2] propagating mode, sound, with velocity $v_s^2 \equiv \left(\frac{\partial p}{\partial \rho}\right)_\epsilon$. As one can easily check the frequency of sound is real $\omega = \pm v_s k$. This implies that sound propagates infinitely in our system. Moreover one can check that there are no other non-trivial modes. This is a very unusual situation. On the one hand we expect propagating modes to be damped and decay with time. In addition, we miss a diffusive mode $\omega \sim -i\Gamma k^2$. We can think of the situation where a perturbation of the density is introduced from the outside; in addition to the appearance of sound waves we would expect the system to diffuse the extra mass included. However our system does not react like that. The reason for this unusual behavior is that to zeroth order in the gradient expansion the concept of dissipation doesn't appear. Actually, in ideal hydro the equation of energy conservation can be expressed as an entropy conservation law. This is the reason why it is called ideal hydro: there is no dissipation.

So the next step is to add the first order corrections to the constitutive relations. As mentioned before, in principle one should add any term compatible with the symmetries of the system. The final result is

$$\Pi_{ij} = p\delta_{ij} + \rho v_i v_j - \eta\left(\partial_i v_j + \partial_i v_j - \frac{2}{3}\delta_{ij}\partial_k v_k\right) - \zeta\delta_{ij}\partial_k v_k\,, \tag{4.10}$$

$$j_i^\epsilon = \left(\epsilon + p + \frac{\rho v^2}{2}\right) v_i - \eta\left(\partial_i v_j + \partial_i v_j - \frac{2}{3}\delta_{ij}\partial_k v_k\right) - \zeta\delta_{ij}\partial_k v_k - \kappa\partial_i T\,. \tag{4.11}$$

The transport coefficients η (shear viscosity), ζ (bulk viscosity) and κ (thermal conductivity) are unknown coefficients that cannot be determined by hydrodynamics. These quantities arise from integratiing out the microscopic degrees of freedom and they can only be computed from the underlying theory. Of course in many cases these coefficients are fixed by phenomenological assumptions. Once these have been added two diffusive

[1] Massive modes have been integrated out in the procedure of obtaining hydrodynamics from a microscopic theory.

[2] It is possible to obtain the same equation for the longitudinal component of δv_it

modes appear in the spectrum (Thermal and mass diffusion) and the previously found sound mode is modified

$$\omega = \pm v_s k - i\Gamma k^2 \,. \tag{4.12}$$

with Γ being a function of both the shear and the bulk viscosities.

The next logical step is to modify our hydrodynamic and constitutive relations to make them compatible with special relativity: relativistic hydrodynamics. For several reasons, however, this is not of central importance in the holographic models that we will analyze along the thesis, so we refer the reader to any of the above mentioned reviews on this subject.

We wish to know how hydrodynamic quantities as conductivities, viscosities, diffusion constants, etc... can be obtained from the underlying theory. As explained in the introdution there are some relations that allow us to compute such quantities from correlators in the linear response (small perturbations) regime. We will now explore these ideas

4.2 Linear response and Kubo formulae

Linear response theory is the formalism designed to study the response of a system to small departures from equilibrium. The basic hypothesis is that small enough external perturbations give rise to a small response on the system. Linear response can be naturally adapted to hydrodynamics if one restricts the perturbations to have small enough momentum. In this chapter we review the basic concepts of linear response. In addition we explore the connection with hydrodynamics and the concept of Kubo formulae, that will appear unceasingly along this thesis.

The objective of linear response theory is to compute the expectation value of any observable in presence of a small perturbation of the system. The great advantage of linear response is that for small enough perturbations it allows us to compute expectation values with the equilibrium ensemble.

Let the Hamiltonian of the system be decomposed as

$$\hat{H}'(t) = \hat{H} + \hat{H}_{ext}(t) \,, \tag{4.13}$$

where H is the time independent Hamiltonian that describes the dynamics of the system in absence of external perturbations and $H_{ext}(t)$ the part of the Hamiltonian that describes the coupling of the system to external perturbations and is only non-zero from an initial time t_0 on. The expectation value in a certain state $|i\rangle$ of the time evolution of an $\hat{\mathcal{O}}(t,x)$ in the Heisenberg picture is

$$\frac{\partial \langle i|\hat{\mathcal{O}}|i\rangle}{\partial t} = i\langle i|[\hat{H}'(t), \hat{\mathcal{O}}(t,x)]|i\rangle \,. \tag{4.14}$$

Let $|i\rangle$ be an eigenstate of $\hat{H}$, then

$$\frac{\partial \langle i|\hat{\mathcal{O}}\ |i\rangle}{\partial t} = i\langle i|[\hat{H}_{ext}(t), \hat{\mathcal{O}}(t,x)]|i\rangle \,. \tag{4.15}$$

Under the assumption that the response is small this can be written as

$$\delta\langle i|\hat{\mathcal{O}}|i\rangle = \int_{t_0}^{t} i\langle i|[\hat{H}_{ext}(t'), \hat{\mathcal{O}}(t,x)]|i\rangle dt' \,. \tag{4.16}$$

Note that the operator inside the integral depends on t instead of t' due to the small response approximation. If we now consider the expectation value of the operator in the grand canonical ensemble

$$\langle\hat{\mathcal{O}}\rangle = \frac{\sum_i e^{-\beta\langle i|\hat{K}|i\rangle}\langle i|\hat{\mathcal{O}}|i\rangle}{\sum_i e^{-\beta\langle i|\hat{K}|i\rangle}} \,, \tag{4.17}$$

with $K = \hat{H} - \hat{N}\mu$. We arrive to

$$\delta\langle\hat{\mathcal{O}}\rangle = i\int_{t_0}^{t} dt' \,\mathrm{tr}\,\left\{\hat{\rho}[\hat{H}_{ext}(t'), \hat{\mathcal{O}}(t,x)]\right\} \,. \tag{4.18}$$

With tr $\hat{\rho} = 1$.Here we see explicitly how in the linear response approximation the average is computed in the unperturbed ensemble. To make connection with future considerations let us consider the typical example

$$\hat{H}_{ext} = \int d^3x J(t,\mathbf{x})\hat{\mathcal{O}}(t,\mathbf{x}) \,, \tag{4.19}$$

substituting in the previous formulas we obtain

$$\delta\langle\hat{\mathcal{O}}(t,\mathbf{x})\rangle = -i\int_{t_0}^{t} dt' \int d^3x' J(t',\mathbf{x}')\,\mathrm{tr}\,\left\{\hat{\rho}\left[\hat{\mathcal{O}}(t,\mathbf{x}), \hat{\mathcal{O}}(t',\mathbf{x}')\right]\right\} \,. \tag{4.20}$$

With the definition of retarded propagator

$$i\,G^R(\mathbf{x},\mathbf{x}',t,t') \equiv \mathrm{tr}\,\left\{\hat{\rho}\left[\hat{\mathcal{O}}(t,\mathbf{x}), \hat{\mathcal{O}}(t',\mathbf{x}')\right]\right\}\,\theta(t-t') \,, \tag{4.21}$$

we can rewrite the the change of the expectation value of the operator as

$$\delta\langle\hat{\mathcal{O}}(t,\mathbf{x})\rangle = \int_{-\infty}^{\infty} dt' \int d^3x' J(t',\mathbf{x}')G^R(\mathbf{x},\mathbf{x}',t,t') \,. \tag{4.22}$$

After fourier transformation of G^R, $\hat{\phi}$ and J and provided that in equilibrium G can only depend on space and time differences we get

$$\delta\langle\hat{\mathcal{O}}(\omega,\mathbf{k})\rangle = J(\omega,\mathbf{k})G^R(\omega,\mathbf{k}) \,. \tag{4.23}$$

In this formula we see explicitly why the retarded propagator is the key quantity in linear response theory. Let us now see an example of the application of this formalism

4.2.1 Correlators in hydrodynamics and Kubo formulae

Following [8], we shall derive the Kubo formula for the diffusion constant of a certain conserved quantity, e.g. particle number. Consider the diffusion equation

$$\partial_t\rho(t,\mathbf{x}) = D\nabla^2\rho(t,\mathbf{x}) \,, \tag{4.24}$$

where D is the diffusion constant that we wish to compute. As explained before this constant only appears if first order corrections in the derivative expansion are considered. It is related to the viscosities and its concrete value can only be determined from the underlying theory. The solution to this equation in spatial Fourier space is

$$\rho(t,\mathbf{k}) = e^{-Dk^2 t}\rho_0(\mathbf{k})\,. \tag{4.25}$$

We can now Laplace transform this in time

$$\rho(\omega,\mathbf{k}) = \int_0^\infty e^{i\omega t}\rho(t,\mathbf{k}) = \frac{\rho_0(\mathbf{k})}{Dk^2 - i\omega}\,. \tag{4.26}$$

To make the connection to the linear response formalism we would like to consider this quantity as a small deviation from the equilibrium value, induced by an external source. Therefore we write $\rho_0(\mathbf{k}) = \chi\mu(\mathbf{k})$, where χ is the homogeneous susceptibility and μ is the source.

$$\rho(\omega,\mathbf{k}) = \int_0^\infty e^{i\omega t}\rho(t,\mathbf{k}) = \frac{\chi\mu(\mathbf{k})}{Dk^2 - i\omega}\,. \tag{4.27}$$

We can now promote ρ to an (particle number) operator, then, we can follow (4.13-4.23) and write

$$\langle\rho(t,\mathbf{k})\rangle = \int_{-\infty}^0 dt' e^{\epsilon t'}\mu(\mathbf{k})G^R_{\rho\rho}(t-t',\mathbf{k})\,. \tag{4.28}$$

where we have chosen the source $\mu(t,\mathbf{x}) = e^{\epsilon t}\mu(\mathbf{x})\theta(-t)$ such that it is turned on adiabatically from $-\infty$ and switched off at $t = 0$. Using the Fourier transform of the retarded correlator we get

$$\langle\rho(t,\mathbf{k})\rangle = -\mu(\mathbf{k})\int\frac{d\omega}{2\pi}\frac{e^{-i\omega t}}{i\omega+\epsilon}G^R_{\rho\rho}(\omega,\mathbf{k})\,. \tag{4.29}$$

Apply Laplace transform in time

$$\langle\rho(\alpha,\mathbf{k})\rangle = -\mu(\mathbf{k})\int\frac{d\omega}{2\pi}\frac{G^R_{\rho\rho}(\omega,\mathbf{k})}{(i\omega+\epsilon)(i(\omega-\alpha)+\epsilon)}\,. \tag{4.30}$$

This can be integrated using Cauchy's theorem choosing the upper contour

$$\langle\rho(\omega,\mathbf{k})\rangle = -\mu(\mathbf{k})\frac{G^R_{\rho\rho}(\omega,\mathbf{k}) - G^R_{\rho\rho}(0,\mathbf{k})}{i\omega}\,. \tag{4.31}$$

Looking at (4.27) we find

$$G^R_{\rho\rho}(\omega,\mathbf{k}) - G^R_{\rho\rho}(0,\mathbf{k}) = \frac{i\omega\chi}{i\omega - Dk^2}\,. \tag{4.32}$$

One can easily prove that $G^R_{\rho\rho}(0,\mathbf{k}) = -\chi$ in the linear response regime and therefore

$$G^R_{\rho\rho}(\omega,\mathbf{k}) = \frac{D\chi k^2}{i\omega - Dk^2}\,. \tag{4.33}$$

This equality allows us to compute the diffusion constant from the retarded correlator of two particle number operators. The concrete Kubo-Green formula is

$$D = \frac{1}{\chi}\lim_{\omega\to0}\lim_{k\to0}\frac{\omega}{k^2}G^R_{\rho\rho}(\omega,\mathbf{k})\,. \tag{4.34}$$

Where clearly the limits don't commute. This non-commutativity of these limits is linked to the existence of a hydrodynamic mode, the "diffusive" $\omega = -iDk^2$ mode that appears as a pole in the correlator. As we will see, the retarded correlators related to some conductivities do not necessarily have a massless pole and therefore the limits in their Kubo-Green formulae can be taken in any order [37] .

4.3 Landau: Symmemtry breaking & Phase transitions

Along the different chapters of this thesis we will explore how different symmetry breaking patterns are realized in holography and how these affect the dynamical (transport) properties of te dual system. Therefore we would like to write a foreword on the relation of transport and symmetries. Undoubtedly, the first name that appears in our minds when thinking of this is Landau. Landau's mean field theory for phase transitions was the best tool for the qualitative characterization of different phases of matter until the 60's. Moreover it is a natural starting point to understand the idea of universality. Let us first explore the idea of phase transitions in this context.

Many phase transitions can be understood as a transition from a (high temperature) disordered phase to a (low temperature) ordered phase. It is precisely to this kind of phase transitions that Landau's theory applies. From the symmetry point of view, the disordered phase is a highly symmetric phase, in which all possible states with equal energy are randomly occupied connected by local fluctuations. Symmetries of the dynamics of the system commute with the Hamiltonian and therefore they connect certain subsets of those states. So one can think of the disordered phase as a fully symmetric phase. This phase exists as long as the population of each excitation is identical to that of its symmetry-equivalent modes. When the phase transition occurs, this is no longer the case and some mode is frozen. In this phase different states connected by a symmetry transformation cannot be connected by local fluctuations. It is in this sense that the symmetry is broken: the state does not present the symmetry of the action. The ordered (broken) phase can be characterized by the deviation that the system shows from the high-symmetry phase. Such deviation is measured by the order parameter. As an example we can think of the order parameter as the mean position squared of spins in a surface

$$\psi = \left(\frac{\sum_{i=0}^{N} S_i^z}{N} \right)^2 . \tag{4.35}$$

Clearly $\psi = 0$ in the disordered phase.

The theoretical tool proposed by Landau to study phase transitions is the Landau Free Energy $\mathcal{F}$. This Free Energy, that can be thought of as an extension of the Gibbs Free Energy, depends on thermodynamic quantities, on external parameters: electric field, stress... and on **all order parameters** of the system. In this approach the microscopic details of the system are unimportant; the order parameters contain coarse grained information about relevant scales in the system. One can think of $\mathcal{F}$ as a coarse grained version of the hamiltonian, that depends only on the physics of large enough scales, and that depends on rather general features: dimensionality, number of relevant components of the order parameter, etc.... From this perspective the idea of universality arises quite naturally. Two microscopically different systems may share same general features at a certain scale. In Wilsoinian language this would correspond to the situation where two different trajectories in the Hamiltonian space converge to the same fixed point.

Let us briefly explore the main ideas in the simplest version of Landau-Ginzburg theory regarding the nature of phase transitions. Close to the phase transition, the order parameter[3] is expected to be very small, since it vanishes in the disordered phase.

[3] We assume that there is only one

Therefore we can decompose it

$$\mathcal{F}(T,\psi) = \mathcal{F}_0(T) + H\psi + a(T)\psi^2 + b(T)\psi^3 + c(T)\psi^4 + \dots . \tag{4.36}$$

Since $\mathcal{F}$ must be invariant under the full symmetry group for any value of the order parameter, the linear term can only be there if H is an external parameter that transforms appropriately. Like this, many other terms are restricted due to symmetry and stability considerations. In order to find the stable state given a certain T one has to find the minimum of $\mathcal{F}$. For the moment let us consider $b(T) = 0$ and no external parameter. Then we find

$$\frac{\partial \mathcal{F}}{\partial \psi} = 0 = 2a(T)\psi + 4c(T)\psi^3 \qquad \longrightarrow \qquad \psi = \begin{cases} 0 \\ \\ \left(\frac{-a(T)}{2c(T)}\right)^{1/2} \end{cases} . \tag{4.37}$$

So we expect the phase transition at the critical temperature where $a(T)$ changes sign. The simplest example we can think of is

$$a(T) = a_0 \frac{T - T_c}{T_c} \qquad\qquad c(T) = c_0 \, . \tag{4.38}$$

Phase transitions can be classified depending on the class of the function $\mathcal{F}$. Ours is a second order phase transitions, also known as continuos transition, for one has to take two derivatives of the Free Energy w.r.t. the temperature to find a discontinuity.

$$\frac{\partial^2 \mathcal{F}}{\partial T^2} = \begin{cases} \mathcal{F}_0'' & T > T_c \\ \\ \mathcal{F}_0'' - \frac{a_0^2}{2c_0 T_c^2} & T < T_c \end{cases} . \tag{4.39}$$

This implies that the entropy of the system $S \sim \frac{\partial \mathcal{F}}{\partial T}$ is continuous trough the phase transition. Other quantities as the specific heat (4.39) are however discontinuous.

An example of first order phase transition can be easily obtained by adding the cubic term in the expansion. If we now consider $b(T) = b_0$ a metastable phase appears. This metastable phase is energetically not favorable and therefore it decays to the stable phase. However, the entropy changes drastically when this transition happens. This abrupt change in the entropy of the system is related to the familiar concept of latent heat.

Once we have the notions about the character of a phase transition and its relation to the breakdown of symmetries, the question we would like to answer is: What happens with the transport phenomena of a system that undergoes a phase transition? The close relation between phase transitions and the breakdown of symmetries allows us to pose a closely related question in the case of continuous symmetries: What happens with the Nambu-Goldstone modes? These are massless and therefore should become very important in the hydrodynamics of the system. In the next section we comment on the hydrodynamic model for superfluidity and its salient features. The role of the NG mode is commented in section 7.1 of chapter 7.

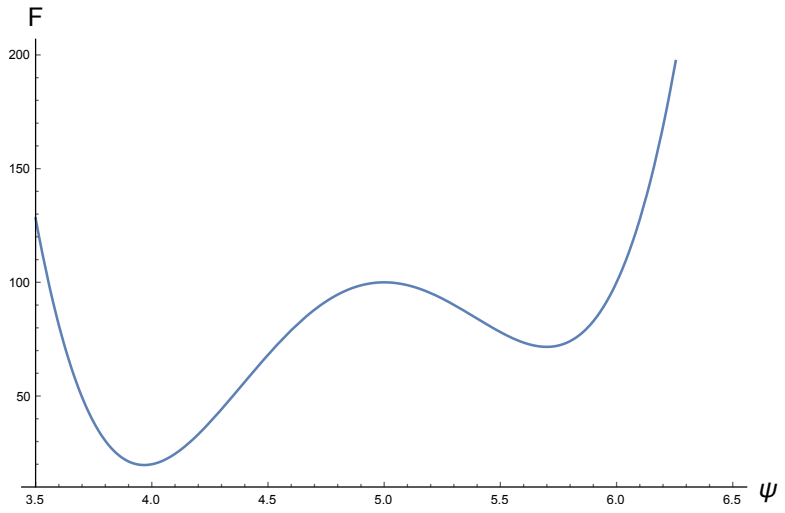

Figure 4.1: Potential with cubic coupling included. Two local minima appear although only one minimizes the energy. The life time of metastable configurations depends on thermodynamic variables and the height of the barrier between vacua.

4.4 Superfluid hydrodynamics: The phenomenological model

The first hydrodynamic model for superfluids was proposed by Tisza and developed by Landau was motivated by the somewhat contradictory experimental observations. The puzzle consisted in the observation that despite of the fact that the superfluid Helium was able to flow dissipationless trough very thin tubes, a pendulum inside the superfluid was found to lose energy. The solution proposed by Landau was to consider the superfluid as a composite of a normal fluid and a superfluid. Within this picture the idea was that the pendulum was loosing energy due to the friction with the normal fluid component. In the capillarities experiment, however, it was only the superfluid component that was being transported. Let us now explore the implications that the two fluid component has in hydrodynamics. In the presence of two different components we are first of all forced to choose a reference frame. So far we have always chosen the rest fluid reference frame, now we have to choose which fluid we want to see at rest, since in principle the superfluid velocity v_s and the normal fluid velocity v_n are independent (think of the capillaries experiment). Let us choose the superfluid rest frame in which only the normal component has non-zero velocity. In this frame we can write the stress tensor, energy and energy current [4] as

$$\Pi_{ij} = \rho_n(v_{ni} - v_{si})(v_{nj} - v_{sj}) + \delta_{ij}(p_n + p_s)\,, \tag{4.40}$$

$$\epsilon = -p_n - p_s + \mu(\rho_n + \rho_s) + T\,s + \frac{\rho_n(v_n - v_s)^2}{2}\,, \tag{4.41}$$

$$j_i^{\epsilon} = (v_{n\,i} - v_{s\,i})\left(\epsilon_n + p_n + \frac{\rho_n(v_n - v_s)^2}{2}\right)\,. \tag{4.42}$$

With these one could write down the conservation relations. For the sake of concreteness we directly jump to the computation of hydrodynamic modes. If we add perturbations on

[4] This is ideal two fluid hydro, so the constitutive relations are expressed to zeroth order in the gradient expansion

top of the equilibrium background (with $v_n = 0$ for simplicity) and linearize the equations we get

$$\partial_t \delta(\rho_s + \rho_n) + \bar{\rho}_n \partial_i \delta v_{n\,i} + \bar{\rho}_s \partial_i \delta v_{s\,i} = 0\,, \tag{4.43}$$

$$\partial_t (\rho_n + \rho_s) S + (\rho_n + \rho_s) S \partial_i \delta v_{n\,i} = 0\,, \tag{4.44}$$

$$\rho_n \partial_t \delta v_{n\,i} + \rho_s \partial_t \delta v_{s\,i} + \partial_i (p_n + p_s) = 0\,. \tag{4.45}$$

Analogously to what we did in 4.1 we can now look for the modes that appear from these equations. Since we are again dealing with idealized hydro we don't expect any dissipation to appear. Moreover, since we have imposed that both fluid components stay at rest, we should find sound modes for both components $\partial_t^2 (p_n + p_s) = k^2 v_s^2 (p_n + p_s)$. Obtaining this is straightforward from what we learned in section (4.1). However, the existence of a second component of the fluid brings a further surprise. Hidden in the equations there is another propagating mode whose equation reads

$$\partial_t^2 S = -S^2 \frac{\rho_s}{\rho_n} k^2 T\,. \tag{4.46}$$

This mode is termed second sound, for it shares the wave structure of sound. However this mode doesn't transport pressure but temperature. Just by construction it should be clear that the appearance of this new mode is an effect of the existence two different components of the same fluid. By looking at the formula we see that this is indeed the case since at zero fluid density the mode becomes time independent.

So now we have a concrete prediction of the phenomenological two component model for superfluids: they should be able to transport temperature gradients in a very effective way (wave, not diffusion) compared to normal fluids. Of course real systems are not properly described by ideal hydro and superfluids are not an exception; however the inclusion of dissipative effects should just shorten the (so far infinite) range of second sound. Indeed this phenomenon has been measured in the lab.

There is an additional mode that can appear termed as fourth sound. Fourth sound appears when the normal component of the fluid is forced to remain at rest. In this case one finds a propagating mode that only involves density fluctuations of the superlfluid component. For certain systems such mode interpolates between first and second sound with increasing temperature: it can be identified with second sound near the pahse transition and with first sound when the density of normal component is small enough. As we will see in chapter 6 this mode appears naturally in certain holographic models of superfluidity.

5
Holography

The gauge/gravity duality was born in 1997 when Maldacena presented his conjecture in [48]. In that paper it was proposed that the large N limit of certain conformaly invariant theories in d dimensions can be described by string theory on AdS space in $d+1$. The most famous example of this is the duality between $\mathcal{N}=4$ super Yang-Mills in d=4 with gauge group $SU(N)$ and Type IIB superstring theory on $AdS_5 \times S^5$. Since then there have been many checks (all positive) of this idea, although no proof has been found yet. The Maldacena conjecture is a realization of a much older idea called holography. This idea was first proposed by t'Hooft [49]. It suggests that theories of quantum gravity (as string theory) should admit a lower dimensional description in terms of non-gravitational theories. These concepts where strongly motivated by the work of Bekenstein and Hawking on the entropy of black holes [50, 51]. In short, the fact that the entropy of a black hole scales with its area, while the entropy of a (non-gravitational) system scales with its volume gives rise to a conflict. Consider the following situation. Take a vast amount of matter and compress it to a sphere with a radius slightly above its Schwarzschild radius. Generically the entropy of such state is $\sim V$. If we now add an extra amount of matter and make the system collapse. Bekenstein formula states that the entropy of the system is now $\sim A$. then, for big enough systems the total entropy has been reduced, in conflict with laws of thermodynamics. The way out given by holography is that such gravitational system is actually describable as a one dimension lower theory without gravity, such that the entropy is actually scaling with the volume of the state in the lower dimension space.

Since 1997, the ideas of the original AdS/CFT conjecture and holography have become a broad area of research in theoretical physics. The initial version of the duality has evolved to the point that nowadays we consider the possibility that any gravity theory has a dual description. For example, the duality has been extended to non asymptotically AdS spaces (Lifshitz holography [52]). This evolution has enlarged the aims that holography may have, with special emphasis in possible applications to condensed matter theory. This has been named AdS/CMT. The work exposed in this thesis mainly belongs to this category.

Along the forthcoming chapters we will take a bottom-up approach to the gauge-gravity duality. This means that we will consider a certain field content in the gravity side motivated by "phenomenological" reasons from the dual theory. Even though one can hope that such models can be obtained from certain consistent truncation of a supergravity, most likely the models considered in bottom-up approaches just don't have a UV completion. This is by no means an inconsistency, but just a restriction on the dual theories considered. In these kind of models one can only explore the large N limit of the dual theory. This

approach to holography has its obvious limitations but serves perfectly for the purpose of understanding certain universal behaviors in the strong coupling and large N limit. Moreover, it opens the door to a new paradigm of the concept of how to define a theory, since many of the dual theories in this approach can only be defined via holography. A key concept in this direction is the holographic renormalization. We will comment on this in subsection 5.2.

It is convenient to clarify some concepts about the terminology. From now on we will refer as the "dual theory" /"boundary theory"/ "CFT" to the $d-1$ theory dual to the gravitational description. The gravitational side will usually be called the "bulk". In addition, when talking about IR or UV we will implicitly mean the IR or UV regions of the dual theory. This means close to the horizon (IR) and at asymptotic infinity (UV) in the bulk by the holographic dictionary. Let us mention that the canonical holographic dictionary states that gauge symmetries in the bulk are mapped to global symmetries in the dual theory. We will always specify which side we refer to when talking about symmetries. Finally, the concept of holographic renormalization refers to the idea of renormalizing the dual theory, by adding certain boundary terms to the bulk theory.

Let us now explore how holography works from a computational point of view. In this sense a central concept in holography is the GKPW formula [53, 54]

$$Z[J] \equiv \langle e^{\int \mathcal{L}} \rangle_{CFT} = e^{-S^{bulk}_{OnShell}}\Big|_{boundary} . \tag{5.1}$$

From this formula, that relates the On-Shell action in the bulk with the generating functional of the dual theory, it is not difficult to obtain a prescription to obtain n-point functions of the dual theory

$$\langle \hat{\mathcal{O}}_1 \hat{\mathcal{O}}_2 .... \hat{\mathcal{O}}_n \rangle = \frac{\delta^n}{\delta J_{\mathcal{O}_1} \delta J_{\mathcal{O}_2} ... \delta J_{\mathcal{O}_n}} \log Z[J] = -\frac{\delta^n}{\delta J_{\mathcal{O}_1} \delta J_{\mathcal{O}_2} ... \delta J_{\mathcal{O}_n}} S^{bulk}_{OnShell} . \tag{5.2}$$

Where J are the sources of the dual theory. So if we are able to identify the gravity duals to the sources of the boundary theory we are almost [1] ready to make explicit calculations from the bulk.

The dual sources are closely related to certain solutions of the equations of motion of the fields in AdS space: the non-normalizable modes. The equations of motion of the fields are second order differential equations and therefore one needs two boundary conditions to find a unique solution. Generically the solutions given by these boundary conditions are said to be either normalizable or non-normalizable. A way to define this is to compute the energy flux of the modes through the boundary of AdS. By imposing the energy to be conserved (flux=0) and the energy[2] to be real, one selects only the normalizable modes (see [13]). Whether none, one or both modes given by the equations of motion are normalizable is in general determined by the mass and the spin of the field. In the case of scalar fields this lower limit is known as Breitenlohner-Friedman (BF) bound. Below this limiting mass both modes become non-normalizable and the theory is unstable. The stable fields with negative mass are sometimes called AdS allowed tachyons, in reference to the flat space case where a negative mass gives rise to a instability. In AdS however this is just a name, since at least one stable solution exists for masses above the BF bound. The reason why this is possible is that the curvature of AdS in a certain way acts as an

[1] We still lack the holographic renormalization.

[2] We refer to energy as the T^0_0 component of the energy-momentum tensor

effective potential preventing the field to become unstable. We will be more precise about this is section 6.1.

Once we know about the existence of normalizable and non-normalizable modes we ask our selves about the role that these play in holography. The canonical prescription is that non-normalizable modes play the role of sources in the dual theory. Since the dual generating functional lives on the boundary, which is the same as saying that the On-Shell action of the gravity side reduces to a boundary term, it is the non-normalizable mode at the boundary what we identify as the source of the dual theory. In the case that both modes are normalizable one has the freedom to choose which to use as the source of the dual operator.
It is tempting to think that the normalizable mode should play the role of the dual operator. Actually in most cases this is the situation. However, as we will see (specially in chapter 8) this is not always true. Let us see the how the simplest example works.

5.1 Massive Scalar Field in AdS_4

Consider the action of a single (real) scalar field in AdS space

$$S = \int \sqrt{-g} d^4x \left(\frac{1}{2} \partial_\mu \phi \partial^\mu \phi + \frac{m^2}{2} \phi^2 \right) , \tag{5.3}$$

where $g_{\mu\nu}$ is the metric of AdS_4. We work in the probe limit, in which we consider that the scalar field does not backreact onto the metric. The equations of motion reads

$$\left(-\Box + m^2 \right) \phi = 0 \, . \tag{5.4}$$

Where the d'Alembertian operator is defined with the AdS metric. Upon substitution of the equations of motion into the action we arise to the On-Shell action, which by the GKPW formula is to be interpreted as the generating functional of the dual theory. Therefore in order to obtain the 1-point function of the dual scalar operator we should differentiate this w.r.t. the coefficient at the boundary of the non-normalizable mode. Then we need to identify such coefficient. For simplicity we impose homogeneity in the transverse directions and look for static solutions. We can solve the equations of motion asymptotically with the ansatz

$$\phi = \sum_{i=0}^{\infty} r^{\alpha - i} \phi_i \, . \tag{5.5}$$

Substituting this in the equations of motion and taking the asymptotic limit $r \to \infty$ one can determine the two allowed values for α

$$m^2 - \alpha_\pm (\alpha_\pm - 3) = 0 \, . \tag{5.6}$$

So we have found the two independent coefficients $\phi_{A(0)}$, $\phi_{B(0)}$

$$\phi_{r \to \infty} = \phi_{A(0)} r^{\alpha_+} + \phi_{A(1)} r^{\alpha_+ - 1} ... + \phi_{B(0)} r^{\alpha_-} + \phi_{B(1)} r^{\alpha_- - 1} + ... \, . \tag{5.7}$$

Where other coefficients as $\phi_{A(1)}$ are determined from the independent ones. We identify the leading term as the non-normalizable mode and compute the 1-point function from

the generating functional

$$\langle O_\phi \rangle = \lim_{r\to\infty} \frac{1}{\sqrt{-\gamma}} \frac{\delta}{\delta \phi_{A(0)}} S_{O.S.} = \phi_{B(0)} + (divergent\, terms)\,, \tag{5.8}$$

where we have substituted Ψ at the boundary by its asymptotic behavior (5.5) and γ is the induced boundary metric. We haven't talked about the need for renormalization so far. Our formula gave rise to a divergent limit plus certain finite values. In the spirit of the early days of holography we just drop out the divergences and keep the finite terms. In section 5.2 we explore the ideas of holographic renormalization in more detail. By dropping the divergences we were left to the leading coefficient of the normalizable mode at the boundary. A very important consideration is in order now. So far we have talked about the normalizable and non-normalizable coefficients related to the independent boundary conditions needed to solve the equations of motion. However if we can just impose any value to the normalizable mode then we have done nothing; we have just defined a theory in which n-point functions can have any value that we desire and we didn't even need to solve any equation. Clearly we lack something. More concretely we lack the entire bulk dynamics. In other words, we have just looked at the UV region; what happens in the IR?. The answer is enlightening: upon solving the equations of motion one finds that most of the possible boundary choices give rise to some irregular behavior in the interior of the bulk. We have not realized this before because we did not solve the equations of motion. The divergence is a very unnatural situation in the gravity side. To avoid it we impose regularity in the interior of the bulk [3]. This condition, together with fixing the non-normalizable mode, fixes the field configuration and therefore the normalizable mode. Moreover, to obtain the value of the 1-point function now we need to solve the bulk equations of motion since one of the conditions is imposed at the interior of AdS space.

5.2 Holographic Renormalization

The goal of the holographic renormalization is to remove the divergent terms of the On-Shell action in the bulk. Since the On-Shell action is the generating functional of the dual theory this procedure ensures that the correlators obtained from it render finite answers. Let us first comment on how one would naively attack the problem. First of all, assume that we can write the On-Shell action as just a boundary term:

$$S_{OS} = \int_\partial \sqrt{-\gamma}\lambda\,. \tag{5.9}$$

This equality is not correct in general but holds for the divergent terms of the O.S action. In principle one can find the explicit expression of λ as a functional of the bulk fields. In order to do so one just needs to substitute the equations of motion in the action, integrate by parts, and look at the boundary term that survives[4].

So what we are after are the divergent terms of (5.9). In order to determine them we could just make an asymptotic expansion of $\sqrt{-\gamma}\lambda$ (say we are in some coordinates such that the boundary is at $r \to \infty$) and look for the divergent terms. For example imagine we have the explicit expression of λ as a functional of the fields of the theory (We just

[3] Generically this happens at the origin of Poincaré patch or at the horizon of a black hole

[4] This is not always the case in the probe limit. Consider ϕ^3 theory for example

consider a scalar field) and, moreover, we know how these fields behave at infinity (which is given by the equations of motion). For concreteness consider a massless scalar field. Then we can write

$$\sqrt{-\gamma}\lambda \sim \sqrt{-\gamma}\phi^2(r) \sim ar^2 + br + c + dr^{-1} + \dots . \tag{5.10}$$

Apparently we are almost done. We just need to subtract $ar^2 + br$ at the boundary. There is however a problem in this construction: the terms we want to subtract are not covariant. They arise form the asymptotic expansion of the covariant expression $\phi^2(r)$. So now, we need an extra step: we have to **invert** the asymptotic series in order to write the counter terms in a covariant fashion. And this is the problematic point, since such an inversion turns out to be extremely complicated in generic cases.

Clearly if the asymptotic expansion had been covariant there would be no problem. Is it possible to do the expansion in a covariant way such that it still allows us to detect the divergent terms? The answer is yes: the strategy is to expand in eigenfunctions of the dilatation operator δ_D. The natural question now is: Why the dilatation operator? The naive asymptotic expansion that we did before can be viewed as an expansion in eigenfucntions of an operator. Let $\hat{\partial} \equiv r\partial_r$. As we will see later, the dilatation operator coincides with the radial derivative **asymptotically** and its eigenfunctions are covariant. Let us emphasize again that we need some notion of degree of divergence of these eigenfucntions. In the case of the operator $\hat{\partial}$ this was given by the weights: terms with an eigenvalue > 0 diverge and others do not. Since $\partial_r \to \delta_D$ the same happens with the dilatation operator. The dilatation operator just reorganizes the asymptotic expansion in covariant terms. It is possible to check that the covariant counterterms given by the dilatation operator procedure coincide with those obtained with the naive strategy after inversion of the series.

Before we go into details, let's sketch the procedure of Holographic Renormalization in the Hamiltonian formalism:

1. Obtain the dilatation operator δ_D
2. Expand $\sqrt{-\gamma}\lambda$ in eigenfunctions of δ_D
3. Determine which weights imply divergence (recall in the naive $\hat{\partial}$ procedure we were looking for those eigenvalues > 0). From now on we call them "dangerous terms".
4. The Counter Terms are just the dangerous terms with a - sign in front of them so that the divergences are canceled.

In what follows we consider an example and show how each step is done

Holographic Renormalization: How to

The following presentation is rather computational. We consider a gauge field and a ($m^2 = -3$) scalar in background AdS space. We stay in the probe limit for simplicity. We will point the parts of the procedure where this limit has an effect.

1. Go to the coordinates where AdS is $ds^2 = dr^2 + e^{2r}dx^2$
2. In this coordinates solve the equations of motion asymptotically, we just need the first term
$$A_i \sim e^{\Delta r} \qquad \phi \sim e^{-r} \qquad \gamma_{ij} \sim e^{2r}\,. \tag{5.11}$$
3. Write the radial derivative as an integrated functional derivative using **all** the fields on your theory :
$$\partial_r = \int dx' \left(\dot{\phi}(x') \frac{\delta}{\delta\phi(x')} + \dot{A}_i(x') \frac{\delta}{\delta A_i(x')} + \dot{\gamma}_{ij}(x') \frac{\delta}{\delta\gamma_{ij}(x')} \right) . \tag{5.12}$$
4. With the asymptotic behavior of the fields obtained in step 2. expand the derivative to leading order; this is the dilatation operator:
$$\partial_r \sim \int dx' \left(-\phi(x') \frac{\delta}{\delta\phi(x')} + \Delta A_i(x') \frac{\delta}{\delta A_i(x')} + 2\gamma_{ij}(x') \frac{\delta}{\delta\gamma_{ij}(x')} \right) \equiv \delta_D\,. \tag{5.13}$$
5. Rewrite the equations of motion substituting the radial derivatives of the fields by another letter, that we will call (although strictly speaking it is not) momentum. Example:
$$\dot{A}_i \equiv E_i \qquad \dot{\phi} \equiv \Pi \qquad \dot{\gamma}_{ij} \equiv K_{ij}\,. \tag{5.14}$$
6. Rewrite the radial derivative using the momenta
$$\partial_r = \int dx' \left(\Pi(x') \frac{\delta}{\delta\phi(x')} + E_i(x') \frac{\delta}{\delta A_i(x')} K_{ij}(x') \frac{\delta}{\delta\gamma_{ij}(x')} \right) . \tag{5.15}$$
7. Now we have to determine the expansions for the momenta and the radial derivative.
8. A very natural question now is: How do we determine which the possible weights in the expansions are? Although there is no need to know this a priori since it is determined by the equations of motion it is actually very useful to have an preliminary idea. The way to obtain this is the following:
   (a) First determine the possible weights of λ. In order to do so just imagine all possible terms appearing in the On-Shell action that respect the symmetries of the system (Lorentz, Gauge, Global...). Now apply the dilatation operator on these terms and see which the eigenvalues are. Stop at eigenvalue -d (4 in our concrete case).
   (b) As said before the derivative of the fields is not exactly the momenta but it is a part of it (if there is a kinetic term). Since the true momenta are obtained differentiating the On-Shell action w.r.t. the different fields, take the terms that you imagined in the On-Shell action and differentiate them w.r.t. the desired

filed. Determine the weights of the terms obtained in this way and that will give you the weights of the momenta. Example

$$\lambda \sim A_i A^i + \partial_i \phi A^i + \phi^2 \tag{5.16}$$

$$\rightarrow E_i \equiv \frac{\delta \lambda}{\delta A_i} \sim A^i + \partial^i \phi \rightarrow E_i = E_{i(-\Delta)} + E_{i(1)}\,. \tag{5.17}$$

9. Now that we know the possible weights for the momenta, we can write down how the expansion of the radial operator will look like. Take the expression in step 6 and introduce the expansions for the momenta. Collect them in groups with same weight and label this groups by this weight (Concrete values are just examples):

$$\begin{aligned}
\partial_r = &\int dx' \left((\Pi(x')_{(1)} + \Pi(x')_{(2-\Delta)} + \Pi(x')_{(2)} + ...) \frac{\delta}{\delta \phi(x')} + \right. \\
&\left. (E_{i(-\Delta)}(x') + E_{i(1)}(x') + E_{i(1-\Delta)}(x') + ...) \frac{\delta}{\delta A_i(x')} + K_{ij(2)}(x') \frac{\delta}{\delta \gamma_{ij}(x')} \right) = \\
&\int dx' \left((\Pi(x')_{(1)}) \frac{\delta}{\delta \phi(x')} + (E_{i(-\Delta)}(x')) \frac{\delta}{\delta A_i(x')} + K_{ij(2)}(x') \frac{\delta}{\delta \gamma_{ij}(x')} \right) \equiv \delta_D + \\
&\int dx' \left(\Pi(x')_{(2-\Delta)} \frac{\delta}{\delta \phi(x')} \right) \equiv \delta_{(1-\Delta)} + \\
&\int dx' \left(\Pi(x')_{(2)} + ...) \frac{\delta}{\delta \phi(x')} + E_{i(1-\Delta)}(x') \frac{\delta}{\delta A_i(x')} \right) \equiv \delta_{(1)} + \\
&\int dx' \left(E_{i(1)}(x') \frac{\delta}{\delta A_i(x')} \right) \equiv \delta_{(1+\Delta)} + \dots\,.
\end{aligned} \tag{5.18}$$

Note that the momentum associated to the metric has no expansion. This is a consequence of the probe limit.

10. This step now is probably the most confusing one so let us be more detailed. What we need now is to determine the explicit expansions (in eigenfunctions of the dilatation operator) for the momenta AND the radial derivative. What makes this part of the procedure so confusing is the fact that these expansions have to be done at the same time; this means that one cannot simply first obtain the expansion for E_i and afterwards the expansion for the radial derivative. Everything is mixed and one has to proceed with caution.

    (a) Using the equations of motion one can determine the FIRST term (highest weight) in the expansions of the momenta. At this point the radial derivative can just be identified with the dilatation operator.

$$\dot{\Pi} + 2\Pi + \partial_i A^i + \phi = 0\,, \tag{5.19}$$

$$(\delta_D + 2)\Pi_{(1)} + \phi = 0 \rightarrow \Pi_{(1)} = -\phi\,. \tag{5.20}$$

    In the backreacted case one should use Einstein equations.

    (b) In the example the $\partial_i A^i$ was not taken into account for its weight was lower $\Delta - 2$.

    (c) Now one can determine the second term. In order to do so one has to use the expansions for the momenta, as well as the expansion for the radial derivative!

The expansions have to be combined in such a way that all terms have the same total weight:

$$\left(\dot{\Pi} + 2\Pi + \partial_i A_i + \phi\right)_{2-\Delta} = 0\,, \tag{5.21}$$

$$\delta_D \Pi_{(2-\Delta)} + \delta_{(1-\Delta)}\Pi_{(1)} + 2\Pi + \partial_i A^i = 0 \to \Pi_{(2-\Delta)} = \dots\,. \tag{5.22}$$

(d) Here one can see why it was not necessary to expand the radial derivative in step 10(a) . There was no combination of operator (except for δ_D) and momentum with the appropriated weight.

(e) Continue with this procedure until the weight that coincides with the normalizable mode (for contravariant momenta this is $d - highestweight$).

11. Now that we have the expansions for the momenta and the radial derivative, solve the equation for λ order by order, as done for the momenta, up to weight -4.

12. The covariant counterterms will be given by all the terms in the expansion of λ with weight bigger than -4.

13. It is important to take into account that the expansions w.r.t. δ look

$$\lambda = \lambda_{(0)} + ... + \lambda_{(d)} + \tilde{\lambda}_{(d)} \log e^{2r}\,. \tag{5.23}$$

Therefore

$$\left(\delta_D X\right)\big|_{(d)} = -dX_{(d)} + 2\tilde{X}_{(d)}\,. \tag{5.24}$$

The coefficient with the tilde gives rise to logarithmic divergences and it must be removed too. It can be obtained in the same manner as the other coefficients.

5.3 Black Holes in holography

Black holes play a crucial role in holography: they allow us to set the dual theory at finite temperature and thus break supersymmetry and conformal invariance. There are several heuristic ways to understand why black hole have this effect. Consider a black hole of a certain radius r_h in the center of AdS space. From the (classical) bulk point of view we can forget about the interior of the black hole and just consider it as a one way door (the horizon); what crosses it never comes back. Then, from the holographic point of view, the horizon is an IR cutoff since we only have to integrate along the part of bulk outside of it. This picture is already appealing: in QFT at finite temperature one imposes certain periodicity to imaginary time $0 < \tau < \beta$ with $\beta = 1/KT$, so the temperature serves as a cutoff for long times i.e. low energies. This relation becomes more explicit when one considers the analytic extension of a black hole metric to imaginary time. The complex time metric is diffeomorphic (and conformally equivalent) to the metric of a cone. Only by imposing the appropriated periodicity in the angular ($\sim \tau$) direction can one remove the conical defect. As it is well known this is the correct recipe to compute the temperature of the black hole. So in holography the thermal circle is naturally implemented in the generating functional by the presence of a black hole in the bulk. In contrast, in standard finite temperature QFT the thermal circle is imposed after comparison of the path integral and the Boltzman distribution in statistical quantum mechanics.

Let us be more specific and study in more detail some characteristics of black holes in AdS space. The idea of considering black holes in AdS space arise much earlier than the AdS/CFT conjecture. The motivation for this was the development of black hole thermodynamics and the striking discovery that black holes in flat space are unstable from the thermodynamic point of view. Consider the metric of a Schwarzschild black hole in Minkowski

$$ds^2 = -\left(1 - \frac{2GM}{r}\right) dt^2 + \left(1 - \frac{2GM}{r}\right)^{-1} dr^2 + r^2 d\Omega^2 \,. \tag{5.25}$$

To compute the temperature associated to it we can use the imaginary time (Gibbons-Hawking) prescription. Taking $t \to i\tau$ and defining $\rho \equiv r - 2GM$ we obtain

$$ds^2 = \frac{\rho}{r} d\tau^2 + \frac{r}{\rho} d\rho^2 + r^2 d\Omega^2 \,. \tag{5.26}$$

With another coordinate change $\rho = \Theta^2$

$$ds^2 = \frac{\Theta^2}{r} d\tau^2 + 4r d\Theta^2 + r^2 d\Omega^2 = 4r \left(\frac{\Theta^2}{4r^2} dt^2 + d\Theta^2\right) + r^2 d\Omega^2 \,. \tag{5.27}$$

This change is important since now the prefactor of $d\tau^2$ goes to zero when $r \to r_H$. Inside the brackets we recognize the metric of a plane in polar coordinates. However, this plane is actually a cone if the angular direction τ doesn't have the appropriate periodicity conditions $\frac{\tau}{2r} = \frac{\tau}{2r} + 2\pi$. By comparison with the closed Euclidean time formalism $\tau = \tau + \frac{1}{\beta}$

$$T = \frac{1}{4\pi r_H} \,. \tag{5.28}$$

With $r_H = 2GM$. From this we can easily derive the specific heat $\partial T / \partial M < 0$. This implies that the hotter the black hole the smaller it becomes, thus radiating more and eventually disappearing. Or the other way around, with the picture of a black hole increasing forever as it swallows the outside radiation. Of course all these considerations arise from the application of thermodynamics to black holes. Specially, the idea of a black hole radiating as a black body is not compatible with GR and only by introducing quantum effects this process becomes possible, by means of the Hawking radiation. The instability of black hole is however not universal and depends not only on the near black hole metric but on the asymptotics of the space-time too. Consider the Schwarzschild-AdS metric

$$ds^2 = -\left(1 - \frac{2GM}{r} + \frac{r^2}{L^2}\right) dt^2 + \left(1 - \frac{2GM}{r} + \frac{r^2}{L^2}\right)^{-1} dr^2 + r^2 d\Omega^2 \,. \tag{5.29}$$

Where L is the AdS radius. We can proceed analogously to the previous example and find

$$T = \frac{L^2 + 3r_H^2}{4\pi L^2 r_H} \,, \tag{5.30}$$

where the horizon radius is a complicated function of M and L. In figure 5.1 we show the behavior of T against L for a fixed value of L. One can see that for a given temperature above T_0 there are two different black hole solutions, usually referred as small and big black hole for obvious reasons. The specific heat of small black hole is negative as it was in Minkowski space. However big black hole have positive specific heat and therefore are

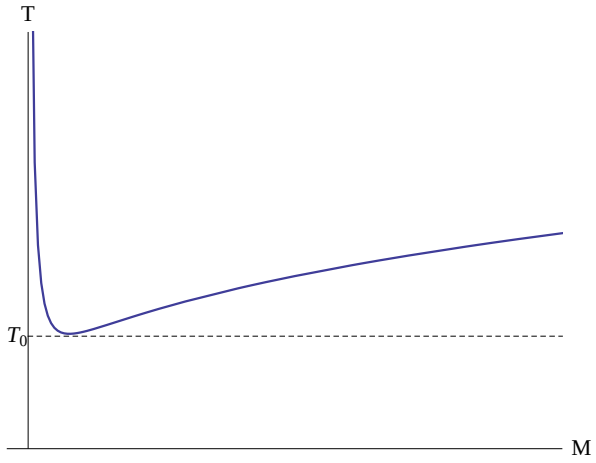

Figure 5.1: Temperature of the Schwarzschild black hole in AdS against its mass for a fixed value of L. Black hole solutions only exist above a critical temperature T_0

stable against small temperature perturbations.

A concept that will appear repeatedly in the principal chapters of this thesis is that of thermodynamically favored phases. Given several possible states of a same system, with equal thermodynamic variables, the one with lowest Gibbs Free Energy (FE) is the stable one. Other possible configurations may be long lived if the transition amplitude to the lowest energy state is strongly suppressed. From the comparison of the path integral and the partition function of statistical physics one can easily obtain the formula for the FE as a functional of the action

$$F = -T \log Z = TI \,. \tag{5.31}$$

Where I is the action evaluated in a certain minimum. The configuration that minimizes the FE dominates the partition function. Using this concept Hawking and Page studied the stability of big black hole in AdS, comparing their associated FE to that of empty[5] AdS. By doing so they found that although stable, big black hole where not the preferred metric for low enough temperatures. At a certain critical temperature T_{HP} the AdS metric is energetically more economic than the black hole. This is the Hawking-Page transition. Its holographic interpretation was given by Witten who showed that in the holographic picture this was the gravitational description of a deconfinement (black hole) - confinement (AdS) phase transition in the dual theory. This idea supposed a great boost for the search of a AdS/QCD duality.

Let us now jump to a related topic regarding the relation between black holes and finite temperature QFTs: the Quasi Normal Modes. In a system at finite temperature we expect the modes produced by small perturbations to have a finite life time. This is the same as saying that we expect to have a finite damping rate, given by an imaginary part in the dispersion relations. These are called quasi normal modes (QNMs). As we saw in section 4.2, linear response is the suited formalism to study these phenomena. Therefore, in order to study the QNMs of a system we want to compute retarded correlators. More

[5]One may think of the energy concentrated in the black hole as a dilute graviton gas in the case of empty AdS

concretely, dispersion relations appear as the poles of these correlators. Previously we saw that the GKPW formula provides us with a prescription for computing n-point functions in holography. Now we want to go beyond that and compute retarded correlators. To this aim will comment on some important aspects shown in [55, 56].
A suggestive issue appears when one tries to compute real time correlators in holography. When one studies perturbations on top of the gravitational background in real time, one finds that several boundary conditions are possible at the horizon. In contrast, if one does the analysis in euclidean time, there is only one "reasonable" choice: regularity. This ambiguity is related to the different possible propagators thatone can define (advanced, retarded...). Interestingly, in order to compute retarded correlators one has to choose "infalling" boundary conditions. This means that only perturbations that go into (instead of come out) the horizon are considered. Let us give a naive sketch with the prescription for computing retarded 2-point funtions

- Solve the linearized equations for the perturbations with finite momentum and frequency on top of the background.
- Impose infalling boundary conditions at the horizon.
- Differenciate the On-Shell action with respect to the appropiated sources.
- The previous step gives rise to a combination of derivatives of the perturbations evaluated at the horizon.
- Using the Fefferman-Graham expansion one can see that the previous step generically gives rise to the cocient of the normalizable mode coefficient over the non-normalizable mode coefficient.
- Obtain the poles of this quantity as a function of frequency and momentum.

This sketch is correct although in general unsolvable analytically and therefore requires numericall techniques. In addition, another interesting phenomenon may arise: mixing. At the beginning of this chapter we showed that the non-normalizable modes where to be understood as the sources of the dual theory. We saw too how the normalizable modes are to be identified as (or at least closely related to) the expectation values of the dual operators. Now one has to pay attention to the fact that in presence of several fields in the bulk the modes mix. In other words, the non-normalizable mode of a field is possibly sourcing not just the operator associated to its field but other operators too. This ultimately implies that the bulk to boundary propagator is matix valued. This situation implies that the QNMs can be computed from the study of the zeros of the determinant of the inverse correlator [57]. We will use this technique in the following chapters to compute QNMs of several theories in holography.

6

Spontaneous Symmetry Breaking I

In this chapter we explore the implementation of spontaneous symmetry breaking in the dual theory. In order to do so we generalize the results of the so-called Holographic Superconductor [58, 59]. The Holographic Superconductor is one of the most celebrated achievements within the duality and the first example of the implementation of spontaneous symmetry breaking in holography. In order to explore its main features and to better understand the phenomenon of spontaneous symmetry breaking and its relation to transport in holography we extend the Holographic Superconductor by inducing the spontaneous breakdown of a $U(2)$ symmetry. This allows us to study how the transport phenomena of the Holographic Superconductor generalize to the non-abelian case and to check how the QNM spectrum is modified according to what we expect from QFT. In addition, the model that we are going to explore is expected to feature exotic Nambu-Goldstone modes. Although the existence and behavior of such modes is well stablished in QFT, there is almost no appearance of these in holography. To our knowledge ours is the first careful study of non-standard NG-Bosons in this context.

Due to the link between local symmetries and global symmetries via the holographic dictionary, it is usually overlooked that global symmetries in the bulk do have an impact in the dual theory. Therefore we do not only extend the usual Holographic Superconductor in the sense of adding a richer and more complicated gauge group. In addition, we perform a thorough study of the implications of the spontaneous symmetry breaking of a global symmetry living in the bulk. We present two models, one featuring an ungauged version of the symmetry in the bulk and another that contains a full gauge symmetry group.
In the former, we just add a second scalar field of the same mass as the one in the usual Holographic Superconductor. This promotes the $U(1)_{gauge}$ to a $U(1)_{gauge} \times SU(2)_{global}$. In the second model we include gauge fields for the whole $U(2)$ symmetry. The difference between the two models is as follows. In the ungauged model only the $U(1)$ symmetry is local in the bulk. It has however a *global* $SU(2)$ symmetry[1] under which the scalar fields transform as a doublet. According to the holographic dictionary this model contains only one conserved current, corresponding to the single gauge field in the bulk. The dual field theory inherits of course the global $SU(2)$ symmetry of the bulk but this symmetry is not generated by operators in the dual conformal field theory. This is similar to the decoupling limit in which we are working and in which the fluctuations of the metric are

[1] Although global symmetries are not expected in a consistent theory of quantum gravity they can be obtained in certain decompactification limits of string theory: e.g. by wrapping branes on cycles and then taking the volume of the cycle to infinity so that the effective gauge coupling on the branes goes to zero leaving only a global symmetry on them.

suppressed. The dual field theory has then strictly speaking no energy momentum tensor. In usual four dimensional Lagrangian field theories, Noether's theorem guarantees that we can always construct a conserved charge generating a given symmetry of the Lagrangian. In holographically defined field theories the existence of a four dimensional Lagrangian is a priori not guaranteed and therefore Noether's theorem does not straightforwardly apply. This is the case here. Although the dual field theory has the $SU(2)$ symmetry it does not contain operators generating these symmetries. We can speak of these symmetries as an outer automorphism of the operator algebra of the dual field theory. Physically the difference between the two models is that the ungauged one is a one-component fluid (there is only one notion of charge) whereas the gauged one is a two component fluid. In the latter case the charges are the expectation values of the zero-component of the currents in the Cartan subalgebra of the $U(2)$ symmetry.

Although the ungauged model does not contain conserved currents for the $SU(2)$ symmetry and therefore many of the standard proofs about existence of Goldstone bosons do not strictly apply we find a new ungapped mode in the QNM spectrum of the scalars. This mode is however not a standard Goldstone boson with linear dispersion relation but a type II Goldstone mode whose energy depends quadratically on momentum.

The second model we consider has a scalar field doublet coupled to the full set of $U(2)$ gauge fields. We switch on a chemical potential only for the overall $U(1)$ symmetry. Therefore the high temperature phase has the full $U(2)$ symmetry. At low temperatures this symmetry is broken to $U(1)$. In this model the dual field theory contains currents for all the $U(2)$ symmetries. We can therefore also study the conductivities associated to the different "colors".

In the context of condensed matter physics it has been pointed out long ago in [60] that such multicomponent superfluids have unusual Goldstone modes with quadratic dispersion relation. In the high energy context such models have been considered as models for Kaon condensation in the color-flavor locked phase of QCD in [31, 61] again emphasizing the existence of the quadratic Goldstone mode. Our gauged holographic model is a straightforward holographic analogue of the model in [31, 61] and indeed we also find the presence of a Goldstone mode with quadratic dispersion relation. Let us also note that in the holographic context a type II Goldstone boson was found before in magnetized $D3/D5$ defect theory [62].

We shall then consider the symmetry breaking pattern of the boundary theory dual to the gauged holographic model. We will see that trough the theorems in section 2.2 the presence of a type II Goldstone boson in the spectrum is guaranteed.

This chapter is organized as follows. In section 6.1 we review the main features of the spontaneous symmetry breaking mechanism in holography and the usual Holographic Superconductor. In section 6.2 we review a simple field theoretical model featuring type II NG-Bosons. This model has been introduced in the context of Kaon condensation in color-flavor locked QCD. It served us as inspiration for constructing the holographic models. Section 6.3 is devoted to the analysis of the ungauged model. Since the well-known s-wave superconductor is a subsector of both the ungauged and the gauged model we also briefly review first the findings of [63]. Then we show that even with this drastic simplification, i.e. not gauging the global $SU(2)$ symmetry in the bulk, the model presents Goldstone modes with quadratic dispersion relation. Hence, within this model a type II NG boson is found as a consequence of having broken *just one* charge generator (the one associated to the $U(1)$ symmetry).

In section 6.4 we study the fully gauged $U(2)$ model. Then we analyze the fluctuation equations to linear order. They decompose into three decoupled sectors. One being the already encountered $U(1)$ s-wave superfluid, the other describing the non-Abelian sector in which the type II Goldstone mode resides and a third one with the unbroken $U(1)$ symmetry. We proceed to study the conductivities which now arrange naturally into a two by two matrix. We show that the diagonal conductivities have delta-functions at zero frequency and are in this sense superconducting. Furthermore we find indications that for temperatures below $T = 0.4T_c$ another instability arises in the gauge field sector leading to an additional p-wave condensate. Then we study the low lying quasinormal modes and analyze the results. We find the type II Goldstone mode and also study the fate of the diffusion modes in the broken phase. Since now four symmetry generators participate there are 4 diffusion modes that in the broken phase pair up and can move away from the imaginary axis. We find that this is precisely what happens. Therefore the response in this sector does not show the purely exponential decay induced by the gapped pseudo diffusion mode of the $U(1)$ sector.

6.1 Spontaneous symmetry breaking in holography

In this section we review the main features of spontaneous symmetry breaking of global symmetries in the gauge/gravity duality. We will focus in the original holographic superconductor and its hydrodynamic properties. Let us remark that this review is based on the work of other authors [58].

The questions that we would like to answer along this chapter are: How does one implement spontaneous symmetry breaking in dual theory from the bulk point of view? What is its effect in the transport phenomena? What happens to the spectrum?

Let's try to give an heuristic answer to these. A key to the first question relies in the holographic dictionary. Since gauge symmetries in the bulk are mapped to global symmetries in the conformal field theory, the most natural guess is that we must spontaneously break the gauge symmetry in order to induce spontaneous symmetry breaking in the boundary. However, Eliztur's theorem shows that spontaneously breaking a gauge symmetry leads to inconsistencies (negative norm states) in the theory. Since we expect unitarity to be respected in the bulk in order to preserve it at the boundary, we should look for the "closest" version to spontaneous symmetry breaking in gauge theories. This is, of course, the Higgs mechanism. The Higgs mechanism does not break the local symmetry, but the global remanent that appears after gauge fixing. In this sense it is not surprising at all that such a mechanism is translated into a breakdown of the global symmetry in the dual theory. Moreover, this picture pushes us to the following question: If we just had to break the global part of the symmetry, why do we need a gauge symmetry at all? Since analogous questions will arise many times along this chapter, we would like to summarize our concerns in three question: What difference does it make to have a global or a gauge symmetry in the bulk? Can this shed some light on our understanding of the effect of symmetries in QFT? We will explore these issues in the following sections.
Let us now focus on the Higgs mechanism in the bulk. It turns out that this mechanism is slightly different from what we know in flat space. The first important concept to understand this is the Breitenlohner-Friedman bound. This bound fixes the minimum value for the mass squared of a scalar field. As it is widely known, this minimum is negative. So we can say that, as long as the mass squared is not too negative, the system is stable. Why is that so? Our intuition from flat space tells us that if there is no potential to compensate for this, the field will just "roll down" over the hill of a mount-like effective potential given by the mass. Such an intuition relies however on the assumption that the field can be considered constant along the space directions. However such assumption is wrong in AdS. For not too negative masses, the normalizable mode of the scalar field is still forced to decay close to the boundary. Therefore, the field cannot just grow infinitely with time; since it must vanish at the boundary the growth in the bulk induces a gradient which costs energy (the Hamiltonian is proportional to $(\nabla\phi)^2$). So what we should expect from the Higgs mechanism is an instability, i.e. a too negative effective mass, that occurs only in a certain regime of space. Let us briefly review how this works (see section 6.3 for a more thorough study) in the first and simplest example of the literature: the Holographic Superconductor. Consider the following action

$$\mathcal{L} = \left(-\frac{1}{4} F^{\mu\nu} F_{\mu\nu} - m^2 \Psi^* \Psi - (D^\mu \Psi)^* D_\mu \Psi \right) . \tag{6.1}$$

Where D^μ contains both the gravitational and gauge connections. As we will see, the gauge field allows us to tune the effective mass of the scalar field. The background metric is taken to be the Schwarzschild-AdS black brane

$$ds^2 = -f(r)dt^2 + \frac{dr^2}{f(r)} + \frac{r^2}{L^2}(dx^2 + dy^2)\,,$$
$$f(r) = \frac{r^2}{L^2} - \frac{M}{r}\,. \tag{6.2}$$

The need of a BH to implement the spontaneous symmetry breaking mechanism can be understood from two different points of view. From the gravity side, the BH induces an effective curvature close to the horizon that differs from the asymptotic region. This allows to generate different space regions. In the close horizon region the effective mass will violate the BF bound and condensation will happen. Close to the boundary however the effective mass will be above this bound and the field will not condense. From the conformal field thoery point of view it is may be easier to understand this. In order to induce the spontaneous symmetry breaking we need te comparison of two dimensionfull parameters. The chemical potential induced by the non-normalizable mode of the gauge field needs some other reference quantity such that their ration is meaningful. Both pictures connect nicely within the duality: the notions of IR and UV are needed in order to have spontaneous symmetry breaking in a theory.

With the ansatz $\Psi = \psi(r)$, $A_0 = \phi(r)$ and all other components set to zero, the e.o.m. are

$$\psi'' + \left(\frac{f'}{f} + \frac{2}{r}\right)\psi' + \frac{\phi^2}{f^2}\psi - m^2\psi = 0\,, \tag{6.3}$$
$$\phi'' + \frac{2}{r}\phi' - \frac{2\psi^2}{f}\phi = 0. \tag{6.4}$$

In (6.3) one can clearly see how the gauge field plays the role of an effective mass for the scalar field. We have two second order coupled ordinary differential equations, which means that there are four boundary conditions to be fixed. Imposing regularity at the horizon gives two constraints. In addition we want to impose the source for the scalar field to vanish, since otherwise we would explicitly induce a non-zero vev. Therefore we are left with one parameter. We choose it to be the non-normalizable mode of the gauge field, that is interpreted as the chemical potential μ of the dual theory. One now solves numerically the above equations for different values of μ. For small enough values of μ there is only one solution that can be found analytically

$$\psi = 0 \qquad\qquad \phi = \mu\left(1 - \frac{1}{r}\right)\,. \tag{6.5}$$

It corresponds to the unbroken phase, in which the vev of the scalar operator vanishes. On the other hand, a second possible solution appears for big enough values of μ. In these solutions the scalar field doesn't vanish and therefore the expectation value of the dual operator is non-zero. The plot in figure 6.1 shows how this quantity grows with $\mu \sim 1/T$ In order to determine which the energetically favored solution is one has to compute and compare the Free Energy (FE) of the system. The FE of the boundary theory can be computed from the On-Shell action of the bulk. In our concrete case it reads

$$F = -TS_{ren} = -T\left(\frac{1}{2}\mu\, n - \int_{r_H}^{\infty} dr\, \frac{r^2\psi^2\chi^2}{f}\right)\,. \tag{6.6}$$

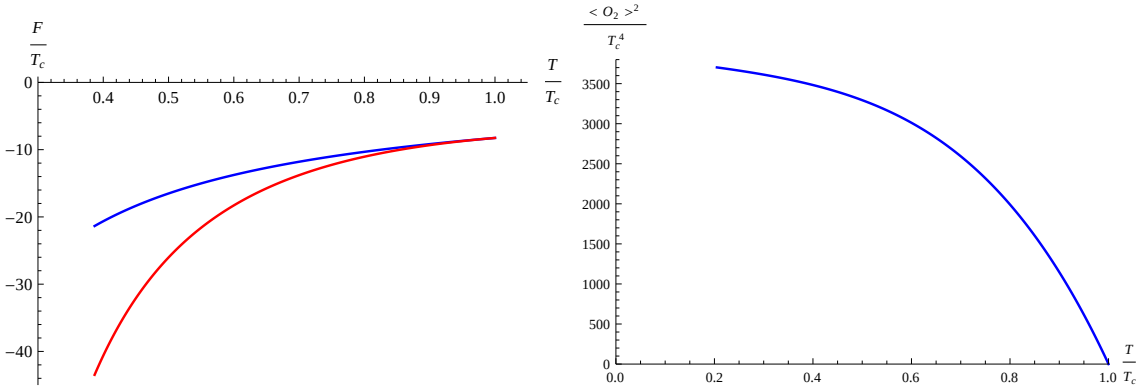

Figure 6.1: (Left) The free energy of the trivial (blue) and condensate (red) background solutions at low temperatures, $T < T_c$. (Right) Value of the condensate in the grand canonical ensemble as a function of T/T_c.

We show the result in Figure 6.3.

Indeed the global symmetry of the dual theory has been spontaneously broken by the implementation of the Higgs mechanism in the bulk. This original version of the Holographic Superconductor is contained in the extended models that we study in the following sections. Since the goal of this section was to give an introduction to the spontaneous symmetry breaking phenomenon in holography, we refer the reader to section 6.3 to see how the conductivities and the spectrum are computed as well as the interpretation for the results.

6.2 A field theoretical model with type II Goldstone boson

Motivated by the physics of Kaon condensation in the color-flavor locked phase of QCD the authors of [31, 61] studied QCD at a nonzero chemical potential for strangeness. It was shown that at a critical value of the chemical potential equal to the Kaon mass, Kaon condensation occurs through a continuous phase transition. Moreover, a Goldstone boson with the non-relativistic dispersion relation $\omega \sim p^2$ appears in the Kaon condensed phase. To illustrate this fact, they considered the following (Euclidean) toy model:

$$\mathcal{L} = (\partial_0 + \mu)\phi^\dagger(\partial_0 - \mu)\phi + \partial_i\phi^\dagger\partial_i\phi + M^2\phi^\dagger\phi + \lambda(\phi^\dagger\phi)^2\,, \tag{6.7}$$

where ϕ is a complex scalar doublet,

$$\phi = \begin{pmatrix} \phi_1 \\ \phi_2 \end{pmatrix}. \tag{6.8}$$

As long as $\mu < M$ the masses of the four excitations in the model are the positive roots in ω of

$$(\omega \pm \mu)^2 = M^2\,. \tag{6.9}$$

All are doubly degenerate. It is straightforward to check that at $\mu = M$ the global $U(2)$ symmetry gets broken and the new vacuum can be chosen to be:

$$\phi = \frac{1}{\sqrt{2}}\begin{pmatrix} 0 \\ v \end{pmatrix}, \qquad \text{with} \quad v^2 = \frac{\mu^2 - M^2}{\lambda}\,. \tag{6.10}$$

Studying the fluctuations of the doublet ϕ around this background one finds two massless and two massive modes with the following dispersion relations:

$$\omega_1^2 = \frac{\mu^2 - M^2}{3\mu^2 - M^2} p^2 + O(p^4) \,, \tag{6.11}$$

$$\omega_2^2 = 6\mu^2 - 2M^2 + O(p^2) \,, \tag{6.12}$$

$$\omega_3^2 = p^2 - 2\mu\omega_3 \,, \tag{6.13}$$

$$\omega_4^2 = p^2 + 2\mu\omega_4 \,. \tag{6.14}$$

If we concentrate on the positive roots we see that ω_1 is a normal, linear Goldstone mode. The positive root of equation (6.13) is

$$\omega_3 = \frac{p^2}{2\mu} + O(p^4) \,. \tag{6.15}$$

This is the type II Goldstone mode. It has formally a non-relativistic dispersion relation. Since the underlying theory has however Lorentz invariance there is of course also a negative energy mode with quadratic dispersion. This arises as the negative root of ω_4. Finally ω_2 and ω_4 are gapped modes with

$$\omega_4 = 2\mu + O(p^2) \,. \tag{6.16}$$

Since the symmetry breaking pattern is $U(2) \to U(1)$ there are three broken generators but only two massless Goldstone modes in the spectrum. This model fulfills all the counting theorems noted in the introduction. In particular the Chadha-Nielsen rule in section 2.2 is exactly saturated. The role of ω_4 is special. It is the mode that pairs up with the type II Goldstone mode in the dispersion relations (6.13) and (6.14). It has been argued that this mode is a universal feature and that its energy at zero momentum is exact and protected against quantum corrections [29, 64, 65]. The spectrum obtained from this model is summed up in Figure 6.2. In our holographic models we will look for this special gapped partner mode of the type II Goldstone mode. It will turn out that the gauged and ungauged models differ significantly here: only the mode in the gauged model shows the characteristic linear dependence on the chemical potential.

This simple Lagrangian model serves as our motivation and guideline to construct a holographic model featuring type II Goldstone modes. In fact we can use the same kind of matter Lagrangian in a holographic setup. According to the usual holographic dictionary a local bulk symmetry corresponds to a global symmetry in the boundary conformal field theory. We would therefore most naturally be led to a model in which we gauge the global $U(2)$ symmetry of (6.7) and put it into an AdS Schwarzschild background. In order to trigger spontaneous symmetry breaking we introduce a chemical potential via a boundary value for the temporal component of the overall, Abelian $U(1)$ gauge field. This is then our *gauged model*.

Alternatively we might ask what are the minimal ingredients necessary to trigger spontaneous symmetry breaking. The chemical potential resides entirely in the overall $U(1)$ factor. The other three $SU(2)$ gauge fields are not needed to achieve symmetry breaking. Therefore we can choose as a sort of minimal setup a model in which the $SU(2)$ symmetry stays global in the bulk of AdS. As already mentioned in the introduction this is a somewhat unusual realization of the symmetry from the boundary conformal field

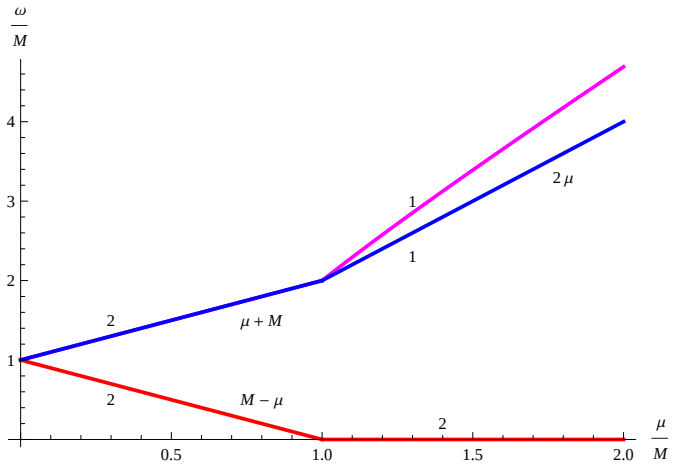

Figure 6.2: The spectrum of the field theoretical model. Below the critical value $\mu = M$ there are four massive modes. The masses are $M - \mu$ and $M + \mu$, the numbers indicate that they are doubly degenerate. In the broken phase $\mu > M$ there are two Goldstone modes with exactly zero mass and two gapped modes. The special gapped mode has mass 2μ.

theory point of view. There are no conserved currents associated to this $SU(2)$ symmetry, nevertheless all states and operators fall naturally into representations of this symmetry group since it is a global symmetry of the bulk and it is also not broken by any of the boundary conditions. This setup constitutes our *ungauged model* and we will study it in detail in the next section.

Let us note here one more technical detail: the field theoretic model of this section is most naturally viewed as living in four space time dimensions. In the following our holographic models will be dual to field theories living in three space time dimensions in order to stay as close as possible to the well-studied holographic $U(1)$ s-wave superfluid of [59, 63]. This is however of no relevance to the essential features of the models, i.e. the existence and the nature of the hydrodynamic and Goldstone modes.

6.3 SSB in Holography with TypeII NG-Bosons: The ungauged model

We will now study the holographic model where the condensation of a charged scalar breaks a global $SU(2)$ symmetry in the bulk. We shall look at the spectrum of quasinormal modes on both sides of the phase transition and study their dispersion relations. Since the simple $U(1)$ s-wave holographic superfluid constitutes a subsector of this as well as of the gauged model we will also use the opportunity to briefly review the most salient features of its QNM spectrum.

The minimal holographic model containing a type II Goldstone boson consists of a scalar doublet of $SU(2)$ charged under a $U(1)$ gauge field. The Lagrangian is given by

$$\mathcal{L} = \left(-\frac{1}{4} F^{\mu\nu} F_{\mu\nu} - m^2 \Psi^\dagger \Psi - (D^\mu \Psi)^\dagger D_\mu \Psi \right) , \tag{6.17}$$

where

$$\Psi = \begin{pmatrix} \lambda \\ \psi \end{pmatrix} , \qquad D_\mu = \partial_\mu - i A_\mu , \tag{6.18}$$

and A_μ is the Abelian gauge field. The mass of the scalar field is chosen to be $m^2 = -2/L^2$. This is basically the same as the model in [59] except that we have added a second scalar field λ with the same mass. Because of the degeneracy in the mass the model possesses in addition to the bulk-local $U(1)$ symmetry a bulk-global $SU(2)$ symmetry. Note that the global $SU(2)$ symmetry is a priori not enough to set the field $\lambda(r) = 0$. But we are interested in un-sourced static solutions for the scalar fields, i.e. we assume that the leading non-normalizable mode is not switched on. The solution space is then a two dimensional complex vector space spanned by the vevs of the operators dual to the scalar fields. On this parameter space we can act with the global $SU(2)$ symmetry to set the operator corresponding to the field λ equal to zero. Since now the non-normalizable and the normalizable mode of λ are set to zero it follows that $\lambda(r) = 0$.

We will be working in the probe limit, in which the coupling of the gauge field is very large and the backreaction of the matter fields onto the metric can be neglected. The background metric is then taken to be the Schwarzschild-AdS black brane

$$\begin{aligned} ds^2 = -f(r) dt^2 + \frac{dr^2}{f(r)} + \frac{r^2}{L^2}(dx^2 + dy^2) , \\ f(r) = \frac{r^2}{L^2} - \frac{M}{r} . \end{aligned} \tag{6.19}$$

The horizon of the black hole is located at $r_H = M^{1/3} L^{2/3}$ and its Hawking temperature is $T = \frac{3 r_H}{4\pi L^2}$. In the following we use dimensionless coordinates

$$(r,\, t,\, x,\, y) \to \left(r_H\, \rho,\, \frac{L^2}{r_H} \bar{t},\, \frac{L^2}{r_H} \bar{x},\, \frac{L^2}{r_H} \bar{y} \right) . \tag{6.20}$$

These rescalings allow us to set $M = r_H = 1$ in the dimensionless system. In order to switch on a finite chemical potential in the boundary theory, the bulk Maxwell field

$$A = \chi(\rho) d\bar{t} , \tag{6.21}$$

must take a non-zero value at the boundary.

The equations of motion for the background fields are

$$\chi'' + \frac{2}{\rho}\chi' - \frac{2\psi^2}{f}\chi = 0\,, \tag{6.22}$$

$$\psi'' + \left(\frac{f'}{f} + \frac{2}{\rho}\right)\psi' + \frac{\chi^2}{f^2}\psi - \frac{m^2}{f}\psi = 0\,. \tag{6.23}$$

Notice that the system above is precisely the original $U(1)$ holographic superconductor first studied in [59]. To ensure finiteness of the norm of the current at the horizon, we have to demand the scalar field to be regular whereas the gauge field has to vanish $\chi(\rho = 1) = 0$. With these boundary conditions, the asymptotic behavior of the fields at the conformal boundary is

$$\chi = \bar{\mu} - \frac{\bar{n}}{\rho} + O\left(\frac{1}{\rho^2}\right)\,, \tag{6.24}$$

$$\psi = \frac{\psi_1}{\rho} + \frac{\psi_2}{\rho^2} + O\left(\frac{1}{\rho^3}\right)\,. \tag{6.25}$$

For the chosen value of the scalar mass, both terms in the scalar asymptotics correspond to normalizable modes [66]. Considering one or the other as the vacuum expectation value of a dual boundary operator leads to two different theories. In what follows we will consider only the case in which ψ_1 is interpreted as the coupling and ψ_2 as the vev of a mass dimension two operator.

The dimensionless parameters are related with the physical quantities by

$$\bar{\mu} = \frac{3}{4\pi T}\,\mu\,, \tag{6.26}$$

$$\bar{n} = \frac{9}{16\pi^2 T^2 L^2}\,n\,, \tag{6.27}$$

$$\psi_1 = \frac{3}{4\pi T L^2}\,J_{\mathcal{O}}\,, \tag{6.28}$$

$$\psi_2 = \frac{9}{16\pi^2 T^2 L^4}\,\langle\mathcal{O}\rangle\,, \tag{6.29}$$

where μ, n and $J_{\mathcal{O}}$, $\langle\mathcal{O}\rangle$ are the chemical potential, charge density and source and expectation value of an operator $\mathcal{O}$ of dimension 2, respectively. From now on we set $L = 1$. In the following we will work in the grand canonical ensemble. In practice we vary the dimensionless parameter $\bar{\mu}$. Because of the underlying conformal symmetry this can then be thought of as either fixing the chemical potential μ and varying the temperature T or fixing the temperature and varying the chemical potential. We define the temperature by $T/T_c = \bar{\mu}_c/\bar{\mu}$ and fix $\mu = 1$.

Spontaneous symmetry breaking is driven by low temperature or high chemical potential. It triggers a non trivial expectation value for the scalar field without switching on any source $J_{\mathcal{O}}$. For small $\bar{\mu}$ the scalar field is trivial and the gauge equation is solved by $\chi = \bar{\mu}(1 - 1/\rho)$ and $\psi = 0$. The system is then in the symmetric phase. However, by decreasing the temperature the system becomes unstable towards condensation of the scalar [58, 59]. In [63] it was shown that at the critical temperature indeed the lowest quasinormal mode of the scalar field becomes unstable, i. e. it crosses over to the upper half plane.

The free energy density of the system is given by the on-shell renormalized action,

$$F = -TS_{ren} = -T\left(\frac{1}{2}\mu\, n - \int_{r_H}^{\infty} dr\, \frac{r^2\psi^2\chi^2}{f}\right) . \tag{6.30}$$

The second term vanishes in the absence of a condensate and it works against the phase transition if it is present. In Figure 6.3 the free energies for the symmetric and broken phase are compared. It is clear that for $T < T_c$ the condensate solution is always preferred and therefore the system undergoes a second order phase transition to the superconducting phase. Note that the presence of the second scalar plays no role for the phase structure. It simply vanishes in the broken and unbroken phase $\lambda = 0$.

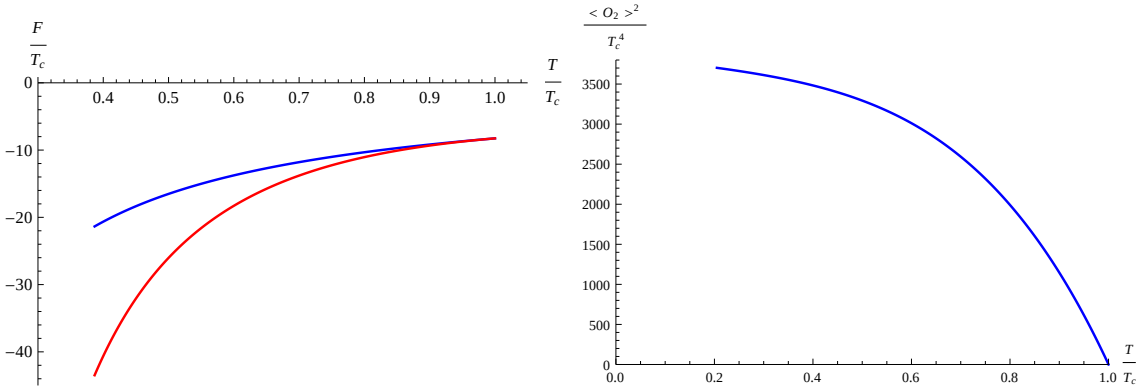

Figure 6.3: (Left) The free energy of the trivial (blue) and condensate (red) background solutions at low temperatures, $T < T_c$. (Right) Value of the condensate in the grand canonical ensemble as a function of T/T_c.

In order to extract the quasinormal mode spectrum, we switch on fluctuations of the background fields

$$\Psi^{\mathrm{T}} = (\eta(\rho,t,x),\, \psi(\rho) + \sigma(\rho,t,x)) , \tag{6.31}$$

$$A = (\chi(\rho) + a_t(\rho,t,x))\, dt + a_x(\rho,t,x)dx . \tag{6.32}$$

We do not include transverse fluctuations because they decouple from the interesting physical features of the model at hand.

In the normal phase, i.e. expanding around $\psi(\rho) = 0$, the system reduces to the $U(1)$ holographic superconductor studied in [63] with two copies of the scalar fluctuations,

$$fs'' + s'\left(f' + \frac{2f}{\rho}\right) + \left(\frac{(\chi+\omega)^2}{f} - \frac{k^2}{\rho^2} - m^2\right) s = 0 , \tag{6.33}$$

$$fa_t'' + \frac{2f}{\rho}a_t' - \frac{k^2}{\rho^2}a_t - \frac{\omega k}{\rho^2}a_x = 0 , \tag{6.34}$$

$$fa_x'' + f'a_x' + \frac{\omega^2}{f}a_x + \frac{\omega k}{f}a_t = 0 , \tag{6.35}$$

$$\frac{i\omega}{f}a_t' + \frac{ik}{\rho^2}a_x' = 0 , \tag{6.36}$$

where s stands for both η and σ fluctuations. The equation for the complex conjugate scalar $\bar{s}$ can be obtained by changing the sign of the potential χ in (6.33). The frequency

and momentum are related to the physical ones by

$$\omega = \frac{3}{4\pi T}\omega_{ph}\,, \tag{6.37}$$

$$k = \frac{3}{4\pi T}k_{ph}\,. \tag{6.38}$$

The scalar and gauge fluctuations completely decouple in the symmetric phase. This is a consequence of working in the probe limit. The quasinormal mode spectrum of the $U(1)$ field in the normal phase is just that of an electromagnetic field on an AdS-Sch background. The longitudinal fluctuations contain one hydrodynamic mode, $\omega = -iDk^2$, reflecting the diffusive behavior of normal fluids. In physical units $D = 3/(4\pi T)$. Due to the lack of an energy-momentum tensor for the dual field theory in the probe limit, the diffusion pole is the only hydrodynamic mode in the unbroken phase.

There are two copies of the scalar fluctuations. The quasinormal modes of η and σ move towards the origin when decreasing the temperature, whereas the modes of $\bar{\eta}$ and $\bar{\sigma}$ have larger masses and widths the smaller the temperature. As we approach the critical temperature $T = T_c$, the lowest quasinormal modes of η and of σ become massless, triggering the phase transition: the scalar field acquires a non trivial vev in order to avoid its fluctuations to become tachyonic. By symmetry we can choose the condensate to reside completely in the ψ field. The fluctuations σ couple then to the gauge field fluctuations just as in [63]. Therefore the QNM spectrum in this sector contains a Goldstone mode with linear dispersion relation $\omega = \pm v_s k + O(k^2)$. This is the usual type I Goldstone boson associated with the breaking of the gauge $U(1)$ symmetry. As shown in [63] it can be interpreted as the sound mode of the dual superfluid in the broken phase. What happens then to the QNMs in the fluctuations of the second scalar η? At the critical temperature there is also an ungapped mode present since its QNM spectrum is simply another copy of the scalar sector. Since there are no operators generating the $SU(2)$ symmetry in the dual field theory standard arguments about the appearance of Goldstone modes do a priori not apply. Three logical possibilities arise then: the mode could become unstable for $T < T_c$, it could become gapped again or it stays ungapped, playing the role of an unexpected Goldstone boson for the broken bulk-global $SU(2)$ symmetry. Shortly we will see that the last possibility is realized and that the massless mode of η will indeed correspond to a type II Goldstone boson with quadratic dispersion relation, $\omega \propto k^2$.

In the broken phase, the equations of motion read

$$0 = f\eta'' + \eta'\left(f' + \frac{2f}{\rho}\right) + \left(\frac{(\chi+\omega)^2}{f} - \frac{k^2}{\rho^2} - m^2\right)\eta\,, \tag{6.39}$$

$$0 = f\delta'' + \delta'\left(f' + \frac{2f}{\rho}\right) + \left(\frac{\chi^2}{f} + \frac{\omega^2}{f} - \frac{k^2}{\rho^2} - m^2\right)\delta - \frac{2i\omega\chi}{f}\zeta - i\psi\left(\frac{\omega}{f}a_t + \frac{k}{\rho^2}a_x\right)\,, \tag{6.40}$$

$$0 = f\zeta'' + \zeta'\left(f' + \frac{2f}{r}\right) + \left(\frac{\chi^2}{f} + \frac{\omega^2}{f} - \frac{k^2L^2}{r^2} - m^2\right)\zeta + \frac{2i\omega\chi}{f}\delta + \frac{2\chi\psi}{f}a_t\,, \tag{6.41}$$

$$0 = fa_t'' + \frac{2f}{\rho}a_t' - \left(\frac{k^2}{\rho^2} + 2\psi^2\right)a_t - \frac{\omega k}{\rho^2}a_x - 2i\omega\psi\delta - 4\chi\psi\zeta\,, \tag{6.42}$$

$$0 = fa_x'' + f'a_x' + \left(\frac{\omega^2}{f} - 2\psi\right)a_x + \frac{\omega k}{f}a_t + 2ik\psi\delta\,, \tag{6.43}$$

$$0 = \frac{i\omega}{f}a_t' + \frac{ik}{\rho^2}a_x' + 2\psi'\delta - 2\psi\delta'\,, \tag{6.44}$$

where we have divided $\sigma = \zeta + i\delta$ into real and imaginary part. The system (6.40)-(6.44) is again the one studied in [63]. This sector, that also appears in the gauged model that will be presented afterwards, decouples from the additional scalar fluctuation η. Notice that even if (6.39) is formally the same as in the normal phase, the background χ is different leading to non trivial features in the η sector such as the presence of a massless excitation.

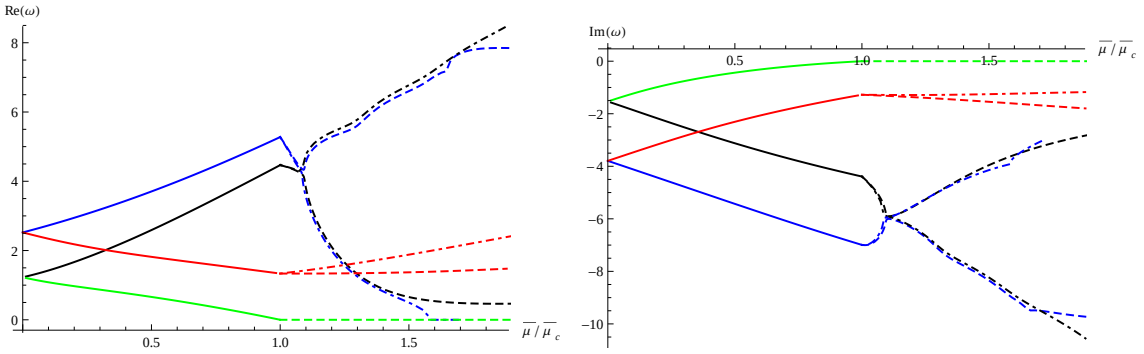

Figure 6.4: Real (left) and imaginary (right) parts of the lowest scalar QNMs as a function of the chemical potential. Solid lines correspond to the unbroken phase. For the broken phase dashed lines stand for modes of the additional scalar while dotdashed lines represent the modes common to the $U(1)$ holographic superconductor.

Figure 6.4 shows the spectrum of quasinormal excitations of the scalar doublet. In the normal phase we have two degenerate copies of the spectrum that partially split after the phase transition. It is clear that the two lowest excitations become massless at the critical chemical potential and then remain massless in the superconducting phase. They can be identified with the two Goldstone bosons at the phase transition. The rest of the excitations remain gapped in the broken phase. Notice that the first $\bar{\eta}$ excitation (dashed black line in figure 6.4) does not follow the expected universal behavior in the broken phase, i.e. it is not linear in μ. This mode is the equivalent of the special gapped mode ω_4 in the field theoretical model of section 6.2. However, it has already been mentioned that the *ungauged model* does not satisfy all the theorems about symmetry breaking and therefore deviations from the universal behavior should not be surprising. The behavior of the gapped modes is actually similar to that of the $U(1)$ model modes. In the unbroken phase we can distinguish the modes that come from the s-type of fluctuations from the ones that come from the complex conjugate $\bar{s}$ fluctuations. The former become lighter whereas the latter become heavier[2]. In the broken phase it is more useful to use real and imaginary parts, at least for the scalar that mixes with the gauge fields fluctuations, i.e. the lower component of the scalar in our conventions. So we can not a priori talk of s and $\bar{s}$ type fluctuations. We still can study to which modes the s and $\bar{s}$ type modes connect to in the broken phase. Here we see an interesting pattern: the s type modes split in the broken phase whereas the $\bar{s}$ type modes stay almost degenerate close to the phase transition (at least at zero momentum). This is surprising given the fact that the fluctuations correspond to two completely different systems, one coming from a single differential equation whereas the others come from a complicated system of coupled equations. However, for small temperatures they split and actually the real part of the lowest one for the $U(1)$ sector goes to zero at a finite temperature. For temperatures below $T \approx 0.63\, T_c$ it becomes a

[2]This behavior is reversed if we had taken the chemical potential to be negative.

purely imaginary mode.

Sound mode: There are two massless modes in the broken phase. The first one is the type I Goldstone boson appearing because of the spontaneous breaking of the $U(1)$ gauge symmetry. In [63], it was shown that this mode corresponds to the sound mode of the dual superfluid and that in the hydrodynamic limit it has a linear dispersion relation

$$\omega_I = \pm \left(v_s\, k + \bar{b}\, k^2\right) - i\Gamma_s\, k^2\,, \tag{6.45}$$

where v_s is the speed of sound and Γ_s is its attenuation. It turns out that the quadratic part of the dispersion relation also has a real component. This component is very small and subleading compared to the linear term that determines the speed of sound. In [63] this real quadratic part has not been studied.

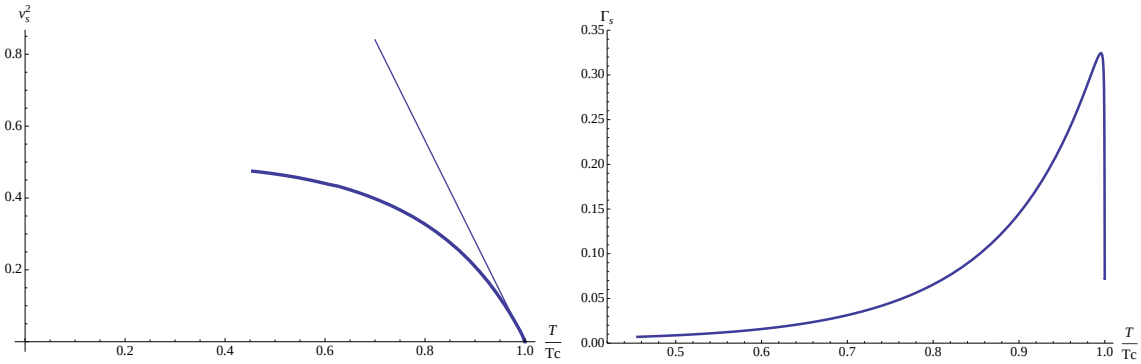

Figure 6.5: Speed of sound and damping for the sound mode. The speed of sound goes to zero at the critical temperature. The damping constant first rises quickly and then falls off again. Precisely at the critical temperature its value is such that the sound modes connect continuously to the scalar modes that become massless there. The peak in the damping constant sits close to the critical temperature and was not resolved in [63].

For very small temperatures the velocity approaches its conformal value $v_s^2 = 1/2$ while the width goes to zero, see figure 6.5. Close to the phase transition, the speed of sound has a mean field behavior as a function of temperature

$$v_s^2 \approx 2.8 \left(1 - \frac{T}{T_c}\right)\,. \tag{6.46}$$

As expected, at $T = T_c$ the speed of sound vanishes. This can be traced back to the fact that at the phase transition the total mass $m_*^2 = M^2 - \mu^2$ fulfills $m_*^2 = v^2 = 0$, as expected, and hence the complex scalar field, charged under a $U(1)$ symmetry, becomes massless.

Indeed, one can write down the effective action, analogous to (6.7), for a complex scalar field with mass M, in the presence of a chemical potential for a $U(1)$ symmetry that is spontaneously broken. The excitations on top of the $U(1)$-breaking background have a dispersion relation equal to (6.11)-(6.12), being (6.11) the type I Goldstone boson. It is a general feature of these linear sigma models that the coefficient in front of the linear term in the momentum depends on m_*^2, as can be explicitly checked for the case at hand (see (6.11)). Therefore, at the phase transition the leading term in the dispersion relation is of

$O(k^2)$; this effect can be seen very clearly with numerical methods, as shown in Figure 6.6. Since the quasinormal mode spectrum has to vary continuously through the second order phase transition the real and complex coefficients of the k^2 term have to coincide at $T = T_c$ with the ones obtained from the massless scalars in the unbroken phase. Numerically we find $\bar{b}(T_c) = 0.22$ and $\Gamma_s(T_c) = 0.071$.

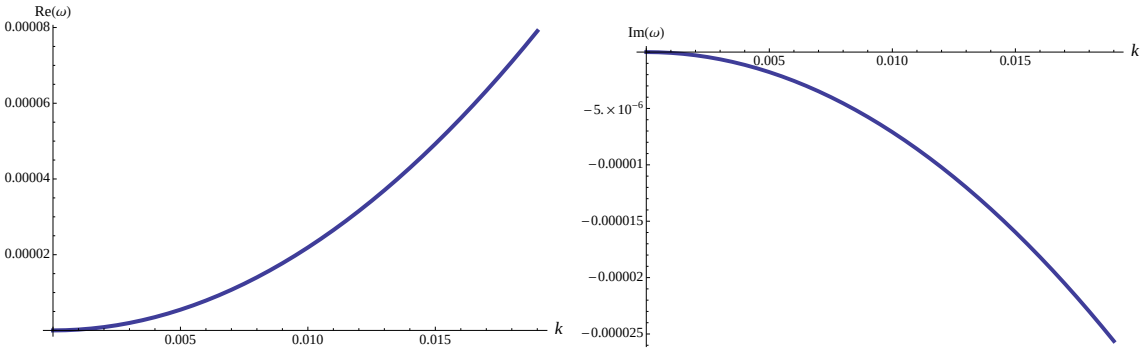

Figure 6.6: Dispersion relations of $\mathrm{Re}\,\omega$ (left) and $\mathrm{Im}\,\omega$ (right) at $T = T_c$ for the type I Goldstone boson in the system studied by [63]. The behavior $\mathrm{Re}\,\omega \sim k$ becomes quadratic right at this temperature: $\mathrm{Re}\,\omega = \bar{b}k^2$. The coefficient is $\bar{b} = 0.22$, which in turn matches the value that one finds if approaches T_c from above (i.e. from the unbroken phase).

Pseudo diffusion mode: In the unbroken phase our model has only one hydrodynamic mode, the diffusion mode $\omega = -iDk^2 + O(k^4)$ with $D = 3/(4\pi T)$ in physical units. The shear and normal sound modes have their origin in the metric fluctuations and therefore are absent in the decoupling limit we are studying. The phase transition to the broken phase is second order. For the spectrum of quasinormal modes this implies that the modes of the broken and unbroken phase must connect continuously through the phase transition. In the case of the diffusion mode there must therefore exist a quasinormal mode with purely imaginary frequency. Hydrodynamics implies however that the only ungapped modes are the sound modes corresponding to the type I Goldstone mode. Not too far from the phase transition, i.e. for $T \lesssim T_c$ the diffusion mode of the broken phase must develop into a mode with dispersion relation

$$\omega = -i\gamma(T) - iD(T)k^2 + O(k^4)\,, \tag{6.47}$$

as shown in Figure 6.7.

We might say that the diffusion mode develops a gap in the broken phase and becomes what has been called a *pseudo diffusion mode* in [63]. Precisely at zero momentum $k = 0$ this gapped pseudo diffusion mode explains the observation made in [67] on the late time response of holographic superconductors. For temperatures $T \lesssim T_c$ the pseudo diffusion mode is the mode that lies closest to the real axis and therefore it dominates the long time response to any perturbation, such as the quenches studied in [67]. It follows that the order parameter shows a purely exponential decay since this mode does not have a real frequency. The existence of that mode can ultimately be traced back to the universality of the diffusion mode in the unbroken phase. We expect therefore the pseudo diffusion mode to be a universal feature of a wide class of superfluids (not necessarily holographic ones).

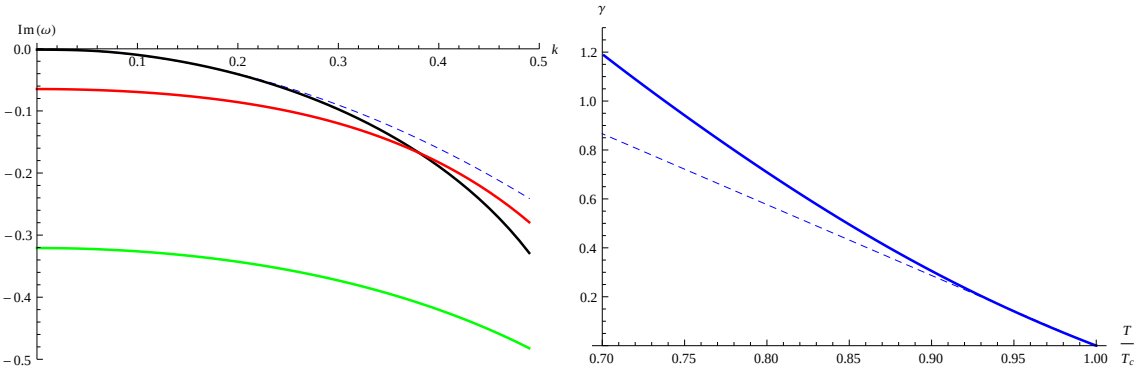

Figure 6.7: (Left) Dispersion relation of the gapped pseudo diffusion mode in the broken phase for three different temperatures. The gap widens as the temperature is lowered. (Right) Gap γ as a function of the reduced temperature T/T_c. As one approaches the critical temperature from below the gap vanishes linearly.

The gap γ grows as the temperature decreases. On the other hand there are quasinormal modes (connecting to the QNMs in the scalar sector of the unbroken phase) whose imaginary part is only weakly dependent on the temperature. At a certain crossover temperature T_* the gap of the pseudo diffusion mode is bigger than the imaginary part of these modes, as shown in Figure 6.8. Then the response pattern changes from a purely exponential decay to an exponentially damped oscillation. Numerically we find that the crossover temperature is $T_* = 0.69\,T_c$.[3] Such crossover changes in the long term response appear frequently in the details of the quasinormal mode spectrum of holographic field theories, [57, 68, 69]. In fact this purely exponential decay applies not only to the order parameter but to all operators that correspond to the fields participating in the fluctuation system (6.40)-(6.44), e.g. charge density or x-component of the current.

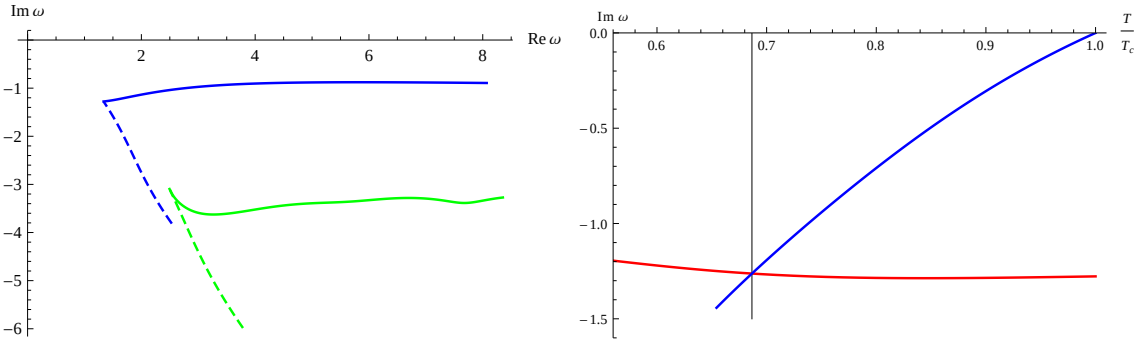

Figure 6.8: (Left) Continuation of the second and third scalar QNM into the broken phase. The real part grows as the temperature is lowered whereas the imaginary part shows very little dependence on T. (Right) The gap γ (blue line) and the imaginary part of the lowest (scalar) mode fluctuation (red line) in the broken phase are shown as function of T/T_c. At $T_* \approx 0.69\,T_c$ the imaginary parts cross. For lower temperatures the late time response is not dominated anymore by the pseudo diffusion mode and consequently is in form of a exponentially decaying oscillation.

[3] This is lower than in the model of [67]. The difference is presumably due to the fact that we work in the decoupling limit.

For finite momentum the response pattern is expected to be different however. Now one also has to take into account the sound mode. While precisely at zero momentum the sound mode, i.e. the Goldstone mode, degenerates to a constant phase change of the condensate at small but non-zero momentum the long time response should be dominated by the complex frequencies (6.45). If one looks however only to the response in the gauge invariant order parameter $|\mathcal{O}|$ the Goldstone modes, being local phase rotations of the order parameter, are projected out.

Type II Goldstone mode: The second massless mode is the Goldstone boson associated with the breaking of the bulk-global $SU(2)$ symmetry. It can be fit to a quadratic dispersion relation of the form

$$\omega_{II} = \pm b\, k^2 - ic\, k^2 + O(k^4)\,, \tag{6.48}$$

in the long wavelength limit. Therefore it has the characteristic of a type II Goldstone mode. In Figure 6.9 the dispersion relation for the η massless mode is shown for various temperatures as well as its fit to the hydrodynamic form. It is clear that there is a good agreement in the regime of validity of the low energy limit.

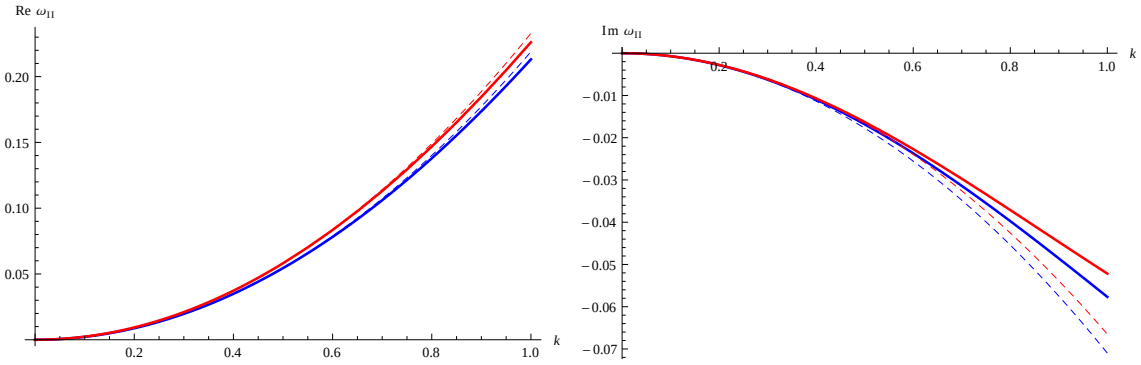

Figure 6.9: Real (left) and imaginary (right) parts of the type II Goldstone mode as a function of the momentum for $T/T_c = 0.9998$ (blue) and $T/T_c = 0.704$ (red) . The solid lines correspond to the numerical result while the dashed lines are the quadratic fit to a dispersion relation $\omega_{II} = b\, k^2 - ic\, k^2$.

The coefficients in the hydrodynamic dispersion relation (6.48) as a function of the temperature are shown in Figure 6.10. Close to the phase transition they have a linear dependence in the reduced temperature

$$\begin{aligned} b(T) &= 0.22 + 0.049\left(1 - \frac{T}{T_c}\right)\,, \\ c(T) &= 0.071 - 0.0014\left(1 - \frac{T}{T_c}\right) \quad \text{near } T_c\,. \end{aligned} \tag{6.49}$$

Notice that at the phase transition the sound mode and the type II Goldstone must behave in the same way due to continuity of the modes through the phase transition and the fact that they are degenerate in the normal phase. In fact, at the transition $b = \bar{b} = 0.22$ and $c = \Gamma_s = 0.071$, values that of course coincide with those of the lowest scalar mode in the normal phase. On the other hand, it is interesting to notice that in the broken

phase the behavior of the coefficients of the type II Goldstone is completely different from that of the coefficients of the sound of the superfluid. Unlike the sound velocity, that vanishes at the phase transition, the coefficient b of the type II Goldstone mode takes a finite value at the critical temperature. This result of course persists for the *gauged model*. The attenuation on the other hand, as it happens for the $U(1)$ sector, has a finite value at the phase transition and then decreases with temperature, reflecting the fact that the fluid is more ideal the lower the temperature.

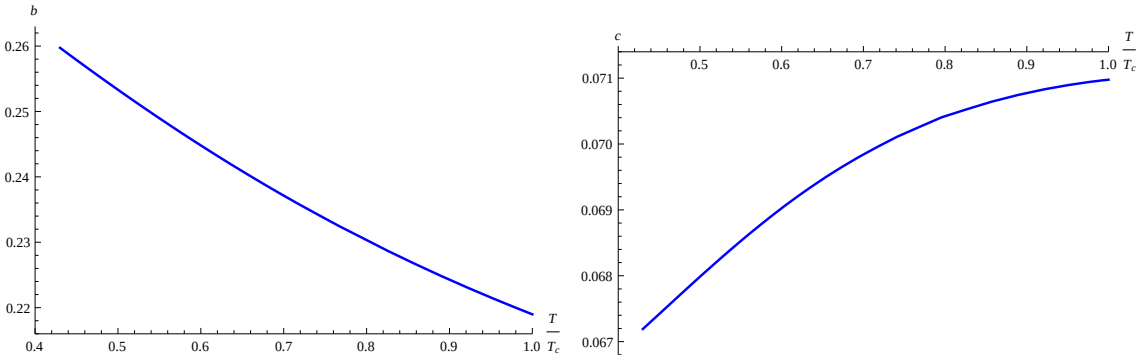

Figure 6.10: Coefficients of the type II Goldstone mode dispersion relation $\omega_{II} = b\,k^2 - ic\,k^2$, as a function of the temperature. Dependence with temperature is very mild.

6.4 SSB in Holography with TypeII NG-Bosons: The gauged model

Let us now discuss the fully gauged model. Consider the following Lagrangian for a complex scalar field living in the fundamental representation of a $U(2)$ gauge symmetry of the bulk,

$$S = \int \sqrt{-g}\mathcal{L} = \int d^4x\sqrt{-g}\left(-\frac{1}{4}F^{\mu\nu c}F^c_{\mu\nu} - m^2\Psi^\dagger\Psi - (D^\mu\Psi)^\dagger D_\mu\Psi\right), \tag{6.50}$$

where

$$\Psi = \begin{pmatrix}\lambda\\ \psi\end{pmatrix}, \qquad A_\mu = A^c_\mu T_c\,, \qquad D_\mu = \partial_\mu - iA_\mu\,, \tag{6.51}$$

and $c = 0,1,2,3$ is the color index. The field Ψ plays the role of the condensate. The expectation value of its dual operator thus triggers the spontaneous breaking of the $U(2)$ global symmetry of the boundary theory. For simplicity, we set $\lambda = 0$ in the background. T_c are the generators of $U(2)$:

$$\begin{aligned} T_0 = \frac{1}{2}\mathbb{I}\,, \qquad T_i = \frac{1}{2}\sigma_i\,,\\ \{T_i, T_j\} = \frac{1}{2}\delta_{ij}\mathbb{I}\,, \qquad \{T_0, T_i\} = \frac{1}{2}\sigma_i\,. \end{aligned} \tag{6.52}$$

Notice that we are again working in the probe limit, so the background metric is taken to be the Schwarzschild-AdS black brane of (6.19). On the other hand, the gauge field is now

$$A^{(0)}_0 \equiv \Phi(r)\,, \quad A^{(3)}_0 \equiv \Theta(r)\,. \tag{6.53}$$

The rest of the components of the gauge field being zero. As in the previous section, we will use dimensionless coordinates defined by the rescaling given in (6.20).

The equations of motion for our ansatz are

$$\psi'' + \left(\frac{f'}{f} + \frac{2}{\rho}\right)\psi' + \frac{(\Phi-\Theta)^2}{4f^2}\psi - \frac{m^2}{f}\psi = 0\,, \tag{6.54}$$

$$\Phi'' + \frac{2}{\rho}\Phi' - \frac{\psi^2}{2f}(\Phi - \Theta) = 0\,, \tag{6.55}$$

$$\Theta'' + \frac{2}{\rho}\Theta' + \frac{\psi^2}{2f}(\Phi - \Theta) = 0\,. \tag{6.56}$$

Notice that from (8.4) it follows that we can not simply switch on Φ without also allowing for a non-trivial Θ. We are of course only interested in switching on a chemical potential in the overall $U(1)$, and therefore we will impose $\Theta(\rho \to \infty) = 0$ and allow for a finite boundary value of Φ.

The coupled system of equations above can be simplified by defining $\chi \equiv \frac{1}{2}(\Phi - \Theta)$ and $\xi \equiv \frac{1}{2}(\Phi + \Theta)$. Using (8.3) and (8.4), we see that the resulting equations for these

fields are[4]

$$\Psi'' + \left(\frac{f'}{f} + \frac{2}{\rho}\right)\Psi' + \frac{\chi^2}{f^2}\Psi - \frac{m^2}{f}\Psi = 0\,, \tag{6.57}$$

$$\chi'' + \frac{2}{\rho}\chi' - \frac{2\Psi^2}{f}\chi = 0\,, \tag{6.58}$$

$$\xi'' + \frac{2}{\rho}\xi' = 0\,, \tag{6.59}$$

where we have redefined $\psi \to \sqrt{2}\Psi$. As usual we choose the boundary conditions $\chi(\rho = 1) = 0$, $\xi(\rho = 1) = 0$ along with regularity of Ψ. Having a dual field theory with only one finite chemical potential switched on, implies that χ and ξ must take the same non trivial value at the boundary in order to ensure that Θ vanishes asymptotically. Notice that ξ decouples completely. The remaining system (6.57)-(8.5) is again the background found for the widely studied s-wave $U(1)$ holographic superconductor. Therefore, the background of the $U(2)$ gauge model contains the Abelian superconductor plus a decoupled conserved $U(1)$ sector.

The field χ lies in the direction of one of the broken generators, which is the linear combination $\frac{1}{2}(T_3 - T_0)$, whereas ξ lies in the direction of the preserved $U(1)$ given by $\frac{1}{2}(T_3 + T_0)$.

The asymptotic expansion of the fields near the conformal boundary reads

$$\chi = \bar{\mu}_\chi - \frac{\bar{n}_\chi}{\rho} + O\left(\frac{1}{\rho^2}\right)\,, \tag{6.60}$$

$$\xi = \bar{\mu}_\xi - \frac{\bar{n}_\xi}{\rho} + O\left(\frac{1}{\rho^2}\right)\,, \tag{6.61}$$

$$\Psi = \frac{\psi_1}{\rho} + \frac{\psi_2}{\rho^2} + O\left(\frac{1}{\rho^3}\right)\,. \tag{6.62}$$

The map of the various coefficients in the previous equations to the boundary conditions is $\bar{\mu}_\chi = \bar{\mu}_\xi = \bar{\mu}$. We will again focus in the $\mathcal{O}_2$ theory exclusively, henceforth we will demand $\psi_1 = 0$.

Equations (6.57)-(8.5) allow for solutions with a non-vanishing condensate, and therefore $\frac{1}{2}(T_3 - T_0)$ will be spontaneously broken. This solution must be found numerically, since the system is non-linear. However, (6.59) *does* have an analytic solution

$$\xi = \bar{\mu}\left(1 - \frac{1}{\rho}\right) \tag{6.63}$$

and thus $\bar{n}_\xi = \bar{\mu}$.

When the symmetry is not broken, $\Psi = 0$, the equation for χ has of course

$$\chi = \bar{\mu}\left(1 - \frac{1}{\rho}\right) \tag{6.64}$$

[4]These equations of motion correspond to the probe limit of the system studied in [70] as a dual of superconductors with chemical potential imbalance. Notice however that in [70] the gauge symmetry was $U(1) \times U(1)$ instead of $U(2)$ as in the present setup.

as a solution as well. Therefore, in the unbroken phase

$$\Theta = 0\,, \tag{6.65}$$

$$\Phi = 2\bar{\mu}\left(1 - \frac{1}{\rho}\right)\,. \tag{6.66}$$

This behavior reflects the fact that T_3 is completely independent from T_0 in the unbroken phase. However, once we switch on the condensate, the interplay between T_3 and T_0 (recall that the remaining symmetry is a combination of the two) makes it impossible to set only one of the fields to zero.

Finally, let us mention that in order to relate the dimensionless parameters with the physical ones, we need to apply the same dictionary (6.26)-(6.29) used for the ungauged model.

6.4.1 Charge Density in the broken phase

According to [26,31] we can expect the presence of type II Goldstone modes if the broken symmetry generators fulfill

$$\langle [Q_a, Q_b] \rangle = B_{ab} \tag{6.67}$$

with at least one $B_{ab} \neq 0$. In our case we have $[Q_1, Q_2] = iQ_3$. Therefore in the broken phase we are interested in a non-vanishing expectation value for the charge density operator $\langle Q_3 \rangle = n_\Theta$. As we argued previously, in the unbroken phase we necessarily have $\Theta(r) = 0$. This happened since both χ and ξ obey the same differential equation and the integration constants had to be set equal in order to do not switch on a source for Θ. Now we would like to find out whether or not an expectation value for Θ will be spontaneously generated in the broken phase.

Independently of the phase the field associated to the unbroken combination of generators is given by (6.63). Since $\Theta = \xi - \chi$, then

$$\bar{n}_\Theta = \bar{\mu} - \bar{n}_\chi\,. \tag{6.68}$$

Hence, what we want to check is the difference between the leading and the subleading coefficients of χ as a function of the temperature. The numerical result is shown in Figure 6.11.

So we conclude that precisely at $T \leq T_c$ this difference is switched on and an expectation value for $\langle Q_3 \rangle$ appears. This can be taken as a clear indication for the appearance of type II Goldstone bosons in the spectrum.

6.4.2 Fluctuations of the gauged model

In order to study the quasinormal spectrum and the conductivities of the system, we switch on longitudinal perturbations on top of the background, so that

$$\hat{\Psi}^T = (\eta(t,\rho,x), \Psi(\rho) + \sigma(t,\rho,x))\,, \tag{6.69}$$

$$A^{(0)} = (\Phi(\rho) + a_t^{(0)}(t,\rho,x))dt + a_x^{(0)}(t,\rho,x)dx\,, \tag{6.70}$$

$$A^{(1)} = a_t^{(1)}(t,\rho,x)dt + a_x^{(1)}(t,\rho,x)dx\,, \tag{6.71}$$

$$A^{(2)} = a_t^{(2)}(t,\rho,x)dt + a_x^{(2)}(t,\rho,x)dx\,, \tag{6.72}$$

$$A^{(3)} = (\Theta(\rho) + a_t^{(3)}(t,\rho,x))dt + a_x^{(3)}(t,\rho,x)dx\,. \tag{6.73}$$

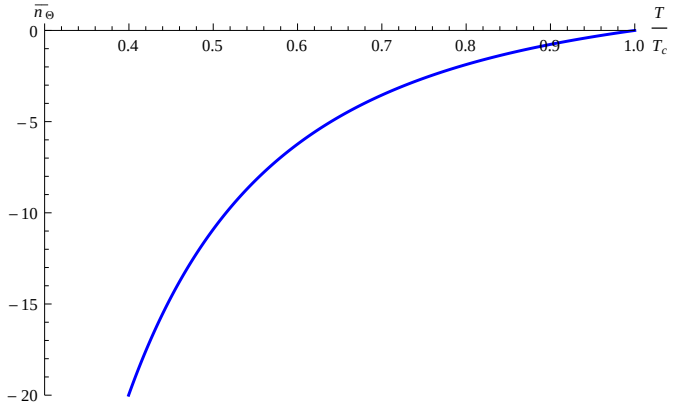

Figure 6.11: Charge density of Θ, $\bar{n}_\Theta$, as a function of the temperature T/T_c.

Perturbations in the Unbroken Phase

In the normal phase, the background value of the condensate vanishes. Moreover, we have $\Theta(\rho) = 0$. The equations of motion for the perturbations read

$$s'' + s'\left(\frac{f'}{f} + \frac{2}{\rho}\right) + \left(\frac{(\frac{\Phi}{2}+\omega)^2}{f^2} - \frac{k^2}{f\rho^2} - \frac{m^2}{f}\right)s = 0\,, \tag{6.74}$$

$$a_t''^{(c)} + \frac{2}{\rho}a_t'^{(c)} - \frac{\omega k}{f\rho^2}a_x^{(c)} - \frac{k^2}{f\rho^2}a_t^{(c)} = 0\,, \tag{6.75}$$

$$a_x''^{(c)} + \frac{f'}{f}a_x'^{(c)} + \frac{\omega^2}{f^2}a_x^{(c)} + \frac{\omega k}{f^2}a_t^{(c)} = 0\,, \tag{6.76}$$

$$\frac{\omega}{f}a_t'^{(c)} + \frac{k}{\rho^2}a_x'^{(c)} = 0\,, \tag{6.77}$$

where $s \in \{\eta, \sigma\}$. Since the color indices do not see each other the system is the same one as (6.33)-(6.36) except that there are four copies of the gauge field fluctuations. Due to the chosen normalization of the $U(2)$ generators the gauge field background Φ enters with an additional factor $\frac{1}{2}$ compared to (6.33). The quasinormal mode spectrum is the same as the one of the holographic s-wave superconductor [63] except that the scalar modes are doubly degenerate and the gauge field modes are fourfold degenerate. In particular there are four copies of the hydrodynamic diffusion mode $\omega = -iDk^2$.

Perturbations in the Broken Phase

The equations of motion in the broken phase decouple in two sets: one mixing the $(0)-(3)$ colors of the gauge field and σ fluctuations and the other mixing the $(1)-(2)$ colors and the η fluctuations.

Writing $\sigma = \zeta + i\delta$, the equations of the $(0)-(3)$ sector are

$$0 = f\zeta'' + \left(f' + \frac{2f}{\rho}\right)\zeta' + \left(\frac{\omega^2}{f} + \frac{\chi^2}{f} - \frac{k^2}{\rho^2} - m^2\right)\zeta + \frac{2i\omega\chi}{f}\delta + (a_t^{(0)} - a_t^{(3)})\Psi\frac{\chi}{f}, \quad (6.78)$$

$$0 = f\delta'' + \left(f' + \frac{2f}{\rho}\right)\delta' + \left(\frac{\omega^2}{f} + \frac{\chi^2}{f} - \frac{k^2}{\rho^2} - m^2\right)\delta - \frac{2i\omega\chi}{f}\zeta + i\Psi\omega\frac{a_t^{(3)} - a_t^{(0)}}{2f} + \\ + i\Psi k\frac{a_x^{(3)} - a_x^{(0)}}{2\rho^2}, \quad (6.79)$$

$$0 = fa_t''^{(0)} + \frac{2f}{\rho}a_t'^{(0)} - \left(\Psi^2 + \frac{k^2}{\rho^2}\right)a_t^{(0)} - \frac{\omega k}{\rho^2}a_x^{(0)} + \Psi^2 a_t^{(3)} - 4\zeta\Psi\chi - 2i\omega\Psi\delta, \quad (6.80)$$

$$0 = fa_x''^{(0)} + f'a_x'^{(0)} + \left(\frac{\omega^2}{f} - \Psi^2\right)a_x^{(0)} + \frac{\omega k}{f}a_t^{(0)} + \Psi^2 a_x^{(3)} + 2ik\delta\Psi, \quad (6.81)$$

$$0 = fa_t''^{(3)} + \frac{2f}{\rho}a_t'^{(3)} - \left(\Psi^2 + \frac{k^2}{\rho^2}\right)a_t^{(3)} - \frac{\omega k}{\rho^2}a_x^{(3)} + \Psi^2 a_t^{(0)} + 4\zeta\Psi\chi + 2i\omega\Psi\delta, \quad (6.82)$$

$$0 = fa_x''^{(3)} + f'a_x'^{(3)} + \left(\frac{\omega^2}{f} - \Psi^2\right)a_x^{(3)} + \frac{\omega k}{f}a_t^{(3)} + \Psi^2 a_x^{(0)} - 2ik\delta\Psi, \quad (6.83)$$

$$0 = \frac{ik}{\rho^2}a_x'^{(0)} + \frac{i\omega}{f}a_t'^{(0)} + 2\Psi'\delta - 2\Psi\delta', \quad (6.84)$$

$$0 = \frac{ik}{\rho^2}a_x'^{(3)} + \frac{i\omega}{f}a_t'^{(3)} - 2\Psi'\delta + 2\Psi\delta'. \quad (6.85)$$

It is trivial to show that by defining new fields $a_t^{(\pm)} \equiv \frac{1}{2}(a_t^{(0)} \pm a_t^{(3)})$ and $a_x^{(\pm)} \equiv \frac{1}{2}(a_x^{(0)} \pm a_x^{(3)})$ the system further decouples into a coupled system for the scalar fluctuations and $a_\mu^{(-)}$ and a background independent set of equations for the $U(1)$ gauge field $a_\mu^{(+)}$. The first subsystem reproduces the eoms (6.40)-(6.44) and therefore corresponds to the s-wave $U(1)$ superconductor contained in the $U(2)$ model. On the other hand, the field $a_\mu^{(+)}$ corresponds to the preserved gauge symmetry surviving the $U(2) \to U(1)$ spontaneous symmetry breaking. The quasinormal mode spectrum in this sector is therefore the same one as in [63] plus the QNMs that are stem from a $U(1)$ gauge field in AdS_4. In particular the hydrodynamic modes in this sector are the sound mode and the diffusion mode of the unbroken $U(1)$.

From now on we will concentrate on the remaining fields. We will call this remaining, inherently non-Abelian sector the $(1)-(2)$ sector and will show that the expected type II Goldstone boson resides there. Writing $\eta = \alpha + i\beta$, we find the following equations in the $(1)-(2)$ sector:

$$0 = f\alpha'' + \left(f' + \frac{2f}{\rho}\right)\alpha' + \left(\frac{\omega^2}{f} + \frac{(\Phi+\Theta)^2}{4f} - \frac{k^2}{\rho^2} - m^2\right)\alpha + \frac{i\omega(\Phi+\Theta)}{f}\beta - \\ -i\Psi\left(\frac{k}{2\rho^2}a_x^{(2)} + \frac{\omega}{2f}a_t^{(2)}\right) + \frac{\Psi\Phi}{2f}a_t^{(1)}\,, \tag{6.86}$$

$$0 = f\beta'' + \left(f' + \frac{2f}{\rho}\right)\beta' + \left(\frac{\omega^2}{f} + \frac{(\Phi+\Theta)^2}{4f} - \frac{k^2}{\rho^2} - m^2\right)\beta - \frac{i\omega(\Phi+\Theta)}{f}\alpha - \\ -i\Psi\left(\frac{k}{2\rho^2}a_x^{(1)} + \frac{\omega}{2f}a_t^{(1)}\right) - \frac{\Phi\Psi}{2f}a_t^{(2)}\,, \tag{6.87}$$

$$0 = fa_t''^{(1)} + \frac{2f}{\rho}a_t'^{(1)} - \left(\Psi^2 + \frac{k^2}{\rho^2}\right)a_t^{(1)} - \frac{\omega k}{\rho^2}a_x^{(1)} + i\Theta\frac{k}{\rho^2}a_x^{(2)} - 2\Phi\Psi\alpha - 2i\omega\Psi\beta \tag{6.88}$$

$$0 = fa_x''^{(1)} + f'a_x'^{(1)} + \left(\frac{\omega^2}{f} - \Psi^2 + \frac{\Theta^2}{f}\right)a_x^{(1)} - 2i\frac{\Theta\omega}{f}a_x^{(2)} - i\Theta\frac{k}{f}a_t^{(2)} + \frac{\omega k}{f}a_t^{(1)}\beta + \\ +2ik\Psi\beta\,, \tag{6.89}$$

$$0 = fa_t''^{(2)} + \frac{2f}{\rho}a_t'^{(2)} - \left(\Psi^2 + \frac{k^2}{\rho^2}\right)a_t^{(2)} - \frac{\omega k}{\rho^2}a_x^{(2)} - i\Theta\frac{k}{\rho^2}a_x^{(1)} + 2\Phi\Psi\beta - 2i\omega\Psi\alpha \tag{6.90}$$

$$0 = fa_x''^{(2)} + f'a_x'^{(2)} + \left(\frac{\omega^2}{f} - \Psi^2 + \frac{\Theta^2}{f}\right)a_x^{(2)} + 2i\frac{\Theta\omega}{f}a_x^{(1)} + i\Theta\frac{k}{f}a_t^{(1)} + \frac{\omega k}{f}a_t^{(2)} + \\ +2ik\Psi\alpha\,, \tag{6.91}$$

$$0 = \frac{ik}{\rho^2}a_x'^{(1)} + \frac{i\omega}{f}a_t'^{(1)} + \frac{1}{f}\left(a_t'^{(2)}\Theta - a_t^{(2)}\Theta'\right) + 2\Psi'\beta - 2\beta'\Psi\,, \tag{6.92}$$

$$0 = \frac{ik}{\rho^2}a_x'^{(2)} + \frac{i\omega}{f}a_t'^{(2)} - \frac{1}{f}\left(a_t'^{(1)}\Theta - a_t^{(1)}\Theta'\right) + 2\Psi'\alpha - 2\alpha'\Psi\,. \tag{6.93}$$

A comment is in order here. This system of equations could be written in a more compact form by using complex field variables η and $a_{t,x}^{(1)} \pm i a_{t,x}^{(2)}$. One has to keep in mind then that the field equations one needs to solve for the QNM spectrum for the complex conjugate fields are not the complex conjugate equations since one has to demand infalling boundary conditions on the fields and on the complex conjugate fields simultaneously. This aspect is somewhat clearer if one works with the (formally) real field variables on paying the price of writing a somewhat lengthy system of equations.

Up to linear order in perturbations, there are three decoupled sectors in the system. Two of them belong to the '$(0)-(3)$ sector' and they are a copy of the $U(1)$ holographic superconductor, already extensively studied, and the preserved $U(1)$ gauge symmetry. The main features of the spectrum of this sector have already been presented in section 6.3 since it is also a subsector of the ungauged model. On the other hand, the so called '$(1)-(2)$ sector' has not been studied before. The physics in this sector is quite different from the holographic superconductors studied up to now and we will concentrate on it in the rest of this chapter.

Before studying the quasinormal modes we will focus on a simpler problem, namely the conductivities.

6.4.3 Conductivities

In order to study the conductivities via Kubo formulae, it is enough to solve the linearized equations in the limit $k = 0$. The retarded correlators that we are interested in have the form $\mathcal{G}_{\mathcal{R}} \sim \left\langle J^x_{(c)}, J^x_{(c')} \right\rangle_{\mathcal{R}}$, with c, c' color indices.

We will be applying the prescription of [57] for computing Green functions in the presence of holographic operator mixing. If one has a set of fields Φ_I, the two-point correlation functions will be

$$\mathcal{G}_{IJ} = \lim_{\Lambda\to\infty} \left(\mathcal{A}_{IM} \mathcal{F}_k^M{}_J(\Lambda)' + \mathcal{B}_{IJ} \right), \tag{6.94}$$

where the matrix $\mathcal{F}_k(r)$ is nothing but the bulk-to-boundary propagator for the fields, normalized to be the unit matrix at the boundary. The matrices $\mathcal{A}$ and $\mathcal{B}$ can be read off from the on-shell renormalized action. The corresponding DC conductivities are given by the following Kubo formula

$$\sigma_{IJ} = \lim_{\omega\to 0} \left(\frac{i}{\omega} \mathcal{G}_{IJ}(\omega, 0) \right). \tag{6.95}$$

At vanishing momentum the longitudinal components of the gauge field perturbations decouple from the scalar perturbations, as well as from the temporal components of the gauge fields. Moreover, the constraints (eqs. (6.84-6.85) and(6.92-6.93)) become trivial. Since we know that the system splits into the $(0) - (3)$ and the $(1) - (2)$ sectors we can rearrange the $a_x^{(c)}$ fields in two vectors

$$\Phi^T_{k\ (0-3)}(\rho) = (a_x^{(0)}(\rho), a_x^{(3)}(\rho)) \quad \text{and} \quad \Phi^T_{k\ (1-2)}(\rho) = (a_x^{(1)}(\rho), a_x^{(2)}(\rho)) \,. \tag{6.96}$$

One can check that in our case the $\mathcal{A}, \mathcal{B}$ matrices take the simple form

$$\mathcal{A} = -\frac{f(r)}{2} \mathbb{I}, \qquad \mathcal{B} = 0 \,, \tag{6.97}$$

for both sectors. A priori we would have a 4×4 matrix of conductivities. We know however that the fluctuations in the $(0) - (3)$ and the $(1) - (2)$ sector decouple from each other. Therefore we can restrict ourselves to study two independent 2×2 matrices of conductivities.

6.4.4 Conductivities in the $(0) - (3)$ sector

The $k = 0$ equations of motion for $a_x^{(0)}$ and $a_x^{(3)}$ can be simplified by using the already defined $a_x^{(-)}$ and $a_x^{(+)}$ fields. This results in

$$0 = f a_x''^{(+)} + f' a_x'^{(+)} + \frac{\omega^2}{f} a_x^{(+)} \,, \tag{6.98}$$

$$0 = f a_x''^{(-)} + f' a_x'^{(-)} + \left(\frac{\omega^2}{f} - 2\Psi^2 \right) a_x^{(-)} \,. \tag{6.99}$$

We see that the resulting system of equations is now completely decoupled. We only have two diagonal conductivities σ_{++} and σ_{--}, corresponding to the unbroken $U(1)$ diffusive sector and a mode which is associated to the broken $U(1)$ coupling to the condensate. The

former is the same as in the unbroken phase and of no further interest for us. The latter is again the well-studied $U(1)$ s-wave superconductor. Its conductivity has been already calculated in [71]. To check our numerics we have re-calculated it and in Figure 6.12 we show its behavior. It coincides completely with [71]. The real part shows the $\omega = 0$ delta function characteristic of superconductivity[5]. Numerically this can be seen through the $1/\omega$ behavior in the imaginary part. The Kramers-Kronig relation (see (A.13) in appendix A.1) implies then infinite DC conductivity. The real part of the AC conductivity also exhibits a temperature dependent gap.

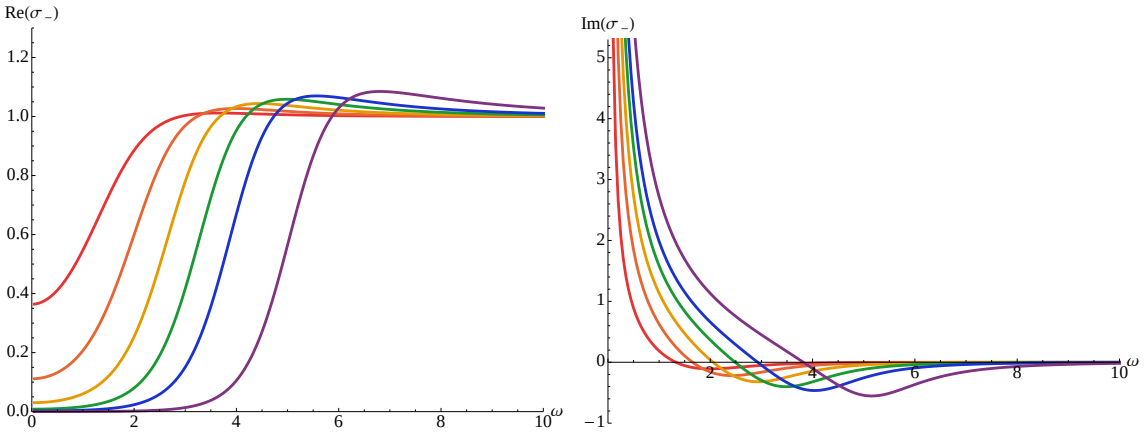

Figure 6.12: Real part (left) and imaginary part (right) of the conductivity as a function of frequency. The plots correspond to temperatures in the range $T/T_c \approx 0.91 - 0.41$, from red to purple. As expected, the plots reproduce the ones of [71].

6.4.5 Conductivities in the $(1) - (2)$ sector

The relevant equations for the $(1) - (2)$ sector read

$$0 = f a_x''^{(1)} + f' a_x'^{(1)} + \left(\frac{\omega^2}{f} - \Psi^2 + \frac{\Theta^2}{f} \right) a_x^{(1)} - 2i \frac{\Theta\omega}{f} a_x^{(2)} \,, \tag{6.100}$$

$$0 = f a_x''^{(2)} + f' a_x'^{(2)} + \left(\frac{\omega^2}{f} - \Psi^2 + \frac{\Theta^2}{f} \right) a_x^{(2)} + 2i \frac{\Theta\omega}{f} a_x^{(1)} \,. \tag{6.101}$$

These equations obey the symmetry

$$(a_x^{(1)} \to a_x^{(2)} \ , \ a_x^{(2)} \to -a_x^{(1)}) \,. \tag{6.102}$$

One can see that the fact that $\Theta(1) = 0$ implies that $a_x^{(1)}(1)$ is independent of $a_x^{(2)}(1)$, so, after imposing infalling boundary conditions at the horizon, the parameter space of boundary conditions is two-dimensional, as expected.

In the unbroken phase the system completely decouples

$$0 = f a_x''^{(c)} + f' a_x'^{(c)} + \frac{\omega^2}{f} a_x^{(c)} \,. \tag{6.103}$$

[5] In general, this behavior is also typical of translation invariant charged media, in which accelerated charges cannot relax. However, working in the probe limit we effectively break translation invariance and therefore the infinite DC conductivity is a genuine sign of superconductivity.

Diagonal Conductivities σ^{11} & σ^{22}

The diagonal components of the conductivity, σ^{11} and σ^{22} have the same behavior, as could be anticipated from the equations (6.100),(6.101). Henceforth, we will only refer to σ^{11}, but all the conclusions also apply to σ^{22}.

Figure 6.13 shows the conductivity for several values of the temperature. We find that these conductivities also show delta-function singularities at $\omega = 0$.

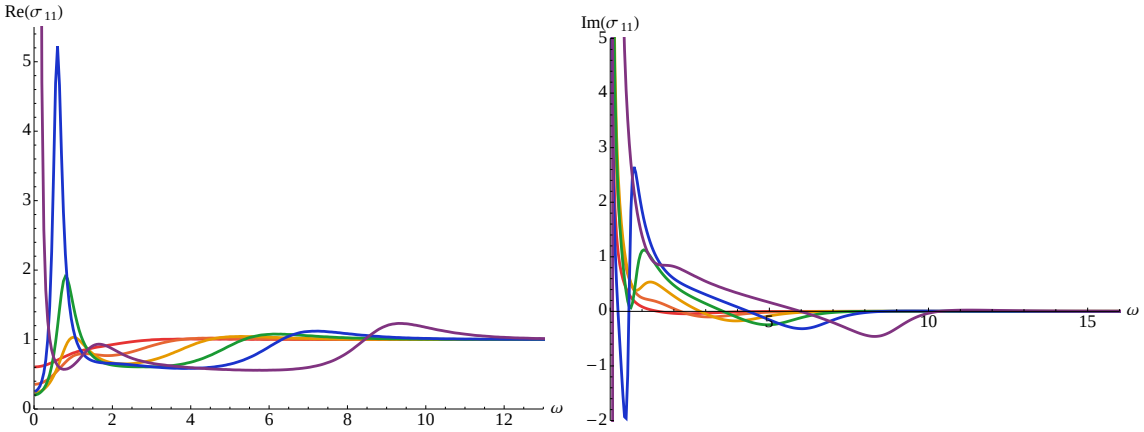

Figure 6.13: Real (left) and imaginary (right) parts of σ^{11} versus ω for five different temperatures chosen in a range $T/T_c \approx 0.91 - 0.41$, from red to purple. $\mathrm{Im}(\sigma^{11})$ clearly blows up as $\omega \to 0$.

The strength of the delta function can also be computed. It is given by the residue of the imaginary part of the conductivity at $\omega = 0$,

$$\lim_{\omega \to 0} \omega \, \mathrm{Im}(\sigma^{11}) \sim n_s \, . \tag{6.104}$$

The residue is plotted in Figure 6.14 as a function of T/T_c. As expected, it starts growing from a zero value. At $T/T_c \approx 0.65$, n_s reaches a maximum and starts decreasing fast, changing sign at $T/T_c = 0.49$. To study n_s down to very low temperature we would need to go beyond the probe limit. However, as we will comment below, this behavior of n_s can be understood in light of the QNM spectra.

Let us look in detail at the behavior of the real part of the conductivity (left plot in figure 6.13). For high enough temperatures the optical conductivity is almost constant, $\mathrm{Re}(\sigma^{11}) = 1$, which is expected since in that regime the dynamics is described essentially by (6.103). As soon as we decrease the temperature, the onset of the DC conductivity also decreases and only approaches the constant value asymptotically, when ω becomes large enough and thus the term $\frac{\omega^2}{f}$ dominates, turning equations (6.100),(6.101) approximately into (6.103). According to the Ferrell-Glover sum rule, the area missing as we lower the temperature is proportional to n_s.

Interestingly, at low temperatures the real part of σ^{11} starts developing a bump at small values of ω ($0 < \omega \lesssim 2$). The bump leaves less area for the delta function to cover, which explains why n_s starts decreasing approximately at this temperature. Moreover, the appearance of these bumps can be traced back to the fact that for a subleading gauge QNM with small $|\,\mathrm{Im}(\omega)|$, $\mathrm{Re}\,\omega(T) >> \mathrm{Im}\,\omega(T)$ holds. Hence, the conductivities affected

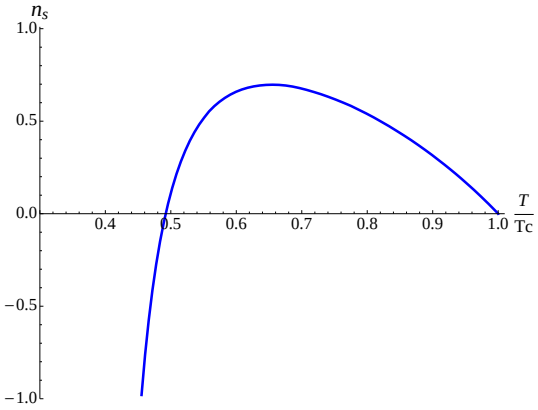

Figure 6.14: Residue at $\omega = 0$ as a function of T/T_c.

by this mode start developing the reminiscence of a resonance at a particular frequency. We have studied the spectrum of low lying QNM for the gauge sector and found that this mode corresponds in the normal phase to the lowest excitation of $a_\mu^{(1,2)}$, $\omega = -1.5i$. But it is at lower temperatures where one finds a remarkable fact: at $T/T_c \approx 0.395$ the mode becomes unstable, and indeed, as we will see, several physical quantities modify their behavior at that temperature.

Therefore, we expect a new phase transition around $T/T_c \approx 0.395$, due entirely to the $(1)-(2)$ sector. Since this phase transition seems to be triggered by an unstable mode in the vector sector it most likely leads to the formation of a p-wave condensate. We will study this possibility in section 8.

Off-diagonal conductivities σ^{12} & σ^{21}

The off-diagonal elements of the conductivity matrix are also related via the symmetry (6.102) and therefore obey $\sigma^{12} = -\sigma^{21}$. Therefore, it is enough to comment on σ^{12}, although the conclusions are valid for both components.

The form of σ^{12} is plotted in Figure 6.15 for various different temperatures as a function of frequency. At $T/T_c = 1$ the system is practically decoupled, so for all temperatures the off-diagonal conductivity goes to zero as ω increases.

Observe that $\sigma^{12}(\omega)$ behaves as a normal conductivity. Its real part vanishes as $\omega \to 0$, whereas the imaginary part tends to a constant value.

6.4.6 Quasinormal Modes

Let us finally study the QNM spectrum in the $(1)-(2)$ sector. This sector contains the fluctuations η, a_μ^i with $i = 1, 2$, therefore in the unbroken phase the spectrum will contain two diffusive modes associated with the two gauge fields. The fluctuations of the scalar field in the normal phase were already discussed in section 6.3. Analyzing the quasinormal mode spectrum in the broken phase amounts to solving the system of equations (6.86)-(6.93). Details of the computation can be found in appendix A.2.

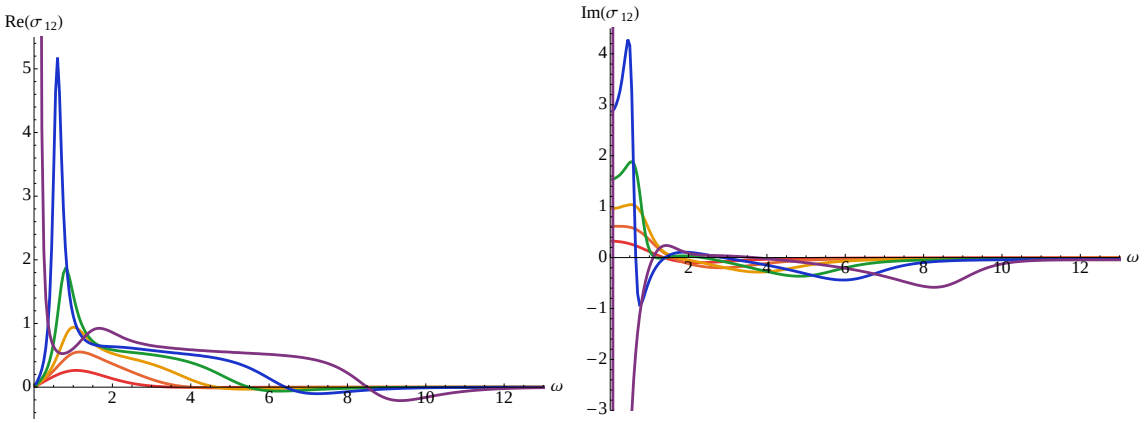

Figure 6.15: Real (left) and imaginary (right) part of σ^{12} as a function of ω for $T/T_c \approx 0.91 - 0.41$, from red to purple.

Type II Goldstone mode

As expected within the $(1) - (2)$ sector we find a type II Goldstone mode. As in the ungauged model for small enough momentum its dispersion relation can be fitted to

$$\omega = \pm \mathcal{B} k^2 - i \mathcal{C} k^2 \,. \tag{6.105}$$

Figure 6.16 shows the dispersion relation for various values of the temperature in the hydrodynamic regime. The quadratic behavior with momentum is apparent.

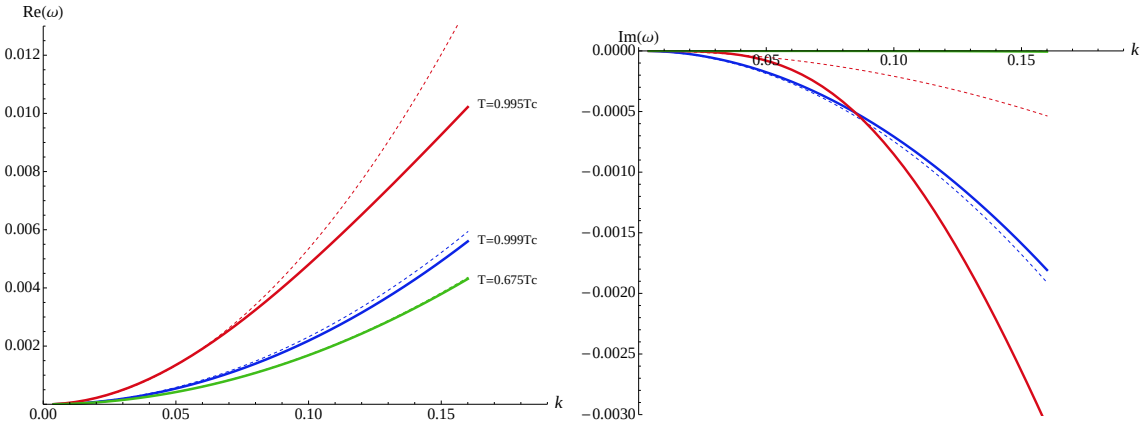

Figure 6.16: Plots of $\mathrm{Re}(\omega)$ (left) and $\mathrm{Im}(\omega)$ (right) as a function of the momentum. Thick lines correspond to data and thin lines to quadratic fit. At $T = 0.995\, T_c$ the real quadratic parameter $\mathcal{B}(T)$ shows a maximum, see Figure 6.17. Relation (6.105) is fulfilled with high accuracy.

The temperature dependence of $\mathcal{B}$ and $\mathcal{C}$ is plotted in Figure 6.17. The value at $T = T_c$ is given by the same value as in the ungauged model (6.49) and in fact can also be cross checked by calculating the scalar mode dispersion relation in the unbroken phase at $T = T_c$ since the QNMs must be continuous through the phase transition. We find a rather surprising dependence of $\mathcal{B}$ with the temperature. It starts at a finite value at the transition and then it rises rather sharply and falls off slower. It reaches a minimum at

$T \approx 0.49\,T_c$, temperature at which we found the change of sign in the residue of current-current correlators. We also find another peak around $T \approx 0.4\,T_c$. We expect that it is again related with the instability found in the gauge sector around that temperature. It would also be interesting to calculate $\mathcal{B}(T)$ using an alternative method e.g. as the sound velocity can be calculated from thermodynamic considerations alone. In order to do this one would need to formulate the hydrodynamics of type II Goldstone modes. We are however not aware of such a hydrodynamic formulation and leave this for future research.

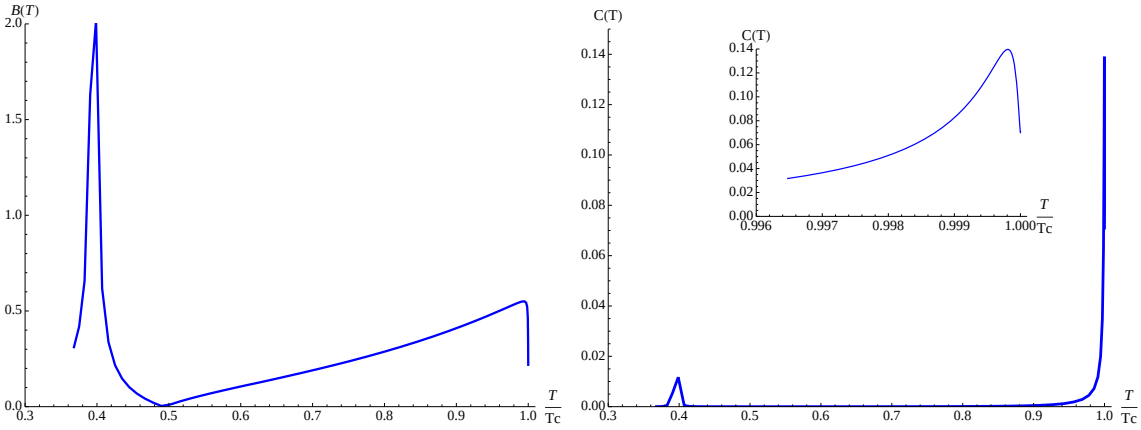

Figure 6.17: $\mathcal{B}$ (left) and $\mathcal{C}$ (right) as a function of T/T_c. The zoom-in shows the peak of $\mathcal{C}$ close to the transition. Furthermore at $T \simeq 0.4T_c$ a sharp peak shows up in both coefficients. We relate this feature also to the instability arising in the vector sector.

The attenuation $\mathcal{C}(T)$ decreases rapidly with temperature. For temperatures $T/T_c < 0.9$ it is negligible and the width of the type II Goldstone scales with k^4 in the hydrodynamic limit. This fast decreasing with temperature reflects that this mode propagates almost ideally in the fluid at low temperature. No further ungapped modes can be found in this sector.

Higher quasinormal modes

Higher quasinormal modes correspond to gapped modes in the QNM spectrum and thus represent subleading contributions to the low energy Green's functions. We will focus here only on two of them: the continuation of the two diffusive modes of the unbroken phase and the special gapped mode that appears as the partner mode of the type II Goldstone mode in the field theoretical model.

Analyzing the first one is interesting in order to understand if also a qualitative change in the response pattern, such as that characterized by T_* in the $U(1)$ superconductor sector, exists in the $(1)-(2)$ sector. Since in this sector there exist however two diffusive modes in the unbroken phase it is also possible that the diffusive modes do not simply develop a gap but that they pair up and move off the imaginary axis in the broken phase. Indeed as we will see this is what happens.

The special gapped mode corresponds to a mode that is associated to the complex conjugate of the scalar perturbation in the unbroken phase. At $k = 0$ and $\mu = 0$ the scalar mode and its complex conjugate are degenerated. As we lower the temperature they split into two different modes. When we reach $T = T_c$, the lowest scalar mode becomes the

type II Goldstone mode whereas the mode of the complex conjugate scalar field turns into the special gapped mode. The gap of this mode is expected to be given by the tree level result (6.16) [65].

Fate of diffusive modes: As already mentioned, in the $(1)-(2)$ sector we have two degenerate diffusive modes in the unbroken phase. When going through the phase transition these modes can therefore pair up and move off the imaginary axes such that their quasinormal frequencies develop real parts and lie symmetrically around the imaginary axis. We expect therefore that in the low energy limit the dispersion relation takes the form

$$\omega = \Gamma(T) + \mathcal{M}(T)k^2\,, \tag{6.106}$$

where both coefficients are complex functions and the second mode is located at $\omega' = -\omega^*$. Besides, we expect the QNMs to be continuous through the phase transition, which in particular means that for $T = T_c$, our pseudo-diffusive modes should match the unbroken phase values, i.e. $\Gamma(T_c) = 0$ and $\mathcal{M}(T_c) = -i$.

The modes at zero momentum are plotted in Figure 6.18. We see that indeed the gap vanishes as $T \to T_c$, whereas the modes split and develop a real part as we decrease the temperature. This last feature is exclusive of the non-Abelian system and thus does not take place in the usual $U(1)$ holographic superconductor, where the gap is purely imaginary (see [63] and comments above). Close to the phase transition, they present a linear behavior in temperature,

$$\Gamma(T) = (4.1 - 0.8\,i)\left(1 - \frac{T}{T_c}\right) \quad \text{near } T_c\,. \tag{6.107}$$

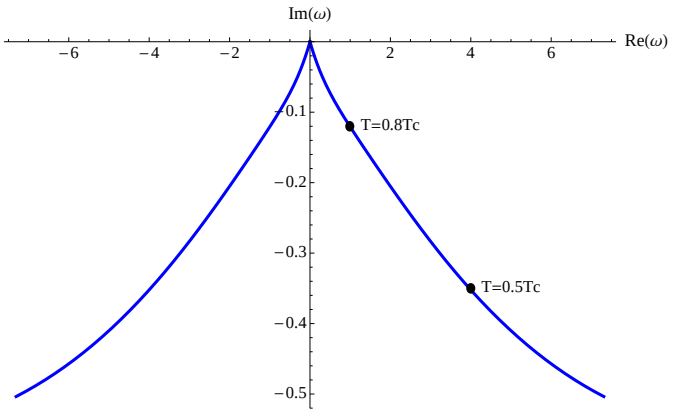

Figure 6.18: $\mathrm{Im}\,\omega$ versus $\mathrm{Re}\,\omega$ at $k = 0$ as a function of the temperature. The shape of the figure is compatible with T symmetry, since there are two pseudo-diffusive modes. Having $\mathrm{Re}\,\omega(k = 0) \neq 0$ is characteristic of the non-Abelian case.

The temperature dependence of the coefficient of the momentum in (6.106), $\mathcal{M}(T)$, is shown in Figure 6.19. The real part rises very steeply just below the phase transition. The imaginary part approaches the unbroken phase value at the critical temperature, i.e. $\mathcal{M}(T_c) = -i$, as is expected for the pseudo-diffusion modes to continuously connect to the normal diffusion modes through the phase transition. Notice $\mathrm{Im}\,\mathcal{M}(T)$ decreases when lowering the temperature.

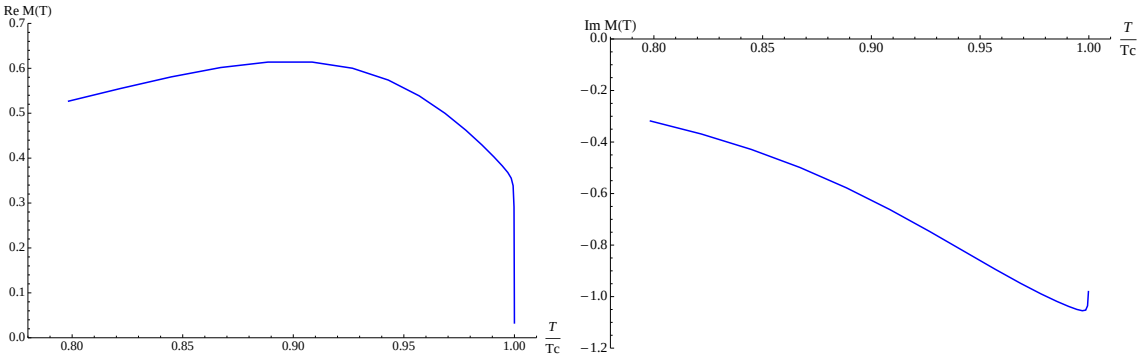

Figure 6.19: Real (left) and imaginary (right) part of $\mathcal{M}(T)$ as a function of T/T_c. As the temperature approaches T_c, the value of $\mathcal{M}(T)$ reaches the one prescribed by continuity through the phase transition.

Another check of the fact that the pseudo diffusion modes come from the pairing up of the diffusion modes of the normal phase is that their dispersion relation at the phase transition matches. Therefore the two diffusive modes are continuous through the transition, as expected for second order phase transitions, however instead of simply developing an imaginary gap to drop out of the hydrodynamic spectrum as for the usual $U(1)$ superconductor, they pair up in two modes that on top of this gap also develop a real part.

The fact that $\mathrm{Re}(\omega)$ does not vanish for these modes implies that sufficiently close to T_c and in the limit $k = 0$, the late-time response of the perturbed state will present an oscillatory decay of the perturbations, meaning that, contrary to the $U(1)$ case, there will not be a temperature at which the late-time behavior changes *qualitatively*.

Special Gapped mode: Seeking for this mode is computationally much more involved. Its behavior is characterized by a gap that is proportional to μ. In particular, in [65] it was argued that a type II Goldstone mode is accompanied by a gapped mode obeying $\omega(0) = q\mu$ with q being the charge of the corresponding field. In our conventions here we have $q = 1$. So we have to look for a mode with $\omega(k = 0) = \mu$. Furthermore we expect that it connects to the lowest mode of the complex conjugate scalar in the unbroken phase.

In Figure 6.20 we depict such mode at zero momentum with respect to the chemical potential $\bar{\mu}$ in numerical units. Notice that the mode is continuous at the phase transition, as expected. We observe the linear behavior with the chemical potential that is predicted theoretically, at least near $\bar{\mu}_c$. It is very difficult to do the analysis when $\bar{\mu} > 6$ due to the high computational power demanded to carry out the computation. The mode shows of course also a non-vanishing imaginary part which is due to the dissipation at finite temperature. We find that the real part above the phase transition can be approximated by

$$\mathrm{Re}\,\omega = 1.10\,\bar{\mu} \quad \text{near } \bar{\mu}_c\,. \tag{6.108}$$

This result shows a deviation from the conjectured behavior. On the one hand this could be due to uncertainties in the numerics. Let us emphasize here that the numerics involved in tracking this mode through the phase transition were rather challenging. However, on the other, it was recently found that the symmetry that this quantity is protected by a larger (O(4)) symmetry present in absence of chemical potential **??**. Since our model does

not contain the generators of this enlarged symmetry the results don't necessarily agree with those findings.

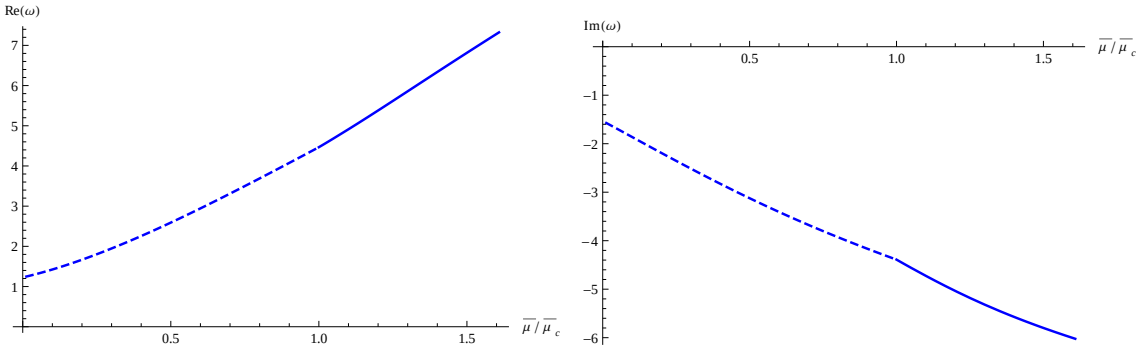

Figure 6.20: Real (left) and imaginary (right) part of the special gapped mode versus the chemical potential. We encounter the expected linear behavior with μ. The plot covers both the unbroken (dashed line) and the broken (solid line) phases.

6.5 Discussion

The aim of this chapter was to study certain extensions of the spontaneous symmetry breaking mechanism in holography. Among others, we were able to stablish the existence of type II Goldstone modes in the quasinormal mode spectrum of a holographic theory dual to a strongly coupled superfluid with $U(2)$ symmetry.

We studied two models, one in which only the overall $U(1)$ symmetry is gauged in the AdS bulk and another in which all the $U(2)$ symmetry is gauged. The most important finding is that indeed there exist ungapped excitations represented by quasinormal modes in the AdS bulk that show the expected but somewhat unusual quadratic dispersion relation of type II Goldstone bosons.

For the ungauged model this does constitute a surprising result. After all, the field theory dual to this model does not contain the necessary conserved currents that would correspond to the generators of the global $SU(2)$ symmetry. Standard proofs of the Goldstone theorem take the existence of such conserved currents for granted. On the other hand it is basically guaranteed that one can construct an effective field theory, a simple Landau-Ginzburg type model, that captures the essential dynamics of the light modes, i.e. the lowest lying quasinormal modes. Such a model would be essentially given by the field theoretical model of section 6.2 and this guarantees the existence of the type II Goldstone modes. However one can expect that such an effective field theory approach can capture only the physics of the low lying QNMs but not the higher modes. This is indeed what happens: the partner mode of the type II Goldstone mode in the ungauged model does not behave in the supposed universal way $\omega = q\mu$. In contrast the corresponding mode in the gauged model does obey this relation approximately.

One rather interesting perspective on the ungauged model opens up if we vary the masses of the scalar fields in the AdS bulk. If the masses are slightly different, then at the critical temperature only one of the two scalars will feature an ungapped QNM (the one with smaller mass). The lowest scalar mode of the second one will still be gapped at that temperature. As one goes through the phase transition we do not expect this mode to become massless at lower temperatures. Rather it should become a pseudo-Goldstone mode with a gap that is proportional to the mass splitting. The appearance of the type II Goldstone mode can then be interpreted as the effect of a symmetry enhancement at the point in parameter space where the masses of the scalars become degenerate. Since this symmetry is not represented by bulk-gauge fields we might call it an accidental symmetry. At this point it is difficult to resist the temptation to draw a parallel to the conjectured symmetry enhancement of high T_c superconductors. In [72] it was suggested that the phase diagram of high T_c superconductors can be captured by a unified model with and enhancement of the $SO(3) \times U(1)$ symmetry of rotations and electromagnetism to a larger $SO(5)$ symmetry. Since high T_c superconductors are d-wave rather than s-wave it remains to be seen how our symmetry enhancement mechanism and the resulting type II Goldstone mode can be combined with holographic models of d-wave superfluids such as [73, 74] [6].

The second model we studied has bulk gauge fields for all of the $U(2)$ symmetry. There are several important differences compared to the ungauged model. The most eye-jumping one is that now we can also define and study the full set of conductivities corresponding to the $U(2)$ symmetry. Nothing special occurs of course in the unbroken

[6] The appearance of unexpected massless modes related to symmetry enhancement in the context of Bose condensates was as well found in [75]

phase, there are simply four diagonal conductivities for all the four bulk gauge fields. In the broken phase there are however interesting new phenomena. In particular there are now off-diagonal conductivities that do not simply vanish. In addition we have found that also the diagonal conductivities in the $(1)-(2)$ sector, the one containing the type II Goldstone mode, have delta-function poles at zero frequency. In this sense this sector is still superconducting. Moreover, going to a decoupling basis for this sector leads to a very suggestive result: the conductivity develops a Drude-like peak characteristic of metals on top of the infinite DC conductivity. On the other hand Landau's criterion for superfluidity does not hold in this sector. Recall that this says that superfluidity takes place for flow velocities v that are smaller than the critical velocity v_c where $v_c = \min_i \omega_i(k)/k$ for all excitation branches i and over all momenta k [76, 77]. For a type II NG mode the critical flow velocity is expected to be zero; we explore this in the next subsection.

A second difference concerns the fate of the diffusive modes. In the unbroken phase there are simply four diffusive modes, one for each gauge field in the AdS bulk. In the broken phase there is one purely imaginary gapped 'pseudo-diffusive' mode in the $(0)-(3)$ sector, i.e. in the sector isomorphic to the $U(1)$ s-wave superfluid. Since there is still one unbroken $U(1)$ symmetry there is also a normal diffusive mode for the preserved $U(1)$ symmetry. In the $(1)-(2)$ sector we have however two diffusive modes in the unbroken phase. Going through the phase transition these two modes can pair up and move off the imaginary axis, becoming a pair of usual gapped quasinormal modes with real and imaginary parts in their frequencies. Generically the imaginary part of this gap is smaller (i.e. it lies closer to the real axis) then the gap of the purely imaginary mode in the $(0)-(3)$ sector. A large, generic perturbation will in its late time response pattern excite both the $(0)-(3)$ and the $(1)-(2)$ sector. The late time response of the $U(2)$ invariant order parameter $\sqrt{|\mathcal{O}_1|^2+|\mathcal{O}_2|^2}$ will therefore be dominated by these paired modes and show an oscillatory behavior in contrast to the response pattern of the order parameter in the $U(1)$ case [67].

Another remarkable QNM is the special gapped mode, i.e. the partner mode of the type II NG boson. At very high temperatures this mode and the one which at $T = T_c$ leads to the sound mode are degenerate. As we lower the temperature the gap of these modes becomes different and, for $T < T_c$, it is expected that $\mathrm{Re}(\omega(k=0))$ for the Special Gapped mode is proportional to $q\mu$ [29, 65]. In particular we find $\omega \sim 1.1\mu$ even if $q = 1$ in our conventions. The deviation we found is possibly related to the absence of certain generators in our model **??**. Numerical uncertainties cannot, however, be discarded. It would be interesting to test this by considering an enlarged symmetry model in the bulk.

7

Spontaneous Symmetry Breaking II

In this section we continue our study of the SSB in holography. More concretely, we answer an opened question that arose in our model: Is the Landau criterion still valid?. Which are the implications of applying such criterion on the usual HS and on the non-abelian extension that we have presented?.

In order to answer these questions we investigate the stability of the different phases in presence of superflow via a QNM analysis of the $U(2)$ model. This automatically will give new and valuable information about the usual $U(1)$ holographic superfluid since a subsector of the linear fluctuations in the $U(2)$ model is isomorphic to it.

The chapter is organized as follows: In section 7.1 we first review the concept of the Landau criterion. After this, in section 7.2 we explain how to introduce superfluid velocity in holography following [78, 79]. Making the comparison of the free energy of the superflow with the normal phase we are able to reproduce the usual phase diagram. Then, in section 7.3, we study the QNM spectrum with the superflow. In particular we calculate the direction dependent speed of sound. We indeed find that as the superfluid velocity is increased the speed of sound in opposite direction to the superflow is diminished and eventually vanishes at a critical velocity v_c. Increasing the superfluid velocity even further this sound velocity becomes negative. This is to be interpreted as the appearance of a negative energy state in the spectrum. In principle that would be enough to argue for instability but at basically no price the QNM analysis can give us an even clearer sign of instability. It is well-known that the imaginary part of the QNMs have to lie all in the lower half plane. If they fail to do so an exponentially growing mode with amplitude $\phi \propto \exp(\Gamma t)$ appears in the spectrum. It is not necessary for this mode to have zero momentum. In fact we see that if we increase the superfluid velocity beyond the critical value the imaginary part of the sound mode quasinormal frequency moves into the upper half plane. And it does so attaining a maximum for non-zero momentum. We see that this behavior is necessary to connect the phase diagram continuously to the normal phase. Then moving slightly aside we study the conductivities with superflow. This has been done before but only in the transverse sector and here we present results for the longitudinal sector.

Finally, in section 7.4 we briefly investigate the fate of the type II Goldstone mode in the $U(2)$ model. We study both the gauged and the ungauged model of previous chapter. Landau's criterion suggests that these setups do not sustain any finite superflow since $\min \frac{\epsilon(p)}{p} = 0$ for quadratic dispersion relations. Again we can not only look at the real part but also at the imaginary part. We indeed find poles in the upper half plane for non-zero momenta for all temperatures and superfluid velocities for the gauged and the

ungauged model [1].

Let us also mention some shortcomings of our analysis. We always work in the so-called decoupling limit in which the metric fluctuations are suppressed. Therefore we do not see the pattern of first and second (and fourth) sound typical for superfluids. In the decoupling limit only the fourth sound, the fluctuations of the condensate, survive. Another shortcoming is that we can apply the Landau criterion only to the QNMs. As in superfluid Helium there exist most likely other excitations, such as vortices, that might modify the value of the critical velocity. The question of if and how solitons of holographic superfluids determine the critical superfluid velocity has been investigated in [83].

[1] Models with one $U(1)$ gauge field and two complex scalars similar to our ungauged model were studied before in [80] and recently in [81] (see also [82]). There the two scalars had however different masses and this should prevent the appearance of the ungapped type II Goldstone mode.

7.1 The Landau criterion

The characteristic property of a superfluid is its ability to flow totally frictionless through thin capillaries. It is useful to think of a superfluid as a two component liquid. One component is the ground state with a macroscopic occupation number and the other is the normal component, subject to friction and viscosity. At very low temperatures the normal component can be described as the gas of elementary quasi particle excitations above the macroscopically occupied ground state. A famous argument due to Landau [76,84,85] sets a limit to the flow velocity that the condensate can obtain. The essence of the argument is as follows. At zero temperature the energy of a quasiparticle excitation of momentum $\vec{p}$ is $\epsilon(\vec{p})$ in the rest frame of the condensate. If we imagine a situation in which the condensate moves with constant velocity $\vec{v}$ the energy cost in creating a quasiparticle is

$$\epsilon'(\vec{p}) = \epsilon(\vec{p}) + \vec{v} \cdot \vec{p}\,. \tag{7.1}$$

In particular if $\vec{p}$ is anti-parallel to the flow velocity $\vec{v}$ this energy is diminished and eventually goes to zero. If $\epsilon' < 0$ it is energetically favorable for the system to create elementary excitations and populate states with this effective negative energy. Since the superfluid velocity $\vec{v}$ is kept constant this means that eventually the condensate gets completely depleted and the superflow stops. It follows that there is a critical flow velocity above which the superfluid ceases to exist. The famous Landau criterion for the existence of superflow is therefore

$$v_{\max} = \min \frac{\epsilon(p)}{p}\,, \tag{7.2}$$

where the minimum over all elementary excitation branches has to be taken. It is known for example for superfluid helium that the low temperature normal component can be well described as a gas of phonons and rotons and that the critical velocity is not determined by the minimum of the phonon and roton dispersion relation but rather by the excitation of vortices, resulting in a much lower critical velocity.

At higher temperatures there is always a normal component present and therefore the energy of an excitation of a superfluid with superflow can not be obtained by a (Galilean) boost as in equation (7.1). It is however still true that the energy will depend on the superfluid velocity and that it can become negative if the superfluid velocity is too large. At finite temperature the criterion is therefore that the superflow is stable as long as the energy of all quasiparticle excitations is positive. If in a superfluid the only low energy excitations are the phonons that criterion is basically the statement that the superflow dependent sound velocity is positive for all directions.

In [78, 79] an s-wave superfluid in 2+1 dimensions with superflow was constructed and it was pointed out that there is indeed a critical velocity above which the superfluid state ceases to exist. The phase diagram obtained in these works was based on comparing the free energy of the superflow with the free energy of the normal phase. It turned out that the phase transition from the superfluid phase to the normal phase was either first or second order depending on the temperature. Remarkably enough, in 3+1 dimensions there is some range of masses of the condensate for which the phase transition is always of second order type [86]. Another way of establishing the phase diagram has been used in [87]. There the supercurrent was fixed and it was argued that the phase transition is always first order.

The physical significance of the comparison of the free energies of the state with superflow and the normal state is not totally clear, since for all temperatures below the critical temperature the normal state is unstable towards condensation to the superfluid state without superflow. Indeed the superflow by itself is a metastable state only [85] as emphasized already in [78]. We propose a different method of characterizing the phase diagram more directly related to the stability criterion (7.2).

7.2 The $U(2)$ superfluid with superflow

We consider the gauged model introduced in the previous chapter (see 6.4). In order to find background solutions corresponding to a condensate with non-vanishing superfluid velocity we proceed as follows. First note that the scalar field $\lambda(r)$ can be set to zero by a $U(2)$ gauge transformation. For the scalar Ψ we demand then that the non-normalizable mode vanishes. By a residual $U(1)$ gauge transformation we can also take Ψ to be real.

Now we need to define what we mean by the superflow. Let us discuss this for a moment from a field theory perspective. In a multi-component superfluid with $U(2)$ symmetry we can in principle construct the four (super) currents

$$J_a^\mu = \Phi^\dagger T_a \nabla^\mu \Phi - (\nabla^\mu \Phi)^\dagger T_a \Phi \,, \tag{7.3}$$

where $\nabla^\mu = \partial^\mu - i A_a^\mu T_a$ is the covariant derivative and Φ is the condensate wave function which transforms as a doublet under $U(2)$. If the condensate is such that one of the spatial currents does not vanish we can speak of a state with non-vanishing superflow. By a gauge transformation we can always assume the condensate to take some standard form, e.g. $\Phi = (0, \phi)^T$ and represent the non-vanishing superflow in terms of constant gauge fields. Since we are interested in the case where we break the $U(2)$ symmetry spontaneously to $U(1)$ we only allow a non-zero gauge field in the overall $U(1)$ corresponding to the generator T_0. Furthermore by an $SO(2)$ rotation we can take the gauge field to point into the x direction. From (7.3) it is easy to see that such a superflow has non-vanishing currents $J_x^{(0)}$ and $J_x^{(3)}$. In order to find solutions with non-trivial charge we also need to introduce a chemical potential. Again in order to preserve the full $U(2)$ symmetry we also allow a chemical potential only for the overall $U(1)$ charge.

Returning now to Holography these considerations determine the ansatz for the gauge fields to be of the form

$$A^{(0)} = A_t^{(0)}(r) dt + A_x^{(0)}(r) dx \,, \qquad A^{(3)} = A_t^{(3)}(r) dt + A_x^{(3)}(r) dx \,. \tag{7.4}$$

While we introduce sources only for $A^{(0)}$ the fact that also the current $J_\mu^{(3)}$ is non-vanishing demands that $A^{(3)} \neq 0$. The physical interpretation for this fact is that the system forces the appearance of a charge density $\rho^{(3)} \neq 0$ (as noticed already in previous chapter) and a current $J_x^{(3)}$ in the vacuum with superflow. This is in turn closely related to the presence of type II Goldstone bosons in the spectrum [26].

amounts

At this point it is important to note that the above identification is only valid in the superfluid phase, that is, whenever $\Psi \neq 0$. A constant background value of the gauge field A_x in the normal phase is not physically meaningful since there is no notion of superflow.

For the reasons outlined above we choose the asymptotic boundary conditions for the gauge fields to be

$$\begin{aligned} A_t^{(0)}(r \to \infty) &= 2\bar{\mu} \,, & A_t^{(3)}(r \to \infty) &= 0 \,, \\ A_x^{(0)}(r \to \infty) &= 2\bar{S}_x \,, & A_x^{(3)}(r \to \infty) &= 0 \,, \end{aligned} \tag{7.5}$$

where $\bar{\mu}$ is to be identified with the chemical potential of the dual theory and $\bar{S}_x$ is related to the superflow velocity. We have included a factor of two in the definitions of $\bar{\mu}$ and

$\bar{S}_x$ for the following reason. The background field equations can be recast in the form of those derived from the $U(1)$ model in [78, 79] by using the field redefinitions

$$\begin{aligned} A_0 &= \frac{1}{2}(A_t^{(0)} - A_t^{(3)})\,, & \xi &= \frac{1}{2}(A_t^{(0)} + A_t^{(3)})\,, \\ A_x &= \frac{1}{2}(A_x^{(0)} - A_x^{(3)})\,, & \varsigma &= \frac{1}{2}(A_x^{(0)} + A_x^{(3)})\,, \end{aligned} \tag{7.6}$$

for which the background equations now read

$$\Psi'' + \left(\frac{f'}{f} + \frac{2}{r}\right)\Psi' + \left(\frac{A_0^2}{f^2} - \frac{A_x^2}{r^2 f} - \frac{m^2}{f}\right)\Psi = 0\,, \tag{7.7}$$

$$A_0'' + \frac{2}{r}A_0' - \frac{2\Psi^2}{f}A_0 = 0\,, \tag{7.8}$$

$$A_x'' + \frac{f'}{f}A_x' - A_x\frac{2\Psi^2}{f} = 0\,, \tag{7.9}$$

$$\xi'' + \frac{2}{r}\xi' = 0\,, \tag{7.10}$$

$$\varsigma'' + \frac{f'}{f}\varsigma' = 0\,. \tag{7.11}$$

It can be checked that we recover the usual $U(1)$ system describing the $U(1)$ holographic superconductor in the presence of superfluid velocity (see for instance [86]). The chemical potential $\bar{\mu}$ is therefore the chemical potential for the field A_0 which plays the role of the temporal component of the (single) gauge field, and A_x plays the role of the spatial component of the single gauge field of [78,79,86]. This explicitly shows that the background of the $U(2)$ model is identical to that of the $U(1)$ superconductor, even for a nonzero superfluid velocity.

An immediate consequence of the fact that the background equations are those of the $U(1)$ holographic superfluid is that, at first sight, the $U(2)$ system seems to be able to accommodate a superflow. However, as already argued, this is in direct contradiction with the Landau criterion of superfluidity [85] due to the presence of a type II Goldstone in the spectrum. Of course, having found solutions to the equations of motion does not yet say anything about the stability. In fact as we will explicitly see the type II Goldstone will turn into an unstable mode and therefore make the whole $U(2)$ solution with superflow unstable.

Equations (7.7)-(7.9) are non-linear and have to be solved using numerical methods. Notice that (7.10) and (7.11) are decoupled. They correspond to the preserved $U(1)$ symmetry after having broken spontaneously $U(2) \to U(1)$. The asymptotic behavior of the fields close to the conformal boundary is

$$\begin{aligned} A_0 &= \bar{\mu} - \frac{\bar{\rho}}{r} + \dots\,, \\ A_x &= \bar{S}_x - \frac{\bar{\mathcal{J}}_x}{r} + \dots\,, \\ \Psi &= \frac{\psi_1}{r} + \frac{\psi_2}{r^2} + \dots\,. \end{aligned} \tag{7.12}$$

The asymptotic quantities are related to the physical ones by

$$\begin{aligned} \bar{\mu} &= \frac{3}{4\pi T}\mu\,, & \bar{\rho} &= \frac{9}{16\pi^2 T^2}\rho\,, \\ \bar{S}_x &= \frac{3}{4\pi T}S_x\,, & \bar{\mathcal{J}}_x &= \frac{9}{16\pi^2 T^2}\mathcal{J}_x\,, \\ \psi_1 &= \frac{3}{4\pi T}\langle\mathcal{O}_1\rangle\,, & \psi_2 &= \frac{9}{16\pi^2 T^2}\langle\mathcal{O}_2\rangle\,. \end{aligned} \tag{7.13}$$

We are working in the grand canonical ensemble, then we fix the chemical potential μ. The temperature is defined by $T/\mu \propto 1/\bar{\mu}$. For studying the evolution of the condensate as a function of the superfluid velocity, the natural way to proceed is to work with S_x/μ as our free parameter together with temperature. Notice that both asymptotic modes of the scalar field are actually normalizable [66]. From now on we stick to the $\mathcal{O}_2$ theory, for which $\psi_1 = 0$ and $\langle\mathcal{O}_2\rangle$ is the vev of a scalar operator of mass dimension two in the dual field theory. Notice that the fields ξ and ζ corresponding to the unbroken $U(1)$ are given by

$$\begin{aligned} \xi &= \bar{\mu} - \bar{\rho}/r\,, \\ \zeta &= \bar{S}_x\,, \end{aligned} \tag{7.14}$$

even with non-vanishing condensate.

The values of the condensate as a function of temperature and superfluid velocity shown in Figure 7.1 reproduce the previous results of [78, 79]. In the plot and in the rest of this chapter the temperature is measured with respect to the critical temperature of the phase transition with no superfluid velocity, i.e. $T_c \approx 0.0587\mu$.

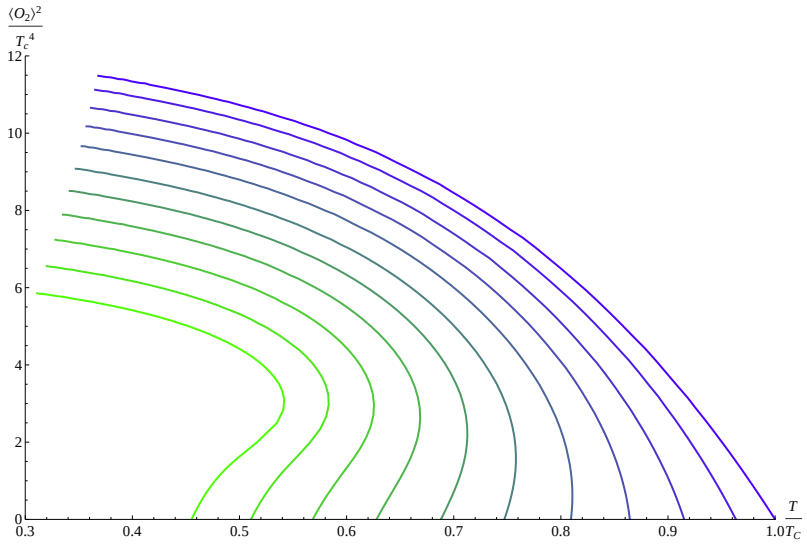

Figure 7.1: The condensate for different values of the superfluid velocity, ranging from $\frac{S_x}{\mu} = 0.005$ (right) to $\frac{S_x}{\mu} = 0.530$ (left).

7.2.1 Free Energy

In this section we compute the free energy of the condensed phase and compare it to the free energy of the unbroken phase as done in [78, 79]. After appropriate renormalization

of the Euclidean on-shell action and using the boundary conditions (7.12), the free energy density reads

$$F = -TS_{ren} = -\bar{\mu}\bar{\rho} + \bar{S}_x\bar{\mathcal{J}}_x + \int_1^\infty dr \left(\frac{2r^2A_0^2}{f} - 2A_x^2\right)\Psi^2\,. \tag{7.15}$$

In the normal phase $\Psi = 0$, regularity at the horizon forces the A_x gauge field to have a trivial profile along the radial direction in the bulk and therefore not to contribute to the free energy, i.e. $\bar{\mathcal{J}}_x = 0$. This is in accordance with the fact that in absence of a scalar condensate it is not possible to switch on a superfluid velocity anymore. Switching on the spatial component of the gauge field in the normal phase describes a pure gauge transformation that does not affect the free energy of the system. In the broken phase instead, different superfluid velocities are physically distinguishable. It is important to emphasize that one is actually comparing the normal phase at vanishing superfluid velocity with the superconducting phase at different values of the superfluid velocity, and that the normal phase is unstable towards condensation without superflow for any $T < T_c$. Therefore, the physical relevance of this comparison is not completely clear. We will see later on that actually the Landau criterion establishes a different transition temperature for the superfluid phase. Nevertheless the free energy gives a natural first approach to characterize the phase diagram of the system. We would like to remark that the superflow phase is just a metastable phase, since the true background is the static condensed phase which always has lower free energy [85], [78].

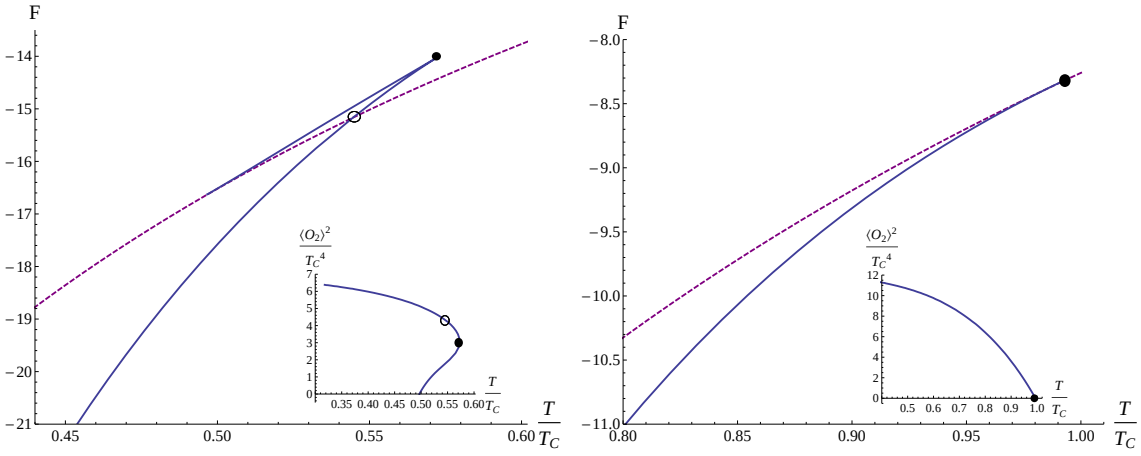

Figure 7.2: Free energy of the condensed (solid line) and normal (dashed line) phases for $\frac{S_x}{\mu} = 0.5$ (left) and $\frac{S_x}{\mu} = 0.05$ (right). The small plots show the behavior of the condensate. The open circle corresponds to the critical temperature $\tilde{T}$ whereas the filled circle corresponds to the spinodal point (max. overheating).

In Figure 7.2 the free energy of both the normal and condensate phase is plotted for different values of $\frac{S_x}{\mu}$. The different behavior for large and small values of the superfluid velocity is apparent. For large superfluid velocity the transition is first order as can be seen from the left panel in Figure 7.2, indicated by the open circle. Coming from low temperatures the system can still be overheated into a metastable state until the point of spinodal decomposition where the order parameter susceptibility $\partial\langle\mathcal{O}\rangle/\partial\mu$ diverges, indicated by the filled circle.

For low superfluid velocities the normal phase free energy and the condensate free energy match smoothly at a second order phase transition. The resulting phase space is contained in Figure 7.6 and reproduces the previous analysis in [78, 79].

The phase transition found from considerations of the free energy is however only apparent. We call the temperature at which the free energies of the condensate phase with superflow and the free energy of the normal phase coincide $\tilde{T}$ from now on. The temperature at which the (second order) phase transition occurs without superflow we will denote by T_c. As we will show now the superflow becomes unstable at temperatures below $\tilde{T}$ as implied by the Landau criterion applied to the sound mode. This temperature we denote by T^*.

7.3 Landau criterion for the $U(1)$ sector

In this section we analyze the QNM spectrum of the $(0)-(3)$ sector, which is identical to the original $U(1)$ holographic superconductor in the presence of superfluid velocity [78, 79]. We focus on the behavior of the lowest QNM, the type I Goldstone boson, with special emphasis on the velocity and the attenuation constant and their dependence on the superfluid velocity and on the angle of propagation with respect to the flow.

To study the QNM spectrum we consider linearized perturbations around the background of the fields of the form $\delta\phi_I = \delta\phi_I(r)\exp[-i(\omega\, t - |k|\, x\cos(\gamma) - |k|\, y\sin(\gamma)]$. Specifically we consider the fluctuations

$$\begin{aligned} \delta\hat{\Psi}^T &= (\eta(r), \sigma(r))\,, \\ \delta A^{(0)} &= a_t^{(0)}(r)dt + a_x^{(0)}(r)dx + a_y^{(0)}(r)dy\,, \\ \delta A^{(3)} &= a_t^{(3)}(r)dt + a_x^{(3)}(r)dx + a_y^{(3)}(r)dy\,, \end{aligned} \tag{7.16}$$

where in the case of the gauge fluctuations we work with the linear combinations already defined by (7.6), i.e. $a_\mu^{(-)} \equiv \frac{1}{2}(a_\mu^{(0)} - a_\mu^{(3)})$ and $a_\mu^{(+)} \equiv \frac{1}{2}(a_\mu^{(0)} + a_\mu^{(3)})$. The linearized equations are rather complicated and we list them in appendix A.3. The numerical techniques used to obtain the hydrodynamic modes in coupled systems are well known. We don't elaborate on them here, referring the interested reader to [63] and [57].

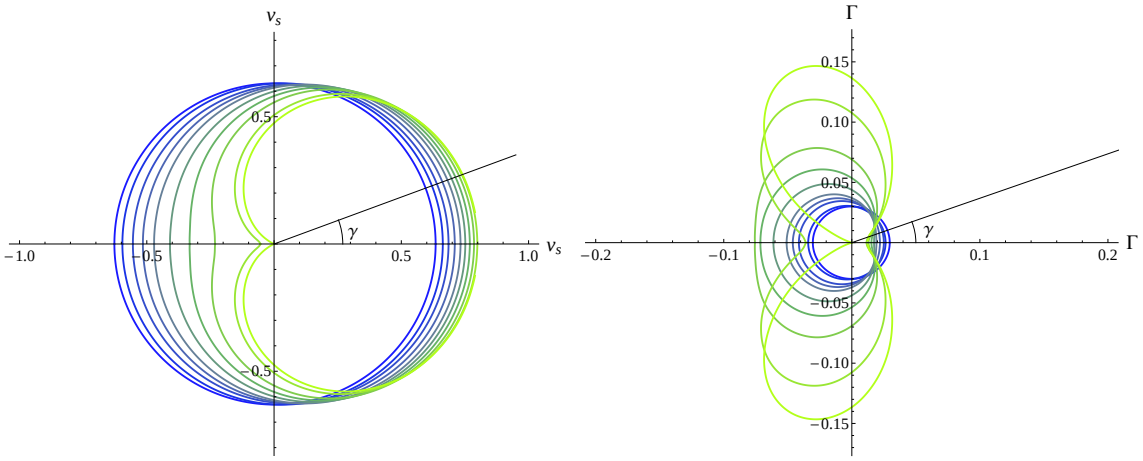

Figure 7.3: Sound velocity and damping for $T = 0.7T_c$ and several superfluid velocities from $S_x/\mu = 0$ (blue) to $S_x/\mu = 0.325$ (green). The radius represents the absolute value of the sound velocity (left) and attenuation constant (right) as a function of the angle γ between the momentum and the superfluid velocity.

In Figures 7.3 and 7.4 we represent the velocity and the attenuation of the type I Goldstone mode. Its dispersion relation is given by $\omega(k) = v_s(\gamma)k + (b - i\Gamma(\gamma))k^2$ at low momentum [2]. Figure 7.3 shows the angle dependent variation of the sound velocity and damping constant for a fixed temperature and varying values of the superfluid velocity. Figure 7.4 shows the same at fixed superfluid velocity but with varying temperature. As one would expect for small S_x/μ and low enough temperature the velocity and damping

[2] The small real constant b does not play a role here since for small enough momentum the linear part proportional to v_s dominates.

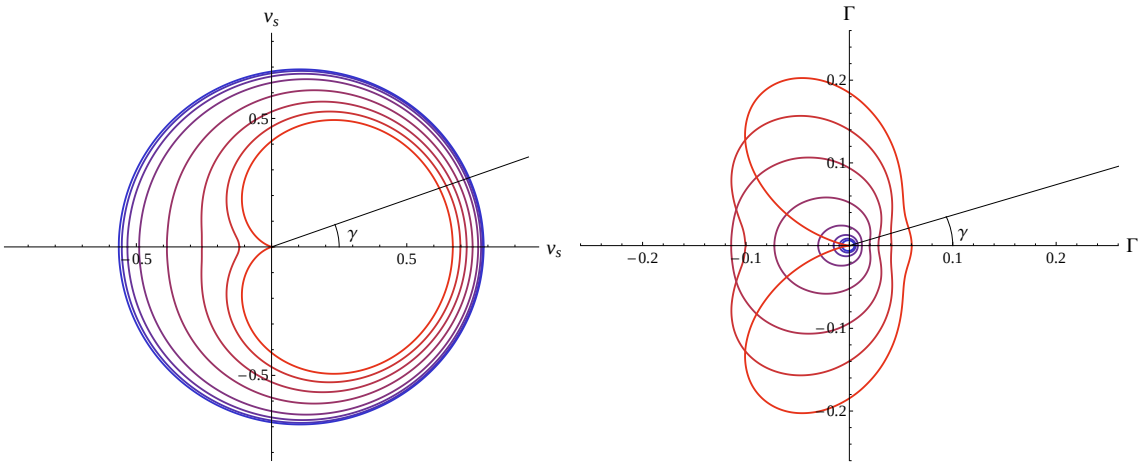

Figure 7.4: Sound velocity (left) and attenuation constant (right) for $S_x/\mu = 0.2$ as a function of the angle γ and for a range of temperatures from $T = 0.85T_c$ (red) to $T = 0.57T_c$ (blue).

constant are almost isotropic. As the superfluid velocity is increased or the temperature is increased the plot becomes more and more asymmetric. The anisotropy of the system is such that we see an enhancement of the sound velocity and a reduction of the damping in the direction of the superflow.

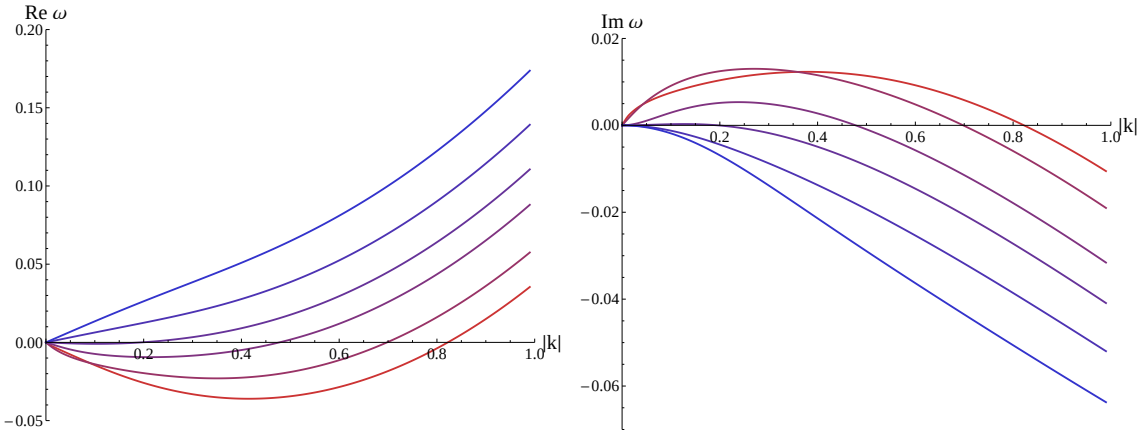

Figure 7.5: Real (left) and imaginary (right) parts of the frequency of the lowest hydrodynamic mode (type I Goldstone mode) versus momentum at $S_x/\mu = 0.1$ and $\gamma = \pi$ for different temperatures from $T = \tilde{T} = 0.970T_c$ (red) to $T = 0.905Tc$ (blue). The instability appears at $T^* = 0.935T_c$.

The most interesting feature of the system is found however in the opposite direction to the superfluid velocity. As one can see in both plots, at $\gamma = \pi$ the reduction in the sound velocity is strongest and eventually both the attenuation constant and the sound velocity vanish simultaneously. It is important to stress that this happens below the temperature $\tilde{T}$. If one continues increasing the temperature (or equivalently increasing the superfluid velocity at fixed temperature) one finds that the real part of the frequency becomes negative and that its imaginary part crosses to the upper half plane, as depicted in

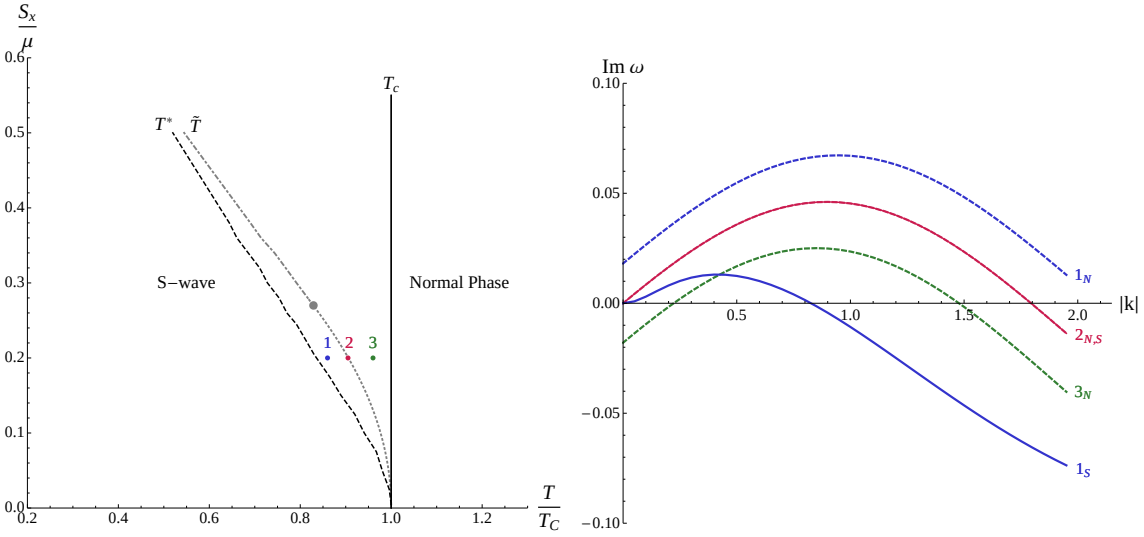

Figure 7.6: (Left) Phase diagram after the study of the QNMs . The grey dashed line corresponds to $\tilde{T}$, the apparent transition temperature found by direct analysis of the free energy. At a certain point (disk) the transition in free energy changes from 2nd order (dotted) to 1st order (dash-dotted). The black solid line corresponds to the critical temperature in absence of superfluid velocity. The black dashed line signals the physical phase transition at T^*, the temperature at which the local instability appears. Points 1, 2 and 3 indicate the values of temperature and velocity used in the plot on the right. (Right) Imaginary part of the lowest QNM for different temperatures at fixed $S_x/\mu = 0.2$ and $\gamma = \pi$. Dashed lines were obtained in the normal phase whereas solid lines were calculated in the superfluid phase.

Figure 7.5. This signals the appearance of a tachyonic mode. T^* is the temperature where both the instability appears and the speed of sound becomes negative. This temperature actually signals the end of the superfluid phase according to the Landau criterion, and therefore we interpret it as the physical phase transition temperature.

In Figure 7.6 (left) we present the phase diagram resulting from the QNM analysis. To illustrate the situation, on the right plot we show the behavior of the relevant QNM[3] at three different points of the phase diagram[4] (points labelled 1, 2, 3 on the left plot). At $\tilde{T} < T < T_c$ in the unbroken phase (line 3_N), the mode that was responsible for the transition to the homogeneous superfluid phase without superfluid velocity is shifted and becomes unstable at finite momentum. This behavior reflects the fact that the system is unstable for $T \leq T_c$, the mode being shifted in momentum due to the constant nonzero value of A_x. At $T = \tilde{T}$ (lines $2_{N,S}$) the lowest mode becomes unstable at $k = 0$. It is at this point that the free energy of the homogeneous superfluid phase equals that of the normal phase. Hence, the free energy analysis, which only captures the $k = 0$ dynamics, predicts a phase transition at this temperature. For the particular superfluid velocity in the plot the phase transition is second order. Finally, the fate of the QNM for $T^* < T < \tilde{T}$ is shown in lines 1_N (for the normal phase) and 1_S (for the homogeneous superflow phase).

[3] In the unbroken phase this is just the lowest scalar QNM, while in the broken phase it is the sound mode at fixed S_x/μ.

[4] An analogous discussion and phase space was found at weak coupling in [88] after the appearance of the first version of the paper in which this chapter is based.

One can see that the Goldstone mode in the superfluid phase is unstable for a finite range in momentum. Only at T^* this mode becomes stable again as shown in Figure 7.5. It is at this temperature that the homogeneous superflow phase becomes stable according to the Landau criterion since the sound velocity becomes positive (moreover the imaginary part of the QNM dispersion relation lies entirely in the lower half plane).

Therefore the QNM results indicate that a phase transition occurs at a lower temperature $T^* < \tilde{T}$. Similarly, if we imagine the system at fixed temperature and start rising the superfluid velocity, both v_s and Γ will vanish at some value of S_x/μ, which we claim is indeed the critical velocity v_c of the superfluid, in the sense of the Landau criterion.

As a very interesting fact, notice that the imaginary part of the mode exhibiting the instability has a maximum at finite momentum as well. The fact that the instability appears at finite momentum suggests that there might exist a new (meta)stable intermediate phase above T^* with a spatially modulated condensate. Examples of such instabilities towards spatial modulation have been discussed before in [89–91].

It is important to remark that, as shown in Figure 7.6 (right), for temperatures $T^* < T < \tilde{T}$ the mode responsible for the transition to the (shifted) homogeneous stationary phase (line 1_N) and the new unstable mode (line 1_S) show maxima at different momenta. We take this as an indication for existence of a new metastable in- homogeneous phase. The wave number of the modulation in this phase should be determined by the maximum of the line 1_S.

Recall that the Landau criterion is formulated uniquely in terms of $\mathrm{Re}(\omega)$. At a given temperature the critical velocity corresponds to the superfluid velocity at which $v_s = 0$, or equivalently to the value of S_x/μ where $\mathrm{Re}(\omega)$ becomes negative (see Figure 7.5). That the criterion is a statement about $\mathrm{Re}(\omega)$ reflects the fact that it holds also at zero temperature. At finite temperature the dispersion relation of the gapless mode gets itself altered due to both the superfluid velocity and the temperature [85, 92], implying that generically the critical value of S_x/μ at fixed temperature *does not* correspond to the velocity of sound at the same temperature and vanishing superfluid velocity.

An extra comment is in order here regarding the phase of the system for $T_c > T > \tilde{T}$. The fact that in the unbroken phase the lowest QNM is unstable in this regime (see line 3_N in Figure 7.6) of course indicates that the normal phase is unstable. Let us comment on this. Since the condensate vanishes in the normal phase, there exists no physical notion of superfluid velocity in this phase; different choices of A_x are just different frame choices. In particular, a constant A_x simply acts as a shift in momentum in the unbroken phase, as can be seen from the fact that the maximum of the QNM is centered at a momentum equal to the value of the gauge field at the conformal boundary. Therefore the normal phase is unstable for any temperature lower than the critical temperature T_c towards the formation of a superfluid without superflow. On the other hand, we know that the homogeneous condensate solution with finite velocity does not exist in this region, and moreover it is unstable for $T > T^*$. We see two possibilities for the completion of the phase diagram in this region. First, the system could simply fall down to the true ground state, which is the condensate with no superflow. At finite S_x/μ this is still a solution which minimizes the energy albeit with a condensate that is not real anymore but rather has a space dependent phase such that $\vec{\nabla}\Phi = 0$. This is simply the gauge transformed homogeneous ground state without superflow. On the other hand, the fact that we found an instability at finite momentum in the temperature range $T^* < T < \tilde{T}$ could indicate that there is a spatially modulated (metastable) phase even in the range $T^* < T < T_c$, namely a striped superfluid.

Due to the smooth appearance of the unstable mode we expect the transition at T^* to that phase to be 2nd order, although this should be studied in detail by constructing the correct inhomogeneous background. The explicit construction of this phase goes however substantially beyond the purpose of this chapter.

7.3.1 Longitudinal conductivities in the $U(1)$ sector

In this section we compute the conductivities in the $(0)-(3)$ sector in the presence of superfluid velocity. As far as we are aware, only the transverse conductivities have been computed so far (see for instance [86, 87]). In contrast, here we focus on the longitudinal conductivities. These are calculated, via the Kubo formula

$$\sigma = \frac{i}{\omega}\langle J^x J^x \rangle \,, \tag{7.17}$$

from the two point function

$$\mathcal{G}_{IJ} = \lim_{\Lambda\to\infty} \left(\mathcal{A}_{IM}\mathcal{F}^M_{kJ}(\Lambda)'\right) \,, \tag{7.18}$$

where the matrix $\mathcal{A}$ can be read off from the on-shell action. $\mathcal{F}$ is the matrix valued bulk-to-boundary propagator normalized to the unit matrix at the boundary. Since we are only interested in the entry of the matrix corresponding to $\langle J^x J^x \rangle$ and the matrix $\mathcal{A}$ is diagonal, we just need one element, i.e. $\mathcal{A}_{xx} = -\frac{f(r)}{2}$. In order to construct the bulk-to-boundary propagator one needs a complete set of linearly independent solutions for the perturbations of the scalar and gauge fields. This implies solving the system of equations given in appendix A.3 at zero momentum. The method follows closely the one detailed in [57]. Notice that there is a surviving coupling between the gauge fields and the scalar perturbations mediated by A_x. This makes the computation of the conductivities more involved than in the case without superflow.

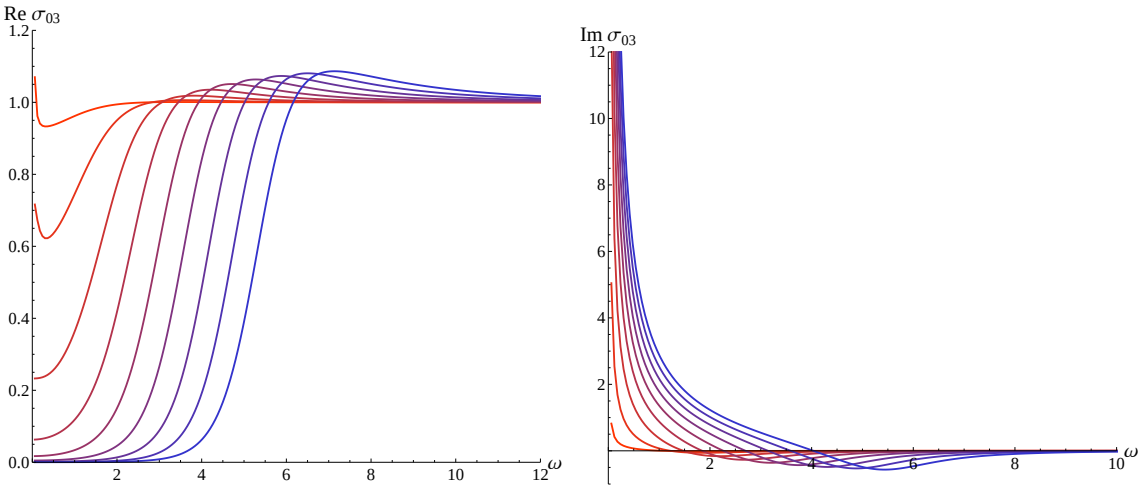

Figure 7.7: Plots of the Real (left) and Imaginary (right) parts of the conductivity for fixed $S_x/\mu = 0.05$. Different lines correspond to different temperatures from $T = 0.99T_c$(red) to $T = 0.38T_c$ (blue).

Our results show little deviation from what was found at zero superflow. The most interesting new feature is a low frequency peak which appears due to the coupling between

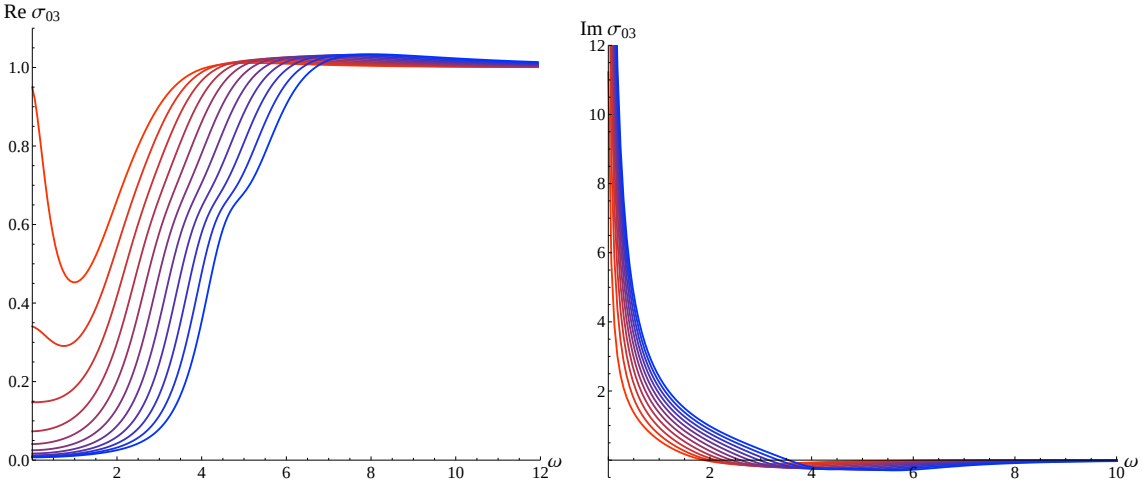

Figure 7.8: Real (left) and imaginary (right) parts of the conductivity for fixed $S_x/\mu = 0.4$. Different lines correspond to different temperatures in the range $T = 0.35T_c$ (blue) - $0.65T_c$ (red).

the gauge and the scalar sectors induced by the superfluid velocity. In Figures 7.7 and 7.8 we present the results for different values of S_x/μ. As expected the behavior for small superfluid velocity far from the critical temperature is the same as the one obtained in [59]. Close to T^* a bump is generated in the real part of the conductivity at $\omega \approx 0$. This indicates the existence of a mode with very small imaginary gap. The mode responsible for this behavior is the pseudo-diffusive mode described in [63]. Due to the conserved $U(1)$ symmetry of the unbroken phase, there exists a diffusive (gapless) mode in the QNM spectrum of the theory. Once the symmetry is spontaneously broken, this mode develops a purely imaginary gap that increases as we lower the temperature. Therefore, for high enough temperatures below the phase transition, the gap of the pseudo-diffusive mode at $k = 0$ is very small and this implies the appearance of a peak at small frequencies in the conductivity as we can see in the figures. If we lower the temperature, the bump starts disappearing simply because the gap of the pseudo-diffusive mode becomes larger. Although this mode was already present in the analysis of the conductivities without superflow, it is only in our present case that it affects the conductivity, due to the coupling at zero momentum between the gauge and scalar sectors mediated by the field A_x. The size of the peak is proportional to the size of that coupling, i.e. it grows with S_x/μ.

7.4 Landau criterion for holographic Type II Goldstone bosons

In the previous section we studied the lowest lying QNM contained in the $(0)-(3)$ or $U(1)$ sector of the theory for various values of the superfluid velocity and arbitrary angle between the momentum and the direction of the superflow. In this section we extend the analysis to the $(1)-(2)$ sector, which is particular of the $U(2)$ model and contains a type II Goldstone boson in the spectrum.

The equations describing the system can be found in appendix A.4. In this case we choose the momentum to lie always in the direction opposite to the superflow because, as we will see, this mode is always unstable. Along with the scalar perturbations prescribed by (7.16) we have to consider the following gauge perturbations in the $(1)-(2)$ sector

$$\begin{aligned} A^{(1)} &= a_t^{(1)}(t,r,x)dt + a_x^{(1)}(t,r,x)dx\,, \\ A^{(2)} &= a_t^{(2)}(t,r,x)dt + a_x^{(2)}(t,r,x)dx\,. \end{aligned} \tag{7.19}$$

Again we use the determinant method of [57] to find the QNMs in this sector. Our results are summarized in Figure 7.9, where the dispersion relation for the lowest QNM mode is shown at a particular superfluid velocity. We checked that the result is qualitatively the same for arbitrary S_x/μ.

The type II Goldstone mode becomes unstable for arbitrarily small superfluid velocities and temperatures below $\tilde{T}$. However, an important difference arises with respect to the $U(1)$ sector. The tachyonic mode does not become stable at any temperature below $\tilde{T}$, contrary to the situation in the $(0)-(3)$ sector, there is no analogous of T^* in this sector. This behavior can be easily interpreted as a reflection of the Landau criterion of superfluidity in our holographic setup: according to (7.2), the critical velocity is zero in any system featuring type II Goldstone bosons, hence for any $T<\tilde{T}$ the superfluid phase is not stable at any finite superfluid velocity. In addition notice that the maximum in the imaginary part occurs at higher values of the momentum as we lower the temperature. In fact as we can see from the figure, lowering the temperature below $\tilde{T}$ the maximum in $\mathrm{Im}(\omega)$ first increases but then starts to decrease again as the temperature is lowered. At the same time it moves out to ever larger values of the momentum.

Note that plots analogous to Figures 7.3 and 7.4 do not make any sense in the $U(2)$ model, since the $(1)-(2)$ sector is unstable at any temperature we have been able to check.

7.4.1 Ungauged model

As it happened before, the background solution is again that of the $U(1)$ superfluid, hence the superflow solution can be accommodated also in the ungauged model. The difference now is that the type II Goldstone mode appears now in the fluctuations of the upper component of the scalar field η, whose equation of motion reads

$$f\eta'' + \left(f' + \frac{2f}{r}\right)\eta' + \left(\frac{(\omega+A_0)^2}{f} - \frac{(k-A_x)^2}{r^2} - m^2\right)\eta = 0\,, \tag{7.20}$$

and is completely decoupled of all other field fluctuations. As noticed in chapter 6 the change of the background due to the condensate is enough to trigger the appearance of the type II Goldstone.

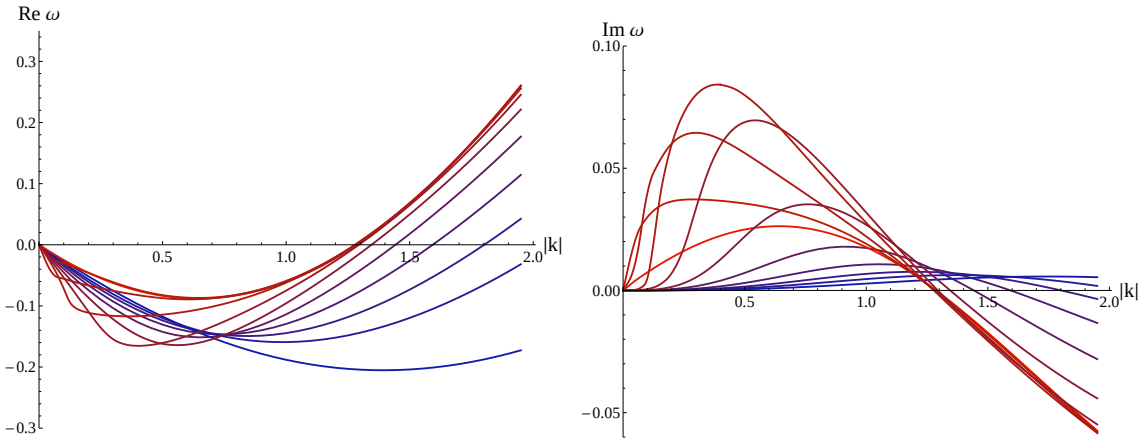

Figure 7.9: Real (left) and imaginary (right) parts of the dispersion relation of the lowest QNM of the $(1)-(2)$ sector in the gauged model for fixed $S_x/\mu = 0.15$ and a range of temperatures from $T = \tilde{T} = 0.95T_c$ (red) to $T = 0.45T_c$ (blue) and momentum anti-parallel to the superfluid velocity.

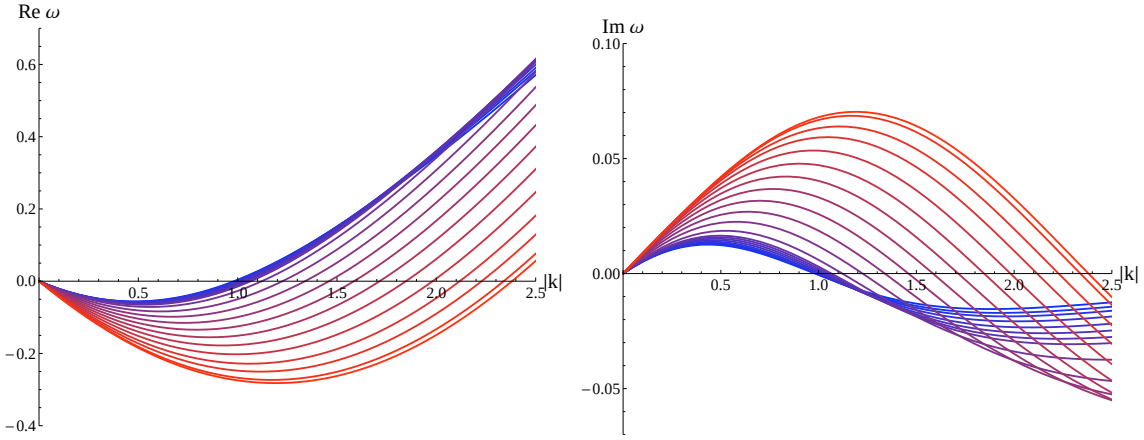

Figure 7.10: Real (left) and imaginary (right) parts of the dispersion relation of the lowest QNM in the $(1)-(2)$ sector of the ungauged model for fixed $S_x/\mu = 0.25$ and a range of temperatures from $T = \tilde{T} = 0.853T_c$ (red) to $T = 0.306T_c$ (blue). Momentum is taken anti-parallel to the superfluid velocity.

It is remarkable that in the ungauged model the type II Goldstone mode is still unstable at any temperature below $\tilde{T}$ for any value of the superfluid velocity. Notice that not including conserved currents for the $SU(2)$ symmetry, the model does not satisfy all theorems on existence of Goldstone bosons. However, the Landau criterion of stability is still valid.

The ungauged model presents a qualitative difference with respect to the gauged model. The value of the momentum at the maximum now decreases as we lower the temperature. This is shown in Figure 7.10, where the dispersion relation of the type II Goldstone at fixed superfluid velocity and for a long range of temperatures is plotted. For arbitrary values of the superfluid velocity we obtained analogous results. increasing the value of the maximum momentum.

7.5 Discussion

We have analyzed the holographic realization of the Landau criterion of superfluidity. The study was motivated by the appearance of type II Goldstone bosons in the model presented in the previous chapter. The quadratic nature of the dispersion relation of the type II Goldstone mode should be responsible for driving the system out of the superfluid phase for arbitrarily small superfluid velocity.

Taking advantage of the fact that the usual $U(1)$ holographic s-wave superconductor is contained in the model, we have revisited the Landau criterion for holographic type I Goldstone modes. When addressing the question of the stability of the condensate at finite superfluid velocity the analysis of the free energy does not give the correct answer. The QNM spectrum contains a tachyonic mode at finite momentum for temperatures $T^* < T < \tilde{T}$. As defined $\tilde{T}$ is the temperature at which free energies of the normal and condensate phase coincide. In contrast, T^* is the temperature where the tachyonic instability arises. Hence, the homogeneous superfluid is stable only for $T < T^*$, see Figure 7.6. The results for the sound velocity as a function of the angle γ between the propagation direction and the superfluid velocity, depicted in Figures 7.3 and 7.4, are perfectly consistent with this statement: at $T = T^*$ and $\gamma = \pi$ the velocity of sound vanishes. This condition can be seen to be equivalent to the Landau criterion and signals the existence of a critical velocity above which the superfluid is not stable anymore.

Since the maximum of the imaginary part of the unstable mode has non-vanishing wave number it is natural to suggest that there might be another, spatially modulated phase for $T > T^*$. The nature or this inhomogeneous phase is however unknown and we leave its explicit construction of even the question of its very existence for future research.

We have also computed the longitudinal conductivities for various superfluid velocities. We see a peak at $\omega = 0$, due to the coupling with the spatial component of the gauge field A_x. The peak decreases as we lower the temperature until it gets completely suppressed (Figure 7.7). We believe that this enhancement of the DC conductivity is caused by the gap of the pseudo-diffusive mode [63] which in the presence of superfluid velocity is formed due to the coupling between the gauge and scalar sectors that takes place even at $k = 0$.

Moving to the $(1) - (2)$ sector, we worked out the impact of the superflow on the type II Goldstone mode. We found that the Landau criterion is effective for arbitrarily small superfluid velocity as depicted in Figure 7.9. The tachyon persists for the whole range of temperatures and (finite) superfluid velocities we have been able to analyze. Hence, we conclude that the critical superfluid velocity for this sector vanishes, in complete accordance with the Landau criterion applied to modes with dispersion relation $\omega \propto k^2$. An analogous result holds for the type II Goldstone mode in the ungauged model.

8

Spontaneous + Explicit Symmetry Breaking

In this chapter we further explore the SSB mechanism and its consequences in holography. To this end we make a deeper exploration of the phase space of the U(2) model introduced in chapter 6. More concretely we focus on the instability that appeared at low temperatures (see figure 6.14). In that model we found that the s-wave superfluid phase is unstable at low temperatures and argued that this instability signaled the appearance of a non-trivial p-wave order parameter. Therefore we would like to construct the true vacuum in that regime. Doing so will lead us to the ideas of competition of phases and of mixed (with both scalar and vector condensates) phases. Therefore not only internal symmetries but spacetime symmetries will break down too. In addition, in this context the possibility of studying the implementation of unbalanced mixtures will naturally appear. As we will see, this implies the explicit breaking of some generators in addition to the spontaneously broken ones.

Let us remark that this is not only interesting from the holographic point of view. An interesting problem in the arena of unconventional superfluids and superconductors is that of the competition and coexistence of different order parameters [93]. A paradigmatic example in the realm of superfluids is that of ^{3}He. At low temperature ^{3}He presents two distinct superfluid phases, denoted as A and B phases [94]. ^{3}He-B is the low temperature (and low pressure) phase and it corresponds to a p-wave superfluid, where the order parameter transforms as a vector under spatial rotations. ^{3}He-A is the higher temperature (and pressure) superfluid phase. It is a chiral p-wave superfluid whose order parameter is a complex vector, and time-reversal and parity symmetry are spontaneously broken. In the domain of unconventional superconductors it has been shown in [95] that for doped three dimensional narrow gap semiconductors such as $Cu_xBi_2Se_3$ and $Sn_{1-x}In_xTe$ there is a competition between s and p-wave superconducting states. Dialing the coupling constants of the two different channels (corresponding to the s and p pairings) leads to a phase diagram where both a p and an s-wave phase exist. Moreover, at the interface of both phases a new $p+is$ state appears. The order parameter for this phase is the combination of a vector and a pseudoscalar, and breaks both time-reversal and parity symmetry, making this state an interesting example of a topological superconductor[1].

In this chapter, building upon the U(2) model of the previous sections, we develop a holographic dual of a superconductor with both s-wave and p-wave condensates. Subse-

[1]This is actually an example of an axionic state of matter. This $p+is$ phase belongs to the class D in the classification [96] of 3D topological superconductors. It possesses gapped Majorana fermions as edge states which give rise to an anomalous surface thermal Hall effect. It would be very interesting to realize holographically this axionic superconducting state (see [97] for a holographic time-reversal symmetry breaking $p+ip$ superconductor).

quently we study the phase diagram of unbalanced mixtures (where two chemical potentials are turned on) finding a competition of s, p, and s+p-wave superconducting phases.

The chapter is organized as follows. In section 8.1 we construct the solutions in the low temperature regime of the U(2) model. For this temperature we find the condensation of a vector mode that breaks the remaining $U(1)$ and gives rise to a new phase with two condensates: the s+p-wave holographic superconductor. The study of these new solutions allows us to determine the phase diagram of the two-component superfluid. The final picture is the following: for small chemical potential μ (high temperature) the system is in the normal phase where no condensate is present. For μ larger than a critical value μ_s the scalar field acquires an expectation value and the system enters the s-wave superfluid phase. Going to even larger chemical potential a new phase transition happens: at $\mu_{sp} > \mu_s$ a vector condensate appears and for $\mu > \mu_{sp}$ the system is in an s+p-wave phase with both scalar and vector non-vanishing order parameters.

Finally, in section 8.2 we shall study new configurations of the system where the two chemical potentials corresponding to the two $U(1)$s $\subset U(2)$ are switched on. This setup, where the $U(2)$ is explicitly broken to $U(1) \times U(1)$, realizes an unbalanced mixture, characterized by the presence of two species of charges with different chemical potentials. Examples of such systems are unbalanced Fermi mixtures [98], and QCD at finite baryon and isospin chemical potential [99]. Moreover, unbalanced superconductors are interesting systems where anisotropic and inhomogeneous phases are expected to appear. Holographic realizations of unbalanced systems where only one kind of order parameter can be realized have been constructed in [70, 100]. Here we construct new solutions of the system in chapter 6 corresponding to unbalanced mixtures that allow for competition of different order parameters. We determine its phase diagram as a function of the two chemical potentials and find that s-wave, p-wave and s+p-wave phases exist.

8.1 The s+p-wave holographic superconductor

Let us consider again the holographic model of a multi-component superfluid consisting of a scalar doublet charged under a $U(2)$ gauge field living in a 3+1 dimensional Schwarzschild-AdS black brane geometry constructed in 6. We would like now to consider the following (consistent) ansatz for the fields in our setup

$$A_0^{(0)} = \Phi(r)\,, \quad A_0^{(3)} = \Theta(r)\,, \quad A_1^{(1)} = w(r)\,, \quad \psi = \psi(r)\,, \tag{8.1}$$

with all functions being real-valued. All other fields are set to zero, in particular we set $\lambda = 0$ (see 6.18) without loss of generality. The resulting equations of motion read

$$\psi'' + \left(\frac{f'}{f} + \frac{2}{r}\right)\psi' + \left(\frac{(\Phi-\Theta)^2}{4f^2} - \frac{m^2}{f} - \frac{w^2}{4r^2 f}\right)\psi = 0\,, \tag{8.2}$$

$$\Phi'' + \frac{2}{r}\Phi' - \frac{\psi^2}{f}(\Phi-\Theta) = 0\,, \tag{8.3}$$

$$\Theta'' + \frac{2}{r}\Theta' + \frac{\psi^2}{f}(\Phi-\Theta) - \frac{w^2}{r^2 f}\Theta = 0\,, \tag{8.4}$$

$$w'' + \frac{f'}{f}w' + \frac{\Theta^2}{f^2}w - \frac{\psi^2}{f}w = 0\,. \tag{8.5}$$

In what follows we choose the scalar to have $m^2 = -2$ and the corresponding dual operator to have mass dimension 2.

The UV asymptotic behavior of the fields, corresponding to the solution of equations (8.2 - 8.5) in the limit $r \to \infty$, is given by

$$\Phi = \mu - \rho/r + O(r^{-2})\,, \tag{8.6}$$

$$\Theta = \mu_3 - \rho_3/r + O(r^{-2})\,, \tag{8.7}$$

$$w = w^{(0)} + w^{(1)}/r + O(r^{-2})\,, \tag{8.8}$$

$$\psi = \psi^{(1)}/r + \psi^{(2)}/r^2 + O(r^{-3})\,, \tag{8.9}$$

where, on the dual side, μ and ρ are respectively the chemical potential and charge density corresponding to the overall $U(1) \subset U(2)$ generated by T_0, whereas μ_3 and ρ_3 are the chemical potential and charge density corresponding to the $U(1) \subset SU(2)$ generated by T_3. $\psi^{(1)}$ is the source of a scalar operator of dimension 2, while $\psi^{(2)}$ is its expectation value. Finally $w^{(0)}$ and $w^{(1)}$ are the source and vev of the current operator $J_x^{(1)}$ (recall that $A_\mu^{(1)}$ is dual to the current $J_\mu^{(1)}$). Notice that in a background where $w(r)$ condenses the $SU(2) \subset U(2)$ is spontaneously broken, and moreover spatial rotational symmetry is spontaneously broken too.

We are looking for solutions of the equations (8.2 - 8.5) where ψ, w, or both acquire non-trivial profiles. We want them to realize spontaneous symmetry breaking so we impose that their leading UV contributions (dual to the sources of the corresponding operators) vanish. We switch on a chemical potential μ along the overall $U(1)$, while requiring that the other chemical potential μ_3 remains null. Therefore our UV boundary conditions are

$$\psi^{(1)} = 0\,, \quad w^{(0)} = 0\,, \quad \mu_3 = 0\,. \tag{8.10}$$

In the IR regularity requires A_t to vanish at the BH horizon.

Notice that after using the scaling symmetries of the system to fix the black hole parameters in the metric, the only scale in the problem is given by the chemical potential μ. In the grand canonical ensemble, in which the physical chemical potential is held fixed, the temperature is proportional to the rescaled chemical potential as $T \propto 1/\mu$. Therefore, varying μ is equivalent to changing the temperature of the system. For that reason the results are sometimes presented in terms of μ instead of T.

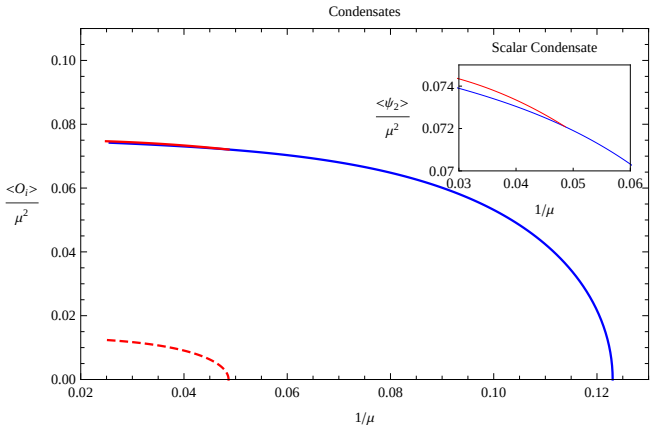

Figure 8.1: Condensates $\psi^{(2)}$ (solid) and $w^{(1)}$ (dashed) as a function of $1/\mu$ in the s-wave (blue) and s+p-wave (red) phases. The p condensate appears at μ_{sp} such that $\mu_s/\mu_{sp} = 0.395$ as found in chapter 6. The inset zooms in on the plot of $\psi^{(2)}$ to show the difference in the scalar condensate between the s (blue) and the s+p (red) solutions.

We have looked for numerical solutions with non-zero ψ and w, shooting from the IR towards the UV where we impose the boundary conditions (8.10). We have found the following solutions:
Normal phase: for all values of μ there exists an analytic solution where $\psi = w = \Theta = 0$ and $\Phi = \mu(1 - 1/r)$. This solution describes the normal state of the system.
***s*-wave phase**: for $\mu \geq \mu_s \approx 8.127$ we find solutions with non-zero ψ. For these solutions the equations decouple into two sectors: one corresponding to the Abelian holographic superconductor [59] and the other to the unbroken $U(1)$ symmetry. Although μ_3 is zero as required in (8.10), both charge densities ρ and ρ_3 are non-vanishing and therefore a two-component s-wave superfluid is realized. Indeed as one can see in eq. (8.4) a non-trivial scalar ψ acts a a source for the field $\Theta(r)$, and therefore the only pure s-wave solutions satisfying the boundary conditions (8.10) are those with $\rho_3 \neq 0$. Hence two different charge densities (ρ and ρ_3) corresponding to the two different $U(1)$s $\subset U(2)$ are turned on for these solutions and it is in this sense that this phase was denoted a two-component holographic superfluid earlier.[2]
***s*+*p*-wave phase**: for $\mu \geq \mu_{sp} \approx 20.56$ there are solutions satisfying (8.10) with non-zero

[2]From eqs. (8.2 - 8.4), one can see that the scalar condensate is only charged under a linear combination of Φ and Θ, whereas in the absence of a vector condensate, the orthogonal combination completely decouples corresponding to the unbroken $U(1)$ gauge field.

ψ and w. In these solutions the $U(2)$ symmetry is completely broken, and moreover since $w^{(1)} \sim \langle J_x^{(1)} \rangle$ spatial rotational symmetry is broken too. Again $\mu_3 = 0$ while ρ and ρ_3 are non-vanishing, thus realizing an s+p-wave phase of a two-component superfluid.

Usually p-wave superconductivity is triggered by a μ_3 chemical potential [101]. Here instead the p component of the s+p superfluid is supported by the spontaneously induced charge density ρ_3. For that reason no solutions with only p condensate are present in this system.[3]

In figure 8.1 we plot the condensates $\langle O_2 \rangle \sim \psi^{(2)}$ and $\langle J_x^{(1)} \rangle \sim w^{(1)}$ as a function of the chemical potential. Notice that the solution where both condensates coexist extends down to as low $1/\mu$ (or equivalently low temperatures) as where we can trust the decoupling limit and thus neglect backreaction.

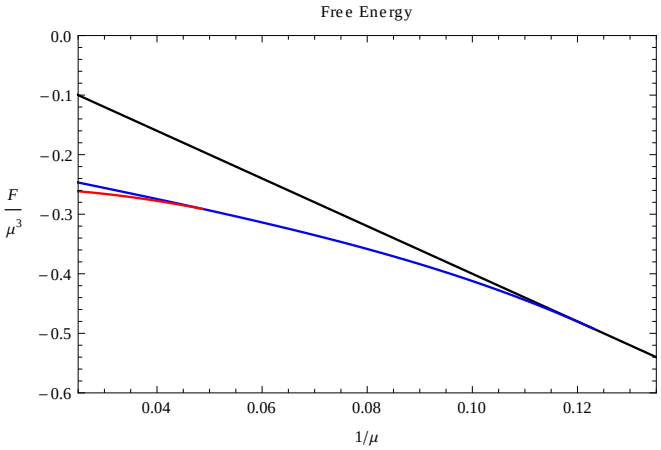

Figure 8.2: Free energy of the different solutions versus $1/\mu$: normal phase in black, s-wave phase in blue, and s+p-wave phase in red.

To determine the phase diagram of our system we compute the free energy of the different solutions and establish which is preferred when more than one exist. The free energy density is given by the on-shell action, and for our ansatz it reads

$$F = -\frac{T}{V} S_E = -\frac{1}{2}\left(\mu\,\rho + \mu_3\,\rho_3\right) + \\ + \int \frac{dr}{2f}\left(-f\,w^2\,\psi^2 + r^2\left(\Phi - \Theta\right)^2\,\psi^2 + \frac{f}{r^2} w^2\,\Theta^2\right). \tag{8.11}$$

The free energy for the different solutions is shown in figure 8.2. At small chemical potential only the normal phase solution exists. At $\mu = \mu_s \approx 8.127$ there is a second order phase transition to the s-wave solution. If one keeps increasing μ, at $\mu_{sp} \approx 20.56$ there is a second order phase transition from the s-wave phase to the s+p-wave phase. The system stays in the s+p-wave phase for $\mu > \mu_{sp}$.

[3] It is clear from eq. (8.5) that the p-wave condensate only couples directly to the $U(1) \subset SU(2)$, i.e to $\Theta(r)$. Actually, this equation reduces to that of the standard p-wave holographic superconductor [101] when the scalar is switched off. As in [101], only a non-zero Θ in the bulk can source the vector condensate since the coupling to the scalar ψ increases the effective mass of w and therefore hinders condensation. In contrast to the standard p-wave scenario we are fixing $\mu_3 = 0$, but solutions with non-zero Θ are still possible in presence of the s-wave condensate (realized by a non-zero ψ) as explained above.

8.2 Unbalanced Superconductors

In this section we relax the condition $\mu_3 = 0$ and study the phase diagram of the system as a function of μ and μ_3/μ. Notice that turning on a second chemical potential means to explicitly break $U(2) \to U(1) \times U(1)$. The system can now be interpreted as a holographic dual to an unbalanced mixture [70, 100].

Now that the $U(2)$ is explicitly broken, we can not generically impose that $\lambda = 0$ by using gauge transformations. Therefore, in principle both components of the scalar doublet may condense. In [102] it was studied which option is thermodynamically favored. Following their analysis, choosing the condensate to be on the lower component forces us to set $\mu_3/\mu < 0$ for the solutions to be stable.

The UV boundary conditions now read

$$\psi^{(1)} = 0\,, \quad w^{(0)} = 0\,. \tag{8.12}$$

As before we use numerical integration to solve the system (8.2 - 8.5). We are presented with a scenario where four different solutions exist:
Normal phase: an analytic solution where $\psi = w = 0$, $\Phi = \mu(1 - 1/r)$ and $\Theta = \mu_3(1 - 1/r)$ exists for any value of μ and μ_3, and it describes the normal state of the system.
***s*-wave phase**: for $\mu - \mu_3 \geq 8.127$ we find solutions with non-zero ψ resembling those in the balanced case.
***p*-wave phase**: for $|\mu_3|/\mu \geq 3.65/\mu$ solutions with $\psi = 0$, but $w \neq 0$ satisfying (8.12) exist. The scalar condensate $\langle O_2 \rangle$ is null while $\langle J_x^{(1)} \rangle \neq 0$. These solutions break the $U(1) \times U(1)$ down to $U(1)$ and also break the $SO(2)$ corresponding to spatial rotations. Notice that $w(r)$ is not charged under the overall $U(1)$ and therefore this solution is insensitive to the value of μ. This would change if the backreaction of the matter fields on the geometry was taken into account as in [70, 100].
***s*+*p*-wave phase**: for small values of μ_3/μ we find the extension of the s+p-wave solution found in the previous section for $\mu_3 = 0$. However, the larger $|\mu_3|/\mu$ the larger the μ at which the phase appears. We have also found solutions with two condensates in an intermediate region in which μ_3 is large and μ is close to the critical value μ_s. But they are always energetically not favored with respect to the pure s-wave solutions (see Figure 8.3).

By computing the free energy (8.11) of the different solutions we determine the phase diagram of the system as a function of $1/\mu$ and μ_3/μ which we plotted in figure 8.3. For small values of μ_3/μ the situation is very similar to what we found in the previous section for $\mu_3 = 0$. As already mentioned, as $|\mu_3|/\mu$ gets larger, the transition to the s+p-wave phase happens at a higher value of μ. It might be the case that the phase eventually disappears at a finite value of that ratio, but this would happen beyond the region of applicability of the decoupling limit, and thus backreaction should be taken into account[4]. For $|\mu_3|/\mu$ large enough, the p-wave phase is preferred at intermediate values of μ. Therefore, as μ is increased above a critical value μ_p the system goes from the normal to the p-wave phase through a second order phase transition. If μ is increased even further

[4]Notice that if the s+p-wave phase survived down to $1/\mu = 0$ for μ_3/μ lower than a critical value (as the phase diagram 8.3 seems to imply) we would be in the presence of a quantum critical point at which the system goes from the s+p to the s-wave phase. This resembles what happens in [95] for the p+is superconductor.

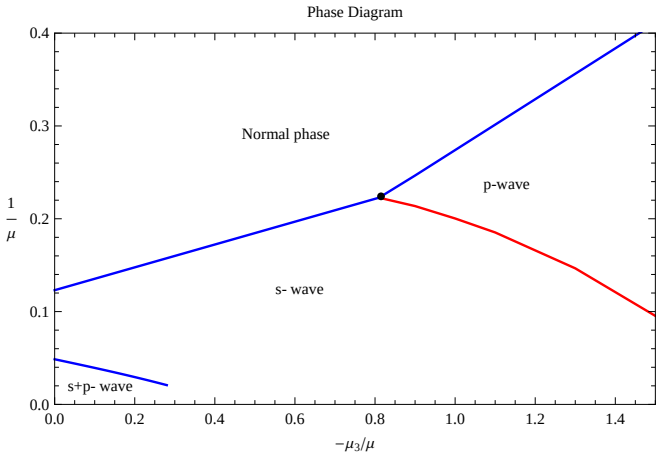

Figure 8.3: Phase diagram of the unbalanced system as a function of $1/\mu$ and μ_3/μ. Second order phase transitions are denoted by blue lines, whereas the red line corresponds to a first order phase transition.

a first order phase transition takes the system from the p-wave to the s-wave phase. This p- to s-wave first order phase transition is illustrated by figure 8.4 where we plot the free energy of both phases (and that of the normal phase) as a function of μ at a fixed value of $\mu_3/\mu = -1$. The tricritical point where the normal, s-wave and p-wave phases meet happens at $1/\mu \approx 0.223$ and $|\mu_3|/\mu \approx 0.815$. The p-wave solution is never energetically preferred for $|\mu_3|/\mu < 0.815$.

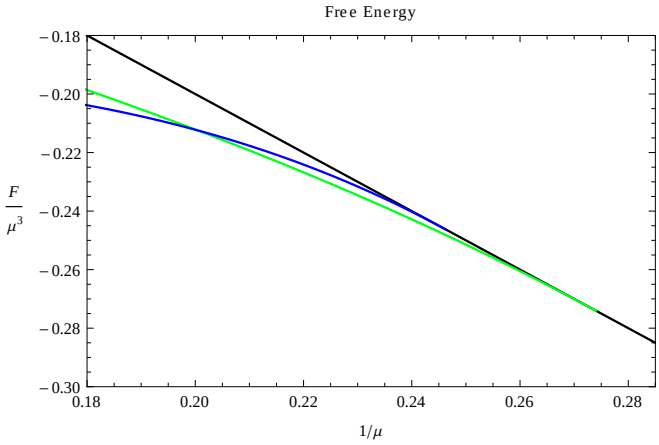

Figure 8.4: Free energy as a function of $1/\mu$ for $\mu_3/\mu = -1$. Black corresponds to the normal phase, blue to the s-wave phase, and green to the p-wave phase.

A cautionary comment about the phase diagram of figure 8.3 is in order. In the regions of the parameter space where $|\mu_3|/\mu \gg 1$ or $1/\mu \ll 1$ the probe limit is not valid anymore, and therefore the phase diagram might be modified once backreaction is taken into account [5]. Indeed, the nature of the different phase transitions, as well as the critical

[5] Remember that the decoupling limit corresponds to taking the gauge coupling (and charge of the scalar

values of the chemical potentials could be altered in those regions [103, 104]. However, in 2+1-dimensions both the s-wave and p-wave superconducting phase transitions separately are known to remain second order even lor large backreaction [70, 100]. Therefore, we expect the main features of the phase diagram like the existence of distinct s and p-wave phases meeting at a tricritical point will not be very sensitive to backreaction. The order of the phase transition between the s and p-wave phases could still be modified by backreaction.

8.3 Discussion

In this chapter we have constructed a holographic s+p-wave superconducting state. This phase, where both an s-wave and p-wave condensates exist, is the preferred state at low temperatures of our holographic two-component superfluid. Our main results are summarized by figures 8.1 and 8.3. Figure 8.1 shows that an s+p-wave state appears at low temperatures. A free energy analysis determined that the system enters this state through a second order phase transition, and stays in it for as low temperature as we can go. On the other hand, figure 8.3 presents the phase diagram for the unbalanced system: chemical potentials for the two $U(1)$s $\subset U(2)$ are turned on, and hence $U(2)$ is explicitly broken to $U(1) \times U(1)$. In this phase diagram three different superconducting phases are present. These are the standard s-wave phase where a scalar condensate breaks the $U(1) \times U(1)$ down to $U(1)$; a p-wave phase where $\langle J_x^{(1)} \rangle \neq 0$, $U(1) \times U(1)$ is broken to (a different) $U(1)$, and also spatial rotational symmetry is broken; and an s+p-wave phase where the $U(1) \times U(1)$ is completely broken by the s and p-wave condensates, and again spatial rotational symmetry is broken. Remarkably, while the system goes from the normal phase to the s-wave and p-wave phases through second order phase transitions, the phase transition between the s and p-wave phases is always a first order one. The existence of this first order phase transition between superconducting phases in the unbalanced system is an interesting prediction of our holographic model. These conclusions could be sensitive to the inclusion of backreaction since, as already mentioned, in principle the order of the phase transitions could change when the parameters are large and the decoupling limit breaks down. Yet in the proximity of the tricritical point, where the p- and s-wave phases meet, the matter fields and its derivatives are small enough for the probe limit to be trusted. Hence the existence of this point and the first order phase transition between the p- and s-wave phases in its proximity will survive once backreaction is considered, at least for large enough gauge coupling. Let as remark that, as we have seen in the previous chapter, in order to ensure the stability of the different phases it is important to study the quasinormal mode spectrum of the model. We leave this for future investigation.

field) $g_{\rm YM}$ to be very large, so the effect of the matter fields on the metric is negligible. Hence it is valid as far as $\mu_i \ll g_{\rm YM}$ and the condensates are small.

9 Anomalies

As emphasized in chapter 3, anomalies in the quantum theories of chiral fermions belong to the most emblematic properties of relativistic quantum field theory. As exposed there, there is a clear distinction between anomalies in presence of external/dynamical gauge fields. We would like to answer the following questions: How can we implement anomalies in presence of external/dynamical gauge fields within holography? How is transport affected by these? We will answer these questions, with special emphasis in the implementation and study of anomalies in presence of dynamical gauge fields.
The chapter is organized as follows. In section 9.1 we review the implementation of anomalies for U(1) symmetries in the presence of external gauge fields in holography. We explain how the anomaly is implemented and summarize the main findings of the last years regarding anomalous transport in holography. After this, in section 9.2, we explore the possibility of introducing the effect of the dynamical gauge fields in a model with just one abelian internal symmetry. In order to do so we define a simple model with one massive vector field in the bulk. We calculate the (holographically) normalized non-conserved current and compare to the massless case. Then we study the generalization of the chiral magnetic conductivity defined via Kubo formulae. We find that the chiral conductivity still exists and in terms of an appropriately defined dimensionless number gets even enhanced compared to the massless case. In the limit of vanishing mass we recover the value of the chiral magnetic conductivity in the **consistent current**. As is well-known this is 2/3 of the standard value most commonly cited (which corresponds to the covariant definition of the current).
We remind the reader of the fact that the chiral magnetic effect in the consistent current for the $U(1)^3$ anomaly of a single Weyl fermion takes the form

$$\vec{J} = \left(\frac{\mu}{4\pi^2} - \frac{A_0}{12\pi^2}\right)\vec{B}\,, \tag{9.1}$$

whereas for the AVV anomaly of a single Dirac fermion with a vector current preserving regularization it is

$$\vec{J}_V = \left(\frac{\mu_5}{2\pi^2} - \frac{A_0^5}{2\pi^2}\right)\vec{B}\,, \tag{9.2}$$

with μ, μ_5 the (axial) chemical potentials and A_0 and A_0^5 the background values of the (axial) gauge fields that do not necessarily coincide with the chemical potentials. The customary gauge choice $A_0 = \mu$ and $A_0^5 = \mu_5$ leads to the factor 2/3 in the $U(1)^3$ case and

to a vanishing CME in the AVV case[1]. In contrast the chiral separation effect

$$\vec{J}_5 = \frac{\mu_V}{2\pi^2}\vec{B} \tag{9.3}$$

shows no explicit dependence on the temporal gauge field. This is a consequence of the fact that the vector-like symmetry is non-anomalous, i.e. μ_V is the chemical potential conjugate to a truly conserved charge.

If one expresses the CME however in terms of the covariant currents the terms depending on the gauge fields are absent. Finally we note that the relation between covariant and consistent currents are $J^\mu_{\text{cov}} = J^\mu_{\text{cons}} + \frac{1}{24\pi^2}\epsilon^{\mu\nu\rho\lambda}A_\nu F_{\rho\lambda}$ for the AVV anomaly and $J^\mu_{\text{cov},V} = J^\mu_{\text{cons,V}} + \frac{1}{12\pi^2}\epsilon^{\mu\nu\rho\lambda}A^5_\nu F_{\rho\lambda}$.

Finally, in section 9.3 we explore a richer model with a U(1)×U(1) symmetry, which allows us to mimic the situation of massless QED. Our motivation is that the proper chiral magnetic effect stems from an interplay of vector- and axial symmetries. The vector symmetry can be taken as the usual electromagnetic $U(1)$. While the electromagnetic gauge fields are still quantum operators we can assume in the quark gluon plasma context that electromagnetic interactions are weak and to first approximation we might model the vector $U(1)$ as a non-dynamical gauge field. Furthermore the vector current of electromagnetic interactions has to be exactly conserved. We compute the chiral magnetic conductivity and the conductivity related to the chiral separation effect. We find that the chiral separation effect is fully realized whereas the chiral magnetic conductivity vanishes. Again we point out that these are the same results that hold for the consistent currents in the case when also the axial current is modeled by a massless vector field. Then we study the chiral magnetic wave [46] and compare our findings to a simple hydrodynamic model in which we include a decay width for the axial charge by hand. We find basically a perfect match between the modes of the phenomenological model and the low lying quasinormal modes of the holographic model. For small momenta we find absence of a propagating wave, whereas for large enough momentum there is indeed a propagating (damped) wave which is the generalization of the chiral magnetic wave. Finally we also study the negative magneto resistivity induced by the anomaly in a constant magnetic field background. We find by numerical analysis that the negative magneto resistivity depends quadratically on the magnetic field. The optical conductivity has a Drude peak form whose height is determined by the inverse of the bulk mass. For large magnetic field a gap opens up in the optical conductivity and we also check that the spectral weight gets shifted from the gap region into the peak region such that a sum rule of the form $d\left(\int d\omega\sigma(\omega)\right)/dB = 0$ holds.

[1] If an axion background is present there is also a term proportional to $\partial_t\theta\vec{B}$. We also emphasize that the anomaly makes the (axial) "gauge" field an observable precisely via the terms in (9.1), (9.2). See e.g. the discussion in [7].

9.1 Chiral anomalies with external gauge fields in holography

The first studies regarding anomalies in holography were [53, 105]. In those pioneering works it was found that the non-conservation of the dual current was related to the existence of boundary-noninvariant terms in the bulk theory. Later [106], it was found that massive gauge fields in the bulk can give rise to the effect of anomalies in the dual theory too. As we will see later in this chapter, the difference between both mechanisms is precisely related to whether the effect of dynamical gauge fields is taken into account or not. In this section we briefly review how the addition of certain terms (not gauge invariant at the boundary) in the bulk Lagrangian affects the (non)conservation of the dual currents and how this affects transport phenomena[2]. This review will be mainly based on the work [45].

Consider the Maxwell-Chern Simons Lagrangian in AdS_{4+1}

$$S = \int d^5x\sqrt{-g}\left(-\frac{1}{4}F_{\mu\nu}F^{\mu\nu} + \frac{\kappa}{3}\epsilon^{\mu\alpha\beta\gamma\delta}A_\mu F_{\alpha\beta}F_{\gamma\delta}\right), \tag{9.4}$$

The CS term of this theory is a bulk term, i.e. it appears in the e.o.m.. Nevertheless it has an interesting property from the symmetry point of view. Upon gauge transformation

$$\delta_\lambda S = \int d^4x\sqrt{-\gamma}\frac{\kappa}{3}\lambda(x)F\wedge F. \tag{9.5}$$

This not a problem from the bulk perspective, since only transformations that vanish at infinity are important in order for the theory to be consistent. Let us emphasize that, although (9.5) is a boundary term, the effect of the CS cannot be cancelled by a local counterterm at the boundary. A comment is in order here regarding the dimensions of space-time. As we know chiral anomalies can only happen in even space-time dimensions. From the holographic point of view the difference in the CS term in even/odd dimensions is then quite appealing. For even space-time dimensions, the CS term is of the form $F\wedge F\wedge F....$ Such a term can be written as a pure boundary term and, therefore, entirely cancelled with local counterterms. The odd case is however different, as one can see in our example, since $A\wedge F\wedge F...$ cannot be written in a pure boundary form.

If we compute the dual current, using the usual prescription we get

$$J^\mu_{cons} = \lim_{r\to\infty}\sqrt{-g}F^{\mu r} + \frac{4}{3}\kappa\epsilon^{\mu\alpha\beta\rho}A_\alpha F_{\beta\rho} \tag{9.6}$$

$$\partial_\mu J^\mu_{cons} = -\frac{\kappa}{3}\epsilon^{\mu\alpha\beta\rho}F_{\mu\alpha}F_{\beta\rho}. \tag{9.7}$$

This current, obtained form the variation of the generating functional is called the consistent current. Note that (9.6) is not covariant. In addition, the consistent current is not unique, since it may be changed by adding finite boundary terms in the action. Moreover, these terms can bo chosen such that the divergence is zero. In massless QED

[2] In the literature the study of anomalies in the context of holography is focused on the Weyl anomaly and on Chiral anomalies. We focus in the latter

such a transformation corresponds to the shift that one can make to "locate" the anomaly in any linear combination of the vector and axial currents. On the other hand, there is one precise choice of the contact term in the dual theory that renders a covariant expression for the current

$$J^{\mu}_{cov} = \lim_{r\to\infty} \sqrt{-g} F^{\mu r} \tag{9.8}$$

$$\partial_\mu J^{\mu}_{cov} = -\kappa \epsilon^{\mu\alpha\beta\rho} F_{\mu\alpha} F_{\beta\rho}. \tag{9.9}$$

Let us remark that the covariant version of the (anomalous) current is always non-conserved. From the holographic point of view, the only way to obtain this current is by direct subtraction of the non-covariant terms in the expression of the consistent current.

9.1.1 Anomalous transport in holography

As we have seen along this thesis, one possible way to obtain transport coefficients is via Kubo formulae. This is specially suited in holography since it relates the desired coefficient to an n-point function of the dual operators. It will be useful to have the results for the anomalous transport obtained from the Maxwell-Chern-Simons holographic theory that we are considering.
The concrete Kubo formula for the chiral magnetic effect is

$$\sigma = \lim_{k\to 0} \frac{i}{k_z} \langle J_x J_y \rangle \Big|_{\omega=0} \tag{9.10}$$

Note that we have not specified which definition of the current is to be used in this formula. Let us jump directly to the results (see [45] for details). With the straightforward definition of the current i.e. using the consistent version of the current in (9.6) the result is

$$\langle J_{x(cons)} J_{y(cons)} \rangle = -4ik_z\kappa(3\mu_5 - \alpha) \tag{9.11}$$

where μ_5 and α arise from the definition of chemical potential in holography and the asymptotic behavior of the gauge field

$$\mu_5 = \int_{r_h}^{\infty} \partial_r A_0 \qquad\qquad A_{0r\to\infty} \sim \alpha - \frac{\beta}{r}. \tag{9.12}$$

For some time people made the mistake of considering that both were the same thing. A way to avoid such problems is to calculate a different correlator

$$\langle J_{x(cov)} J_{y(cons)} \rangle = -12ik_z\kappa\mu_5, \tag{9.13}$$

which is directly free from the presence of sources. Clearly, in the absence of sources both quantities are the same.

Despite of these important technicalities, the result is in agreement with those from QFT and is a nice example of how anomalous transport phenomena can be studied in holography.

9.2 Holographic Stückelberg mechanism with a U(1) Gauge Field

As discussed in 3.2, chiral conductivities do get renormalized however in the case when the gauge fields appearing in the anomalous divergence of the current are dynamical [107,108]. An example is the singlet $U(1)_A$ current in QCD. Its anomaly is of the form

$$\partial_\mu J^\mu_A = \epsilon^{\alpha\beta\gamma\delta}\left(\frac{N_c\sum_f q_f^2}{32\pi^2}F_{\alpha\beta}F_{\gamma\delta}+\frac{N_f}{16\pi^2}\mathrm{tr}(G_{\alpha\beta}G_{\gamma\delta})+\frac{N_cN_f}{96\pi^2}F^5_{\alpha\beta}F^5_{\gamma\delta}\right) \tag{9.14}$$

Here F is the electromagnetic field strength, G the gluon field strength and F^5 the field strength of an axial gauge field A^5_μ whose only purpose is to sum up insertions of the axial current in correlation functions, i.e. there is no associated kinetic term. N_c and N_f are the numbers of colors and flavors respectively. In this case it has been shown in [107, 108] that the vortical conductivity receives two loop corrections whereas later on is has been argued in an effective field theory approach that all chiral conductivities receive higher loop corrections once dynamical gauge fields enter the anomaly equation [109].

It has been argued long ago by 't Hooft that in such a situation one should not think of the classically present $U(1)_A$ symmetry as a symmetry at all on the quantum level [110]. In asymptotically free theories such as QCD there might survive only a discrete subgroup because of instanton contributions. This discrete subgroup can be further broken spontaneously via chiral symmetry breaking but since it was not a symmetry to begin with there is also no associated Goldstone boson, which explains the high mass of the η' meson in QCD. A related fact is that the corresponding triangle diagram receives higher loop corrections via photon-photon or gluon-gluon re-scattering. These higher order diagrams lead to a non-vanishing anomalous dimension for the axial current operator J^μ_A. See [111, 112] for recent reviews.

These considerations motivate us to study the anomalous magneto response of massive vector fields in holography. Our philosophy is as follows. In quantum field theory we would have to study the path integral

$$Z=\int D\Psi D\bar\Psi D\mathcal{A}_q\,\exp\left[i\int d^4x\left(-\frac{1}{2}\mathrm{tr}(G.G)+\bar\Psi\not{D}\Psi+\theta\mathcal{O}_A+J.A\right)\right], \tag{9.15}$$

where $\mathcal{A}_q$ stands collectively for the dynamical gauge fields, G is their field strength tensor and $\mathcal{O}_A$ is the (operator valued) anomaly

$$\mathcal{O}_A=\epsilon^{\alpha\beta\gamma\delta}\left(\frac{N_f}{16\pi^2}\mathrm{tr}(G_{\alpha\beta}G_{\gamma\delta})+\frac{N_cN_f}{96\pi^2}F_{\alpha\beta}F_{\gamma\delta}\right). \tag{9.16}$$

Since the anomaly is a quantum operator we need to define a path integral that allows to calculate correlations functions of this anomaly operator. This means that we need to introduce the source field $\theta(x)$ coupling to $\mathcal{O}_A$. For the same reason we also have to include a source for the anomalous current J^μ. This source is the non-dynamical gauge field which from now on we denote by A_μ. The covariant derivative in (9.15) contains only the dynamical gauge fields. The non-dynamical gauge fields are coupled with the last term in (9.15). If we define the effective action $\exp(iW_{\text{eff}}[A,\theta])=Z$ it is basically guaranteed by construction that this effective action enjoys the gauge symmetry

$$\delta A_\mu=\partial_\mu\lambda\,,\qquad \delta\theta=-\lambda\,,\qquad \delta W_{\text{eff}}=0\,. \tag{9.17}$$

We now replace the (strongly coupled) dynamics of the gluon (and fermion) fields, i.e. the path integral over $\mathcal{A}_q$, Ψ and $\bar{\Psi}$ by the dynamics of classical fields propagating in Anti-de Sitter space. The gravity dual should allow to construct $W_{eff}[A,\theta]$ as the on-shell action of a field theory in Anti-de Sitter space containing a vector field A_μ and a scalar θ obeying the gauge symmetry (9.17). In addition, as we have argued before, the vector field should source a non-conserved current. Since Anti-de Sitter space implies the dual theory to have an additional conformal symmetry the four-dimensional current is non-conserved if and only if its dimension is different from three. This in turn means that the bulk vector field in our AdS theory has to be a massive vector and it is precisely the gauge symmetry (9.17) that allows the inclusion of a gauge invariant Stückelberg mass in the bulk AdS theory. The anomaly also includes the global part proportional to the field strengths of the non-dynamical gauge field therefore we also need to include a five dimensional Chern-Simons term in our AdS dual. The relation of the Stückelberg field in holography to the anomaly has been first pointed out in [106] and the necessity to include it in holographic studies of the anomalous transport has very recently also been emphasized in [113].
Moreover, since we have application to the physics of the strongly coupled quark gluon plasma in back of our head, we are lead to study a massive Stückelberg theory with Chern-Simons term at high temperature, i.e. in the background of an AdS black brane. We make one more simplifying assumption. We do not study any correlations functions including the energy momentum tensor. Therefore we can resort to the so called probe limit in which we ignore the back reaction for the gauge field theory onto the geometry. In our concrete model we consider Maxwell-Chern-Simons theory in the bulk and give a mass to the gauge field via Stückelberg mechanism

$$S=\int d^5x\sqrt{-g}\left(-\frac{1}{4}F_{\mu\nu}F^{\mu\nu}-\frac{m^2}{2}(A_\mu-\partial_\mu\theta)(A^\mu-\partial^\mu\theta)+\frac{\kappa}{3}\epsilon^{\mu\alpha\beta\gamma\delta}(A_\mu-\partial_\mu\theta)F_{\alpha\beta}F_{\gamma\delta}\right), \tag{9.18}$$

The above model provides a mass for the gauge field in a consistent gauge-invariant way. Stückelberg terms indeed arise as the holographic realization of dynamical anomalies, as pointed out for the first time in [106] (see also [114] for similar conclusions in the context of AdS/QCD). This has been also emphasized by the authors of [113] for a class of non-conformal holographic models.
As it is well-known, in holography we do not have access to the strongly coupled gauge field directly [3]. This implies that the dynamical contribution to the divergence of the current enters as a mass-term for the gauge field thereby inducing an explicit non-conservation. In contrast the global anomaly is implemented by an explicit Chern-Simons term. This fits the general expectation that the dynamical anomaly cannot be switched off because it is not simply a given by a functional of external fields.
Let us also comment on a crucial difference between model (9.18) and models of holographic superconductors. Holographic superconductors [71] also give a bulk mass term to the gauge field and they might be written in Stückelberg form as well [117]. The difference is that the Higgs mechanism in the bulk uses a massive scalar field that decays at the boundary and does therefore not change the asymptotic behavior of the gauge field. In our case the mass is constant in the bulk and does therefore change the asymptotic behavior of the vector field as one approaches the boundary of AdS.

[3] Note however that dynamical gauge fields emerge in the "alternative" quantization scheme in AdS_4 [115]. They can also be introduced via inclusion of boundary kinetic terms [116].

We work in the probe limit with Schwarzschild-AdS_5 as background metric

$$ds^2 = -f(r)dt^2 + \frac{dr^2}{f(r)} + \frac{r^2}{L^2}\left(dx^2+dy^2+dz^2\right), \qquad f(r) = \frac{r^2}{L^2} - \frac{r_H^4}{r^2}. \tag{9.19}$$

As usual we make use of rescaling invariance of the theory to set $r_H = 1$ and $L = 1$, and therefore $\pi T = 1$.
The equations of motion are

$$\nabla_\nu F^{\nu\mu} - m^2(A^\mu - \partial^\mu\theta) + \kappa\epsilon^{\mu\alpha\beta\gamma\rho}F_{\alpha\beta}F_{\gamma\rho} = 0, \tag{9.20}$$

$$\nabla_\mu\left(A^\mu - \partial^\mu\theta\right) = 0. \tag{9.21}$$

The asymptotic analysis shows that the non-normalizable and the normalizable modes of the gauge field behave as

$$A_{i(N.N.)} \sim A_{i(0)}r^{\Delta}, \qquad A_{i(N.)} \sim \tilde{A}_{i(0)}r^{-2-\Delta}, \qquad \Delta = -1+\sqrt{1+m^2}. \tag{9.22}$$

Since the mass has to be positive (for the massless case saturates the unitarity bound), there is no possible alternative quantization and the leading term is always to be identified with the non-normalizable (N.N.) mode. Moreover, there is an upper bound to the value of the mass prescribed by $\Delta = 1$. As we will show via holographic renormalization, the operator dual to the coefficient of the non-normalizable mode is essentially given by the normalizable mode. Its dimension can be found via the following argument. The AdS metric is invariant under the scaling $r \to \lambda r$, $(t,\vec{x}) \to \lambda^{-1}(t,\vec{x})$. Since a gauge field is a one form we have to study the behavior of $A_\mu(r,x)dx^\mu$ under these scalings one finds then that the normalizable mode has a scaling dimension of

$$\dim(\tilde{A}_{i(0)}) = [J_i] = 3+\Delta. \tag{9.23}$$

This implies that if $\Delta > 1$ the dual operator is irrelevant (in the IR) and thus destroys the AdS asymptotics. In the holographic renormalization in appendix A.5 we find that accordingly the number of counterterms diverges for $\Delta > 1$[4].
It is clear that the number of counterterms depends on the value of the mass. From now on we work in the range of masses that minimizes it, namely

$$\Delta < \frac{1}{3} \longleftrightarrow m^2 < \frac{7}{9}. \tag{9.24}$$

Henceforth we refer to Δ as the anomalous dimension of the dual current.
The procedure of renormalization for this theory is explained and discussed in detail in the appendix A.5. The boundary action with the counter-terms such that $S_{\mathcal{R}en} = S + S_{CT}$ reads

$$S_{CT} = \int_\partial d^4x\sqrt{-\gamma}\left(\frac{\Delta}{2}B_iB^i - \frac{1}{4(\Delta+2)}\partial_iB^i\partial_jB^j + \frac{1}{8\Delta}F_{ij}F^{ij}\right), \tag{9.25}$$

with $B_i \equiv A_i - \partial_i\theta$.

Remarkably, the coupling of the Stückelberg field to the Chern-Simons term in (9.18) is not optional once the mass is turned on; if one does not add it to the action it appears as a counterterm when holographic renormalization is carried out. More precisely the coefficient in front of $d\theta \wedge F \wedge F$ in (9.18) is not arbitrary once the mass is turned on. It is fixed to be the negative of the coefficient in front of the Chern-Simons term $A \wedge F \wedge F$, which renders a completely gauge invariant action. If we had not added this term directly from the start it would thus have appeared as a counterterm.

[4]We thank Ioannis Papadimitriou for pointing this out.

9.2.1 The one-point function

From the renormalized action we compute correlators of the dual operators in the boundary theory by means of the usual prescription. In this section we show our results, sticking only to the strictly necessary technical details for the discussion. A detailed discussion of the calculations can be found in appendix A.6.1.

Due to the anomalous dimension of the operator the analysis of the 1-point function becomes more subtle than in the massless case. In previous works, at zero mass, the leading terms of the expressions where finite. Therefore it made sense to look at expression for the current VEV as a functional of the covariant fields before taking the limit $r \to \infty$. This is however not the case when $m \neq 0$, since now all terms are divergent to leading order. Nevertheless, to make comparison with the results at zero mass, we want to look at the result before explicitly taking the limit. In order to do so, we split the unrenormalized 1-pt. function into a term lacking a (sub leading) finite contribution (called X below) and terms which do lead to a finite contribution after renormalization

$$\langle J^i \rangle = \lim_{r\to\infty} \sqrt{-g} r^{\Delta} \left(F^{ir} + r\Delta A^i \right) + X^i \,. \tag{9.26}$$

We see that the contribution arising from the Chern-Simons term in (9.18) is contained in X^i, which means that it does not contribute **explicitly** to the current. The renormalized one-point function reads

$$\langle J^i \rangle_{ren.} = 2(1+\Delta)\tilde{A}^i_{(0)} \,, \tag{9.27}$$

where $\tilde{A}_{(0)m}$ is the coefficient of the normalizable mode. Let us compare this with the expression for the **consistent** current that one obtains in absence of mass[5]

$$\begin{aligned} \langle J^i \rangle &= \lim_{r\to\infty} \sqrt{-g} \left(F^{ir} + \frac{4\kappa}{3} \epsilon^{ijkl} A_j F_{kl} \right) + X^i \,, \\ &\overset{\text{Ren.}}{=} 2\tilde{A}^i_{(0)} + \frac{8\kappa}{3} \epsilon^{ijkl} A_{j(0)} \partial_k A_{l(0)} \end{aligned} \tag{9.28}$$

Here we see that in the massless case ($\Delta = 0$) the Chern Simons term indeed gives a finite contribution to the current which is explicitly proportional to the sources. It is precisely this term what makes the difference between the covariant and the consistent definition of the current. We remind the reader that in the case of global anomalies one can define a covariant current by demanding that it transforms covariantly under the anomalous gauge transformation. In the AdS/CFT dictionary this covariant current is given by the normalizable mode of the vector field. In contrast the consistent current is defined as the functional derivation of the effective action with respect to the gauge field and in the AdS/CFT correspondence includes the Chern-Simons term in (9.28).

Equations (9.26) and (9.27) establish that we are no longer able to make such a distinction if $m \neq 0$, for there is no explicit finite local contribution of the Chern Simons term to the current operator. Quite remarkably, all of our results show that (9.27) corresponds

[5]Notice that in the zero mass limit θ becomes a non-dynamical field defined at the boundary. The divergence of this field also contributes to the current [7]. In order to keep the discussion simple we chose to take this non-dynamical field to vanish since this is the natural value that arises from our background in the the zero mass limit.

to the *consistent* current in the zero mass limit. This ultimately implies that in the limit $m \to 0$ the highly non-local expression $\tilde{A}_{(0)i}$ gives rise to the two terms in the last line of (9.28), which include a local term in the external sources. Hence, along the chapter we will only refer to consistent or covariant currents when analyzing the massless limit.

Another remarkable difference with the massless model is the Ward identity of the current operator. Using the equations of motion we can write the divergence of the current on-shell

$$\begin{aligned}\langle \partial_i J^i \rangle &= \lim_{r\to\infty} \sqrt{-g} r^{\Delta} \left(m^2 \partial^r \theta + r\Delta \partial_i A^i - \frac{\kappa}{3}\epsilon^{ijkl} F_{ij} F_{kl} + \tilde{X} \right) , \\ &\overset{\text{Ren.}}{=} 2(1+\Delta)\partial_i \tilde{A}^i_{(0)} \, , \end{aligned} \tag{9.29}$$

where we have extracted the (infinite) Chern Simons term from (9.26)[6] because it is convenient for the following discussion. As mentioned before, the fact that the terms in these expressions diverge obscures the interpretation if one does not take the limit $r \to \infty$. Once we take it we find that the ward identity (9.29) becomes a tautology since the only term on the right hand side that give a finite contribution is determined in the large r expansion directly by the divergence of the normalizable mode of the vector field. Therefore the divergence of the current on-shell is unconstrained.
If we now look at what happens when we take the limit $m \to 0$ before we take $r \to \infty$ we see that we recover the expression for the divergence of the consistent current

$$\langle \partial_i J^i \rangle = \lim_{r\to\infty} \sqrt{-g} \left(\frac{\kappa}{3}\epsilon^{ijkl} F_{ij} F_{kl} + \tilde{X} \right) \overset{\text{Ren.}}{=} \sqrt{-g}\frac{\kappa}{3}\epsilon^{ijkl} F_{ij} F_{kl} \, . \tag{9.30}$$

contained in the (non-local) normalizable mode of the filed. As we will see now the behavior of the conductivity points in the same direction.

9.2.2 Two-point functions & anomalous conductivity

Our main interest is to study the effect that the anomalous dimension has on the response of the system in presence of a magnetic field. As a first step in this direction we compute the anomalous conductivity $J_i = \sigma_{55} B_i$ that is related to a correlator of current operators via the Kubo formula

$$\sigma_{55} = \lim_{k\to 0} \frac{i}{k_z} \langle J_x J_y \rangle \Big|_{\omega=0} \, . \tag{9.31}$$

We emphasize however, that B_i does not have the simple interpretation of a magnetic field since its dimension is $2-\Delta$. We want to study the anomalous conductivity in an analogous fashion to [45] and find the dependence of the chiral anomalous conductivity on the source for J^μ. In order to generalize the concept of chemical potential to the situation at hand we we switch on a temporal component of the gauge field in the background $A = \Phi(r)\, dt$. We choose the axial gauge $A_r = 0$. The equation of motion is

$$\Phi'' + \frac{3}{r}\Phi' - \frac{m^2}{f}\Phi = 0 \, . \tag{9.32}$$

[6] In other words, $\partial_i X^i = -\frac{\kappa}{3}\epsilon^{ijkl} F_{ij} F_{kl} + \tilde{X}$.

We solve the equation (9.32) numerically[7], with the following boundary conditions

$$\phi(r_H) = 0\,, \qquad\qquad \phi(r \to \infty) \sim \mu_5 r^{\Delta}\,, \tag{9.33}$$

with μ_5 being the source. Notice that μ_5 does not correspond to a thermodynamic parameter in our massive model. Rather it should be interpreted as a coupling in the Hamiltonian. Different values of μ_5 correspond therefore to different theories. Different values of a chemical potential correspond only to different filling levels of the low lying fermionic states in the same theory. In the case of an anomalous symmetry one has to distinguish this filling level from the presence of a background constant temporal component of the gauge field [45].

The near horizon analysis shows that we are forced to impose $\Phi(r_H) = 0$. In absence of the mass term the gauge filed is not divergent at the horizon, independently of the finite value it takes at the boundary. This reflects the remnant (recall we work in the axial gauge) gauge freedom that one has in this case: the value of the source can be shifted by a gauge transformation[8]. However the mass term in the e.o.m. is divergent at the horizon and forces the field to vanish there. Remarkably, this and the asymptotic behavior of the field illustrate the fact that speaking of a chemical potential does no longer make sense. Computing the chemical potential as the integrated radial electric flux in the bulk one obtains

$$\mu = \lim_{r\to\infty} \int_{r_H}^{r} \partial_r A_t dr \to \infty. \tag{9.34}$$

This can be understood heuristically from the non-conservation of the charge: the energy to introduce and maintain a quantum of charge that is not conserved is infinite.
Since our background is homogeneous in the transverse directions it is easy to see that $\langle \partial_i J^i \rangle = 0$. In particular, the fact that a stationary solution exists implies that it is possible to choose a homogeneous configuration of μ_5 such that it compensates for the decay of the charge that is naturally caused due to the mass term. Namely,

$$\frac{d\rho}{dt} = 0\,, \tag{9.35}$$

with ρ the charge density of the system. We will see that the source necessary to ensure (9.35) equals the axial chemical potential in the massless limit (recall that only when $m = 0$ we can identify μ_5 with a chemical potential).

Once we have built the background we can proceed to switch on perturbations on top of it in order to compute the 2-point function (9.31). To linear order in the external source $\tilde{A}^i_{(0)} \approx \tilde{A}^i_{(0)} + \delta\tilde{a}^i_{(0)}$. From (9.27) we have

$$\langle J^n J^m \rangle = 2(1+\Delta)\eta^{ml} \frac{\delta \tilde{a}_{(0)l}}{\delta a_{(0)n}}\,. \tag{9.36}$$

Here $\tilde{a}_{(0)m}$ is the coefficient of the normalizable mode of the perturbation. We compute

[7] The analytic solution can be worked out in terms of hypergeometric functions. Since we need to resort to numerical methods later on, when studying fluctuations around the background, we found it more convenient to apply purely numerical methods also for the background.

[8] Gauge transformations that are non-zero at the horizon are not true gauge transformations but global transformations!

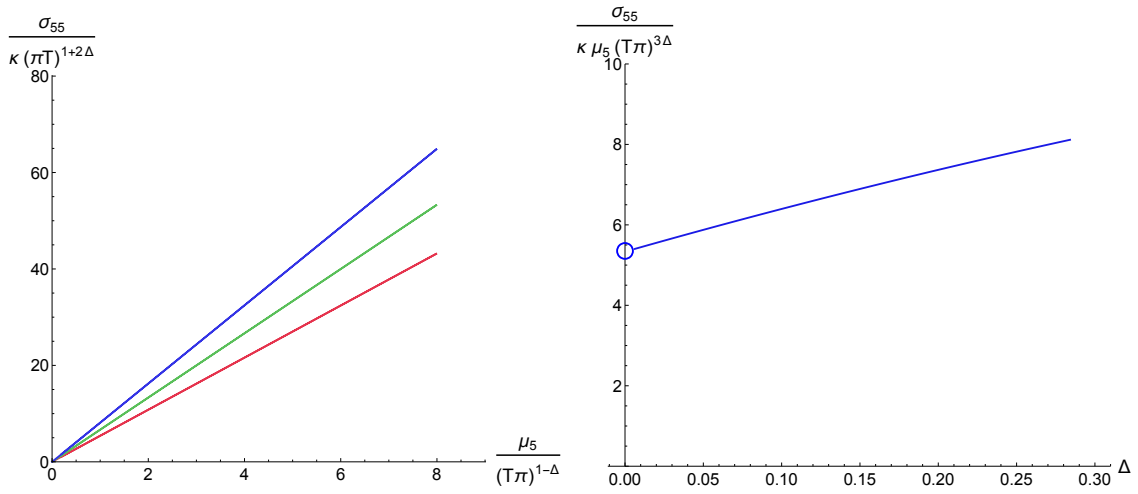

Figure 9.1: Left: Plot of the conductivity versus the source for: $m^2 = 1/2$ (Blue), $m^2 = 1/4$ (Green), $m^2 = 0.01$ (Red). Right: Plot of the conductivity coefficient as a function of the anomalous dimension; the circle stands for the asymptotic value in the limit $\Delta \to 0$.

the above expression numerically. Again we leave technical details for appendix (A.6.2) because the analysis is tedious and it is based on standard techniques. We show the result in figure 9.1. A comment is in order here regarding the temperature dependence on the plots. Dimensional analysis of the correlator $[\langle JJ \rangle] = 6+2\Delta$ implies that the conductivity has now dimension $[\sigma] = 1 + 2\Delta$. This in turn causes the physical conductivity to have a temperature dependence $\sigma \sim T^{3\Delta}$. As usual, from numerics we can only plot dimensionless quantities $\sigma/(\pi T)^{3\Delta}$ and $\mu_5/(\pi T)^{1-\Delta}$.

The plot on the left panel of figure 9.1 shows the dependence of the conductivity with the source for different values of the mass. Despite the fact that the slope changes the behavior is always linear in the dimensionless source parameter. The plot on the right panel shows the conductivity coefficient vs. the anomalous dimension of the current Δ. Remarkably the conductivity gets enhanced by the presence of the mass term in the bulk. In addition to this enhancement the plot shows another feature that deserves a comment. In the limit $\Delta(m) \to 0$ the conductivity goes to the numerical value $5.333 \sim \frac{16}{3}$. Let us now look at the analytic solution for zero mass shown in (2.25) of [45][9]

$$\langle J_5^i J_5^j \rangle = -4i\tilde{\kappa}k(3\mu_5 - \alpha)\epsilon_{ij}\,, \tag{9.37}$$

where μ_5 here is the thermodynamic chemical potential, α is the source, i.e. the boundary value of the temporal component of the gauge field and $\tilde{\kappa} = \frac{2\kappa}{3}$ in our convention. If one chooses the gauge $\alpha = \mu_5$ then one obtains

$$\langle J_5^i J_5^j \rangle = -8i\tilde{\kappa}k\mu_5\epsilon_{ij}\,, \tag{9.38}$$

In our numerical results we have absorbed the Chern Simons coupling in the definition of the external B-field (or equivalently set it to one in the fluctuation equations). Taking into account the difference in the normalizations of the Chern Simons couplings in [45] we can

[9]This model contained two massless vector fields in the bulk. One modeling the conserved vector and the other the anomalous axial symmetry. It is clear that the result obtained in our model with one massive vector should be compared in the zero mass limit to the axial vector sector of the model in [45].

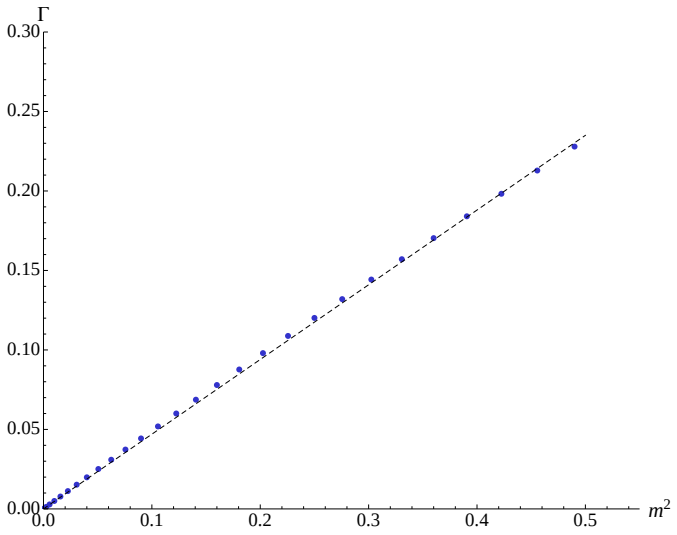

Figure 9.2: The gap Γ versus m^2. Black line corresponds to a linear fit.

extract from (9.37) the numerical value $\sigma_{55} = 16/3$ which coincides with the $m \to 0$ limit in our case! We conclude that our result matches the analytic formula only if we identify $\alpha = \mu_5$, as mentioned right after equation (9.35). This is also consistent with what we found in the expression for the current.

The fact that we found a time-independent background solution obscures the non-conservation of the charge. The best way to shed light onto the explicit decay of charge is by considering a trivial background (in particular, all the sources vanish) and look at the spectrum of quasinormal modes. In the massless case the lowest QNM shows a diffusion-type behavior, namely $\omega = -iDk^2$. This diffusive mode has to develop a gap when $m \neq 0$ due to the non-conservation of the charge. Technical details on how to compute QNM can be found in [57]. Indeed we find that the lowest QNM is no longer massless. The gap Γ depends on the value of the bulk mass as depicted in figure 9.2.

This indicates that the charge is no longer conserved. Furthermore a simple phenomenological model including only the dynamics of the lowest quasinormal mode suggests that the non-conservation can be modeled by writing $\partial_\mu J^\mu = -\frac{1}{\tau} J^0$, where τ is the inverse of the gap Γ of the lowest quasinormal mode. Indeed, such a phenomenological decay law together with Fick's law $\vec{J} = -D\vec{\nabla}J^0$ suggests a gapped pseudo diffusive mode $\omega + i/\tau + iDk^2 = 0$ which indeed is what we find from the QNM spectrum (see next section).

9.3 The Stückelberg U(1)xU(1) model

In this section we introduce an extra unbroken abelian symmetry in the bulk. This allows us to switch on an "honest" external magnetic field in the dual theory and therefore study not only the axial conductivity but the chiral magnetic conductivity and the chiral separation conductivity as well. In addition we are able to study the effect of the mass on

the chiral magnetic wave and on the electric conductivity. The Lagrangian reads

$$\mathcal{L} = \left(-\frac{1}{4}F^2 - \frac{1}{4}H^2 - \frac{m^2}{2}(A_\mu - \partial_\mu\theta)(A^\mu - \partial^\mu\theta) + \frac{\kappa}{2}\epsilon^{\mu\alpha\beta\gamma\delta}(A_\mu - \partial_\mu\theta)\left(F_{\alpha\beta}F_{\gamma\delta} + 3H_{\alpha\beta}H_{\gamma\delta}\right)\right), \tag{9.39}$$

where $F = dA$ and $H = dV$. The new dynamical U(1) in the bulk is massless and couples to the Chern-Simons term in the usual way. As in the previous section we work in the probe limit with Schwarzschild-AdS_5 as background metric. The scalar field transforms non-trivially only under the massive $U(1)$. From now on we refer to the massless $U(1)$ as "vector" V_μ and to the massive $U(1)$ as "axial" A_μ. The equations of motion for the gauge fields are

$$\nabla_\mu F^{\mu\nu} - m^2(A^\nu - \partial^\nu\theta) + \frac{3\kappa}{2}\epsilon^{\nu\alpha\beta\gamma\rho}(F_{\alpha\beta}F_{\gamma\rho} + H_{\alpha\beta}H_{\gamma\rho}) = 0\,, \tag{9.40}$$

$$\nabla_\nu H^{\nu\mu} + 3\kappa\epsilon^{\mu\alpha\beta\gamma\rho}F_{\alpha\beta}H_{\gamma\rho} = 0\,. \tag{9.41}$$

The equation of motion of the scalar remains unchanged (see equation (9.21)). Non-normalizable and normalizable modes of the axial gauge field have the same asymptotics for large r as the gauge field in the $U(1)$ model. The vector field shows the same behavior at infinity as usual

$$V_{i(N.N.)} \sim V_{i(0)}r^0\,, \qquad V_{i(N.)} \sim \tilde{V}_{i(0)}r^{-2}\,. \tag{9.42}$$

The holographic renormalization of this model is discussed in appendix A.5.2. The result is the following boundary term

$$S_{CT} = \int_\partial d^4x\sqrt{-\gamma}\left(\frac{\Delta}{2}B_iB^i - \frac{1}{4(\Delta+2)}\partial_iB^i\partial_jB^j + \frac{1}{8\Delta}F_{ij}F^{ij} + \frac{1}{8}H_{ij}H^{ij}\log r^2\right), \tag{9.43}$$

with $B_i = A_i - \partial_i\theta$. There are two differences from the result in the previous model. On the one hand, the appearance of the usual $\sim$ log term for the vector gauge field. On the other, the role of the coupling of the Stückelberg field to the C.S term in (9.39) is different because now we have two independent couplings $d\theta \wedge F \wedge F$ and $d\theta \wedge H \wedge H$. The former is mandatory, as in the the $U(1)$ model. The latter however is optional since it is a finite boundary term[10]. We have chosen to include it. As we will see, this will not affect the results in our concrete background, but it is potentially useful for other models since it cancels possible finite contributions to the vector current stemming from the Stückelberg field.

9.3.1 One-point functions

First we compute the 1-point functions of the gauge fields. The technical details of the calculations can be found in appendix A.7.1. As in (9.26) we hide all terms that do not contain any finite contribution in vectors X^i and Y^i, obtaining

$$\langle J_V^i\rangle = \lim_{r\to\infty}\sqrt{-g}\left(H^{ir} + 6\kappa\epsilon^{ijkl}\left(A_j - \partial_j\theta\right)H_{kl}\right) + X^i\,, \tag{9.44}$$

$$\langle J_A^i\rangle = \lim_{r\to\infty}\sqrt{-g}r^\Delta\left(F^{ir} + r\Delta A^i\right) + Y^i\,. \tag{9.45}$$

[10] At zero mass this coupling corresponds to the axion term discussed in [118].

The axial current behaves as in the previous model. Recall that the leading term in the asymptotic expansion of the axial gauge field diverges and so does the Chern Simons term in (9.44). Nevertheless, contrary to the axial current, this term has a subleading finite part (which is the reason why we do not include it in X^i). Looking at the complete expansion for the axial gauge field (A.79), we see that this finite contribution is proportional to the source of θ instead of the source of the gauge field. This is of course different from what one finds in the massless case. In addition, it is here where we see the effect that the coupling $d\theta \wedge H \wedge H$ has. It cancels this finite contribution proportional to the source dual to the Stückelberg field. As mentioned before, this cancellation comes from the choice we made in the action and can be removed at will.
We can now look at the Ward identities. Substituting the e.o.m. in the divergence of the current we find

$$\langle \partial_i J_V^i \rangle_{\text{Ren.}} = 0\,, \qquad \langle \partial_i J_A^i \rangle_{\text{Ren.}} = (2+2\Delta)\partial_i \tilde{A}_{i(0)}\,. \tag{9.46}$$

The vector current is conserved as in the massless case. The result for the axial current is the same as in the previous model: its divergence is unconstrained reflecting the fact that it is a non-conserved current.

9.3.2 Two-point functions & anomalous conductivities

The presence of an extra $U(1)$ allows us to obtain the following anomalous conductivities from Kubo formulae [45, 119]

$$\sigma_{CME} = \lim_{k\to 0} \frac{i\epsilon_{ij}}{2k} \left\langle J^i J^j \right\rangle (\omega = 0, k)\,, \tag{9.47}$$

$$\sigma_{CSE} = \lim_{k\to 0} \frac{i\epsilon_{ij}}{2k} \left\langle J_5^i J^j \right\rangle (\omega = 0, k)\,, \tag{9.48}$$

$$\sigma_{55} = \lim_{k\to 0} \frac{i\epsilon_{ij}}{2k} \left\langle J_5^i J_5^j \right\rangle (\omega = 0, k)\,. \tag{9.49}$$

In order to study these we have to switch on a source for both axial and vector charges. Since the vector charge is conserved at the boundary it is possible to define a non-divergent chemical potential for it. In fact, since the vector charge is conserved we do not need to source it by a constant V_0 at the boundary. Formally V_0 is just a pure gauge and therefore does not enter any physical observables. It is however a convenient and standard choice to reflect the presence of the chemical potential in the vector sector by choosing $V_0 = \mu$ at the boundary and $V_0 = 0$ at the horizon. In this case the difference of potentials at the boundary and the Horizon is the energy needed to introduce one unit of charge into the ensemble. This is a finite quantity and by definition the chemical potential μ.

We want to see how the dependence of the conductivities on the source and/or chemical potential is affected by the mass. Our background consists of the non-trivial temporal components of both gauge fields. It is static and homogeneous in the dual theory so the bulk fields only depend on the radial coordinate (again we work in the axial gauge $A_r = 0,\ V_r = 0$)

$$\theta(r) = 0\,, \quad A = \phi(r)dt\,, \quad V = \chi(r)dt\,. \tag{9.50}$$

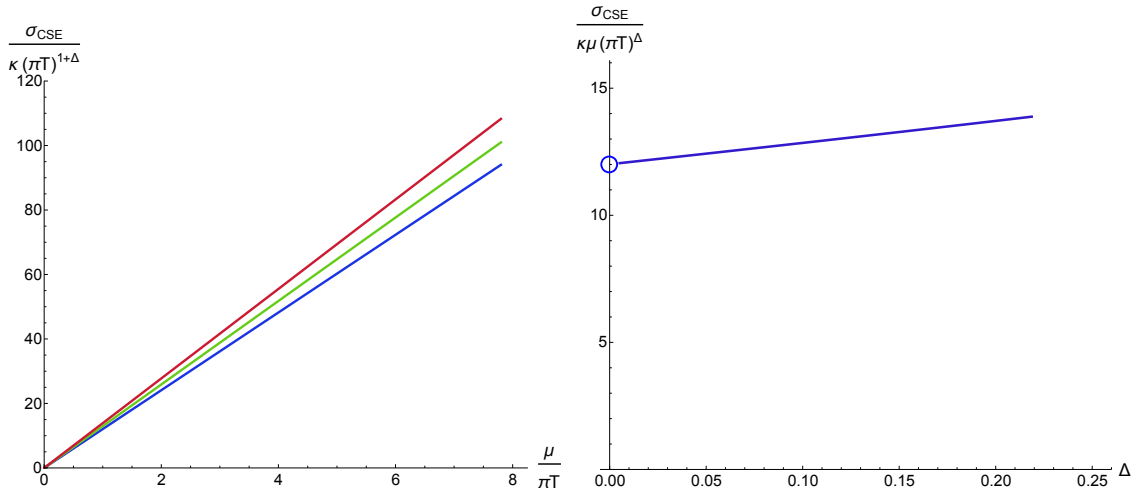

Figure 9.3: Left: Plot of the CSC versus the chemical potential μ for: $m^2 = 1/2$ (Red), $m^2 = 1/3$ (Green), $m^2 = 0$ (Blue). This conductivity is independent of the axial source μ_5. Right: Plot of the CSC coefficient as a function of the anomalous dimension $\Delta = \sqrt{m^2+1} - 1$.

The equations to solve are

$$\phi'' + \frac{3}{r}\phi' - \frac{m^2}{f}\phi = 0\,, \tag{9.51}$$

$$\chi'' + \frac{3}{r}\chi' = 0\,. \tag{9.52}$$

The boundary conditions for the gauge fields at infinity $\phi(r\to\infty) = \mu_A r^{\Delta}$; $\chi(r\to\infty) = \mu_V$ determine the value of the sources. As usual, (9.52) has the analytic solution

$$\chi(r) = \mu_V - \frac{\mu_V}{r^2}\,. \tag{9.53}$$

Expanding the action to second order in the perturbations and differentiating w.r.t. the sources we obtain the concrete expressions for the renormalized correlators

$$\langle J_i^V J_j^V\rangle_{\text{Ren.}} = 2\eta_{mj}\frac{\delta\tilde{v}_{i(0)}}{\delta v_{m(0)}}\,, \tag{9.54}$$

$$\langle J_i^A J_j^A\rangle_{\text{Ren.}} = (2+2\Delta)\eta_{mj}\frac{\delta\tilde{a}_{i(0)}}{\delta a_{m(0)}}\,, \tag{9.55}$$

$$\langle J_i^A J_j^V\rangle_{\text{Ren.}} = 2\eta_{mj}\frac{\delta\tilde{v}_{i(0)}}{\delta a_{m(0)}} = (2+2\Delta)\eta_{mj}\frac{\delta\tilde{a}_{i(0)}}{\delta v_{m(0)}}\,. \tag{9.56}$$

We compute the above correlators numerically. For a detailed explanation see appendix A.7.2. In the following we comment on the outcome.

Axial Conductivity: the conductivity σ_{55} related to the correlator of two axial currents behaves identically to section 9.2.2. Hence, we refer the reader to figure 9.1 and the corresponding discussion.

Chiral Separation Conductivity: we show the result in figure 9.3. In the plot on the l.h.s. we show the behavior of the conductivity with the vector chemical potential μ. We find that there is no dependence on the source μ_5 for any value of the mass/anomalous dimension. As in the axial conductivity we observe an enhancement with increasing mass. In addition, in the massless limit the conductivity approaches the value $\sigma_{CSE} \approx 12$ in numerical units. Again this is in agreement with the analytic solution for $m = 0$ [45]. Notice that for this conductivity even in $m = 0$ there is no dependence on the value of the vector field at the horizon (the source).

Chiral Magnetic Conductivity: the CME vanishes in our background. This is in perfect agreement with all the findings so far. As it happened with the rest of anomalous conductivities, in the massless limit the CMC approaches the value that one obtains for the consistent currents. We believe that the fact that it vanishes even in the massive case is a consequence of the the presence of the source μ_5. The necessary source to achieve a stationary solution for any value of m is such that it forces the anomalous response of J_V^i to B_V^i to vanish, very much as it occurs at zero mass. This does however not imply that the Chiral Magnetic effect does not exist in this model. As we will see in what follows, if we allow the axial charge to fluctuate freely (as opposed to fixing its value via a source term) the chiral magnetic effect is realized. In particular it gives rise to a (generalization of the) chiral magnetic wave and to a negative magneto resistivity. Both of which can be understood as a manifestation of the chiral magnetic effect.

9.3.3 The Chiral Magnetic Wave

We start be reviewing the essential features in the case when also the axial current is a canonical dimension three current. The chiral magnetic wave (CMW) is a collective massless excitation that arises form the coupling of vector and axial density waves in presence of a magnetic field [46]. In addition, this mode can only appear in the spectrum if there is an underlying axial anomaly. The dispersion relation for this mode corresponds to a damped sound wave

$$\omega(k) = \pm v_\chi k - iDk^2\,, \tag{9.57}$$

although it is related to transport of electric and axial charge. This mode can be thought of as a combination of the CME and the CSE. The vector charge and the axial charge oscillate one into the other giving rise to a propagating wave. This wave mode is present even in the absence of net axial or vector charge. The CMW is expected to play an important role in the experimental confirmations of anomaly induced transport effects. It has been argued in the case of heavy ion collisions that the CMW induces a quadrupole moment in the electric charge distribution of the final state hadrons [47, 120].

Let us analyze how this propagating mode is affected by the Stückelberg mechanism in the bulk. Before we proceed to study holographic numerical results we can perform a purely hydrodynamic computation as follows. As we have already shown in the previous section, the presence of the mass term for the axial vector field leads to a non-vanishing, purely imaginary gap for the lowest quasinormal mode. We include this gap as a decay constant for axial charge. Consider thus a model with axial and vector symmetries. Under the assumption of the existence of a AVV anomaly in the system, the constitutive relations

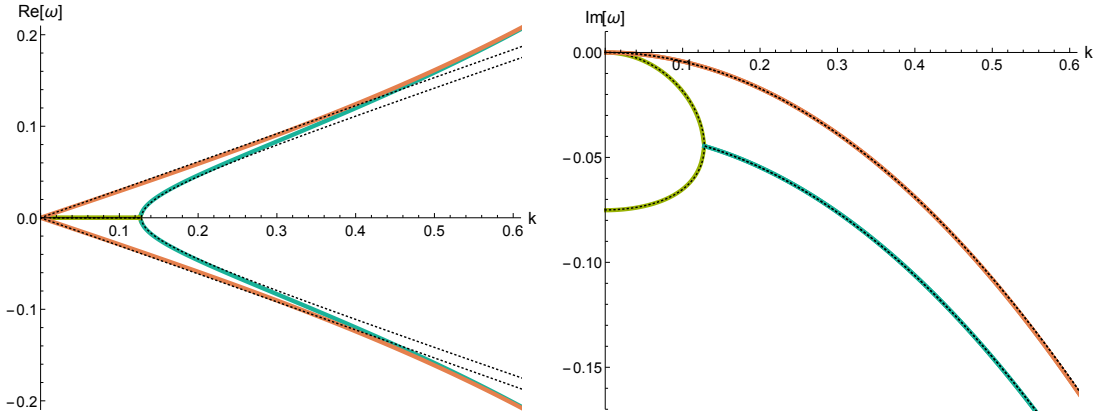

Figure 9.4: (Color online) Real and Imaginary parts of the frequency of the lowest QNM as a function of k. Solid lines correspond to numerical data with $\kappa B = 0.05$ and two different values of the mass: $m^2 = 0$ (orange) and $m^2 = 0.15$ ($\Delta = 0.08$) (blue, green). The Massive case is given two different colors to highlight the regimes $k < k_c$ (green) and $k > k_c$ (blue). Dashed lines correspond to the analytic formula (9.62). The massless case shows the behavior of the CMW. With a non-vanishing mass such a behavior s recovered for $k > k_c$.

for the current in the presence of a background magnetic field B read

$$j_V^x = \frac{\kappa \rho_A B}{\chi_A} - D\partial_x \rho_V \,, \qquad\qquad j_A^x = \frac{\kappa \rho_V B}{\chi_V} - D\partial_x \rho_A \,. \tag{9.58}$$

with D the Diffusion constant and κ the anomaly coefficient. We assume CME and CSE to be present. They are expressed in terms of charge densities and the susceptibilities χ_A, χ_V [46]. On the other hand we have the (non-)conservation equations

$$\partial_\mu j_V^\mu = 0 \,, \qquad\qquad \partial_\mu j_A^\mu = -\Gamma \rho_A \,. \tag{9.59}$$

Where $\Gamma(m)$ is the charge dissipation induced by the coupling to the underlying gauge anomaly[11]. From here we get the coupled equations

$$\omega \rho_V + \frac{k\kappa \rho_A B}{\chi_A} + ik^2 D \rho_V = 0 \,, \tag{9.60}$$

$$(\omega + i\Gamma)\rho_A + \frac{k\kappa \rho_V B}{\chi_V} + ik^2 D \rho_A = 0 \,. \tag{9.61}$$

Assuming now that the equations are linearly dependent we get

$$\omega_\pm = -\frac{i\Gamma}{2} - iDk^2 \pm \sqrt{\frac{B^2 k^2 \kappa^2}{\chi_A \chi_V} - \frac{\Gamma^2}{4}} \,. \tag{9.62}$$

The mode associated to ω_+ is massless and expected to arise due to the fact that the vector symmetry is conserved. It basically represents the Diffusion law for the conserved vector charge. The ω_- mode is gapped, i.e. $\omega_-(k = 0) = -i\Gamma$. Both combine at a critical value for the momentum $k_C(\Gamma, B, \chi_{(V,A)})$ that makes the term inside the square root vanish.

[11] We also assume vanishing external electric field and therefore there is no $\vec{E}.\vec{B}$ term present in the equation for the axial current.

- If $4B^2\kappa^2k^2 > \chi_A\chi_V\Gamma^2$ the square root is real and we obtain a contribution linear in k (which boils down to the well-known linear dispersion relation of the chiral magnetic wave in the limit $\Gamma = 0$).
- If $4B^2\kappa^2k^2 < \chi_A\chi_V\Gamma^2$ the square root contribution is completely contained in the imaginary part of the frequency.

In summary, we see that

$$k_C = \frac{\chi_A\chi_V\Gamma^2}{4B^2\kappa^2}\,. \tag{9.63}$$

For $k > k_C$ we get a propagating mode whose dispersion relation approximates the one of the CMW[12]. On the contrary, if $k < k_C$, there is no real part of the frequency (i.e. no chiral magnetic wave); one of the modes remains massless and the other develops a gap Γ.

With this phenomenological model in mind we look for these modes in our holographic model. In order to find the CMW we look at the QNM spectrum in presence of a constant magnetic field B in the z-direction. Since the CMW is present at zero axial and vector charge densities, we do not switch on any chemical potential in the background. The only non-zero field in our ansatz for the background is $A_x = By$. It is easy to check that such an ansatz satisfies the equations of motion trivially. Subsequently we study the perturbations, with momentum k aligned with the magnetic field. Applying the determi-

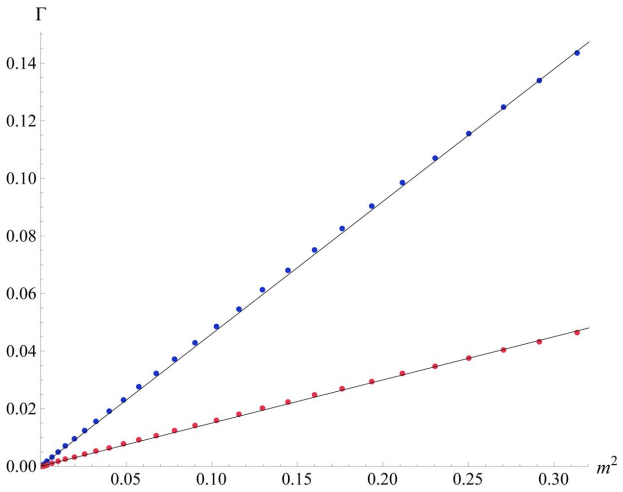

Figure 9.5: (Color online) The gap Γ versus m^2 for different values of the magnetic field $\kappa B = 0.01$ (blue) and $\kappa B = 0.5$ (red) . Black lines correspond to linear fits.

nant method of [57] we are able to obtain the dispersion relation of the CMW as depicted in figure 9.4; we show the dispersion relation of the lowest QNMs for both $m = 0$ (orange) and $m > 0$ (green, blue) in presence of B. On top of this we plot (dashed lines) the predictions of the phenomenological model (9.62).
The numerical results are in perfect agreement with the analytic analysis. We observe the appearance of a critical momentum k_C, induced by the mass term. Below this momentum

[12] Observe that for $k >> k_c$ the slope $\mathrm{Re}(\omega)/k$ is the same as in the case $\Gamma = 0$.

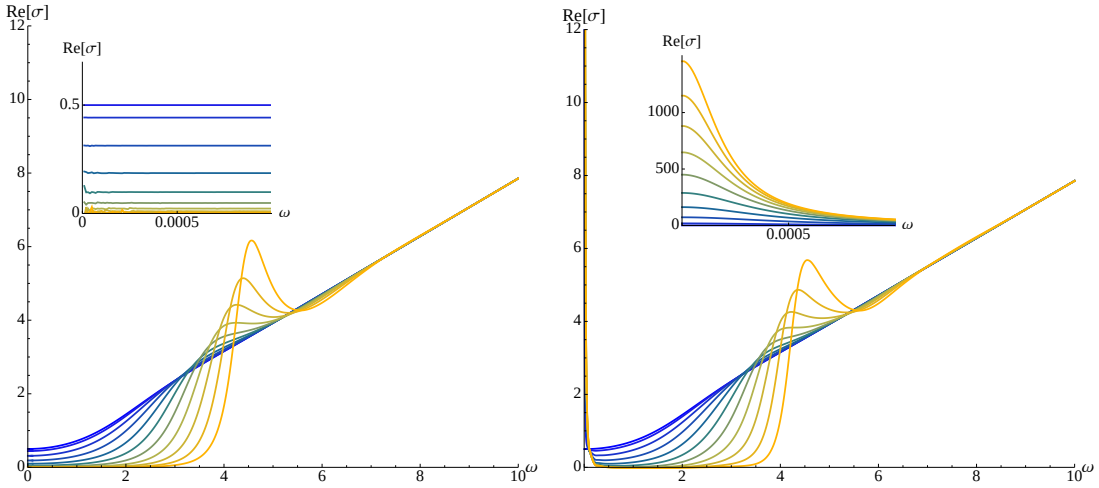

Figure 9.6: Real part of the conductivity in the longitudinal sector for $\Delta = 0$ (Left) and $\Delta = 0.1$ (Right). Different colors correspond to different values of the magnetic field B, from $\kappa B = 0$(blue) to $\kappa B = 0.5$ (yellow). The behavior of the conductivity at high frequencies is qualitatively the same for both values of Δ. The DC conductivity however shows a Drude peak as soon as the mass (Δ) is switched on whereas it is a delta function peak centered at $\omega = 0$.

the chiral magnetic wave is not really wave-like (i.e. $\mathrm{Re}[\omega(k)] = 0$ for $k < k_C$); the two modes decouple, giving rise to a diffusive mode and gapped purely imaginary mode. Such a spectrum is what one would expect to find in the model if there was no CMW, that is, the unbroken vector charge exhibits diffusive behavior, with a massless mode protected by the symmetry, whereas the analogous mode for broken axial U(1) symmetry develops a gap Γ. This gap is proportional to the mass and gets diminished the stronger the magnetic field. Above the critical momentum the two modes fuse again, giving rise to the expected behavior of the CMW. Since the CMW is a propagating oscillation between axial and vector charge we see that for small momentum the decay of the axial charge dominates, i.e. the axial charge decays before it can oscillate back into vector charge. The strength of the mixing of the charges is proportional to the momentum. This mixing becomes large enough and the oscillation fast enough to allow the build up of a propagating (damped) wave at large enough momentum.

We show the behavior of the gap Γ with the mass for different values of the magnetic field in figure 9.5. We find that the gap goes as $\sim m^2$ and that it is inversely proportional to the strength of the magnetic field.

9.3.4 Negative Magneto Resistivity

As a last step we study how the electric conductivity is affected by the mass. In the absence of mass the CMW induces perfect (i.e. infinite) DC conductivities for both the electric and the axial conductivities along the magnetic field. However, from the QNM analysis of the previous section we know that this cannot hold anymore. We expect a finite conductivity but with a strong Drude like peak at zero frequency. As we will see this is indeed what is happening.

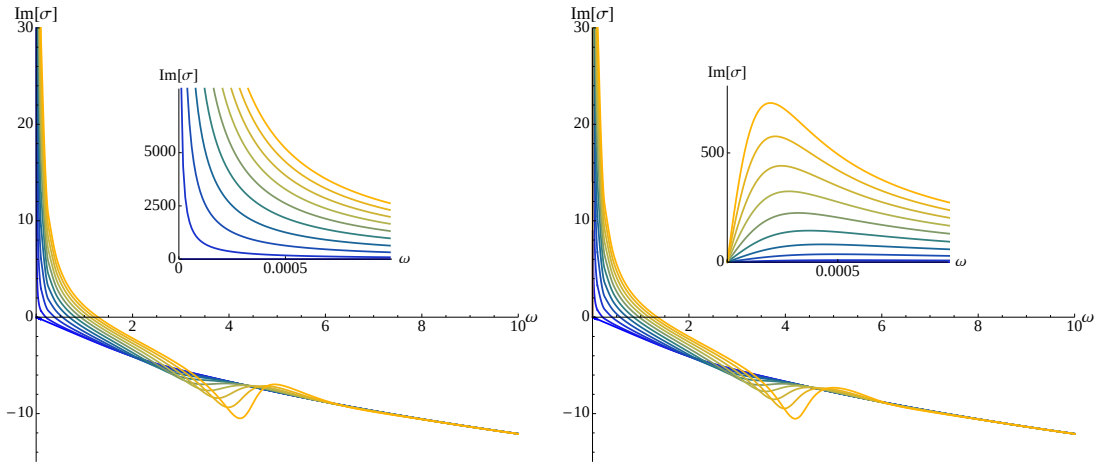

Figure 9.7: Imaginary part of the conductivity in the longitudinal sector for $\Delta = 0$ (Left) and $\Delta = 0.1$ (Right). Different colors correspond to different values of the magnetic field B, from $\kappa B = 0$(blue) to $\kappa B = 0.5$ (yellow). In agreement with the real part in figure 9.6 the zero frequency behavior shows a pole only when the mass is absent, signaling the presence of a delta function in the real part. As soon as the mass is switched on $\mathrm{Im}[\sigma]$ vanishes at the origin.

In order to analyze the longitudinal conductivity along the magnetic field we switch on perturbations on top of the background that we used to study the CMW, namely, an external magnetic field pointing in the z-direction. The electric conductivity along the magnetic field can be extracted from the correlator

$$\sigma_{||} = \lim_{\omega\to 0} \frac{i}{2\omega} \left\langle J^z J^z \right\rangle (\omega, k = 0) \,, \tag{9.64}$$

Since this conductivity is obtained at zero momentum we can assume spatial homogeneity for the perturbations. The coupled equations of motion can be found in appendix A.8. The analysis of the two-point function reveals that for this configuration of the background the correlator we want to compute has the usual expression

$$\left\langle J^z J^z \right\rangle_{\text{Ren.}} = \lim_{r\to\infty} r^3 \partial_r \mathbb{H} + \omega^2 \log(r) \,. \tag{9.65}$$

We solve the equations numerically with infalling boundary conditions and build the bulk-to boundary propagator (BBP from now on). Our results are shown in figures 9.6,9.7,9.8.

The well-known Kramers-Kronig relations imply that a pole in the imaginary part of the conductivity at zero frequency signals the presence of a delta function peak in the real part, i.e. and infinite DC conductivity. As soon as we turn the mass on, we observe that the DC conductivity is not a delta function anymore (see figures 9.6 and 9.7). This fact has important consequences in the Ohm's law for an anomalous system with an explicit breaking term. It has been first pointed out that the axial anomaly induced a large DC conductivity in a magnetic field (or a negative magneto resistivity) in [121]. More recent studies of this phenomenon are [122, 123]. In these studies Weyl fermions of opposite chirality appear as the effective electronic excitations at low energies in a crystal

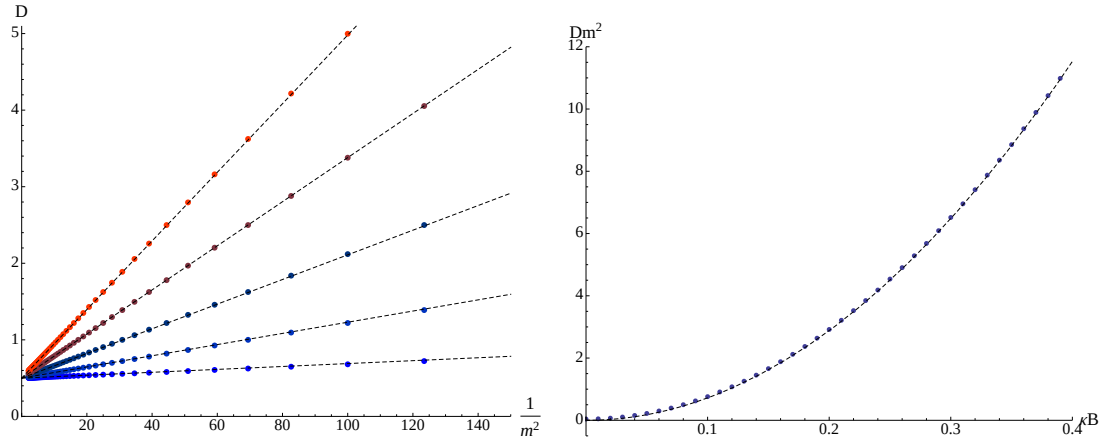

Figure 9.8: Left: We show the value of the highest point of the Drude peak (D) against $\frac{1}{m^2}$ for several values of κB from $\kappa B = 0.005$ (Blue) to $\kappa B = 0.25$ (Red) . Dashed lines corresponds to linear fits. Right: Dependence of the slopes in the l.h.s. plot as a function of κB. Dashed line corresponds to a quadratic fit; we find the coefficient to be ≈ 72.

(Weyl semi-metal). The associated axial symmetry is however only an approximate one since the electronic quasiparticles can be scattered from one Weyl cone into another. The associated scattering rate is called the inter-valley scattering rate τ_i. It turns out that the conductivity in these Weyl semi-metals is indeed proportional to the inter-valley scattering rate. Our findings are in complete analogy, the inverse of the gap in figure 9.5 plays the role of the inter-valley scattering time leading to a finite but strongly peaked DC magneto conductivity.
By numerical analysis we find the dependence of the DC conductivity on m, κ and B. Results are shown in figure 9.8. We can approximate it by

$$D \approx 72 \frac{\kappa^2 B^2}{m^2} \,. \tag{9.66}$$

Since in figure 9.5 we found that the gap is proportional to m^2 we indeed see that the DC conductivity scales linearly with the inverse of the gap as expected. We also find that it depends quadratically on the magnetic field. Again this is the expected result at least for small magnetic fields. For larger magnetic fields the weak coupling analysis shows however a linear dependence on the magnetic field that can be traced back to the fact that all fermionic quasiparticles are in the lowest landau level.

We found that our results show a kind of instability for too large magnetic field such that we were not able to see this cross over to linear behavior. This might be an artifact of the probe limit or a genuine instability of the theory at high magnetic fields (similar to the Chern-Simons term induced instabilities in an electric field found in [89]). We leave this issue for further investigation.

Finally we note that we have checked that the sum rule is fulfilled for several values of the mass and the magnetic field. This sum rule takes the form $\frac{d}{dB} \int \mathrm{Re}(\sigma(\omega)) d\omega = 0$. The sum rule implies that the peak is built up by shifting spectral weight from higher frequencies towards $\omega = 0$. In fact this is precisely what can be seen in figure 9.6 where it is evident that the region of intermediate frequencies gets depleted and correspondingly a gap in the magneto-optical conductivity opens up as the magnetic field strength is

increased. Note that this gap is present still in the region where we found quadratic scaling (9.66).

9.4 Discussion

In this chapter we have explored the implementation of chiral anomalies in holography. Concretely, we have studied anomaly related transport phenomena in a bottom-up holographic model with massive vector fields and Stückelberg axion. One of our motivations was that the dynamical part of the axial anomaly, i.e. the gluonic contribution, is dual to the dynamics of axions in holography. Its precisely this axion that can be used in the bulk Stückelberg mechanism to give mass to the bulk gauge field. The operator dual to this massive gauge field is a non-conserved current and this non-conservation is manifest in the fact that we did not find a constraint on the divergence of the current. Throughout the chapter, we have restricted ourselves to the probe approximation.

Equipped with the above model for an anomalous massive $U(1)$ gauge field, in section 9.2 we have studied carefully the form of the current one-point function, showing that the well-known Bardeen-Zumino polynomial does not exist if the mass $m \neq 0$. The resulting form of the (holographically renormalized) current tends to the *consistent* definition in the massless limit. Moreover, as described by (9.29) the divergence of such a current is not constrained. Moving to the two-point functions, the anomalous conductivity σ_{55} has been computed using its definition via a Kubo formula. We find that its value corresponds to the one associated to to the consistent current in the zero mass limit. We also showed that the QNM spectrum has a gap in contrast to the massless case in which there exists a hydrodynamic diffusion mode. We stress that the non-conserved current J^i is not a hydrodynamic degree of freedom because of this gap. Furthermore the parameter μ_5 is not a chemical potential but a coupling constant. Nevertheless we think it would be an interesting exercise to work out constitutive relations of for the non-conserved current extending the well-established methods of the fluid/gravity correspondence [124] to this case.

In section 9.3 we implemented the interplay between non-conserved axial and conserved vector currents. We also studied a wider set of anomalous conductivities using Kubo formulae (9.47), (9.48) and (9.49) We found that (as expected) the axial conductivity is identical to the case with only one axial gauge field. The chiral separation conductivity is independent of the source μ_5, behaves linearly with μ and increases with the mass, as depicted in figure 9.3. Finally, the chiral magnetic conductivity vanishes for all the values of m that we have studied; we interpret this fact as an effect of the source that ensures that the background is time-independent. As $m \to 0$, all the conductivities approach the value corresponding to consistent definition of the currents. Subsection 9.3.3 is devoted to the study of the chiral magnetic wave (CMW) [46] in the presence of mass. First, we perform an analytic analysis of the modes in a phenomenological model that implements the axial non-conservation via a relaxation term (see equation (9.59)). This model predicts that a propagating wave like mode can build up only for large enough momentum. Indeed we find from our quasinormal mode analysis that the model can be fitted very well to the QNM spectrum and that indeed a propagating chiral magnetic wave is absent for small momenta.

Finally we have also studied the negative magneto resistivity and showed that a sum rule holds for the magneto-optical conductivity. The strength of the DC conductivity is proportional to the square of the magnetic field and inverse proportional to the gap. This is in agreement with weak coupling considerations for small magnetic fields and an inter-valley scattering relaxation time for axial charge. Unfortunately we were not able to see the expected cross-over to linear behavior in the magnetic field because our numerics indicated a possible instability at large B-field. If this is an artifact of the probe limit (which assumes negligible backreaction of the gauge field on the geometry) or a genuine instability we leave to further investigation.

10

Spontaneous Symmetry Breaking & Anomalies

It could be stated that the study of the interplay between anomalous transport and superfluids started a decade ago; the first approaches to chiral transport (concretely, the Chiral Separation Effect) where analyzed for high-density QCD, assuming for instance that baryon symmetry is spontaneously broken, see [125, 126]. However, a systematic study of Chiral Superfluids has only been undertaken recently, using different techniques to obtain the hydrodynamic expansion, with particular emphasis on the anomalous response [127–131].
The results indicate that the effect of the background condensate is two-fold. On the one hand, unlike the case of ordinary fluids, anomalous conductivities are not fully determined by anomaly coefficients anymore. On the other, in addition to the Chiral Vortical and Chiral Magnetic effects, there exist new types of transport phenomena driven by the anomalies. However, until now, we lack clear predictions for the anomalous response parameters in superfluids. Moreover it has been recently pointed out that, for a certain class of holographic models of chiral superfluids [132] the zero-temperature behaviour of the CMC and CVC is universal and given by [22]

$$\sigma_{55}^{\text{brok.}}(T \to 0) = \frac{\sigma_{55}^{\text{unbrok.}}}{3}\,, \tag{10.1}$$

$$\sigma_{CVC}^{\text{brok.}}(T \to 0) = 0\,, \tag{10.2}$$

where "brok." and "unbrok." refer to broken and unbroken phases, respectively.

Motivated by this, we would like to address the question of how the interplay between anomalies and spontaneously broken symmetries affect transport phenomena in holography. In order to calculate possible corrections of the anomalous transport coefficients due to the presence of condensates, we perform an explicit computation of them. For simplicity we stick to s-wave condensates, adding a Chern-Simons term to the gauge fields in the bulk.
Contrary to the usual approaches to transport in Chiral Superfluids, here we rely on linear response theory to analyze the possible corrections. Kubo formulae provide us with the response driven by a small external perturbation. These are powerful because they account automatically for all the corrections to the coefficients and sometimes prove the existence of new transport phenomena which is difficult to analyze by means of hydrodynamic expansions. Hence, we assume that it is possible to define the anomalous conductivities in terms of correlators in the broken phase, which is to say, that there exists a current due

to an external magnetic field in both the unbroken and broken phases[1]

$$\mathcal{J}^i = \sigma_{\{CME,CSE,55\}} B^i \,, \tag{10.3}$$

$$\mathcal{J}^i = \sigma_{CEE} \epsilon^{ij} E_j \,. \tag{10.4}$$

Where $\mathcal{J}, B, E$ correspond to a generic $U(1)$ covariant current, magnetic and electric field, respectively, whereas σ denotes generic conductivities[2]. Equation (10.4) represents the Chiral Electric Effect (CEE), an anomalous transport phenomenon which is present only for Chiral Superfluids at finite superfluid velocity [130]. We propose a Kubo formula for the Chiral Electric Conductivity (CEC) and compute its value in our models.
In addition, we emphasize the existence of a type of transport phenomena in Chiral Superfluids that to our knowledge has been overlooked so far. We call it Chiral Charge Generation Effect (CCGE). It establishes the presence of a charge density whenever the supervelocity is aligned with an external magnetic field

$$\rho = \hat{\sigma}\ \vec{\xi} \cdot \vec{B} \tag{10.5}$$

here $\vec{\xi}$ is the superfluid velocity and $\hat{\sigma}$ the corresponding conductivity (CCGC). We provide a Kubo formula for it in Section 10.0.2 and compute its value, showing that it is generically different from zero. The response prescribed by (10.5) is not formally new, even though we believe its physical importance has not been stressed before. It has appeared in the literature and for instance it can be mapped to the term S_1 of equation (2.31) of [131] [3]. Such a term establishes the presence of a charge density whenever a transverse London-type-current $S_1 = \epsilon^{ijk}\zeta_i \partial_j \zeta_k$ is acting on the system. Since $\zeta_k = -\partial_k \phi + A_k$ (see [131]) we propose that there is an effective response of the form (10.5) arising from $S_1 = \epsilon^{ijk}\zeta_i^0 \partial_j A_k + ...$ We believe that such a transport phenomenon leads to interesting phenomenological implications.

Notice that, for the above formulae to make sense, it is important in general that the background we are considering is stable in the presence of a (perturbatively small) magnetic field, i.e. that there exists a perturbative expansion in the amplitude of a external magnetic field. Given such a perturbative expansion, at zeroth order the holographic superfluid corresponds to the background considered here. This is consistent with the usage of Kubo Formulae to compute the transport coefficients. However, for finite external magnetic fields, the holographic superfluid gets affected and, in particular, it generates London-type currents [71]. Therefore, one could argue against the validity of our results beyond perturbatively small external sources. In order to avoid that potential issue, in Section 10.2 we study a $U(1) \times U(1)$ model, in which only one of the $U(1)$'s undergoes a phase transition and thus we can study how the (unscreened) magnetic field associated to the unbroken symmetry enters the chiral transport properties.
In what follows we restrict ourselves to external gauge fields, which allows for configurations that do not excite the anomaly. This is a pertinent remark, since as we saw in the previous chapter, having a dynamical photon would imply the existence of general loop corrections to the anomalous transport coefficients [109] which are important even in the hydrodynamic approximation. Despite the fact that there is no photon here, in the broken

[1] For a detailed analysis of some of the Kubo formulae applied to Chiral Superfluids, see [133]
[2] CSE stands for Chiral Separation Effect.
[3] We thank Carlos Hoyos for pointing this out. See also [134]

phase the Goldstone boson could in general give important corrections at strong coupling. However, we expect our calculation not to capture all these contributions, for they are subleading in the classical gravity approximation.
A source of the corrections that we should be able to capture within holography is the one associated to the background scalar field. For instance, in [135] the Chiral Separation Conductivity (CSC) was indeed found to present corrections in the case of a linear sigma model (the background scalar field gives an effective mass to the fermions through the Yukawa coupling and contributes to the CSC).

Entropic arguments were used in [130] to extract the Hydrodynamics of Chiral Superfluids in the presence of external unbroken gauge fields. The Chiral Electric Effect was predicted and some possible generic corrections to the CMC and CVC were found. Moreover, in [22] it was argued that such corrections do not vanish but become universal (model independent) at low temperatures and the CMC and the CVC were computed at $T = 0$, indeed finding a universal result. Our models are restricted to the probe limit and hence we are not able to reach $T \to 0$; furthermore, we cannot induce metric perturbations and hence the CVC cannot be calculated. However, we observe that the chiral conductivities stabilize fast enough to be able to observe their $T = 0$ behaviour even at temperatures close enough to T_c, where our computations are reliable.
In what follows we consider two models, one in which a $U(1)$ anomalous symmetry undergoes a phase transition and one in which we have two $U(1)$ symmetries and only one of them develops a condensate. In the absence of supervelocity the former case reduces to a truncation of the model of [22] and indeed we observe that σ_{55} approaches the value prescribed by equation (10.1). In the latter model (not considered so far in the literature) we can define three non-vanishing anomalous conductivities at zero supervelocity [45]; our results suggest that all of them approach universal values at low temperatures. Remarkably enough, the universal ratio is always different from 1/3 and, in particular, the CMC vanishes as we increase the chemical potential.

10.0.1 Remarks on the definition of the current

At this point it is important to point out several remarks related to the definition of the currents. In the presence of a condensate, regularity imposes that the gauge field must be zero at the horizon. Hence, it is better to work from the start with the covariant definition of the current, as in [136]. Notice that this amounts to neglecting the contribution to the current operator coming from the holographic Chern-Simons term. With this manipulation there is no trace of the sources in the correlators and one can perfectly work with a boundary condition such that the background gauge field vanishes at the horizon. The resulting correlators are the ones of [45] with $\alpha = \beta = 0$. Physically, we thus will be working with the covariant current[4], and our computed retarded two-point functions contain therefore one covariant and one consistent current, namely

$$\mathcal{G}_{\mathcal{R}} \sim \langle \mathcal{J}^{\text{cov}} \mathcal{J}^{\text{cons}} \rangle \ . \tag{10.6}$$

[4]The covariant current is a gauge-invariant object and thus the source that couples to it is a good chemical potential. Therefore, by working from the beginning with the covariant current we avoid the necessity of taking into account the difference between the source for the consistent current, A_0, and the actual (gauge-invariant) chemical potential, μ (see [45] for a detailed discussion on this issue).

Notice that this in particular implies that, no matter the model under consideration, none of our (covariant) currents is conserved in general. However, this is not a problem at all since our background gauge field configurations are such that the anomaly is not excited.

10.0.2 Remarks on the Kubo Formulae

Let us point out some remarks on the Kubo formulae we are going to use. We lack formal derivation of the one corresponding to the CEC. However, assuming a constitutive relation of the form (10.4), we can derive a suitable Kubo formula for it. We point out that we do not intend to make contact with the hydrodynamic construction of [130] (for example, our Kubo relations are associated to the laboratory frame, not the Landau frame). Instead, we propose suitable Kubo formulae for the conductivities we aim to study, based on the fact that we know which the gauge-invariant sources are, as well as the type of response that we expect. Our Kubo formulae read

$$\sigma_{\{55,CSE,CME\}} = \lim_{k\to 0} \frac{i}{2k} \left\langle J^y J^z \right\rangle_{\mathcal{R}} (\omega = 0, k)\,, \tag{10.7}$$

$$\sigma_{CEC} = \lim_{\omega\to 0} \frac{i}{2\omega} \left\langle J^y J^z \right\rangle_{\mathcal{R}} (\omega, k = 0)\,, \tag{10.8}$$

$$\sigma_{CCGE} = \lim_{k\to 0} \frac{i}{2k_\perp} \left\langle J^0 J^y \right\rangle_{\mathcal{R}} (\omega = 0, k)\,. \tag{10.9}$$

Where $k_\perp$ means that the momentum points in a direction transverse to the supervelocity. All the conductivities in (10.7) are associated to similar correlators. The distinction between them comes from the nature of the currents inside the two point functions and it only makes sense in the presence of more than one $U(1)$. This will be made explicit in Section 10.2. We believe the above provide suitable expressions due to the following

- All the above conductivities vanish in the absence of anomaly.
- For $\sigma_{\{55;CSE;CME\}}$ we rely on the fact that they are related to the response to an external magnetic field by definition. Moreover, as we will see, (10.7) is continuous through the phase transition, matching the value that $\sigma_{\{55,CSE,CME\}}$ shows in the unbroken phase. In addition to this, our formula coincides with the one of [133].
- In the case of σ_{CEC}, we take into account that it corresponds to the effect of an external electric field, as in [130]. With this in mind, we choose a kinematic limit such that it can be drastically distinguished from the other anomalous transport coefficients. Moreover, we observe that $\sigma_{CEC} \sim \xi$ at low temperatures.
- The formula (10.9) can be derived from the discussion of [133] (our notation is also taken from that reference). We start with the term $J^0 = -T_0 e^\sigma g_{1,\nu} S_1$ [5] and take the variation

$$\frac{\delta S_1}{\delta A_l} = 2ik_j \epsilon^{ijk} \zeta_i^{eq.} \frac{\delta \zeta_k^{eq.}}{\delta A_l}|_{\text{sources}=0} \tag{10.10}$$

[5] $g_{1,\nu}$ is the derivative of the thermal coefficient g_1 with respect to $\nu \equiv \mu/T$ [131]

where the 2 comes from the fact that we have twice the same contribution $\epsilon^{ijk}\zeta_i^{eq.}\partial_j\frac{\delta\zeta_k^{eq.}}{\delta A_l}$. For transverse momentum, we use equation (3.29) of [133], yielding

$$\frac{\delta\zeta_i^{eq.}}{\delta A_l} = \delta_i^l - \frac{k_i k^l}{k^2} - 2iT_0 c_3 k_i \zeta_0^l \,, \tag{10.11}$$

$$\frac{\delta S_1}{\delta A_l} = 2ik_j\epsilon^{ijk}\zeta_i^0\left(\delta_k^l - \frac{k_k k^l}{k^2} - 2iT_0 c_3 k_k \zeta_0^l\right) . \tag{10.12}$$

Now, $k_k k_j \epsilon^{kj} = 0$ and hence, to first order in k we have

$$\left\langle J^0 J^l \right\rangle = -2iTg_{1,\nu}k_j\epsilon^{ijl}\zeta_i + \mathcal{O}(k^2) \tag{10.13}$$

where all the equilibrium super/subscripts "0" have been omitted. From here,

$$\epsilon_{lmn}\mathcal{G}_R^{0l} = -2iTg_{1,\nu}k_j\zeta_i\left(\delta_m^i\delta_n^j - \delta_m^j\delta_n^i\right) \tag{10.14}$$

where $\mathcal{G}_R^{0l} \equiv \left\langle J^0 J^l \right\rangle$. The formula (10.5) can be recovered by assuming $m = z, n = x$. In our notation $\zeta_i \equiv \xi_i$ and we get[6]

$$\sigma_{CCGE} \equiv T\xi_z g_{1,\nu} = \lim_{k_x\to 0}\frac{i}{2k_x}\mathcal{G}_R^{0y}(\omega = 0) \tag{10.15}$$

To avoid any possible confusion let us point out that, taking advantage of the fact that we work with a fixed component of the supervelocity, throughout this work we usually absorb the supervelocity factors into the conductivities, as prescribed by equations (10.8) and (10.9). This can be seen explicitly in (10.15). Of course, in general one has to take into account that the CEE and CCGE are linear in the supervelocity (a vector) and write expressions like (10.5) instead.

In Section 10.1 we present a simple model in which we only have one $U(1)$ anomalous symmetry that gets broken spontaneously. We reproduce the outcomes of [22] and we also include finite supervelocity and analyze the results; in particular, we compute the CEC and the CCGC via Kubo formulae, showing that they do not vanish in general. Then we move to Section 10.2, where a more realistic model is considered: we work with a $U(1)\times U(1)$ symmetry, which can be interpreted as having both axial and vector currents (for a different interpretation, see the main text), with the condensate coupled to the vector sector. The richer set of chiral conductivities is analyzed (both at zero and finite supervelocity) with special emphasis on the $T \to 0$ behaviour suggested by data. Section 10.3 includes interpretations, conclusions and future directions of the present work.

10.1 Broken Anomalous symmetry

We want to analyze, from the holographic point of view, how anomalous conductivities are altered due to the presence of an s-wave condensate. To this end we consider a holographic superconductor plus a Chern-Simons term that induces a $U(1)^3$ anomaly in the dual field theory.

[6] Notice in passing that the coefficient g_1, as defined in [131], is associated to a gauge-invariant term and hence cannot be fixed by anomaly matching. This makes the relation between chiral transport coefficients and underlying anomalies more subtle than in the case of ordinary fluids (see however Section 10.3.1).

From the point of view of the dual field theory we have a spontaneously broken $U(1)$ anomalous global symmetry. The action of the bottom-up model reads

$$S = \int d^5x\sqrt{-g}\left(-\frac{1}{4}F_{MN}F^{MN} + \frac{\kappa}{3}\epsilon^{MABCD}A_M F_{AB}F_{CD} - \overline{D_M\Psi}D^M\Psi - m^2\bar{\Psi}\Psi\right) \tag{10.16}$$

This is the model of [22] with $V_\psi = 1$, $V = m^2\bar{\Psi}\Psi$ and $\kappa = c/8$. In what follows we work with the covariant definition of the current, meaning that we are neglecting the Chern-Simons contribution to the definition of J^μ.
We take the Schwarzschild AdS Black Brane in 5 dimensions as our background metric in the bulk

$$ds^2 = -f(r)dt^2 + \frac{dr^2}{f(r)} + \frac{r^2}{L^2}(dx^2 + dy^2 + dz^2) \tag{10.17}$$

being $f(r) = \frac{r^2}{L^2} - \frac{r_H^2}{r^2}$. From now on we work in adimensional units, rescaling all the L^2 factors to one. Our ansatz for the background fields consists of a non-vanishing temporal and spatial component of the gauge field and the real component of the scalar field. All of them with just radial dependence

$$A = \phi(r)dt + V(r)dx; \qquad \Psi(r) = \psi(r) \tag{10.18}$$

With this ansatz the background equations of motion reduce to

$$\phi'' + \frac{3}{r}\phi' - \frac{2\psi^2}{f}\phi = 0 \tag{10.19}$$

$$\psi'' + \left(\frac{f'}{f} + \frac{3}{r}\right)\psi' + \frac{\phi^2}{f^2}\psi - \frac{V^2}{r^2 f}\psi - \frac{m^2}{f}\psi = 0 \tag{10.20}$$

$$V'' + \left(\frac{f'}{f} + \frac{1}{r}\right)V' - \frac{2\psi^2}{f}V = 0 \tag{10.21}$$

The equations boil down to the ones which govern the usual s-wave holographic superconductor in the presence of supervelocity (see 7.2). This could have been anticipated by noticing that the ansatz does not excite the Chern-Simons contribution $\kappa\epsilon^{MABCD}F_{AB}F_{CD}$ to the gauge field equation. Hence, the anomaly is absent at the level of the background. However, it has important implications for the perturbations.
In our convention we choose to fix the temperature and interpret the adimensional quantities

$$\bar{\mu} = \frac{\mu}{T}; \qquad \vec{\bar{\xi}} = \frac{\vec{\xi}}{T} \tag{10.22}$$

as the chemical potential and the supervelocity of the system (along this work we make some abuse of language and refer to the $\bar{\mu} \to \infty$ regime as the $T \to 0$ limit), which are determined by the boundary conditions of the fields to be imposed at spatial infinity:

$$\phi(r)_{r\to\infty} \sim \mu_5 \qquad V(r)_{r\to\infty} \sim \xi_{\{x,z\}} \tag{10.23}$$

By $\xi_{\{x,z\}}$ we mean that the supervelocity will be taken to be pointing either in the x or the z-direction. In addition, we choose the standard quantization, by imposing the boundary

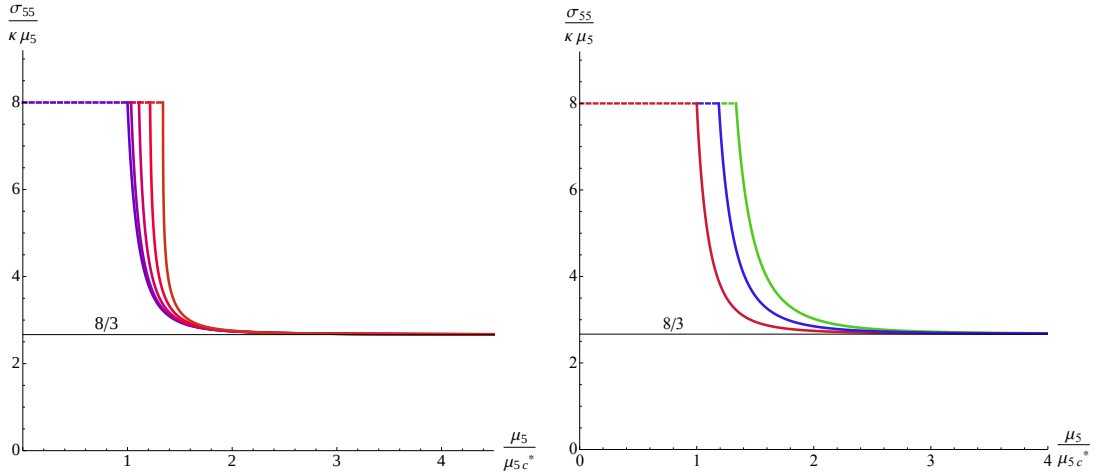

Figure 10.1: Axial conductivity divided by the chemical potential and the anomaly coefficient versus chemical potential. μ_{5c}^* is the critical chemical potential at zero supervelocity . (Left) Each line corresponds to same mass value $m^2 = -7/2$ and different superfluid velocity, from $\xi_x/T = 0.1$ (blue) to $\xi_x/T = 2.1$ (orange). The dashed horizontal line corresponds to the unbroken phase, where $\sigma_{55} \sim \mu_5$. In the broken phase this conductivity approaches $1/3$ of the unbroken phase value for large enough chemical potential. This is compatible with the results of [22]. (Right) Each line corresponds to a different mass (red $m^2 = -7/2$, blue $m^2 = -3$, green $m^2 = -5/2$) of the scalar field in the bulk. As one can see the $1/3$ factor is unaltered by the dimension of the operator that condenses. The conductivity depends linearly with κ.

conditions to the leading term in the asymptotic expansion of the scalar field

$$\psi(r)_{r\to\infty} \sim \frac{\psi_1}{r^{\Delta_-}} + \frac{\psi_2}{r^{\Delta_+}} + \ldots$$

$$\psi_1 = 0 \qquad\qquad \psi_2 = \langle O \rangle \tag{10.24}$$

We solve equations (10.19)-(10.21) with this boundary conditions numerically.

Before we proceed to discuss our results for the conductivities a comment is in order regarding the background we have constructed. In our study of the Landau criterion for holographic superfluids in chapter 7 we showed that the system presents instabilities at finite momentum close to the phase transition for a large range of supervelocities. Although this analysis was made in AdS_{3+1} we expect it to apply in AdS_{4+1} as well. We do not discard those issues to have some influence, even though, as we will see later on, all of our results seem to be perfectly consistent for every value of the chemical potential. In any case, let us emphasize that our forthcoming main observations have to do with the behaviour of the conductivities far from the transition point, where the above potential issues are not expected to play any role.

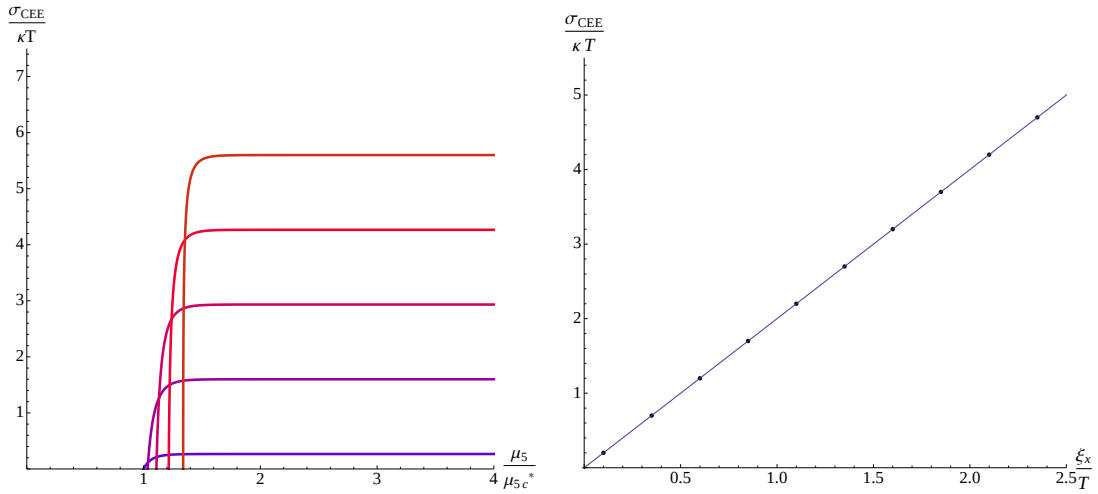

Figure 10.2: (Left) Chiral electric conductivity versus chemical potential. Each line corresponds to a different superfluid velocity, $\xi_x/T = 0.1 - 2.1$. We observe that $\sigma_{CEE}/\kappa T = 0$ at μ_{5c} and it approaches a constant value at low temperatures/ large chemical potential. (Right) Dots correspond to $\sigma_{CEE}/\kappa T$ versus $\bar{\xi}_x$ in the large μ_5 region in which $\sigma_{CEE}/\kappa T$ is independent of μ_5. The solid line corresponds to a linear fit; the slope is 2.667. The conductivity depends linearly with κ.

10.1.1 The Chiral conductivities in the broken phase: Axial conductivity and CEC

In order to compute the chiral conductivities from the Kubo formulae (10.3)-(10.5) we study perturbations on top of the background we have built. We first want to explore the axial conductivity[7] and the CEC, therefore we switch on the perturbations with non-vanishing frequency and momentum pointing in the direction parallel to the supervelocity (that we choose to be the x-direction). The sector we are interested in decouples from the rest of the field perturbations in this kinematic setup, leaving us with just the perturbations of the transverse gauge fields

$$\delta A_y = a_y(r,t,x); \qquad \delta A_z = a_z(r,t,x) \tag{10.25}$$

In momentum space the equations read

$$a_y'' + \left(\frac{f'}{f} + \frac{1}{r}\right) a_y' + \frac{1}{f}\left(\frac{\omega^2}{f} - \frac{k^2 L^2}{r^2} - 2\psi^2\right) a_y + 16ik\frac{\kappa L}{rf}\phi' a_z + 16i\omega\frac{\kappa L}{rf}V' a_z = 0 \tag{10.26}$$

$$a_z'' + \left(\frac{f'}{f} + \frac{1}{r}\right) a_z' + \frac{1}{f}\left(\frac{\omega^2}{f} - \frac{k^2 L^2}{r^2} - 2\psi^2\right) a_z - 16ik\frac{\kappa L}{rf}\phi' a_y - 16i\omega\frac{\kappa L}{rf}V' a_y = 0 \tag{10.27}$$

[7] In the literature this conductivity has often been directly associated to the CMC, for the qualitative dependence of the three conductivities of (10.3) on the axial/vector chemical potentials is the same in the absence of condensate. However, there are significant differences when a condensate distinguishing between axial and vector currents is present, as we will see. Thus, we stick to the notation of [45] and denote as CMC the conductivity related to a vector-vector correlator when a AVV anomaly is switched on.

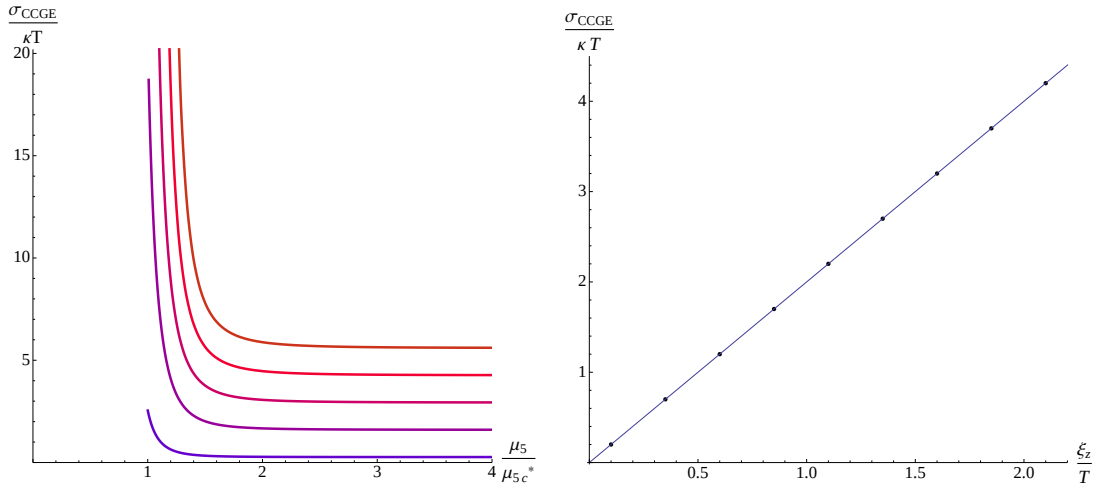

Figure 10.3: (Left) Chiral charge generation conductivity versus chemical potential, different lines correspond to different values of the supervelocity, $\xi_x/T = 0.1 - 2.1$. (Right) Dots correspond to σ_{CCGE} versus supervelocity for large values of the chemical potential. The solid line corresponds to a linear fit; the slope is 2.667. The conductivity depends linearly with κ.

In the unbroken phase it is possible to find an analytic solution to the above system of equations in the kinematic limit $\omega = 0$ and to first order in momentum $k_x \equiv k$. Recall that this is all that we need in order to obtain σ_{55}, making use of Kubo formulae [119]. However, in the case at hand the background has been computed numerically and therefore we look directly for numerical solutions to the system (10.26)-(10.27).
We are now ready to calculate the Kubo formulae shown in (10.3)-(10.5). The problem reduces to numerically computing the two retarded 2-point functions with the usual holographic prescription [57] (see the appendix for details on the computation).

A comment that applies to all figures is in order here. The critical value of the chemical potential depends on the value of the supervelocity and the mass of the scalar field. In our convention, μ_c^* is the critical value at zero supervelocity and $m^2 = -7/2$.

Our results for σ_{55} are depicted in Figure 10.1. We observe that σ_{55} is proportional to the (axial) chemical potential even in the broken phase. However, the coefficient of proportionality decreases from 1 to 1/3 in units of $e^2 N_c/4\pi^2$. Numerically, in terms of κ we get[8]

$$\frac{\sigma_{55}\left(\frac{\bar{\mu}_5}{\bar{\mu}_{5c}} >> 1\right)}{\kappa\mu_5} = 2.668 \approx \frac{8}{3}\,. \tag{10.28}$$

This reduction has been predicted to be universal. In our model, we can check that this is independent from the mass of the bulk scalar field (right plot of Figure 10.1). Remarkably, finite supervelocity does not alter these conclusions, as depicted in Figure 10.1 (left); the correction to the transport coefficient is independent of the supervelocity. As a final

[8] In order to make contact with the computation in the unbroken phase of [119], notice that we have set $16\pi G \equiv 1$ in (10.16). Hence, their result $\sigma_B^{\text{unbrok.}} = 8\kappa\mu_5/(16\pi G)$ corresponds to $\sigma_{55}^{\text{unbrok.}} = 8\mu_5\kappa$ with our conventions.

remark, we find that the dependence of the axial conductivity with κ is unaffected by the presence of the condensate and the supervelocity, namely $\sigma_{55} \sim \kappa$.
Moving to the CEC, we observe that it starts increasing but rapidly approaches a constant value, independent of μ_5/T. On the contrary, it linearly increases with the superfluid velocity for large chemical potential, see Figure 10.2. Or results thus strongly suggest that, at low temperatures,

$$\frac{\sigma_{CEE}\left(\frac{\bar{\mu}_5}{\bar{\mu}_{5c}} >> 1\right)}{\kappa T} = 2.667\frac{\xi_x}{T} \approx \frac{8}{3}\frac{\xi_x}{T}\,. \tag{10.29}$$

Notice that this value is essentially the same as the observed for σ_{55} at large axial chemical potential. Again the dependence with κ is linear.

10.1.2 The Chiral Charge Generation Effect

Let us now induce a supervelocity in the z-direction, by turning on $A_z(r)$ instead of $A_x(r)$ in the bulk. This, as anticipated, influences the quasinormal modes, even though the background equations remain the same as in the previous subsection (due to the fact that, without superflow, the background is isotropic), with the replacement $A_x \leftrightarrow A_z$. On top of this we switch on perturbations with non-vanishing frequency and momentum pointing in the x-direction (transverse to the supervelocity). The equations for the perturbations in the transverse sector are more involved now for they couple to all other perturbations. They can be found in appendix A.10.1 .
As mentioned in the introduction, the CCGE corresponds to a "generation" of charge proportional to the scalar product of the supervelocity and the magnetic field

$$\rho = \hat{\sigma}\ \vec{\xi}\cdot\vec{B}\,. \tag{10.30}$$

As aforementioned, for convenience we absorb the supervelocity component into the conductivity, i.e. $\sigma_{CCGE} = \hat{\sigma}\xi_z$. Note that the charge vanishes if the supervelocity is parallel to the external momentum. In order to observe such an effect, we use (10.9).
We proceed as before and present our result in Figure 10.3 . We observe that indeed this phenomenon is not negligible in the presence of supervelocity. Moreover, it stabilizes at large enough chemical potential; in the region in which σ_{CCGE} does not depend on $\bar{\mu}_5$, it presents a clear linear dependence on the superfluid velocity (right plot of Figure 10.3). We can perform a numerical quadratic fit, obtaining

$$\frac{\sigma_{CCGE}\left(\frac{\bar{\mu}_5}{\bar{\mu}_{5c}} >> 1\right)}{\kappa T} = 2.667\frac{\xi_z}{T} \approx \frac{8}{3}\frac{\xi_z}{T} \tag{10.31}$$

to a good approximation. Again, the slope has the same value as for the CEC. Let us emphasize that the behaviour of this transport coefficient at the phase transition is strange at first sight. Naively, we would have expected $\sigma_{CCGE}(\bar{\mu}_c) = 0$ instead of the observed value. We comment on this issue in Section 10.3.

10.2 Model with axial and vector currents

In this section we study the more realistic model, in which we consider two $U(1)$ bulk gauge fields, being only one of them spontaneously broken. There are two different interpretations of this model:

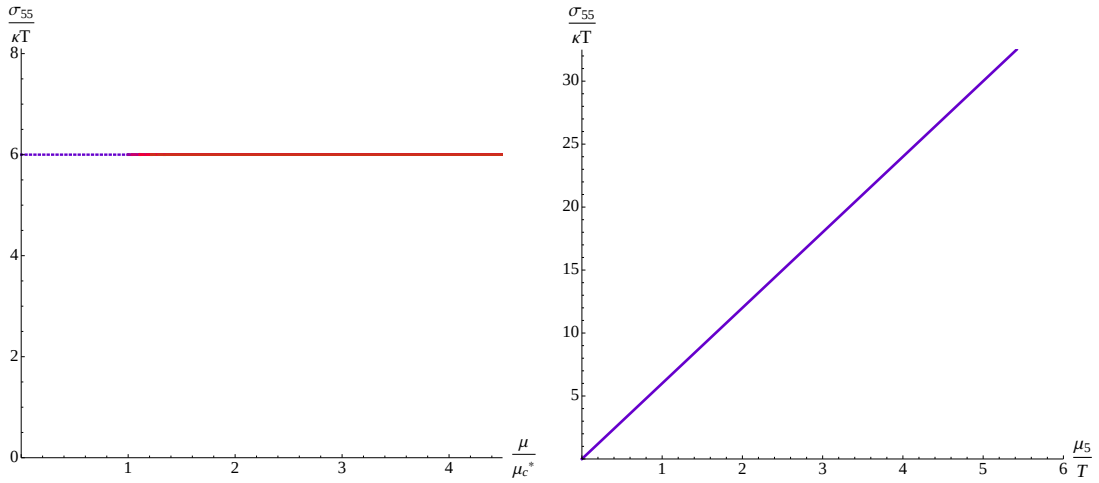

Figure 10.4: (Left) Axial conductivity versus vector chemical potential at $\bar{\mu}_5 = 1$ and $\xi_x/T = 0.1 - 2.1$. We find that σ_{55} is independent of both the vector chemical potential and the superfluid velocity. (Right) σ_{55} versus axial chemical potential. The dependence with μ_5 is linear, as expected. The conductivity depends linearly with κ.

- We have axial and vector currents $U(1)_V \times U(1)_A$ and the condensate is coupled only to the vector part, whereas the axial symmetry is unbroken. This realizes the interplay between anomalous axial and vector currents, first considered in [45]. The fact that the axial current is not coupled to the scalar field means that the axial charge of the condensate is zero, so the axial chemical potential can be made constant through the phase transition and is not affected by the condensation whatsoever.
- The unbroken $U(1)$ is a generic field and the two $U(1)$'s are intertwined in a particular way by the anomaly. With this second interpretation, crossed anomalous correlators can be related to the response of the (broken) current to an external unscreened magnetic field, associated to the unbroken symmetry. This avoids any possible problem with the physical realization external magnetic fields contained in the bulk of the system.

Despite of the two possible interpretations, we use a notation adapted to the first one. The action of the model contains a complex scalar field coupled to the vector sector

$$\mathcal{L} = -\frac{1}{4}F_{MN}F^{MN} - \frac{1}{4}G_{MN}G^{MN} + \frac{\kappa}{2}\epsilon^{MABCD}A_M(3F_{AB}F_{CD} + G_{AB}G_{CD}) - \overline{D_M\Psi}D^M\Psi - m^2\bar{\Psi}\Psi\,. \tag{10.32}$$

Here F is the field strength for the vector gauge field V and G is the analogue for the axial gauge field A. Moreover $D_M\Psi = \partial_M\Psi - iV_M\Psi$. We consider AAA and AVV anomalies. The equations of motion for the background are the same as (10.19)-(10.21), with an additional equation for the background axial gauge field $A(r) = K(r)dt$

$$K'' + \frac{3}{r}K' = 0 \tag{10.33}$$

which has a trivial analytic solution $K(r) = K_0 - K_1/r^2$. The boundary conditions for the gauge fields are:

$$\phi(r)_{r\to\infty} \sim \mu \qquad V(r)_{r\to\infty} \sim \xi_{\{x,z\}} \qquad K(r)_{r\to\infty} \sim \mu_5 \tag{10.34}$$

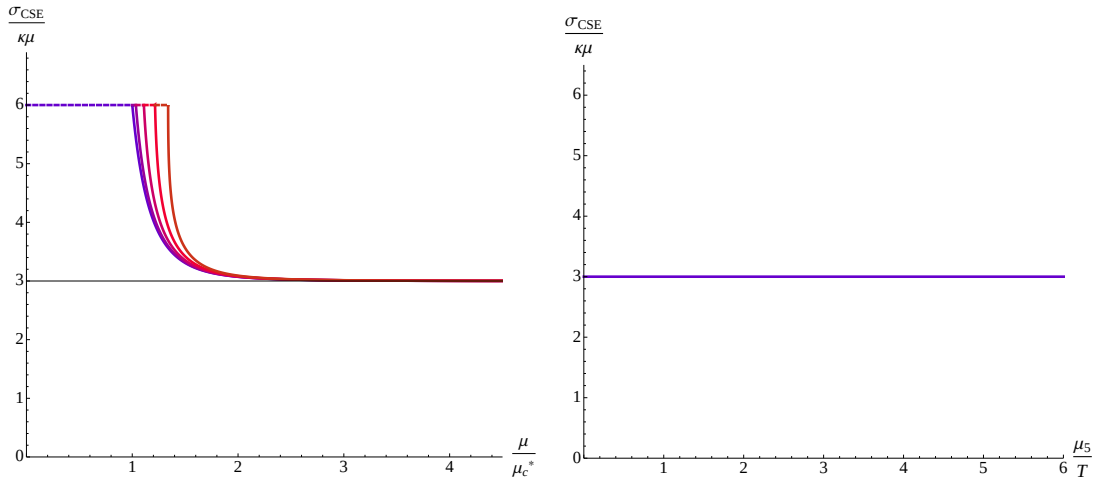

Figure 10.5: (Left) Chiral separation conductivity divided by vector chemical potential versus vector chemical potential, $\bar{\mu}_5 = 1$ and $\xi_x/T = 0.1 - 2.1$. The conductivity now approaches $1/2$ of the value at $\bar{\mu}_c$, independently of ξ_x/T. (Right) The plot shows this conductivity against the axial chemical potential for generic values of μ. σ_{CSE} is independent of the axial chemical potential in both the broken and unbroken phases. The conductivity depends linearly with κ.

We impose again standard quantization for the scalar field. First we choose the supervelocity to point in the x-direction. On top of this we switch on the perturbations with non-vanishing frequency and momentum parallel to the supervelocity. The equations for the perturbations in the transverse sector can be found in appendix A.10.2. There is a wider set of correlators that we can study in this set up

$$\sigma_{55} = \lim_{k\to 0} \frac{i}{2k} \left\langle J_A^y J_A^z \right\rangle_{\mathcal{R}} (\omega = 0, k) \tag{10.35}$$

$$\sigma_{CSE} = \lim_{k\to 0} \frac{i}{2k} \left\langle J_V^y J_A^z \right\rangle_{\mathcal{R}} (\omega = 0, k) \tag{10.36}$$

$$\sigma_{CME} = \lim_{k\to 0} \frac{i}{2k} \left\langle J_V^y J_V^z \right\rangle_{\mathcal{R}} (\omega = 0, k) \tag{10.37}$$

In the superfluid phase, after assuming that the supervelocity is transverse to the momentum, we can also consider the Kubo formulae related to the Chiral Electric Effect and the Chiral Charge Generation Effect

$$\sigma^A_{CCGE} = \lim_{k\to 0} \frac{i}{2k_\perp} \left\langle J_A^0 J_V^y \right\rangle_{\mathcal{R}} (\omega = 0, k) \; ; \qquad \sigma^V_{CCGE} = \lim_{k\to 0} \frac{i}{2k_\perp} \left\langle J_V^0 J_A^y \right\rangle_{\mathcal{R}} (\omega = 0, k) \tag{10.38}$$

$$\sigma^A_{CEE} = \lim_{k\to 0} \frac{i}{2\omega} \left\langle J_A^y J_V^z \right\rangle_{\mathcal{R}} (\omega, k = 0) \; ; \qquad \sigma^V_{CEE} = \lim_{k\to 0} \frac{i}{2\omega} \left\langle J_V^y J_A^z \right\rangle_{\mathcal{R}} (\omega, k = 0) \tag{10.39}$$

We expect them to receive different corrections due to the fact that the condensate distinguishes between the vector and the axial symmetry. Notice that our notation establishes that, for example, $\rho_A = \sigma^A_{CCGE} B_z^V$ and $\rho_V = \sigma^V_{CCGE} B_z^A$.

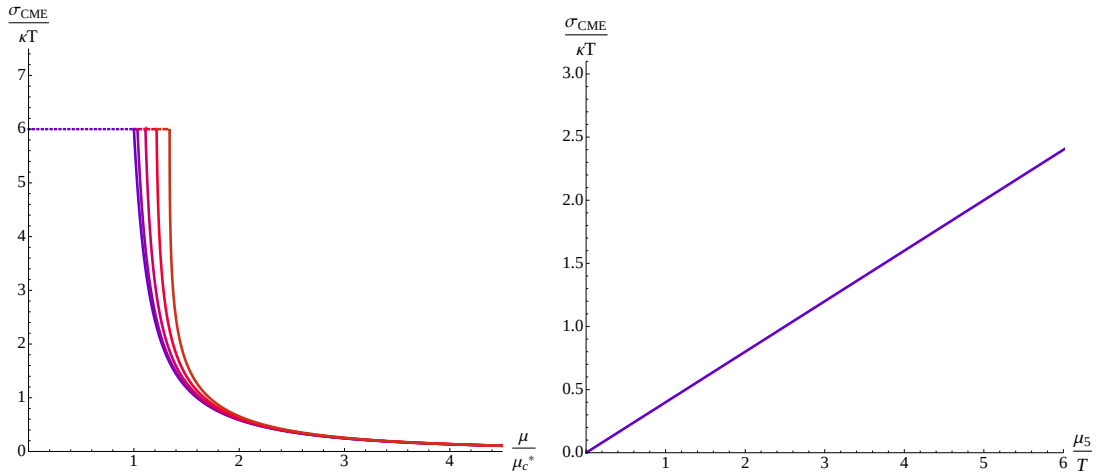

Figure 10.6: (Left) Chiral magnetic conductivity versus vector chemical potential with $\bar{\mu}_5 = 1$. Different lines correspond to different values of the superfluid velocity, with $\xi_x/T = 0.1 - 2.1$. The best fit shows that for large enough values of $\bar{\mu}$ it decreases as $\sigma \sim 1/\bar{\mu}^2$. (Right) $\sigma_{CME}/\kappa T$ vs. axial chemical potential with $\mu/T = 2.5$. The linear dependence with μ_5, characteristic of the unbroken phase, remains unaltered. The conductivity depends linearly with κ.

Our results are as follows. On the one hand, the correlator $\langle J_5^y J_5^z \rangle$ does not get altered due to the condensate, and is linear in μ_5, as depicted in Figure 10.4. The behavior could have been anticipated, since the on-shell action is diagonal in vector/axial sectors and it is clear that in the dynamical equations (A.137)-(A.138) the mixing between a_y and a_z is independent of the condensate. This is ultimately due to the fact that the condensate only couples to the vector sector and that the correlator $\langle J_5^y J_5^z \rangle$ is only sensitive to the AAA anomaly[9].

On the other hand, the results concerning σ_{CSE} are summarized in Figure 10.5. This conductivity acts similarly to that encountered in the first section. This was expected by the form of the equations of motion: in this model, the correlator mixing between a_y and v_z is mediated by the same background fields as in the model with only axial symmetry. Remarkably, unlike the case with a $U(1)^3$ anomaly, at large values of $\bar{\mu}$ we obtain[10]

$$\frac{\sigma_{CSE}\left(\frac{\bar{\mu}}{\bar{\mu}_c} >> 1\right)}{\kappa\mu} = 2.998 \approx \frac{\sigma_{CSE}(\bar{\mu}_c)}{2\kappa\mu}\,, \tag{10.40}$$

independently of the superfluid velocity. This result indicates that the $T \to 0$ behaviour is strongly dependent on the structure of the broken symmetries and the interplay of the anomalies. Moreover, the conductivity does not depend on the axial chemical potential (right plot).

Finally, let us comment on the σ_{CME}. The results are displayed in Figure 10.6. We find a linear dependence on $\bar{\mu}_5$, as expected. However, in the presence of the condensate we observe a new dependence on the vector chemical potential, which is absent in the

[9]The independence of the condensate can be spoiled by altering the model. For instance, by inducing an axial component for the condensate.

[10]The numerical value $\sigma_{CSE}(T_c)/(\kappa\mu) \approx 6$ depends on the strength of the κ-term in the equations of motion and is not of fundamental importance, for it can be easily rescaled (compare to Section 10.1).

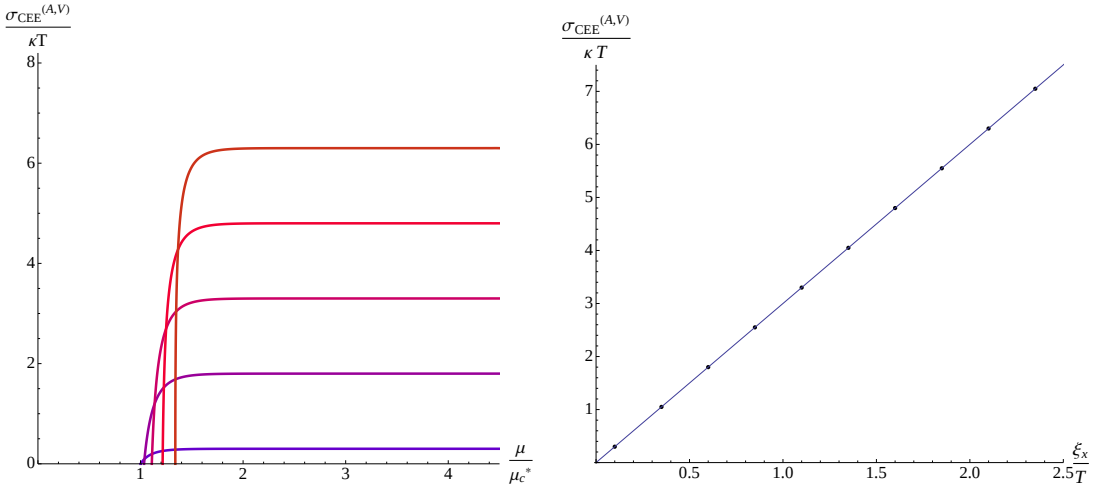

Figure 10.7: (Left) Chiral electric conductivity versus vector chemical potential at $\bar{\mu}_5 = 1$ and $\xi_x/T = 0.1{-}2.1$ (bottom to top). Both σ^V_{CEE}/T and σ^A_{CEE}/T show the same behaviour . (Right) Chiral electric conductivities versus supervelocity at $\bar{\mu}_5 = 1$ in the region where they don't depend on μ. The conductivity depends linearly with κ.

unbroken phase. The chemical potential diminishes the value of the CMC strongly and it tends to zero for large values of $\bar{\mu}$ as

$$\frac{\sigma_{CME}\left(\frac{\bar{\mu}}{\bar{\mu}_c} >> 1\right)}{\kappa T} \approx g\frac{1}{\bar{\mu}^2} \tag{10.41}$$

with a numerical value for $g \approx 2.15$. We elaborate on this in Section 10.3.

For the chiral transport coefficients associated to the CEE, we observe that correlators of the form $\langle J_A J_A\rangle\,(k=0)$ and $\langle J_V J_V\rangle\,(k=0)$ vanish identically. Concerning the ones mixing axial and vector currents, we observe that $\sigma^V_{CEE} = \sigma^A_{CEE} \equiv \sigma^{(V,A)}_{CEE}$. The result is depicted in Figure 10.7. Fitting the right plot to a parabola, we get

$$\frac{\sigma^{(V,A)}_{CEE}\left(\frac{\bar{\mu}}{\bar{\mu}_c} >> 1\right)}{\kappa T} = 3.003\frac{\xi_x}{T}. \tag{10.42}$$

with remarkable precision.

10.2.1 $U(1) \times U(1)$ model with transverse supervelocity

As we did in the previous model, in order to study the CCGE we switch on perturbations with non-zero frequency and momentum pointing in the x-direction, transverse to the superfluid velocity (z-direction). The system of equations with transverse supervelocity can be found in appendix A.10.3. We report the results on the CCGC in Figure 10.8.
As shown in there are now two different conductivities related to the CCGE, which we denote $\sigma^{(V)}_{CCGE}$ and $\sigma^{(A)}_{CCGE}$ They exhibit a very different behavior close to $\bar{\mu}_c$; the conductivity $\sigma^{(V)}_{CCGE}$ is similar to the one found in Section 10.1.2, whereas $\sigma^{(A)}_{CCGE}$ looks like the CEC, with a good continuous behavior at the phase transition. We comment on those differences in Section 10.3. At low temperatures, however, both $\sigma^{(A)}_{CCGE}$ and $\sigma^{(V)}_{CCGE}$ tend

to the same value and the dependence with the supervelocity is linear (Figure 10.9). A quadratic fit yields

$$\frac{\sigma^{(V,A)}_{CCGE}\left(\frac{\bar{\mu}}{\bar{\mu}_c} >> 1\right)}{\kappa T} = 3.003\frac{\xi_z}{T}. \tag{10.43}$$

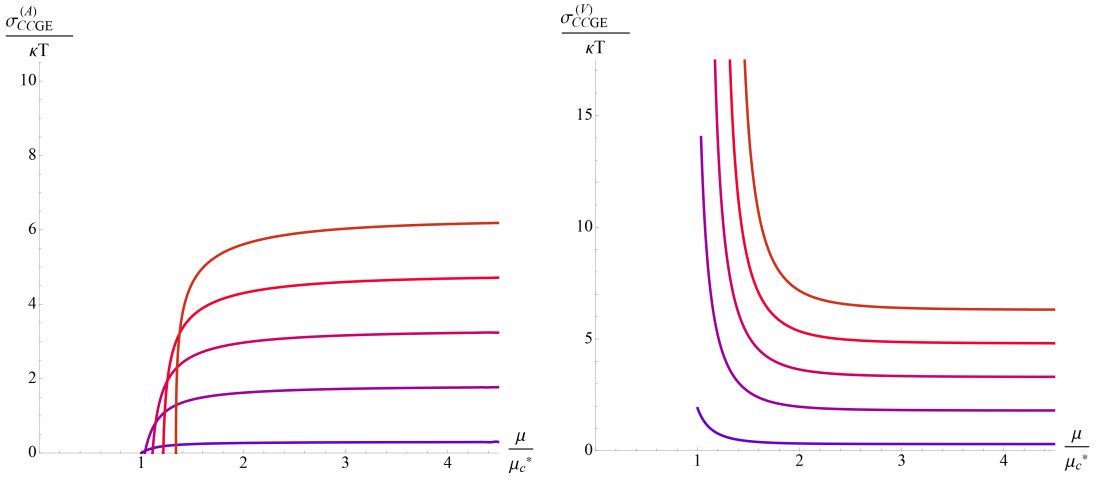

Figure 10.8: $\sigma^{(A)}_{CCGE}/\kappa T$ (Left) and $\sigma^{(V)}_{CCGE}/\kappa T$ (Right) versus vector chemical potential at $\bar{\mu}_5 = 1$ and $\xi_x/T = 0.1 - 2.1$ (bottom to top). For large enough values of the chemical potential both conductivities show the same behaviour. Both depend linearly with κ

Remarkably enough, we point out that the conductivity

$$\sigma^{(VV)}_{CCGE} = \lim_{k\to 0}\frac{i}{2k_\perp}\left\langle J^0_V J^y_V\right\rangle_{\mathcal{R}}(\omega = 0, k)\,, \tag{10.44}$$

depicted in Figure 10.10, is not negligible. In principle we could have anticipated it to vanish because of the structure of the anomalies included in the Lagrangian (10.32). As shown in the plot, this only occurs far enough form the phase transition. This effect points towards an "effective VVV anomaly" (see also the results concerning the CMC) that is present close to the phase transition.

10.3 Discussion

We have analyzed the explicit form of the chiral conductivities in two holographic models with $U(1)$ and $U(1) \times U(1)$ symmetries, in presence of a scalar condensate, at finite superfluid velocity. We have presented an explicit calculation of CEE by using a suitable Kubo formula, which allowed us to prove in a robust way that the CEC is in general not vanishing in superfluids.
Moreover, by means of the Kubo formulae we have found an effect whose existence, as far as we are aware, had not been emphasized before in the literature. This induces the presence of axial charge in the presence of supervelocity and a magnetic field

$$\rho_A \propto \vec{\xi}\cdot\vec{B} \tag{10.45}$$

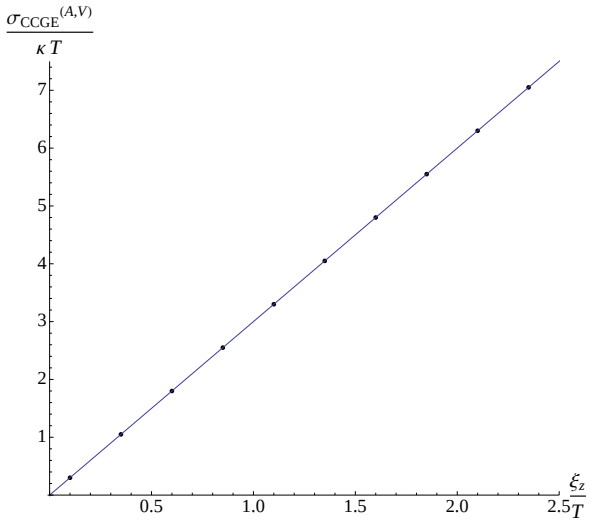

Figure 10.9: Both conductivities $\sigma^{(A,V)}_{CCGE}$ show the same dependence on the vector chemical potential μ and the supervelocity ξ_z for large enough values of μ. The slope coincides with the slope for the CEC, despite the radically different behaviour close to the phase transition.

Such a term has interesting consequences. For instance, the Chiral Magnetic Effect would be dynamically produced in a superfluid in the presence of an external magnetic field aligned with the supervelocity. We believe this term deserves more investigation in the future, in order to fully understand the mechanism by which charge is "generated", as well as to analyze the implications that it could lead to.
In addition, we have found generic corrections, due to the background condensate, to all of the anomalous conductivities. Such corrections seem to take a constant value as $T \to 0$ in all of the cases. We observe that such value is model-dependent, but seems to be strongly constrained by the number of broken symmetries and the interplay between the anomalies.

Section 10.1 is devoted to the study of the chiral transport of a broken anomalous $U(1)$ symmetry. At $\xi = 0$, we found the result previously pointed out, namely, the value of the conductivity is $1/3$ of that in the unbroken phase, i.e,

$$\sigma_{55}(T \to 0) \approx \frac{8\kappa}{3}\mu_5 = \frac{\sigma_{55}(T_c)}{3}\,. \tag{10.46}$$

This fact turns out not to be affected when a supervelocity parallel to the momentum is considered. Moreover, as soon as supervelocity is considered, we have two new anomalous effects present: The Chiral Electric Effect and the Chiral Charge Generation Effect. We proposed suitable Kubo formulae for both the CEE and CCGE and computed their value, finding that both become independent from the chemical potential at sufficiently low temperatures. Moreover, their dependence with the superfluid velocity is linear, i.e.,

$$\sigma_{CEE}(T \to 0) \approx \sigma_{CCGE}(T \to 0) \approx \frac{8\kappa}{3}\xi_x\,, \tag{10.47}$$

Section 10.2 deals with two $U(1)$ global symmetries, giving rise to a more rich set of anomalous conductivities with different behaviors once one of the $U(1)$ symmetries

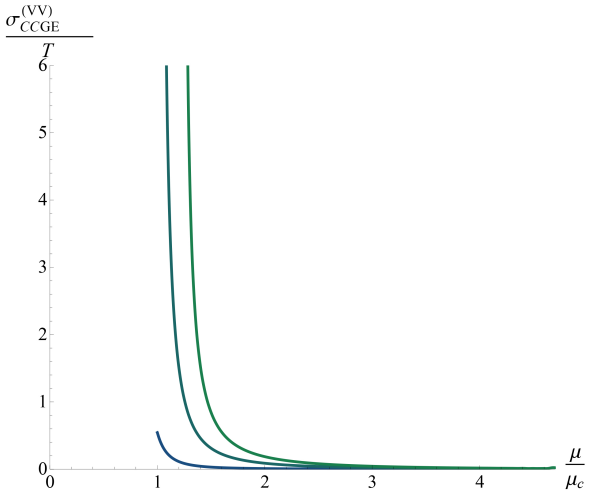

Figure 10.10: Plot of the $\sigma^{(VV)}_{CCGE}$ conductivity (defined in the text) versus vector chemical potential for several values of the supervelocity.

gets spontaneously broken. The transport coefficient σ_{55} remains the same as in the unbroken phase, but the CMC now acquires a dependence of the vector chemical potential that makes it vanish as we lower the temperature. This result suggests that the charged particles stored in the condensate (forming "cooper pairs") do not contribute to the CMC, which hence vanishes at sufficiently low temperatures. The decrease of the CMC seems to be following a law of the form $\sigma_{CME}/T \sim g/\bar{\mu}^2$, with $g \approx 2.15$. The scaling of σ_{CME} with the axial chemical potential is the usual one, namely $\sigma_{CME} \sim \mu_A$. Finally, the CSE decreases up to 1/2 the value that it presents in the unbroken phase, yielding

$$\sigma_{CSE}(T \to 0) \approx \frac{6\kappa}{2}\mu = \frac{\sigma_{CSE}(T_c)}{2}\,. \tag{10.48}$$

These results do not get altered when inducing supervelocity. Furthermore, we observe $\sigma^V_{CEE} = \sigma^A_{CEE}$, both presenting a qualitative behavior that is similar to the one of Section 10.1; however the scaling with supervelocity is now

$$\sigma^{(V,A)}_{CEE}(T \to 0) \approx 3\kappa\xi_x \tag{10.49}$$

Finally, $\sigma^V_{CCGE} \neq \sigma^A_{CCGE}$ close to the phase transition. At low temperatures both tend to the same value and the same dependence on supervelocity, namely

$$\sigma^{(V,A)}_{CCGE}(T \to 0) \approx 3\kappa\xi_z \tag{10.50}$$

10.3.1 On the Low temperature behaviour of the Chiral Conductivities

A simple argument by which the CCGE is expected to arise in superfluids is the following. Imagine that we have free Chiral fermions coupled to an electromagnetic field A_μ.

$$\mathcal{L} = \bar{\psi}(V_\mu - A_\mu)\gamma^\mu\psi \tag{10.51}$$

We also couple them to an external field V_μ associated to a $U(1)$ symmetry that gets spontaneously broken. The axial current $j^\mu_{\text{axial}} = \bar{\psi}\gamma^\mu\gamma^5\psi$ is anomalous. Hence, in general

$$\partial_\mu j^\mu_{\text{axial}} = a\ F\wedge F + b\ G\wedge F + c\ G\wedge G \tag{10.52}$$

where a, b and c are coefficients; F and G are the stress-tensors associated to A_μ and V_μ respectively. There is no external axial field. Let us concentrate on the term proportional to b; due to the Bianchi identities, it can be rewritten as $b\ \partial_\mu(\epsilon^{\mu\nu\rho\lambda}V_\nu F_{\rho\lambda})$[11]. At this point, we substitute the actual value of V_μ, which, assuming that $\mu = 0$, corresponds to $V_\mu = (0, \xi_x, 0, 0)$[12]. Assuming that j^μ_{axial} does not depend on the position, we find, in momentum space

$$\omega j^\mu_{\text{axial}} = \omega b\epsilon^{\mu x\rho\lambda}\xi_x F_{\rho\lambda} + ... \tag{10.53}$$

leading to both the Chiral Electric Effect and the Chiral Charge Generation Effect, i.e,

$$j^y_{\text{axial}} \sim b\epsilon^{yxtz}\xi_x E_z \tag{10.54}$$
$$j^t_{\text{axial}} \sim b\epsilon^{txyz}\xi_x B_x \tag{10.55}$$

The above argument "with the hands" leads us to some notion of covariantization of those effects[13]. This would imply that for the $U(1)^3$ anomaly, the anomalous contribution to the current can be recast in a covariant form

$$J^\mu_{\text{anom}}(T\to 0) = \Sigma^{\mathcal{A}}_{SCE}\epsilon^{\mu\nu\rho\lambda}u^S_\nu F_{\rho\lambda} + ... \tag{10.56}$$

where $u^{S\mu} = -\mu u^\mu + \zeta_\nu P^{\nu\mu}$ is the (non-normalized) superfluid velocity and the "..." indicate possible corrections due to vorticity. This covariant form of the response can be analyzed numerically by establishing the numerical universality (up to the form of the interplay between the anomaly $\mathcal{A}$ and the broken symmetries) of the coefficient $\Sigma^{\mathcal{A}}_{SCE}$. Our results suggest that the superfluid component (the only one present at zero temperature) gives a contribution of the form (10.56) with

$$\Sigma^{AAA}_{SCE} = \frac{C}{3} \tag{10.57}$$

being C a number that is fully determined by the anomaly coefficient.
For the $U(1)\times U(1)$ model the at zero temperatures there exists a subset of non-vanishing chiral conductivities for which (10.56) applies, with

$$\Sigma^{AVV}_{SCE} = \frac{C}{2}\,. \tag{10.58}$$

[11] Notice that, since the symmetry is spontaneously broken, in principle we have to substitute $V_\mu \to V_\mu - \partial_\mu\phi$, where ϕ is the Goldstone mode. However, for simplicity we stick to a gauge in which $\phi = 0$. This will not influence our conclusions.

[12] One can consider $\xi \to \xi e^{-i\omega t}$ instead, to bring down the frequency in 10.53 consistently. At the end of the calculation all the ω factors will cancel.

[13] A cautionary remark is in order here. It is not clear to us whether an argument such as the one presented here gives the complete answer, i.e. whether one can associate the parameter b in (10.55) to the actual σ_{CCGE}. Most likely one cannot. The reason for our concerns is that, for instance, the reasoning does not distinguish between covariant/consistent currents and overlooks the subtleties associated to the introduction of chemical potential/supervelocity in the presence of anomalous symmetries. However, we believe that it serves to illustrate the kind of transport phenomena that we expect, for it works at the formal level.

Equations (10.57) and (10.58) are very suggestive. The nature of the number in the denominator of Σ^{A}_{SCE} appears to be determined by the spontaneously broken symmetries that are contained in the anomaly responsible for the chiral conductivity under consideration.
Furthermore, one could ask whether the conclusions presented here are universal, i.e. valid for all holographic s-wave superfluids or even beyond the holographic approach. If (10.57) and (10.58) held in general, it would imply that at zero temperature the anomalous conductivities have a robust value, entirely determined by anomaly coefficients plus the interplay between the broken symmetries and the anomalies.
We would also like to emphasize that formula (10.15) allows us to extract the coefficient termed $g_1(T, \mu/T, \xi^2/T^2)$ in [131]. At low temperatures, our numerical results for the CCGC and σ_{55} for the $U(1)^3$ anomaly are perfectly compatible with

$$g_1(\bar{\mu} >> 1) = -\frac{C}{3}\frac{\mu}{T} \tag{10.59}$$

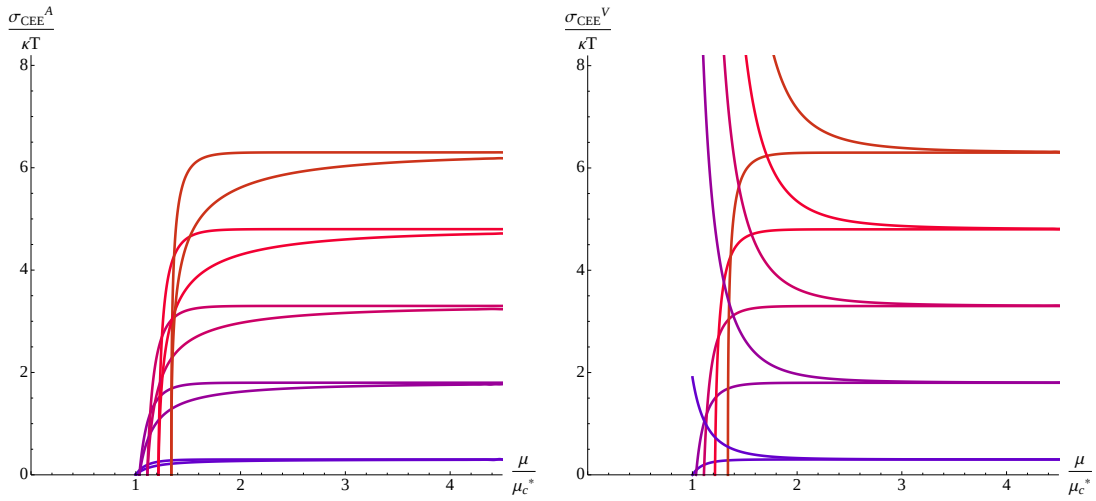

Figure 10.11: $\sigma^{(A)}_{CEE}/T$ (Left) and $\sigma^{(V)}_{CEE}/T$ (Right) versus vector chemical potential at $\bar{\mu}_5 = 1$ and $\xi_x/T = 0.1 - 2.1$ (bottom to top) computed in the two different kinematic limits allowed by gauge invariance. For large enough values of the chemical potential the lines overlap. Notice that one of the limits corresponds to the CCGC.

In the case of the AVV anomaly, the compatibility seems to be not that straightforward.
In the notation of [133], $\sigma_{55} \sim (2Tg_1 + \mu C)$. The coefficient g_1 is continuous at the phase transition but its derivative is not (see Figure 10.1) and hence $\sigma_{CCGE} \sim g_{1,\nu}$ is not continuous at $\bar{\mu}_c$. This fact explains why we do not observe that the CCGC vanishes at the phase transition.
Finally, let us mention that the electric field $E_x = \partial_{[t}A_{x]}$ is a gauge invariant source in our setup, so assuming that $j^y \sim \sigma_{CEE}E_x$ *only*, we would have expected

$$\frac{i}{\xi_z}\lim_{\omega\to 0}\partial_\omega \mathcal{G}^{yx}_{ra}(\omega,k)|_{k_y=k_x=0} = \frac{i}{\xi_z}\lim_{k_x\to 0}\partial_{k_x}\mathcal{G}^{yt}_{ra}(\omega,k)|_{k_y=k_x=0} \tag{10.60}$$

to hold by gauge invariance. Here $\mathcal{G}^{\mu\nu}_{ra}$ are retarded correlators and the subindex "ra" represents the correct combination of time and anti-time ordered sources with respect to

which we vary the generating functional.
Notice that the right hand side of equation (10.60) is also the Kubo formula for σ_{CCGE}, and therefore $\sigma_{CCGE} = \sigma_{CEE}$ should be enforced by gauge invariance of the external sources. This is not what we observe, compare Figures 10.2 and 10.3. The reason is that the constitutive relation of the current receives contributions from terms other than the one associated to the CEE and therefore the limits taken in (10.60) capture the influence of gauge-invariant sources that are not the electric field. Remarkably, the effect of those other sources seems to vanish at low temperatures, as shown in Figure 10.11, for, at $T \to 0$, we recover (10.60). This supports the validity of the relation (10.56).

11
Conclusiones

En esta tesis hemos investigado al relacion entre la ruptura de simetría y fenómenos de transporte en holografía. con este fin hemos profundizado en los conceptos de simetría y su ruptura en holografía. Los puntos más importantes de nuestro análisis han sido los siguientes

En los capítulos 6, 7, 8 se ha considerado la ruptura espontánea de simetría en holografía. Desde el punto de vista gravitatorio esto se consigue mediante un mecanismo de Higgs localizado en el bulk. Concretamente se ha estudiado la ruptura espontánea de una simetría U(2). En este modelo se pudo estudiar la aprición y el comportamiento de bosones de Nambu-Goldstone exóticos en holografía. Se pudo comproba como este modelo no solo respeta los teoremas modernos de contaje, si no que puede servir para extender estos, puesto que provee un ejemplo concreto en el que se evitan las restricciones habituales (existencia de operadores locales que implementen la simetría). Para implmentar esto se considera la ruptura de una simetría global en el bulk. En esta situacion la simetría existe en la teoría dual pero no se puede construir ningún operador local relacionado con esta. De esta manera se puede ver como holografía provee un método único de implementar simetrías en teorías fuertemente acopladas.
La relación de dispersión cuadrática de los modos NG tipo II dio lugar a preguntarse sobre la estabilidad de este tipo de superfluidos. Utilizando el criterio de Landau se encontró que en efecto los superfluidos con modos NG tipo II son inestables cuando se induce una velocidad relativa entre la componente normal y la superfluida. Esto motivó una revisión del análisis de estabilidad del superconductor holográfico habitual (abeliano). Mediante un análisis de los modos quasinormales del sistema se encontró una modificación en el espacio de fases del superconductor holográfico: la región que separa la fase rota y la fase desordenada en presencia de una velocidad de la componente superfluida es inestable. Además dicha inestabilidad ocurre a momento finito. Esto sugiere que una fase modulada podría ser la configuración estable que interpola entre ambas regiones. Para comprobar esto sería necesario construir explicitamente la fase y rehacer el análisis de estabilidad desde el punto de vista de la energía libre y del criterio de Landau.

El modelo de superconductor no abeliano tiene una estructura especialmente rica. Durante el estudio de la configuración estática se encontró una inestabilidad a bajas temperaturas. Esta inestabilidad da lugar a una nueva fase en la que se genera un condensado de tipo p. Sorprendentemente, existe una zona en el espacio de fases en la que ambos condensados coexisten. Esta fue el primer modelo holográfico exihibiendo este comportamiento. En este modelo se exploró la posibilidad de introducir un potencial químico en las direcciones no abelianas. Dicha posibilidad corresponde a la ruptura explícita de la simetría.

En el capítulo 9 se estudió la anomalía axial desde el punto de vista holográfico. En este contexto se encontró una interesante conexión entre anomalías y ruptura espontánea de simetría: el mecanismo de Higgs y el de Stueckelberg en el bulk, intimamente relacionados dessde el punto de vista de espacio plano, dan lugar a dos efectos muy diferentes en la teoría dual.

Utilizando el mecanismo de Stueckelbeg se ha investigado el efecto de incluir fenómenos de rescatterging en cantidades relacionadas con la anomalía en la teoría dual. Se pudo comparar los resultados obtenidos con aquellos en ausencia de dichos fenómenos encontrando interesantes conexiones entre ambdas via renormalización holográfica. Es importante mencionar que la conexión entre términos de Chern-Simons y fotones masivos no es desconocida: en 2+1 dimensiones es sabido que"integrating out" los fermiones masivos da lugar a una teoría efectiva de Chern-Simons que da lugar a una masa efectiva para el campo gauge. Podría ser posible generalizar dicha conexión a dimensiones superiores y profundizar en esta desde el punto de vista holográfico. Una cuestión queda abierta: en el modelo expuesto no fue posible encontrar ua versión covariante de la corriente; sería interesante estudiar cómo generalizar el concepto de corriente covariante a modelos holográficos con fotones masivos en el bulk.

Finalmente, en el captíulo 10 se consideró la interacción entre ambos mecanismos de ruptura de simetría. Haciendo énfasis en los fenómenos de transporte, se ha considerado como la aparicion de un condensado escalar efecta afecta los coeficientes de transporte. Sorprendentemente fue posible identificar un efecto que había sido pasado por alto: el efecto de generación de carga quiral predice la aparición de carga quiral cuando un campo magnético se alinea a la velocidad del superfluido.
A lo largo de los dos últimos capítulos surgieron ciertas sutilezas en el concepto de potencial químico. Esto dio lugar a una interesante observación sobre las distintas maneras de introducir el mismo desde el punto de vista holográfico: cuando el campo gauge en el bulk se ve forzado a desaparecer en el horizonte deja de ser posible diferenciar entre potencial químico y fuente en la teoría dual. Esto ocurre precisamente cuando la carga dual no está conservada.

En esta tesis, como el título prometía, se han estudiado fenómenos de transporte relacionados con ruptura de simetrías en holgrafía. Se ha podido comprobar como holografía nos provee nuevas maneras de estudiar estos conceptos. Junto a esto se ha podido ver como efectos conocidos desde el punto de vista de teorías de campos tienen sorprendentes efectos en la teoría gravitatoria dual.

Aún quedan muchas preguntas por responder en el ámbito del transporte holográfico. ¿ Es posible entender el mecanismo que rige los superconductores de alta temperatura con holografía? ¿ Es posible obtener predicciones cualitativas del comportamiento del plasma de quarks y gluones? ¿ Cómo de lejos se puede llegar al calcular correcciones 1/N? ¿ Se puede encontrar alguna relación más profunda entre anomalías y ruptura espontánea de simetría? ¿ Hasta qué punto es posible ahondar en la filosofía de la holografía? ¿ Tiene un dual cualquier teoría de gravedad?

Abrazar la dualidad gauge/gravedad hasta sus últimas consecuencias promete ser un viaje iluminador.

A
Appendices

A.1 Matrix valued Kramers-Kronig relation

The generically *matrix-valued* spectral function is defined as

$$\rho_{ij}(x) = \langle [\mathcal{O}_i(x), \mathcal{O}_j(0)] \rangle \,, \tag{A.1}$$

where $\mathcal{O}_i$ are Hermitian operators. Its behavior under Hermitian conjugation is

$$\rho(x)^\dagger = \rho(-x) = -\rho(x)^t \,. \tag{A.2}$$

Correspondingly, the Fourier transform $\tilde{\rho}(k) = \int d^4x\, e^{-ikx}\rho(x)$ also satisfies a set of identities

$$\tilde{\rho}(k)^\dagger = \tilde{\rho}(k) = -\tilde{\rho}(-k)^t \,. \tag{A.3}$$

In particular this means that the diagonal components are real and antisymmetric under $k \to -k$. One may also be interested in the behavior under $\omega \to -\omega$. We take now $k = (\omega, \mathbf{q})$. For theories with rotational invariance the spectral function can depend only on $\mathbf{q}^2$. Consequently the diagonal components will also be real and odd in ω

$$\rho_{ii}(\omega, \mathbf{q}^2) = \rho_{ii}(\omega, \mathbf{q}^2)^* = -\rho_{ii}(-\omega, \mathbf{q}^2) \,. \tag{A.4}$$

For the off-diagonal components however, only if one also imposes time reversal or parity symmetry can one prove that the off-diagonal entries must be either even or odd functions of the frequency. In the present case time reversal symmetry is broken by the presence of the chemical potential. Further constraints can however by obtained by supposing that the theory is invariant under $\mathbf{x} \to -\mathbf{x}$. For an odd number of spatial dimensions we could use the parity operators P to take $\mathbf{x} \to -\mathbf{x}$. In the two spatial dimensions we study in this paper we can take P to by a rotation by π (for an arbitrary even number of spatial dimensions $D = 2n$ we could take the angle π for all the rotations in the $i, i+1$-th plane for all $i \leq n$). This P-operator acts as $P\mathcal{O}_i(t, \mathbf{x})P^{-1} = \sigma_i \mathcal{O}_i(t, -\mathbf{x})$ with $\sigma_i = \pm 1$. In odd spatial dimensions σ_i is the parity of the operator. In even spatial dimension $\sigma_i = -1$ if $\mathcal{O}_i$ is the component of a spatial vector. Hence

$$P[\rho_{ij}(t, \mathbf{x})] = \sigma_i \sigma_j \rho_{ij}(t, -\mathbf{x}) \,. \tag{A.5}$$

P-invariance implies $\rho_{ij}(t, \mathbf{x}) = \sigma_i \sigma_j \rho_{ij}(t, -\mathbf{x})$, which for the Fourier transform implies that

$$\tilde{\rho}_{ij}(\omega, \mathbf{q}) = -\sigma_i \sigma_j \tilde{\rho}_{ij}(-\omega, \mathbf{q})^* \,. \tag{A.6}$$

So the off-diagonal entries are either odd or even functions of ω depending on the signs σ_i. In the case where the fields transform in the same way under the parity operator this means that the real (imaginary) part of the off-diagonal components is an odd (even) function of the frequency.

From the spectral function, as defined in (A.1) we can define two causal propagators, namely the retarded and advanced Green's functions

$$G_R(x) = -i\Theta(t)\rho(x)\,, \tag{A.7}$$
$$G_A(x) = i\Theta(-t)\rho(x)\,, \tag{A.8}$$

where $x = (t, \mathbf{x})$. Using (A.3), one can prove the following relation among the Fourier transforms of these

$$\tilde{G}_R(k) = \tilde{G}_R(-k)^* = \tilde{G}_A(k)^\dagger\,. \tag{A.9}$$

From here, we see that the real (imaginary) part, $\mathrm{Re}(G_R)$ ($\mathrm{Im}(G_R)$), is even (odd) under $k \to -k$. We can compute the Fourier transform of the retarded Green's function, which is given by the convolution of the Fourier transform of the Heaviside step function $\tilde{\Theta}(\omega)$ with the Fourier transform of the spectral function $\tilde{\rho}(k)$,

$$\tilde{G}_R(\omega, \mathbf{q}) = -i\int_{-\infty}^{\infty} \tilde{\Theta}(\omega - \mu)\tilde{\rho}(\mu, \mathbf{q})\frac{d\mu}{2\pi}\,. \tag{A.10}$$

Using the Fourier transform of the step function

$$\tilde{\Theta}(\omega) = \frac{i}{\omega + i\epsilon}\,,$$

and the Sokhatsky-Weierstrass theorem we get

$$\tilde{G}_R(\omega, \mathbf{q}) = \mathcal{P}\int_{-\infty}^{\infty} \frac{\tilde{\rho}(\omega', \mathbf{q})}{\omega - \omega'}\frac{d\omega'}{2\pi} - \frac{i}{2}\tilde{\rho}(\omega, \mathbf{q})\,, \tag{A.11}$$

where $\mathcal{P}$ denotes the principle value. From the Hermiticity of $\tilde{\rho}(k)$ we see that we can regard (A.11) as a split of $\tilde{G}^R(k)$ into its Hermitian and anti-Hermitian parts, and find that the spectral function can be computed from the anti-Hermitian part of the Fourier transform of the retarded Green's function

$$\tilde{\rho}(k) = i[\tilde{G}_R(k) - \tilde{G}_R(k)^\dagger] \equiv 2i\tilde{G}_R^{(A)}(k)\,, \tag{A.12}$$

where the (A) stands for anti-Hermitian[1]. Plugging this back into (A.11) and taking the Hermitian part (H) on both sides we arrive at

$$\tilde{G}_R^{(H)}(\omega) = \frac{i}{\pi}\mathcal{P}\int_{-\infty}^{\infty} \frac{G_R^{(A)}(\omega')}{\omega - \omega'}d\omega'\,, \tag{A.13}$$

which is nothing but the Kramers-Krönig relation for the matrix Green's function. It is complemented by the conjugate relation interchanging the Hermitian and anti-Hermitian parts. Imposing P-invariance and using (A.6) and (A.11) if follows that the Green's function satisfies

$$\tilde{G}_{ij}^R(\omega, \mathbf{q}) = \sigma_i\sigma_j\tilde{G}_{ij}^R(-\omega, \mathbf{q})^*\,. \tag{A.14}$$

[1]Using (A.9) we can always work with retarded Green's functions G_R.

This constrains the QNM spectrum. Taking for example a diagonal Green's function with $i = j$ and writing it as a sum over quasinormal frequencies [68, 137] one seems that the quasinormal frequencies have to come either in pairs obeying ω_n and $\tilde{\omega}_n = -\omega_n^*$ or are confined to lie on the imaginary axis. The residues of the pairs are related by complex conjugation and the purely imaginary ones have to have also purely imaginary residue.

A.2 Solving the fluctuation equations

The $(1)-(2)$ sector of the gauged model in the broken phase consists of a system of coupled equations (6.86)-(6.93). In order to extract the spectrum of quasinormal modes we made use of the techniques detailed in [57, 63], where a method to compute the poles of the Green functions in terms of non-gauge invariant fields was developed. The quasinormal frequencies are given by the zeroes of the determinant of the field matrix spanned by a maximal set of linearly independent solutions satisfying infalling boundary conditions on the horizon evaluated at the boundary.

Imposing infalling boundary conditions, the near horizon behavior of the fields solving the mentioned equations reads

$$\alpha = (\rho-1)^{\kappa}\left(\alpha_{(0)} + \alpha_{(1)}(\rho-1) + \dots\right), \tag{A.15}$$

$$\beta = (\rho-1)^{\kappa}\left(\beta_{(0)} + \beta_{(1)}(\rho-1) + \dots\right), \tag{A.16}$$

$$a_t^{(i)} = (\rho-1)^{\kappa+1}\left(a_{t\,(0)}^{(i)} + a_{t\,(1)}^{(i)}(\rho-1) + \dots\right), \tag{A.17}$$

$$a_x^{(i)} = (\rho-1)^{\kappa}\left(a_{x\,(0)}^{(i)} + a_{x\,(1)}^{(i)}(\rho-1) + \dots\right), \tag{A.18}$$

where $\kappa = -i\omega/3$ and $i = 1, 2$. Since the system is subject to two constraints, we can only choose four of the six parameters at the horizon. Without loss of generality, solutions can be parametrized by $\{\alpha_{(0)}, \beta_{(0)}, a_{x\,(0)}^{(i)}\}$. In this way it is possible to construct four independent solutions to the field equations. We can label them as I, II, III, IV.

Two additional solutions, V, VI, can be obtained by performing gauge transformations of the trivial solution,

$$\alpha \to 0,\ \beta \to i\frac{\lambda_1\Psi}{2},\ a_x^{(1)} \to -k\lambda_1,\ a_x^{(2)} \to 0,\ a_t^{(1)} \to \omega\lambda_1,\ a_t^{(2)} \to i\Theta\lambda_1\,, \tag{A.19}$$

$$\alpha \to i\frac{\lambda_2\Psi}{2},\ \beta \to 0,\ a_x^{(1)} \to 0,\ a_x^{(2)} \to -k\lambda_2,\ a_t^{(1)} \to -i\Theta\lambda_2,\ a_t^{(2)} \to \omega\lambda_2\,, \tag{A.20}$$

where λ_i are arbitrary constants. Notice that these pure gauge solutions are not algebraic since they have a nontrivial dependence on the bulk coordinate ρ.

The most general solution for each field $\varphi_i = \{\tilde{\alpha},\ \tilde{\beta},\ a_t^{(i)},\ a_x^{(i)}\}$ is given by a linear combination of the above solutions, including the pure gauge modes,

$$\varphi_i = c_I\varphi_i^I + c_{II}\varphi_i^{II} + c_{III}\varphi_i^{III} + c_{IV}\varphi_i^{IV} + c_V\varphi_i^V + c_{VI}\varphi_i^{VI}\,, \tag{A.21}$$

where we have defined $\{\tilde{\alpha}(\rho),\ \tilde{\beta}(\rho)\} = \{\rho\alpha(\rho),\ \rho\beta(\rho)\}$. This convenient choice allows us to identify the asymptotic boundary values φ_i with the sources of the gauge invariant operators of the dual field theory.

As shown in [63], the poles of the retarded Green functions will be given by the values of the frequency for which the determinant of the matrix spanned by φ_i^N vanishes

asymptotically. Expanding the determinant and evaluating it at a cutoff $\rho = \Lambda$, it reads

$$
\begin{aligned}
0 &= \frac{1}{\lambda_1\lambda_2}\det\begin{pmatrix}
\varphi_\alpha{}^I & \varphi_\alpha{}^{II} & \varphi_\alpha{}^{III} & \varphi_\alpha{}^{IV} & \varphi_\alpha{}^{V} & \varphi_\alpha{}^{VI} \\
\varphi_\beta{}^I & \varphi_\beta{}^{II} & \varphi_\beta{}^{III} & \varphi_\beta{}^{IV} & \varphi_\beta{}^{V} & \varphi_\beta{}^{VI} \\
\varphi_{t(1)}{}^I & \varphi_{t(1)}{}^{II} & \varphi_{t(1)}{}^{III} & \varphi_{t(1)}{}^{IV} & \varphi_{t(1)}{}^{V} & \varphi_{t(1)}{}^{VI} \\
\varphi_{t(2)}{}^I & \varphi_{t(2)}{}^{II} & \varphi_{t(2)}{}^{III} & \varphi_{t(2)}{}^{IV} & \varphi_{t(2)}{}^{V} & \varphi_{t(2)}{}^{VI} \\
\varphi_{x(1)}{}^I & \varphi_{x(1)}{}^{II} & \varphi_{x(1)}{}^{III} & \varphi_{x(1)}{}^{IV} & \varphi_{x(1)}{}^{V} & \varphi_{x(1)}{}^{VI} \\
\varphi_{x(2)}{}^I & \varphi_{x(2)}{}^{II} & \varphi_{x(2)}{}^{III} & \varphi_{x(2)}{}^{IV} & \varphi_{x(2)}{}^{V} & \varphi_{x(2)}{}^{VI}
\end{pmatrix} \qquad \text{(A.22)} \\
&= \omega^2\det\begin{pmatrix}
\varphi_\alpha^I & \varphi_\alpha^{II} & \varphi_\alpha^{III} & \varphi_\alpha^{IV} \\
\varphi_\beta^I & \varphi_\beta^{II} & \varphi_\beta^{III} & \varphi_\beta^{IV} \\
\varphi_{x(1)}^I & \varphi_{x(1)}^{II} & \varphi_{x(1)}^{III} & \varphi_{x(1)}^{IV} \\
\varphi_{x(2)}^I & \varphi_{x(2)}^{II} & \varphi_{x(2)}^{III} & \varphi_{x(2)}^{IV}
\end{pmatrix} + \omega k\det\begin{pmatrix}
\varphi_\alpha^I & \varphi_\alpha^{II} & \varphi_\alpha^{III} & \varphi_\alpha^{IV} \\
\varphi_\beta^I & \varphi_\beta^{II} & \varphi_\beta^{III} & \varphi_\beta^{IV} \\
\varphi_{t(1)}^I & \varphi_{t(1)}^{II} & \varphi_{t(1)}^{III} & \varphi_{t(1)}^{IV} \\
\varphi_{x(2)}^I & \varphi_{x(2)}^{II} & \varphi_{x(2)}^{III} & \varphi_{x(2)}^{IV}
\end{pmatrix} \\
&\quad -\omega k\det\begin{pmatrix}
\varphi_\alpha^I & \varphi_\alpha^{II} & \varphi_\alpha^{III} & \varphi_\alpha^{IV} \\
\varphi_\beta^I & \varphi_\beta^{II} & \varphi_\beta^{III} & \varphi_\beta^{IV} \\
\varphi_{t(2)}^I & \varphi_{t(2)}^{II} & \varphi_{t(2)}^{III} & \varphi_{t(2)}^{IV} \\
\varphi_{x(1)}^I & \varphi_{x(1)}^{II} & \varphi_{x(1)}^{III} & \varphi_{x(1)}^{IV}
\end{pmatrix} + k^2\det\begin{pmatrix}
\varphi_\alpha^I & \varphi_\alpha^{II} & \varphi_\alpha^{III} & \varphi_\alpha^{IV} \\
\varphi_\beta^I & \varphi_\beta^{II} & \varphi_\beta^{III} & \varphi_\beta^{IV} \\
\varphi_{t(1)}^I & \varphi_{t(1)}^{II} & \varphi_{t(1)}^{III} & \varphi_{t(1)}^{IV} \\
\varphi_{t(2)}^I & \varphi_{t(2)}^{II} & \varphi_{t(2)}^{III} & \varphi_{t(2)}^{IV}
\end{pmatrix},
\end{aligned}
$$

where the background boundary conditions $\Theta(\Lambda) = 0$ and $\Lambda\Psi = 0$ have been already imposed. This absence of background sources for the corresponding operators makes the point $(\omega, k) = (0, 0)$ a trivial solution to the vanishing determinant condition, which ensures the existence of a hydrodynamic mode. Notice also that the point $(\omega, k) = (0, 0)$ is a double solution to the previous determinant equation.

Solutions to the equations of motion and to the determinant condition (A.22) have been computed numerically. It has been checked that the election of solution basis, i.e. of initial values of the free parameters, does not affect the result.

A.3 Fluctuation equations in the $(0) - (3)$ sector

The fluctuations in the $U(1)$ theory or the $(0) - (3)$ sector contain the zeroth and third color sectors of the gauge field and the lower component of the scalar field $\sigma = \rho + i\delta$. The

equations of motion for an arbitrary direction of the momentum then read

$$\begin{aligned}
0 =& f\rho'' + \left(f' + \frac{2f}{r}\right)\rho' + \left(\frac{\omega^2}{f} + \frac{A_0^2}{f} - \frac{A_x^2}{r^2} - \frac{|k|^2}{r^2} - m^2\right)\rho + \frac{2i\omega A_0}{f}\delta + 2a_t^{(-)}\Psi\frac{A_0}{f} \\
& - 2\frac{a_x^{(-)}}{r^2}\Psi A_x + |k|\cos(\gamma)\frac{2i}{r^2}A_x\delta\,, \qquad \text{(A.23)} \\
0 =& f\delta'' + \left(f' + \frac{2f}{r}\right)\delta' + \left(\frac{\omega^2}{f} + \frac{A_0^2}{f} - \frac{A_x^2}{r^2} - \frac{|k|^2}{r^2} - m^2\right)\delta - \frac{2i\omega A_0}{f}\rho - i\Psi\omega\frac{a_t^{(-)}}{f} \\
& - |k|\cos(\gamma)\frac{2i}{r^2}A_x\rho - |k|\cos(\gamma)\frac{i}{r^2}\Psi a_x^{(-)} - |k|\sin(\gamma)\frac{i}{r^2}\Psi a_y^{(-)}\,, \qquad \text{(A.24)} \\
0 =& f a_t''^{(-)} + \frac{2f}{r}a_t'^{(-)} - \left(\frac{|k|^2}{r^2} + 2\Psi^2\right)a_t^{(-)} - \frac{\omega|k|}{r^2}\cos(\gamma)a_x^{(-)} - \frac{\omega|k|}{r^2}\sin(\gamma)a_y^{(-)} \\
& - 4\Psi A_0\rho - 2i\omega\Psi\delta\,, \qquad \text{(A.25)} \\
0 =& f a_x''^{(-)} + f' a_x'^{(-)} + \left(\frac{\omega^2}{f} - 2\Psi^2\right)a_x^{(-)} + \frac{\omega|k|}{f}\cos(\gamma)a_t^{(-)} + 2i|k|\cos(\gamma)\Psi\delta \\
& - 4\Psi\rho A_x - \frac{|k|^2\sin^2(\gamma)}{r^2}a_x^{(-)} + \frac{|k|^2\cos(\gamma)\sin(\gamma)}{r^2}a_y^{(-)}\,, \qquad \text{(A.26)} \\
0 =& f a_y''^{(-)} + f' a_y'^{(-)} + \left(\frac{\omega^2}{f} - 2\Psi^2\right)a_y^{(-)} + \frac{\omega|k|}{f}\sin(\gamma)a_t^{(-)} + 2i|k|\sin(\gamma)\Psi\delta \\
& - \frac{|k|^2\cos^2(\gamma)}{r^2}a_y^{(-)} + \frac{|k|^2\cos(\gamma)\sin(\gamma)}{r^2}a_x^{(-)}\,, \qquad \text{(A.27)}
\end{aligned}$$

and the constraint

$$0 = \frac{i\omega}{f}a_t'^{(-)} + \frac{i|k|}{r^2}\cos(\gamma)a_x'^{(-)} + \frac{i|k|}{r^2}\sin(\gamma)a_y'^{(-)} + 2\Psi'\delta - 2\Psi\delta'\,, \qquad \text{(A.28)}$$

where we have used $k_x = |k|\cos(\gamma)$, $k_y = |k|\sin(\gamma)$. The general pure gauge solution in this sector is

$$\delta = i\lambda\Psi; \quad \rho = 0; \quad a_t^{(-)} = \lambda\omega; \quad a_x^{(-)} = -\lambda|k|\cos(\gamma); \quad a_y^{(-)} = -\lambda|k|\sin(\gamma)\,, \qquad \text{(A.29)}$$

where λ is an arbitrary constant.

A.4 Fluctuation equations in the $(1)-(2)$ sector

The perturbations in the $(1)-(2)$ sector of the $U(2)$ theory include the fluctuations of the upper component of the scalar field, $\eta = \alpha + i\beta$, along with that sector of the gauge field.

For momentum in the opposite direction of the superflow, the equations of motion read

$$0 = f a_x''^{(1)} + f' a_x'^{(1)} + \left(\frac{\omega^2}{f} - \Psi^2 + \frac{\left(A_t^{(3)}\right)^2}{f} \right) a_x^{(1)} - 2i \frac{A_t^{(3)} \omega}{f} a_x^{(2)} + i\omega \frac{A_x^{(3)}}{f} a_t^{(2)}$$
$$- \frac{A_t^{(3)} A_x^{(3)}}{f} a_t^{(1)} - 2A_x^{(0)} \Psi \alpha + 2ik\Psi\beta - \frac{ikA_t^{(3)}}{f} a_t^{(2)} + \frac{\omega k}{f} a_t^{(1)} , \tag{A.30}$$

$$0 = f a_x''^{(2)} + f' a_x'^{(2)} + \left(\frac{\omega^2}{f} - \Psi^2 + \frac{\left(A_t^{(3)}\right)^2}{f} \right) a_x^{(2)} + 2i \frac{A_t^{(3)} \omega}{f} a_x^{(1)} - i\omega \frac{A_x^{(3)}}{f} a_t^{(1)}$$
$$- \frac{A_t^{(3)} A_x^{(3)}}{f} a_t^{(2)} + 2\Psi A_x^{(0)} \beta + 2ik\Psi\alpha + \frac{ikA_t^{(3)}}{f} a_t^{(1)} + \frac{\omega k}{f} a_t^{(2)} , \tag{A.31}$$

$$0 = f a_t''^{(1)} + \frac{2f}{r} a_t'^{(1)} - \left(\frac{\left(A_x^{(3)}\right)^2}{r^2} + \Psi^2 + \frac{k^2}{r^2} \right) a_t^{(1)} + \frac{A_t^{(3)} A_x^{(3)}}{r^2} a_x^{(1)} - i\omega \frac{A_x^{(3)}}{r^2} a_x^{(2)} - 2i\omega\beta\Psi$$
$$- 2\phi\Psi\alpha + \frac{ikA_t^{(3)}}{r^2} a_x^{(2)} - \frac{2ikA_x^{(3)}}{r^2} a_t^{(2)} - \frac{\omega k}{r^2} a_x^{(1)} , \tag{A.32}$$

$$0 = f a_t''^{(2)} + \frac{2f}{r} a_t'^{(2)} - \left(\frac{\left(A_x^{(3)}\right)^2}{r^2} + \Psi^2 + \frac{k^2}{r^2} \right) a_t^{(2)} + \frac{A_t^{(3)} A_x^{(3)}}{r^2} a_x^{(2)} + i\omega \frac{A_x^{(3)}}{r^2} a_x^{(1)}$$
$$- \frac{ikA_t^{(3)}}{r^2} a_x^{(1)} + \frac{2ikA_x^{(3)}}{r^2} a_t^{(1)} - \frac{\omega k}{r^2} a_x^{(2)} - 2i\omega\alpha\Psi + 2A_t^{(0)} \Psi\beta , \tag{A.33}$$

$$0 = f\alpha'' + \left(f' + \frac{2f}{r} \right) \alpha' + \left(\frac{\omega^2}{f} + \frac{\left(A_t^{(0)} + A_t^{(3)}\right)^2}{4f} - \frac{\left(A_x^{(0)} + A_x^{(3)}\right)^2}{4r^2} - \frac{k^2}{r^2} - m^2 \right) \alpha$$
$$+ \left(i\omega \left(\frac{A_t^{(0)} + A_t^{(3)}}{f} \right) + \frac{ik}{r^2} \left(A_x^{(0)} + A_x^{(3)} \right) \right) \beta + \frac{A_t^{(0)} \Psi}{2f} a_t^{(1)} - i\omega \frac{\Psi}{2f} a_t^{(2)}$$
$$- \frac{A_x^{(0)} \Psi}{2r^2} a_x^{(1)} - \frac{ik\Psi}{2r^2} a_x^{(2)} , \tag{A.34}$$

$$0 = f\beta'' + \left(f' + \frac{2f}{r} \right) \beta' + \left(\frac{\omega^2}{f} + \frac{\left(A_t^{(0)} + A_t^{(3)}\right)^2}{4f} - \frac{\left(A_x^{(0)} + A_x^{(3)}\right)^2}{4r^2} - \frac{k^2}{r^2} - m^2 \right) \beta$$
$$- \left(i\omega \left(\frac{A_t^{(0)} + A_t^{(3)}}{f} \right) + \frac{ik}{r^2} \left(A_x^{(0)} + A_x^{(3)} \right) \right) \alpha - \frac{A_t^{(0)} \Psi}{2f} a_t^{(2)} - i\omega \frac{\Psi}{2f} a_t^{(1)}$$
$$+ \frac{A_x^{(0)} \Psi}{2r^2} a_x^{(2)} - \frac{ik\Psi}{2r^2} a_x^{(1)} , \tag{A.35}$$

subject to the constraints

$$0 = 2f\left(\Psi\beta' - \Psi'\beta\right) + a_t^{(2)}A_t'^{(3)} - a_t'^{(2)}A_t^{(3)} + \frac{f}{r^2}\left(A_x^{(3)}a_x'^{(2)} - a_x^{(2)}A_x'^{(3)}\right) - i\omega a_t'^{(1)} - \frac{ikf}{r^2}a_x'^{(1)}\,, \tag{A.36}$$

$$0 = 2f\left(\Psi\alpha' - \Psi'\alpha\right) + a_t'^{(1)}A_t^{(3)} - a_t^{(1)}A_t'^{(3)} + \frac{f}{r^2}\left(a_x^{(1)}A_x'^{(3)} - A_x^{(3)}a_x'^{(1)}\right) - i\omega a_t'^{(2)} - \frac{ikf}{r^2}a_x'^{(2)}\,, \tag{A.37}$$

There are two pure gauge solutions in this sector,

$$\alpha = 0\,,\quad \beta = i\lambda_1\Psi/2\,,\quad a_t^{(1)} = \lambda_1\omega\,,\quad a_t^{(2)} = i\lambda_1 A_t^{(3)}\,,\quad a_x^{(1)} = -\lambda_1 k\,,\quad a_x^{(2)} = i\lambda_1 A_x^{(3)}\,, \tag{A.38}$$

$$\alpha = i\lambda_2\Psi/2\,,\quad \beta = 0\,,\quad a_t^{(1)} = -i\lambda_2 A_t^{(3)},\quad a_t^{(2)} = \lambda_2\omega\,,\quad a_x^{(1)} = -i\lambda_2 A_x^{(3)},\quad a_x^{(2)} = -\lambda_2 k\,, \tag{A.39}$$

where λ_1 and λ_2 are arbitrary constants.

A.5 Holographic Renormalization

A.5.1 U(1) Model

In order to renormalize the theory shown in (9.18) we follow the procedure in [15]. Within this approach the renormalization procedure consists of an expansion of the canonical momenta and the On-Shell action λ in eigenfunctions of the dilatation operator. This operator can be obtained taking the asymptotic leading term of the radial derivative

$$\partial_r = \int d^dx\left(\dot\gamma_{ij}\frac{\delta}{\delta\gamma_{ij}} + \dot A_i\frac{\delta}{\delta A_i} + \dot\theta\frac{\delta}{\delta\theta}\right) \sim \int d^dx\left(2\gamma_{ij}\frac{\delta}{\delta\gamma_{ij}} + \Delta A_i\frac{\delta}{\delta A_i} + O(e^{-r})\right)\,, \tag{A.40}$$

$$\delta_D = \int d^dx\left(2\gamma_{ij}\frac{\delta}{\delta\gamma_{ij}} + \Delta A_i\frac{\delta}{\delta A_i}\right)\,. \tag{A.41}$$

Notice that this operator is not gauge invariant. Nevertheless $S_{C.T.}$ must be gauge invariant since the bulk Lagrangian is invariant too. Therefore $S_{C.T.}$ must be expressible as a functional of $B_i \equiv A_i - \partial_i\theta$. We will see that this is indeed the case even though we expand the on-shell action in eigenfunctions of the (non gauge invariant) dilatation operator δ_D. We choose the axial gauge $A_r = 0$. Recall that

$$\Delta(\Delta+2) = m^2. \tag{A.42}$$

Our notation for the eigenfunctions of the dilatation operator reads

$$\delta_D X_{(a)} = -aX_{(a)}\,, \qquad\qquad \delta_D X_{(4)} = -4X_{(4)} - 2\tilde X_{(4)}\,. \tag{A.43}$$

All our results were obtained in the probe limit and therefore, for simplicity, we adapt the renormalization procedure to this limit. This implies that we will use the e.o.m. for the fields, instead of the Hamiltonian constraint in Einstein equations, to determine the

eigenfunctions of the dilatation operator the canonical momenta are expanded in. In addition we set the extrinsic curvature $K_{ij} \equiv \dot{\gamma}_{ij} = 2\gamma_{ij}$, which in our setup is enough for the boundary analysis. The matter e.o.m., written in terms of $E_i \equiv \dot{A}_i$ and $\Pi \equiv \dot{\theta}$ are:

$$\dot{E}_i + 2E_i - m^2\left(A_i - \partial_i\theta\right) + \partial^j F_{ji} + 2\kappa\epsilon^{irjkl}E_j F_{kl} = 0\,, \tag{A.44}$$

$$\dot{\Pi} + 4\Pi - \partial^i\left(A_i - \partial_i\theta\right) = 0\,, \tag{A.45}$$

$$\Pi = \frac{1}{m^2}\left(\partial^i E_i - \kappa\epsilon^{rijkl}F_{ij}F_{kl}\right)\,. \tag{A.46}$$

With (A.41) and the e.o.m. we can determine the explicit form of the different terms in the expansions

$$E_i = E_{i(-\Delta)} + E_{i(0)} + E_{i(2-2\Delta)} + E_{i(2-\Delta)} + E_{i(2)} + \dots\,, \tag{A.47}$$

$$\Pi = \Pi_{i(2-\Delta)} + \Pi_{i(2)} + \dots\,, \tag{A.48}$$

$$E_{i(-\Delta)} = \Delta A_i\,, \tag{A.49}$$

$$E_{i(0)} = -\Delta\partial_i\theta\,, \tag{A.50}$$

$$\Pi_{(2-\Delta)} = \frac{1}{(\Delta+2)}\partial_i A^i\,, \tag{A.51}$$

$$\Pi_{(2)} = \frac{-1}{(\Delta+2)}\Box\theta\,. \tag{A.52}$$

Other terms like $E_{i(2-2\Delta)}$ are non-zero but as we will see they not contribute to the counterterms. We can determine the expressions for the higher order operators needed to expand the radial derivative:

$$\partial_r = \delta_D + \delta_{(\Delta)} + \delta_{(2-2\Delta)} + \delta_{(2-\Delta)} + \delta_{(2)} + \delta_{(2+\Delta)} + \dots\,, \tag{A.53}$$

$$\delta_{(\Delta)} = \int d^dx' E_{i(0)}(x')\frac{\delta}{\delta A_i(x')}\,, \tag{A.54}$$

$$\delta_{(2-\Delta)} = \int d^dx' \left(E_{i(2-2\Delta)}(x')\frac{\delta}{\delta A_i(x')} + \Pi_{(2-\Delta)}(x')\frac{\delta}{\delta\theta(x')}\right)\,, \tag{A.55}$$

$$\delta_{(2)} = \int d^dx' \left(E_{i(2-\Delta)}(x')\frac{\delta}{\delta A_i(x')} + \Pi_{(2)}(x')\frac{\delta}{\delta\theta(x')}\right)\,, \tag{A.56}$$

$$\delta_{(2+\Delta)} = \int d^dx' E_{i(2)}(x')\frac{\delta}{\delta A_i(x')}\,. \tag{A.57}$$

Once we have these we just need the equation for the On-Shell action

$$\dot{\lambda} + \lambda - \mathcal{L}_m = 0\,, \tag{A.58}$$

$$\begin{aligned}\dot{\lambda} + 4\lambda + \frac{1}{2}E_iE^i + \frac{m^2}{2}\Pi^2 + \frac{m^2}{2}(A_iA^i - 2A_i\partial^i\theta + \partial_i\theta\partial^i\theta) + \\ \frac{1}{4}F_{ij}F^{ij} + \frac{4\kappa}{3}(A_i - \partial_i\theta)E_jF_{kl}\epsilon^{irjkl} - \frac{\kappa}{3}\Pi F_{ij}F_{kl}\epsilon^{irjkl} = 0\,.\end{aligned} \tag{A.59}$$

To determine the terms of the eigenfunction expansion of the On-Shell action

$$\begin{aligned}\lambda =&\lambda_{(0)} + \lambda_{(2-2\Delta)} + \lambda_{(2-\Delta)} + \lambda_{(2)} + \lambda_{(4-4\Delta)} + \\ &\lambda_{(4-3\Delta)} + \lambda_{(4-2\Delta)} + \lambda_{(4-\Delta)} + \lambda_{(4)} + \tilde{\lambda}_{(4)} \log e^{2r} + \dots .\end{aligned} \tag{A.60}$$

It is important to remark that depending on the value of $0 \leq \Delta \leq 1$ new terms may appear in this expansion. For example, the next possible term in this expansion is $\lambda_{(6-6\Delta)}$. Therefore, as in the rest of the paper, we restrict our analysis to

$$6 - 6\Delta > 4 \rightarrow \Delta < \frac{1}{3} . \tag{A.61}$$

Furthermore, for a large enough mass ($\Delta = 1$) the number of possible counterterms becomes infinite. This is to be expected since for such a value of the mass the operator dual to the gauge field becomes marginal.

We are now ready to proceed solving (A.59) order by order in dilatation weight

$$\lambda_{(0)} = 0 , \tag{A.62}$$

$$\lambda_{(2-2\Delta)} = \frac{-\Delta}{2} A_i A^i , \tag{A.63}$$

$$\lambda_{(2-\Delta)} = \Delta \partial_i \theta A^i , \tag{A.64}$$

$$\lambda_{(2)} = \frac{-\Delta}{2} \partial_i \theta \partial^i \theta . \tag{A.65}$$

At this point one can see that these first terms of the O.S. action expansion can be rearranged in terms of the B_i field:

$$\lambda_{(2-2\Delta)} + \lambda_{(2-\Delta)} + \lambda_{(2)} = -\frac{\Delta}{2} B_i B^i . \tag{A.66}$$

It is a nice check to find all the terms explicitly and then rearrange them like this although, as mentioned before, this is to be expected. Moreover we can use this in our advantage: once one obtains a counterterm which is only proportional to A_i the following terms can be determined by just imposing that λ has to be gauge invariant.

$$\lambda_{(4-4\Delta)} = 0 , \qquad \lambda_{(4-3\Delta)} = 0 . \tag{A.67}$$

Let us analyze the following term with some detail

$$\begin{aligned}\dot{\lambda}\Big|_{(4-2\Delta)} + 4\lambda_{(4-2\Delta)} + E_{i(-\Delta)} E^i_{(2-\Delta)} + \frac{m^2}{2} \Pi^2_{(2-\Delta)} + \frac{1}{4} F_{ij} F^{ij} + \\ \frac{4\kappa}{3} \epsilon^{rijkl} F_{jk} \left(E_{i(0)} A_l - E_{i(-\Delta)} \partial_l \theta \right) = 0 ,\end{aligned} \tag{A.68}$$

$$(\delta_D + 4)\lambda_{(4-2\Delta)} + \delta_{(2-\Delta)} \lambda_{(2-\Delta)} + \delta_{(2)} \lambda_{(2-2\Delta)} + E_{i(-\Delta)} E^i_{(2-\Delta)} + \frac{m^2}{2} \Pi^2_{(2-\Delta)} + \frac{1}{4} F_{ij} F^{ij} = 0 , \tag{A.69}$$

$$\lambda_{(4-2\Delta)} = \frac{1}{4(\Delta + 2)} \partial_i A^i \partial^j A_j - \frac{1}{8\Delta} F_{ij} F^{ij} . \tag{A.70}$$

It is remarkable that the term proportional to κ vanishes due to the contraction of a symmetric $\left(E_{i(0)}A_l - E_{i(-\Delta)}\partial_l\theta\right)$ and an antisymmetric ϵ^{rijkl} tensor. Here we see the importance of the coupling of the Stückelberg filed to the Chern-Simons term. If we had not added it, at this point we would have found an extra counter term of the form $-\theta\wedge F\wedge F$. In this expression we have neglected total derivatives. From this last equation we can infer the following two orders by imposing gauge invariance. So, in terms of the gauge invariant field B_i the counterterm reads:

$$\lambda_{4-2\Delta} + \lambda_{4-\Delta} + \lambda_4^* = \frac{1}{4(\Delta+2)}\partial_i B^i \partial_j B^j - \frac{1}{8\Delta}F_{ij}F^{ij}\,. \tag{A.71}$$

Note that we cannot determine $\lambda_{(4)}$ with just the boundary analysis. λ_4^* is just a part of λ_4 which is imposed by gauge invariance and that can be obtained from the asymptotics.

We only lack the $\sim$ log term, that is obtained by evaluating the equation to 4th order

$$\tilde{\lambda}_{(4)} = 0\,. \tag{A.72}$$

Thus, the S_{CT} reads:

$$S_{CT} = \int_\partial d^dx\sqrt{-\gamma}\left(\frac{\Delta}{2}B_iB^i - \frac{1}{4(\Delta+2)}\partial_iB^i\partial_jB^j + \frac{1}{8\Delta}F_{ij}F^{ij}\right)\,. \tag{A.73}$$

A.5.2 U(1)xU(1) model

Few things change if we introduce a second gauge field (non-massive, non-anomalous in the boundary). The asymptotic behavior remains unchanged. Specially, the vector gauge field behaves as it usually does and thus it does not contribute to the dilatation operator.

$$\delta_D = \int d^dx\left(2\gamma_{ij}\frac{\delta}{\delta\gamma_{ij}} + \Delta A_i\frac{\delta}{\delta A_i} + O(e^{-r})\right)\,. \tag{A.74}$$

The equation of the O.S. action has to be modified:

$$\begin{aligned}&\dot{\lambda} + 4\lambda + \frac{1}{2}E_iE^i + \frac{1}{2}\Sigma_i\Sigma^i + \frac{m^2}{2}\Pi^2 + \frac{m^2}{2}(A_iA^i - 2A_i\partial^i\theta + \partial_i\theta\partial^i\theta) + \\ &\frac{1}{4}F_{ij}F^{ij} + \frac{1}{4}H_{ij}H^{ij} + 2\kappa(A_i - \partial_i\theta)\left(E_jF_{kl} + 3\Sigma_jH_{kl}\right)\epsilon^{irjkl} - \\ &\frac{\kappa}{2}\Pi\left(F_{ij}F_{kl} + 3H_{ij}H_{kl}\right)\epsilon^{irjkl} = 0\,.\end{aligned} \tag{A.75}$$

Where Σ and H_{ij} are the the momentum[2] and the field strength of the vector gauge field. It is not difficult to realize that the only term proportional to V_i that will contribute to the divergent part of λ is the kinetic term $H_{ij}H^{ij}$. Since this is of order 4, it will only contribute to the logarithmic term and therefore:

$$S_{CT} = \int_\partial d^dx\sqrt{-\gamma}\left(\frac{\Delta}{2}B_iB^i - \frac{1}{4(\Delta+2)}\partial_iB^i\partial_jB^j + \frac{1}{8\Delta}F_{ij}F^{ij} + \frac{1}{8}H_{ij}H^{ij}\log e^{2r}\right)\,. \tag{A.76}$$

[2] as we did with the axial field we define $\Sigma_i \equiv \dot{V}_i$.

A.6 Correlators in the U(1) model

A.6.1 1-point function

In order to derive the 1-point function of the (non-conserved) vector operator dual to the gauge field we write fields as background plus perturbations

$$\mathcal{A}_\mu = A_\mu + a_\mu\,, \qquad\qquad \theta = \theta + \phi\,, \tag{A.77}$$

we expand the **renormalized** action to first order in the perturbations

$$\begin{aligned} S^{(1)}_{\mathcal{R}} = &\int dr\, d^4x\sqrt{-g}\left[a_\mu\left(\nabla_\nu F^{\nu\mu} - m^2(A^\mu - \partial^\mu\theta) + \kappa\epsilon^{\mu\alpha\beta\gamma\rho}F_{\alpha\beta}F_{\gamma\rho}\right) - \phi\nabla_\mu\left(A^\mu - \partial^\mu\theta\right)\right] + \\ &\int_\partial d^4x\sqrt{-g}\left[a_i\left(F^{ir} + \frac{4}{3}\kappa(A_j - \partial_j\theta)F_{kl}\epsilon^{rijkl}\right) - \phi(F_{ij}F_{kl}\epsilon^{rijkl} + m^2(A^r - \partial^r\theta))\right] + \\ &\int_\partial d^4x\sqrt{-\gamma}\; a_i\left(\Delta(A^i - \partial^i\theta) + \frac{1}{2(\Delta+2)}\partial^i(\partial_j A^j - \Box\theta) - \frac{1}{2\Delta}\partial_j F^{ji}\right) + \\ &\int_\partial d^4x\sqrt{-\gamma}\;\phi\left(\Delta(\partial_j A^j - \Box\theta) + \frac{1}{2(\Delta+2)}\Box(\partial_j A^j - \Box\theta)\right)\,. \end{aligned} \tag{A.78}$$

The bulk integral contains the e.o.m. for the background fields. The second line shows the boundary term that arises from the unrenormalized action S whereas the third and fourth lines contain the expansion of the counter term actionS_{CT}. By inspection of the equations of motion one finds that the most general asymptotic expansion of the fields reads

$$\begin{aligned} A_\mu \sim &\sum_{i=0}^{\infty} A_{\mu(i)} r^{\Delta - i} + \sum_{i=0}^{\infty}\tilde{A}_{\mu(i)} r^{-2-\Delta-i} + \sum_{i=0}^{\infty}\tilde{\theta}_{\mu(i)} r^{-i} + \\ &\sum_{n>1, i\geq 2(n-1)}^{\infty}\omega_{\mu(n,i)} r^{n\Delta - i} + \sum_{n>1, i\geq 3n}^{\infty}\tilde{\omega}_{\mu(n,i)} r^{-n\Delta - i} + \sum_{i\geq 4} A_{L(i)} r^{(-i)}\log(r)\,, \end{aligned} \tag{A.79}$$

$$\begin{aligned} \theta \sim &\sum_i \theta_{(i)} r^{(-i)} + \sum_{n\geq 1, i\geq 2n}\tilde{\Psi}_{(n,i)} r^{(n\Delta - i)} + \sum_{n\geq 1, i\geq 3n+2}\tilde{\Psi}_{(-n,i)} r^{(-n\Delta - i)} + \\ &\sum_{i\geq 4}\theta_{L(i)} r^{(-i)}\log(r)\,. \end{aligned} \tag{A.80}$$

With $\Delta = \sqrt{1+m} - 1$ that is bounded to be $\Delta < 1$. The coefficient of the leading (non-normalizable mode) term $A_{(0)x}$ is to be identified with the source of the dual operator. $\tilde{A}_{(0)x}$ is the coefficient of the normalizable mode. $\omega_{(n,i)}, \tilde{\omega}_{(n,i)}$ arise due to the non-linearities of the e.o.m. and can be expressed as functionals of the sources of the "other" components of the gauge field $A_{(0)y\neq x}$. Finally, the $\tilde{\theta}$ and A_L terms arise from the coupling to the Stückelberg field and are functionals of the source of θ; the logarithmic terms are sub leading w.r.t. the normalizable mode, contrary to what happens in the massless case. In the expansion for θ we find the $\theta_{(i)}$ coefficients that contain both the non-normalizable $i = 0$ and the normalizable $i = 4$ mode. The Ψ, $\tilde{\Psi}$ terms appear due to the coupling to the gauge field.
From the boundary term of the O.S. action one can obtain the 1-point function of the dual operator J^i.

As usual, it is convenient to group all the fields in a vector of the appropriately normalized fields[3] $\psi = (r^{-\Delta} a_i, \phi)$ and express them as the (matrix valued) bulk to boundary propagator (BBP) times a vector $\psi_{(0)}$ made of the value of the sources

$$\psi_I(r) = F_{IJ}(r)\psi_{J(0)}\,, \qquad\qquad F(\Lambda) = \mathbb{I}\,. \tag{A.81}$$

Moreover, it will be useful to separate the BBP matrix in a rectangular matrix $\mathbb{F}$ and a vector $\mathbb{G}$ such that

$$F = \left(\begin{array}{c} \mathbb{F} \\ \hline \mathbb{G} \end{array}\right)\,, \qquad\qquad a_I = r^{\Delta}\mathbb{F}_{IJ}\psi_{J(0)}\,, \qquad\qquad \phi = \mathbb{G}_J\psi_{J(0)}\,. \tag{A.82}$$

In terms of these the expectation value of the current reads

$$\begin{aligned}\langle J^m\rangle = &\lim_{r\to\infty}\sqrt{-g}\left(r^{\Delta}\mathbb{F}_{im}\left(F^{ir}+\frac{4\kappa}{3}\epsilon^{ijkl}\left(A_j-\partial_j\theta\right)F_{kl}\right)-\mathbb{G}_m(F_{ij}F_{kl}\epsilon^{rijkl}+m^2(A^r-\partial^r\theta)\right)+\\ &\lim_{r\to\infty}\sqrt{-\gamma}\,r^{\Delta}\mathbb{F}_{im}\left(\Delta(A^i-\partial^i\theta)+\frac{1}{2(\Delta+2)}\partial^i(\partial_jA^j-\Box\theta)-\frac{1}{2\Delta}\partial_jF^{ji}\right)+\\ &\lim_{r\to\infty}\sqrt{-\gamma}\quad\mathbb{G}_m\left(\Delta(\partial_jA^j-\Box\theta)+\frac{1}{2(\Delta+2)}\Box(\partial_jA^j-\Box\theta)\right)\,.\end{aligned} \tag{A.83}$$

The above expression is quite messy and needs some inspection. In the massless case [45] all terms proportional to $\mathbb{F}_{i\neq m}, \mathbb{G}_m$ vanish in the $r\to\infty$ limit and therefore are not explicitly written in the literature. When the mass is present, however, all terms in the expression are divergent. This is easy to check given the expansions (A.79). To have a better understanding of the properties of the current it is convenient to collect the terms that do not contain finite contributions as shown in the main text (9.26).

A.6.2 2-point functions

Equation (9.36) is the correct expression for the correlator $\langle J_y J_z\rangle$. However, one usually does not have an analytic solution for the e.o.m. and therefore one has to construct the BBP numerically. This implies that we are interested in (9.36) expressed as a linear combination of the BBP and its derivatives. In principle one can derive this combination directly from the O.S. action to second order in perturbations but this might be rather tedious. A simpler strategy is to look at the asymptotic expansions for the perturbations and then invert the series to find the expression of the normalizable mode as a combination of $\mathbb{F}, \dot{\mathbb{F}}$. The anomalous conductivity (9.31) is a good opportunity to perform an explicit example.

First we switch on perturbations for all fields with momentum k aligned to the x direction and frequency ω: $\delta\theta = \sigma(r)e^{-i\omega t+ikx}$ and $\delta A_\mu = a_\mu(r)e^{-i\omega t+ikx}$. The linearized

[3] Since the gauge field diverges at the boundary precisely as $\sim r^{\Delta}$, this choice for the normalization allows us to have a finite BBP and to collect the sources of the dual theory in $\psi_{(0)}$.

e.o.m. for these perturbations naturally separate in decoupled sectors, since we are interested in the correlator $\langle J_y J_z \rangle$ we just look at

$$f a_y'' + \left(f' + \frac{f}{r}\right) a_y' + \left(-m^2 + \frac{\omega^2}{f} - \frac{k^2}{r^2}\right) a_y - \frac{8ik\kappa\phi' a_z}{r} = 0 \tag{A.84}$$

$$f a_z'' + \left(f' + \frac{f}{r}\right) a_z' + \left(-m^2 + \frac{\omega^2}{f} - \frac{k^2}{r^2}\right) a_z + \frac{8ik\kappa\phi' a_y}{r} = 0\,, \tag{A.85}$$

that decouple from the other equations.

The asymptotic analysis of equations (A.84,A.85) reveals that close to the boundary the perturbations behave as

$$a_i(r \to \infty) \sim a_{(0)i}\left(r^\Delta - \frac{k^2}{4\Delta} r^{\Delta-2}\right) + a_{(0)j}\epsilon_{ij}\frac{8\mu k\kappa i}{3(\Delta-2)} r^{2\Delta-2} + \frac{\tilde{a}_i}{r^{2+\Delta}}\,. \tag{A.86}$$

Where $\tilde{a}_i$ is the normalizable mode of the perturbation. In principle it has a complicated dependence on the sources but in the linear response regime we can write

$$\tilde{a}_i = \rho a_{i(0)} + \tilde{\rho} a_{j(0)} \longrightarrow \frac{\delta \tilde{a}_i}{\delta a_{(0)j}} = \tilde{\rho}\,. \tag{A.87}$$

that allows us to write (A.86) as

$$a_i(r \to \infty) \sim a_{(0)i}\left(r^\Delta - \frac{k^2}{4\Delta} r^{\Delta-2} + \frac{\rho}{r^{\Delta+2}}\right) + a_{(0)j}\epsilon_{ij}\left(\frac{8\mu k\kappa i}{3(\Delta-2)} r^{2\Delta-2} + \frac{\tilde{\rho}}{r^{2+\Delta}}\right)\,. \tag{A.88}$$

Which is more useful to make the connection to the BBP matrix

$$\mathbb{F} = \begin{pmatrix} b(r) & c_+(r) \\ c_-(r) & d(r) \end{pmatrix}\,, \tag{A.89}$$

with [4]

$$b(r) = d(r) \sim 1 - \frac{k^2}{4\Delta r^2} + \frac{\rho}{r^{2+2\Delta}}\,, \qquad c_\pm \sim \pm\left(\frac{8\mu k\kappa i}{3(\Delta-2)} r^{\Delta-2} + \frac{\tilde{\rho}}{r^{2+2\Delta}}\right)\,. \tag{A.90}$$

At this point we can invert the series to the order of the normalizable mode. In our concrete case we have

$$\tilde{\rho} = \lim_{r\to\infty} r^{2+2\Delta} \frac{(2-\Delta)c(r) + rc'(r)}{-3\Delta}. \tag{A.91}$$

So the last thing to do is to numerically construct the BBP imposing infalling boundary conditions at the horizon and compute the latter formula. For a detailed explanation on how to numerically construct the BBP we refer the reader to [57]. Due to how we numerically construct $\mathbb{F}$, one may find some issues when computing $\lim_{r\to\infty} c(r)$ so we rather use an alternative expression involving only derivatives of $c(r)$. One can easily derive

$$\tilde{\rho} = \lim_{r\to\infty} r^{3+2\Delta} \frac{(3-\Delta)c'(r) + rc''(r)}{6\Delta(\Delta+1)}. \tag{A.92}$$

This expression combined with equations (9.36,9.31) leads finally to a expression for the conductivity

$$\sigma_{55} = \lim_{k\to 0} \frac{i}{k_x} \lim_{r\to\infty} r^{3+2\Delta} \frac{(3-\Delta)c'(r) + rc''(r)}{6\Delta}\bigg|_{\omega=0}\,. \tag{A.93}$$

[4] Here we make some abuse of language when we refer the block in $\mathbb{F}$ that affects a_x, a_y as $\mathbb{F}$. The true $\mathbb{F}$ is actually a 4×5 matrix as explained in (A.82).

A.7 Correlators in the U(1)xU(1) model

A.7.1 1-point functions

First of all we expand the action to first order in perturbations

$$
\begin{aligned}
S^{(1)}_{\mathcal{R}} = &\int dr\, d^4x\sqrt{-g}\left[a_\mu\left(\nabla_\nu F^{\nu\mu} - m^2(A^\mu - \partial^\mu\theta) + \frac{3\kappa}{2}\epsilon^{\mu\alpha\beta\gamma\rho}(F_{\alpha\beta}F_{\gamma\rho} + H_{\alpha\beta}H_{\gamma\rho})\right)\right] + \\
&\int dr\, d^4x\sqrt{-g}\left[v_\mu\left(\nabla_\nu H^{\nu\mu} + 3\kappa\epsilon^{\mu\alpha\beta\gamma\rho}F_{\alpha\beta}H_{\gamma\rho}\right) - \phi\nabla_\mu\left(A^\mu - \partial^\mu\theta\right)\right] + \\
&\int_\partial d^4x\sqrt{-g}\left[a_i\left(F^{ir} + 2\kappa(A_j - \partial_j\theta)F_{kl}\epsilon^{rijkl}\right)\right] + \\
&\int_\partial d^4x\sqrt{-g}\left[v_i\left(H^{ir} + 6\kappa(A_j - \partial_j\theta)H_{kl}\epsilon^{rijkl}\right) - \phi(F_{ij}F_{kl}\epsilon^{rijkl} + m^2(A^r - \partial^r\theta))\right] + \\
&\int_\partial d^4x\sqrt{-\gamma}\; a_i\left(\Delta(A^i - \partial^i\theta) + \frac{1}{2(\Delta+2)}\partial^i(\partial_j A^j - \Box\theta) - \frac{1}{2\Delta}\partial_j F^{ji}\right) + \\
&\int_\partial d^4x\sqrt{-\gamma}\; v_i\left(-\frac{1}{2}\partial_j H^{ji}\log(r)\right) \\
&\int_\partial d^4x\sqrt{-\gamma}\;\phi\left(\Delta(\partial_j A^j - \Box\theta) + \frac{1}{2(\Delta+2)}\Box(\partial_j A^j - \Box\theta)\right).
\end{aligned}
\tag{A.94}
$$

From the e.o.m. we find that the expansions for the scalar and the massive gauge field remain qualitatively unchanged up to the normalizable mode w.r.t. what we found in the $U(1)$ model. The expansion for the vector field is

$$
V_\mu = \sum_i V_{\mu(i)} r^{-i} + \sum_{i\geq 2}\tilde{V}_{\mu(i)} r^{-i}\log(r) + \sum_{n,i\geq n+1}\Lambda_{\mu(n,i)} r^{n\Delta - i}\,. \tag{A.95}
$$

Where the $\sim\Lambda$ terms appear due to the mixing with the axial gauge field via Chern Simons. As in the previous case it is convenient to define the BBP with the fields normalized $(r^{-\Delta}a_i, v_i, \phi)$ so that we can impose

$$
\psi_I(0) \equiv \begin{pmatrix} a_{t(0)} \\ \vdots \\ v_{t(0)} \\ \vdots \\ \phi_{(0)} \end{pmatrix}, \qquad F(\Lambda) = \mathbb{I}. \tag{A.96}
$$

I is useful to divide the BBP in two rectangular matrices $\mathbb{F}, \mathbb{H}$ and a vector $\mathbb{G}$

$$
F = \begin{pmatrix} \mathbb{F} \\ \text{------} \\ \mathbb{H} \\ \text{------} \\ \mathbb{G} \end{pmatrix}, \qquad a_I = r^\Delta \mathbb{F}_{IJ}\psi_{J(0)}\,, \qquad v_I = \mathbb{H}_{IJ}\psi_{J(0)}\,, \qquad \phi = \mathbb{G}_J\psi_{J(0)}\,. \tag{A.97}
$$

From this one can derive the renormalized 1-point functions. The expressions can be found in the main text in (9.44).

A.7.2 2-point functions

In order to obtain the 2-point functions in (9.47,9.48,9.49) we switch on perturbations with momentum aligned to the z direction $\delta\theta = \sigma(r)e^{-i\omega t+ikz}$, $\delta A_\mu = a_\mu(r)e^{-i\omega t+ikz}$ and $\delta V_\mu = v_\mu(r)e^{-i\omega t+ikz}$ on top of our background (9.50). The equations decouple and in the sector we are interested in we are left to four coupled equations for a_x, a_y, v_x, v_y.

$$a_y'' + \left(\frac{f'}{f}+\frac{1}{r}\right)a_y' + \left(\frac{\omega^2}{f^2}-\frac{k^2}{r^2 f}-\frac{m^2}{f}\right)a_y - \frac{12ik\kappa\phi'}{fr}a_z - \frac{12ik\kappa\chi'}{fr}v_z = 0\,, \tag{A.98}$$

$$a_z'' + \left(\frac{f'}{f}+\frac{1}{r}\right)a_z' + \left(\frac{\omega^2}{f^2}-\frac{k^2}{r^2 f}-\frac{m^2}{f}\right)a_z + \frac{12ik\kappa\phi'}{fr}a_y + \frac{12ik\kappa\chi'}{fr}v_y = 0\,, \tag{A.99}$$

$$v_y'' + \left(\frac{f'}{f}+\frac{1}{r}\right)v_y' + \left(\frac{\omega^2}{f^2}-\frac{k^2}{r^2 f}\right)v_y - \frac{12ik\kappa\chi'}{fr}a_z - \frac{12ik\kappa\phi'}{fr}v_z = 0\,, \tag{A.100}$$

$$v_z'' + \left(\frac{f'}{f}+\frac{1}{r}\right)v_z' + \left(\frac{\omega^2}{f^2}-\frac{k^2}{r^2 f}\right)v_z + \frac{12ik\kappa\chi'}{fr}a_y + \frac{12ik\kappa\phi'}{fr}v_y = 0\,. \tag{A.101}$$

The asymptotic analysis of these equations allows to write the near boundary expansion

$$a_i(r\to\infty) \sim a_{(0)i}(r^\Delta + Mr^{\Delta-2}) + a_{(0)j}\epsilon_{ij}\tilde{M}r^{2\Delta-2} + \frac{\tilde{a_i}}{r^{\Delta+2}}\,, \tag{A.102}$$

$$v_i(r\to\infty) \sim v_{(0)i}(1) + v_{(0)j}\epsilon_{ij}(\tilde{M}r^{\Delta-2}) + \frac{\tilde{v_i}}{r^2}\,. \tag{A.103}$$

Where M and $\tilde{M}$ are functions of k, κ, A_t', V_t'. In the linear response limit the normalizable modes $\tilde{a}_i\,\tilde{v}_i$ can only depend linearly on the sources, therefore we may rewrite the expansions

$$a_i(r\to\infty) \sim a_{(0)i}(r^\Delta + Mr^{\Delta-2} + \frac{\rho}{r^{2+\Delta}}) + a_{(0)j}\epsilon_{ij}(\tilde{M}r^{2\Delta-2} + \frac{\tilde{\rho}}{r^{2+\Delta}}) + v_{(0)i}\frac{\tilde{\tilde{\rho}}}{r^{2+\Delta}} + v_{(0)j}\epsilon_{ij}\frac{\tilde{\tilde{\rho}}}{r^{2+\Delta}}\,, \tag{A.104}$$

$$v_i(r\to\infty) \sim v_{(0)i}(1+\frac{\eta}{r^2}) + v_{(0)j}\epsilon_{ij}(\tilde{M}r^{\Delta-2} + \frac{\tilde{\eta}}{r^2}) + a_{(0)i}\frac{\tilde{\tilde{\eta}}}{r^2} + a_{(0)j}\epsilon_{ij}\frac{\tilde{\tilde{\eta}}}{r^2}\,. \tag{A.105}$$

This allows us to write

$$\langle J_i^V J_j^V\rangle = 2\frac{\delta\tilde{v}_i}{\delta v_{j(0)}} = 2\tilde{\eta}_i\,, \tag{A.106}$$

$$\langle J_i^A J_j^A\rangle = (2+2\Delta)\frac{\delta\tilde{a}_i}{\delta a_{j(0)}} = (2+2\Delta)\tilde{\rho}_i\,, \tag{A.107}$$

$$\langle J_i^A J_j^V\rangle = 2\frac{\delta\tilde{v}_i}{\delta a_{j(0)}} = 2\tilde{\tilde{\eta}}_i\,. \tag{A.108}$$

Now we perform the same analysis as in (A.6.2), seeking the correct expression of these correlators as a linear combination of the BBP and its derivatives in order to compute the conductivities numerically. We find

$$2\tilde{\eta}_i = \lim_{r\to\infty} -r^3 p'(r)\,, \tag{A.109}$$

$$(2+2\Delta)\tilde{\rho}_i = \lim_{r\to\infty} r^{3+2\Delta}\frac{(3-\Delta)b'(r)+rb''(r)}{3\Delta}\,, \tag{A.110}$$

$$2\tilde{\tilde{\eta}}_i = \lim_{r\to\infty} -r^{3+2\Delta}\frac{v'(r)}{\Delta+1}\,. \tag{A.111}$$

where $p(r)$, $b(r)$ and $v(r)$ are the functions that appear in the matrix valued BBP

$$\begin{pmatrix} r^{-\Delta}a_y(r) \\ r^{-\Delta}a_z(r) \\ v_y(r) \\ v_z(r) \end{pmatrix} = \begin{pmatrix} a(r) & b(r) & c(r) & d(r) \\ i(r) & j(r) & k(r) & l(r) \\ m(r) & n(r) & o(r) & p(r) \\ u(r) & v(r) & w(r) & y(r) \end{pmatrix} \begin{pmatrix} a_{y(0)} \\ a_{z(0)} \\ v_{y(0)} \\ v_{z(0)} \end{pmatrix} . \tag{A.112}$$

A.8 U(1)xU(1) Model: perturbations for the CMW

In order to compute the QNM spectrum and the electric conductivities with a constant and homogeneous background magnetic field we switch on perturbations with momentum k aligned to the magnetic field and frequency ω. The decoupled sector of equations we are interested in reads

$$a_t'' + \frac{3}{r}at' - \left(\frac{k^2}{fr^2} + \frac{m^2}{f}\right)a_t - \frac{\omega k}{fr^2}a_z + \frac{12\kappa B}{r^3}v_z' + \frac{i\omega m^2}{f}\eta = 0\,, \tag{A.113}$$

$$v_t'' + \frac{3}{r}vt' - \frac{k^2}{fr^2}v_t - \frac{\omega k}{fr^2}v_z + \frac{12\kappa B}{r^3}a_z' = 0 \tag{A.114}$$

$$a_z'' + \left(\frac{f'}{f} + \frac{1}{r}\right)a_z' + \left(\frac{\omega^2}{f^2} - \frac{m^2}{f}\right)a_z + \frac{\omega k}{f^2}a_t + \frac{12\kappa B}{fr}v_t' - \frac{ikm^2}{f}\eta = 0\,, \tag{A.115}$$

$$v_z'' + \left(\frac{f'}{f} + \frac{1}{r}\right)v_z' + \frac{\omega^2}{f^2}v_z + \frac{\omega k}{f^2}v_t + \frac{12\kappa B}{fr}a_t' = 0\,, \tag{A.116}$$

$$\eta'' + \left(\frac{3}{r} + \frac{f'}{f}\right)\eta' + \left(\frac{\omega^2}{f^2} - \frac{k^2}{f}\right)\eta + \frac{i\omega}{f^2}a_t + \frac{ik}{fr}a_z = 0\,. \tag{A.117}$$

With a, v, η being the perturbations for the axial, vector and Stückelberg fields respectively and f the blackening factor of the metric. There are as well two constraints:

$$\omega a_t' + \frac{kf}{r^2}a_z' + \frac{12\kappa B}{r^3}\left(\omega v_z + kv_t\right) - im^2 f\eta' = 0\,, \tag{A.118}$$

$$\omega v_t' + \frac{kf}{r^2}v_z' + \frac{12\kappa B}{r^3}\left(\omega a_z + ka_t\right) = 0\,. \tag{A.119}$$

The equations for the electric conductivity can be obtained turning off the momentum.

A.9 Computing the Conductivities

To compute the conductivities we have followed the method developed in [57].

We rearrange the perturbations in a vector $\Phi(r, x^\mu)$ and work with the Fourier transformed quantity

$$\Phi(r, x^\mu) = \int \frac{d^d k}{(2\pi)^d}\Phi_k^I(r)e^{-i\omega t + i\vec{k}\vec{x}} \tag{A.120}$$

with $\Phi_k(r)$ being

$$\Phi_k^\top(u) = (A_t(r), A_x(r), A_z(r), ...) \tag{A.121}$$

(the specific structure depends on the case at hand, the number of coupled fields, etc.). The general form of the boundary action is [57]

$$\delta S^{(2)} = \int \frac{d^d k}{(2\pi)^d} \left[\Phi^I_{-k} \mathcal{A}_{IJ} \Phi'^J_k + \Phi^I_{-k} \mathcal{B}_{IJ} \Phi^J_k\right] \tag{A.122}$$

where the prime stands for d/dr. To calculate the retarded correlators we solve the equations for the perturbations with infalling boundary conditions, on the one hand, and boundary conditions $\Phi^I_k(r \to \infty) = \phi^I_k$ on the other. This procedure should give us the desired Green's functions, after taking the variation of (A.122) with respect to the fields at large values of r. Moreover, if

$$\Phi^I_k(r) = F^I_J(k, r)\phi^J_k \tag{A.123}$$

then $F^I_J(k, r \to \infty) = 1$ is the bulk-to-boundary propagator. The retarded two-point functions, from which we are able to read directly the transport coefficients, are then computed as

$$G^{\mathcal{R}}_{IJ}(k, r \to \infty) = -2 \lim_{r\to\infty} \left(\mathcal{A}_{IM} \left(F^M_J(k, r)\right)' + \mathcal{B}_{IJ}\right) \tag{A.124}$$

The $\mathcal{A}_{IJ}$ and $\mathcal{B}_{IJ}$ matrices depend only on the background and also upon the model under consideration. We provide their values below

A.9.1 $U(1)$ model: $\mathcal{A}_{IJ}$ and $\mathcal{B}_{IJ}$ matrices

The matrices turn out to be independent of the supervelocity and its direction, once we neglect the contribution of the Chern-Simons term to define the covariant currents. We get

$$\begin{aligned} \mathcal{A} &= -\frac{1}{2} r f(r) \mathrm{Diag}(1, 1) \\ \mathcal{B} &= 0 \\ \mathcal{B}_{\mathrm{CT}} &= \frac{\ln r}{4} \left(\frac{k^2\sqrt{f(r)}}{r} - \frac{\omega^2 r}{\sqrt{f(r)}}\right) \mathrm{Diag}(1, 1) \end{aligned} \tag{A.125}$$

Notice that the counterterms do not contribute to the anomalous transport coefficients, for $\mathcal{B}_{\mathrm{CT}}$ only has diagonal entries, which furthermore are of second order in ω and k.

A.9.2 $U(1) \times U(1)$ model: $\mathcal{A}_{IJ}$ and $\mathcal{B}_{IJ}$ matrices

In this case we get the same results as before, independently for the axial and vector fields, namely

$$\begin{aligned} \mathcal{A}_{\text{axial}} &= -\frac{1}{2} r f(r) \text{Diag}(1,1) \\ \mathcal{B}_{\text{axial}} &= 0 \\ \mathcal{B}_{\text{CT}}^{\text{axial}} &= \frac{\ln r}{4} \left(\frac{k^2 \sqrt{f(r)}}{r} - \frac{\omega^2 r}{\sqrt{f(r)}} \right) \text{Diag}(1,1) \end{aligned} \tag{A.126}$$

and

$$\begin{aligned} \mathcal{A}_{\text{vector}} &= -\frac{1}{2} r f(r) \text{Diag}(1,1) \\ \mathcal{B}_{\text{vector}} &= 0 \\ \mathcal{B}_{\text{CT}}^{\text{vector}} &= \frac{\ln r}{4} \left(\frac{k^2 \sqrt{f(r)}}{r} - \frac{\omega^2 r}{\sqrt{f(r)}} \right) \text{Diag}(1,1) \end{aligned} \tag{A.127}$$

A.10 Equations of Motion

A.10.1 Momentum transverse to the supervelocity for the $U(1)$ model

$$0 = f\rho'' + \left(f' + \frac{3f}{r} \right) \rho' + \left(\frac{\omega^2}{f} + \frac{\phi^2}{f} - \frac{V^2}{r^2} - \frac{k^2}{r^2} - m^2 \right) \rho + \frac{2i\omega\phi}{f} \delta + 2a_t \Psi \frac{\phi}{f} - 2\frac{a_z}{r^2} \Psi V \tag{A.128}$$

$$0 = f\delta'' + \left(f' + \frac{3f}{r} \right) \delta' + \left(\frac{\omega^2}{f} + \frac{\phi^2}{f} - \frac{V^2}{r^2} - \frac{k^2}{r^2} - m^2 \right) \delta - \frac{2i\omega\phi}{f} \rho - i\Psi\omega \frac{a_t}{f} - k\frac{i}{r^2} \Psi a_x \tag{A.129}$$

$$0 = f a_t'' + \frac{3f}{r} a_t' - \left(\frac{k^2}{r^2} + 2\Psi^2 \right) a_t - \frac{\omega k}{r^2} a_x - 4\Psi\phi\rho - 2i\omega\Psi\delta - 16ik\kappa \frac{f}{r^3} V' a_y \tag{A.130}$$

$$0 = f a_x'' + \left(f' + \frac{f}{r} \right) a_x' + \left(\frac{\omega^2}{f} - 2\Psi^2 \right) a_x + \frac{\omega k}{f} a_t + 2ik\Psi\delta + \frac{16i\kappa}{r} \omega V' a_y \tag{A.131}$$

$$f a_y'' + \left(f' + \frac{f}{r} \right) a_y' + \left(\frac{\omega^2}{f} - \frac{k^2}{r^2} - 2\psi^2 \right) a_y + 16ik\frac{\kappa}{r} \phi' a_z - \frac{16i\kappa}{r} V' \left(\omega a_x + k a_t \right) = 0 \tag{A.132}$$

$$f a_z'' + \left(f' + \frac{f}{r} \right) a_z' + \left(\frac{\omega^2}{f} - \frac{k^2}{r^2} - 2\psi^2 \right) a_z - 16ik\frac{\kappa}{r} \phi' a_y - 4V\Psi\rho = 0 \tag{A.133}$$

and the constraint

$$0 = \frac{i\omega}{f} a_t' + \frac{ik}{r^2} a_x' + 2\Psi'\delta - 2\Psi\delta' \tag{A.134}$$

Where a_i are the perturbations of the axial gauge field. ρ and δ are the real and imaginary parts of the perturbations of the scalar field, respectively. Momentum points in the x-direction, transverse to the superfluid velocity that points in the z-direction. We observe that now the equations become more complicated, with the perturbations of the scalar coupled to all the fields, including the transverse sector. This can imply that the Quasinormal Modes now get affected by the anomaly.

A.10.2 Momentum parallel to the supervelocity for the $U(1)$ model

The equations for the relevant sector with momentum aligned to the supervelocity read

$$v_y'' + \left(\frac{f'}{f} + \frac{1}{r}\right) v_y' + \frac{1}{f}\left(\frac{\omega^2}{f} - \frac{k^2 L^2}{r^2} - 2\psi^2\right) v_y + 12ik\frac{\kappa L}{rf}\phi' a_z + 12ik\frac{\kappa L}{rf}K' v_z + 12i\omega\frac{\kappa L}{rf}V' a_z = 0 \tag{A.135}$$

$$v_z'' + \left(\frac{f'}{f} + \frac{1}{r}\right) v_z' + \frac{1}{f}\left(\frac{\omega^2}{f} - \frac{k^2 L^2}{r^2} - 2\psi^2\right) v_z - 12ik\frac{\kappa L}{rf}\phi' a_y - 12ik\frac{\kappa L}{rf}K' v_y - 12i\omega\frac{\kappa L}{rf}V' a_y = 0 \tag{A.136}$$

$$a_y'' + \left(\frac{f'}{f} + \frac{1}{r}\right) a_y' + \frac{1}{f}\left(\frac{\omega^2}{f} - \frac{k^2 L^2}{r^2}\right) a_y + 12ik\frac{\kappa L}{rf}\phi' v_z + 12ik\frac{\kappa L}{rf}K' a_z + 12i\omega\frac{\kappa L}{rf}V' v_z = 0 \tag{A.137}$$

$$a_z'' + \left(\frac{f'}{f} + \frac{1}{r}\right) a_z' + \frac{1}{f}\left(\frac{\omega^2}{f} - \frac{k^2 L^2}{r^2}\right) a_z - 12ik\frac{\kappa L}{rf}\phi' v_y - 12ik\frac{\kappa L}{rf}K' a_y - 12i\omega\frac{\kappa L}{rf}V' v_y = 0 \tag{A.138}$$

where $v_{\{y,z\}}$ and $a_{\{y,z\}}$ are the vector and axial perturbations respectively. Momentum points in the x-direction, parallel to the supervelocity. Note that only the vector component couples to the condensate, as could have been anticipated. This equations decouple from the equations for the rest of perturbations.

A.10.3 Momentum transverse to the supervelocity for the $U(1) \times U(1)$ model

The equations read

$$f\rho'' + \left(f' + \frac{3f}{r}\right)\rho + \left(\frac{\omega^2+\phi^2}{f} - \frac{k^2+V^2}{r^2} - m^2\right)\rho - \frac{2}{r^2}\psi V v_z + \frac{2\phi}{f}\left(\psi v_t + i\omega\delta\right) = 0 \tag{A.139}$$

$$f\delta'' + \left(f' + \frac{3f}{r}\right)\delta + \left(\frac{\omega^2+\phi^2}{f} - \frac{k^2+V^2}{r^2} - m^2\right)\delta - \frac{i}{r^2}\psi k v_x - \frac{i\omega}{f}\left(\psi v_t + 2\phi\rho\right) = 0 \tag{A.140}$$

$$fv_t'' + \frac{3f}{r}v_t' - \left(\frac{k^2}{r^2} + 2\psi^2\right)v_t - \frac{\omega k}{r^2}v_x - 2i\omega\psi\delta - 4\phi\psi\rho - 12ik\frac{\kappa f}{r^3}V' a_y = 0 \tag{A.141}$$

$$fv_x'' + \left(f' + \frac{f}{r}\right)v_x' + \left(\frac{\omega^2}{f} - 2\psi^2\right)v_x + \frac{\omega k}{f}v_t + 2ik\psi\delta + 12i\omega\frac{\kappa}{r}V' a_y = 0 \tag{A.142}$$

$$fv_y'' + \left(f' + \frac{f}{r}\right)v_y' + \left(\frac{\omega^2}{f} - \frac{k^2}{r^2} - 2\psi^2\right)v_y + 12ik\frac{\kappa}{r}\phi' a_z + 12ik\frac{\kappa}{r}K' v_z - 12i\omega\frac{\kappa}{r}V' a_x - 24ik\frac{\kappa}{r}V' a_t = 0 \tag{A.143}$$

$$fv_z'' + \left(f' + \frac{f}{r}\right)v_z' + \left(\frac{\omega^2}{f} - \frac{k^2}{r^2} - 2\psi^2\right)v_z - 4V\psi\rho - 12ik\frac{\kappa}{r}\phi' a_y - 12ik\frac{\kappa}{r}K' v_y = 0 \tag{A.144}$$

$$fa_t'' + \frac{3f}{r}a_t' - \frac{k^2}{r^2}a_t - \frac{\omega k}{r^2}a_x - 12ik\frac{\kappa f}{r^3}V' v_y = 0 \tag{A.145}$$

$$fa_x'' + \left(f' + \frac{f}{r}\right)a_x' + \frac{\omega^2}{f}a_x + \frac{\omega k}{f}a_t + 12i\omega\frac{\kappa}{r}V' v_y = 0 \tag{A.146}$$

$$fa_y'' + \left(f' + \frac{f}{r}\right)a_y' + \left(\frac{\omega^2}{f} - \frac{k^2}{r^2}\right)a_y + 12ik\frac{\kappa}{r}\phi' v_z + 12ik\frac{\kappa}{r}K' a_z - 12i\omega\frac{\kappa}{r}V' v_x - 12ik\frac{\kappa}{r}V' v_t = 0 \tag{A.147}$$

$$fa_z'' + \left(f' + \frac{f}{r}\right)a_z' + \left(\frac{\omega^2}{f} - \frac{k^2}{r^2}\right)a_z - 12ik\frac{\kappa}{r}\phi' v_y = 0 \tag{A.148}$$

And the constraints

$$\frac{i\omega}{f}a_t' + \frac{ik}{r^2}a_x' = 0 \tag{A.149}$$

$$\frac{i\omega}{f}v_t' + \frac{ik}{r^2}v_x' + 2\psi'\delta - 2\psi\delta' = 0 \tag{A.150}$$

Where a_i and v_i are the perturbations of the axial and vector gauge fields respectively. ρ and δ are the real and imaginary parts of the perturbations of the scalar field, respectively. Momentum points in the x-direction, whereas the superfluid velocity points in the z-direction.

Bibliography

[1] M. Srednicki, *Quantum Field Theory*. Cambridge, 2007.

[2] T. Brauner, *Spontaneous Symmetry Breaking and Nambu-Goldstone Bosons in Quantum Many-Body Systems*, *Symmetry* **2** (2010) 609–657, [1001.5212].

[3] R. A. Bertlmann, *Anomalies in quantum field theory*. Oxford, UK: Clarendon (1996) 566 p. (International series of monographs on physics: 91).

[4] A. Bilal, *Lectures on Anomalies*, 0802.0634.

[5] S. L. Adler and W. A. Bardeen, *Absence of higher order corrections in the anomalous axial vector divergence equation*, *Phys.Rev.* **182** (1969) 1517–1536.

[6] K. Fukushima, D. E. Kharzeev, and H. J. Warringa, *The Chiral Magnetic Effect*, *Phys. Rev.* **D78** (2008) 074033, [0808.3382].

[7] K. Landsteiner, E. Megias, and F. Pena-Benitez, *Anomalous Transport from Kubo Formulae*, *Lect.Notes Phys.* **871** (2013) 433–468, [1207.5808].

[8] P. Kovtun, *Lectures on hydrodynamic fluctuations in relativistic theories*, *J.Phys.* **A45** (2012) 473001, [1205.5040].

[9] J. Kapusta and C. Gale, *Finite-temperature field theory: Principles and applications*, .

[10] M. Le Bellac, *Thermal Field Theory*, .

[11] P. C. Hohenberg and A. P. Krekhov, *An introduction to the Ginzburg-Landau theory of phase transitions and nonequilibrium patterns*, *ArXiv e-prints* (Oct., 2014) [1410.7285].

[12] A. Schmitt, *Introduction to Superfluidity*, *Lect.Notes Phys.* **888** (2015) [1404.1284].

[13] O. Aharony, S. S. Gubser, J. M. Maldacena, H. Ooguri, and Y. Oz, *Large N field theories, string theory and gravity*, *Phys. Rept.* **323** (2000) 183–386, [hep-th/9905111].

[14] J. McGreevy, *Holographic duality with a view toward many-body physics*, *Adv.High Energy Phys.* **2010** (2010) 723105, [0909.0518].

[15] I. Papadimitriou and K. Skenderis, *AdS / CFT correspondence and geometry*, hep-th/0404176.

[16] K. Skenderis, *Lecture notes on holographic renormalization*, *Class.Quant.Grav.* **19** (2002) 5849–5876, [hep-th/0209067].

[17] P. Zhao, *Black holes in Anti-de Stter Spacetime*, .

[18] I. Amado, D. Arean, A. Jimenez-Alba, K. Landsteiner, L. Melgar, *et. al.*, *Holographic Type II Goldstone bosons*, *JHEP* **1307** (2013) 108, [1302.5641].

[19] I. Amado, D. Aren, A. Jimnez-Alba, K. Landsteiner, L. Melgar, *et. al.*, *Holographic Superfluids and the Landau Criterion*, *JHEP* **1402** (2014) 063, [1307.8100].

[20] I. Amado, D. Arean, A. Jimenez-Alba, L. Melgar, and I. Salazar Landea, *Holographic s+p Superconductors*, *Phys.Rev.* **D89** (2014), no. 2 026009, [1309.5086].

[21] A. Jimenez-Alba, K. Landsteiner, and L. Melgar, *Anomalous magnetoresponse and the Stckelberg axion in holography*, *Phys.Rev.* **D90** (2014), no. 12 126004, [1407.8162].

[22] I. Amado, N. Lisker, and A. Yarom, *Universal chiral conductivities for low temperature holographic superfluids*, 1401.5795.

[23] A. Jimenez-Alba and L. Melgar, *Anomalous Transport in Holographic Chiral Superfluids via Kubo Formulae*, *JHEP* **1410** (2014) 120, [1404.2434].

[24] D. T. Son and P. Surowka, *Hydrodynamics with Triangle Anomalies*, *Phys. Rev. Lett.* **103** (2009) 191601, [0906.5044].

[25] H. B. Nielsen and S. Chadha, *On How to Count Goldstone Bosons*, *Nucl.Phys.* **B105** (1976) 445.

[26] H. Watanabe and T. Brauner, *On the number of Nambu-Goldstone bosons and its relation to charge densities*, *Phys.Rev.* **D84** (2011) 125013, [1109.6327].

[27] H. Watanabe and H. Murayama, *Unified Description of Nambu-Goldstone Bosons without Lorentz Invariance*, *Phys.Rev.Lett.* **108** (2012) 251602, [1203.0609].

[28] Y. Hidaka, *Counting rule for Nambu-Goldstone modes in nonrelativistic systems*, *Phys.Rev.Lett.* **110** (2013) 091601, [1203.1494].

[29] A. Kapustin, *Remarks on nonrelativistic Goldstone bosons*, 1207.0457.

[30] H. Watanabe and H. Murayama, *Redundancies in Nambu-Goldstone Bosons*, *Phys.Rev.Lett.* **110** (2013) 181601, [1302.4800].

[31] T. Schfer, D. Son, M. A. Stephanov, D. Toublan, and J. Verbaarschot, *Kaon condensation and Goldstone's theorem*, *Phys.Lett.* **B522** (2001) 67–75, [hep-ph/0108210].

[32] S. L. Adler, *Axial vector vertex in spinor electrodynamics*, *Phys.Rev.* **177** (1969) 2426–2438.

[33] J. Bell and R. Jackiw, *A PCAC puzzle: pi0 -¿ gamma gamma in the sigma model*, *Nuovo Cim.* **A60** (1969) 47–61.

[34] E. Witten, *Current Algebra Theorems for the U(1) Goldstone Boson*, *Nucl.Phys.* **B156** (1979) 269.

[35] D. E. Kharzeev, L. D. McLerran, and H. J. Warringa, *The effects of topological charge change in heavy ion collisions: 'Event by event P and CP violation'*, *Nucl. Phys.* **A803** (2008) 227–253, [0711.0950].

[36] D. E. Kharzeev and H. J. Warringa, *Chiral Magnetic conductivity*, *Phys. Rev.* **D80** (2009) 034028, [0907.5007].

[37] D. Satow and H.-U. Yee, *Chiral Magnetic Effect at Weak Coupling with Relaxation Dynamics*, *Phys.Rev.* **D90** (2014), no. 1 014027, [1406.1150].

[38] S. A. Voloshin, *Parity violation in hot QCD: How to detect it*, *Phys.Rev.* **C70** (2004) 057901, [hep-ph/0406311].

[39] **STAR Collaboration** Collaboration, B. Abelev *et. al.*, *Observation of charge-dependent azimuthal correlations and possible local strong parity violation in heavy ion collisions*, *Phys.Rev.* **C81** (2010) 054908, [0909.1717].

[40] Y. Akiba, A. Angerami, H. Caines, A. Frawley, U. Heinz, *et. al.*, *The Hot QCD White Paper: Exploring the Phases of QCD at RHIC and the LHC*, 1502.02730.

[41] V. Okorokov, *Strongly interacting matter at RHIC: experimental highlights*, 1410.7160.

[42] V. Koch, A. Bzdak, and J. Liao, *Have we seen local parity violation in heavy-ion collisions?*, *Acta Phys.Polon.Supp.* **5** (2012) 773–780.

[43] D. E. Kharzeev and D. T. Son, *Testing the chiral magnetic and chiral vortical effects in heavy ion collisions*, *Phys.Rev.Lett.* **106** (2011) 062301, [1010.0038].

[44] Q. Li, D. E. Kharzeev, C. Zhang, Y. Huang, I. Pletikosic, *et. al.*, *Observation of the chiral magnetic effect in ZrTe5*, 1412.6543.

[45] A. Gynther, K. Landsteiner, F. Pena-Benitez, and A. Rebhan, *Holographic Anomalous Conductivities and the Chiral Magnetic Effect*, *JHEP* **02** (2011) 110, [1005.2587].

[46] D. E. Kharzeev and H.-U. Yee, *Chiral Magnetic Wave*, *Phys.Rev.* **D83** (2011) 085007, [1012.6026].

[47] Y. Burnier, D. E. Kharzeev, J. Liao, and H.-U. Yee, *Chiral magnetic wave at finite baryon density and the electric quadrupole moment of quark-gluon plasma in heavy ion collisions*, *Phys.Rev.Lett.* **107** (2011) 052303, [1103.1307].

[48] J. M. Maldacena, *The large N limit of superconformal field theories and supergravity*, *Adv. Theor. Math. Phys.* **2** (1998) 231–252, [hep-th/9711200].

[49] G. 't Hooft, *The Holographic principle: Opening lecture*, hep-th/0003004.

[50] J. D. Bekenstein, *Black holes and entropy*, *Phys.Rev.* **D7** (1973) 2333–2346.

[51] S. Hawking, *Black hole explosions*, *Nature* **248** (1974) 30–31.

[52] S. Kachru, X. Liu, and M. Mulligan, *Gravity duals of Lifshitz-like fixed points*, *Phys.Rev.* **D78** (2008) 106005, [0808.1725].

[53] E. Witten, *Anti-de Sitter space and holography*, *Adv.Theor.Math.Phys.* **2** (1998) 253–291, [hep-th/9802150].

[54] S. Gubser, I. R. Klebanov, and A. M. Polyakov, *Gauge theory correlators from noncritical string theory*, *Phys.Lett.* **B428** (1998) 105–114, [hep-th/9802109].

[55] D. T. Son and A. O. Starinets, *Minkowski space correlators in AdS / CFT correspondence: Recipe and applications*, *JHEP* **0209** (2002) 042, [hep-th/0205051].

[56] P. K. Kovtun and A. O. Starinets, *Quasinormal modes and holography*, *Phys.Rev.* **D72** (2005) 086009, [hep-th/0506184].

[57] M. Kaminski, K. Landsteiner, J. Mas, J. P. Shock, and J. Tarrio, *Holographic Operator Mixing and Quasinormal Modes on the Brane*, *JHEP* **1002** (2010) 021, [0911.3610].

[58] S. S. Gubser, *Breaking an Abelian gauge symmetry near a black hole horizon*, *Phys.Rev.* **D78** (2008) 065034, [0801.2977].

[59] S. A. Hartnoll, C. P. Herzog, and G. T. Horowitz, *Building a Holographic Superconductor*, *Phys.Rev.Lett.* **101** (2008) 031601, [0803.3295].

[60] B. Halperin, *Dynamic properties of the multicomponent Bose fluid*, *Phys. Rev. B* **11** (1975) 178190.

[61] V. Miransky and I. Shovkovy, *Spontaneous symmetry breaking with abnormal number of Nambu-Goldstone bosons and kaon condensate*, *Phys.Rev.Lett.* **88** (2002) 111601, [hep-ph/0108178].

[62] V. G. Filev, C. V. Johnson, and J. P. Shock, *Universal Holographic Chiral Dynamics in an External Magnetic Field*, *JHEP* **0908** (2009) 013, [0903.5345].

[63] I. Amado, M. Kaminski, and K. Landsteiner, *Hydrodynamics of Holographic Superconductors*, *JHEP* **0905** (2009) 021, [arXiv:0903.2209].

[64] T. Brauner, *Spontaneous symmetry breaking in the linear sigma model at finite chemical potential: One-loop corrections*, *Phys.Rev.* **D74** (2006) 085010, [hep-ph/0607102].

[65] A. Nicolis and F. Piazza, *A relativistic non-relativistic Goldstone theorem: gapped Goldstones at finite charge density*, *Phys.Rev.Lett.* **110** (2013) 011602, [1204.1570].

[66] I. R. Klebanov and E. Witten, *AdS / CFT correspondence and symmetry breaking*, *Nucl.Phys.* **B556** (1999) 89–114, [hep-th/9905104].

[67] M. Bhaseen, J. P. Gauntlett, B. Simons, J. Sonner, and T. Wiseman, *Holographic Superfluids and the Dynamics of Symmetry Breaking*, *Phys.Rev.Lett.* **110** (2013) 015301, [1207.4194].

[68] I. Amado, C. Hoyos-Badajoz, K. Landsteiner, and S. Montero, *Hydrodynamics and beyond in the strongly coupled N=4 plasma*, *JHEP* **0807** (2008) 133, [0805.2570].

[69] R. A. Davison and A. O. Starinets, *Holographic zero sound at finite temperature*, *Phys.Rev.* **D85** (2012) 026004, [1109.6343].

[70] F. Bigazzi, A. L. Cotrone, D. Musso, N. P. Fokeeva, and D. Seminara, *Unbalanced Holographic Superconductors and Spintronics*, *JHEP* **1202** (2012) 078, [1111.6601].

[71] S. A. Hartnoll, C. P. Herzog, and G. T. Horowitz, *Holographic Superconductors*, *JHEP* **0812** (2008) 015, [0810.1563].

[72] S.-C. Zhang, *A Unified Theory Based on SO(5) Symmetry of Superconductivity and Antiferromagnetism*, *Science* **275 (5303)** (1997) 1089–1096.

[73] F. Benini, C. P. Herzog, R. Rahman, and A. Yarom, *Gauge gravity duality for d-wave superconductors: prospects and challenges*, *JHEP* **1011** (2010) 137, [1007.1981].

[74] J.-W. Chen, Y.-J. Kao, D. Maity, W.-Y. Wen, and C.-P. Yeh, *Towards A Holographic Model of D-Wave Superconductors*, *Phys.Rev.* **D81** (2010) 106008, [1003.2991].

[75] S. Uchino, M. Kobayashi, and M. Ueda, *Bogoliubov Theory and Lee-Huang-Yang Correction in Spin-1 and Spin-2 Bose-Einstein Condensates in the Presence of the Quadratic Zeeman Effect*, *Phys.Rev.* **A81** (2010) 063632, [0912.0355].

[76] I. Khalatnikov, *An Introduction to the Theory of Superfluidity*. Advanced Books Classics, Westview Press.

[77] L. Landau and E. Lifshitz, *Course of Theoretical Physcis, Vol. 9, Statistical Physics*. Pergamon Press.

[78] C. Herzog, P. Kovtun, and D. Son, *Holographic model of superfluidity*, *Phys.Rev.* **D79** (2009) 066002, [0809.4870].

[79] P. Basu, A. Mukherjee, and H.-H. Shieh, *Supercurrent: Vector Hair for an AdS Black Hole*, *Phys.Rev.* **D79** (2009) 045010, [0809.4494].

[80] P. Basu, J. He, A. Mukherjee, M. Rozali, and H.-H. Shieh, *Competing Holographic Orders*, *JHEP* **1010** (2010) 092, [1007.3480].

[81] R.-G. Cai, L. Li, L.-F. Li, and Y.-Q. Wang, *Competition and Coexistence of Order Parameters in Holographic Multi-Band Superconductors*, *JHEP* **1309** (2013) 074, [1307.2768].

[82] D. Musso, *Competition/Enhancement of Two Probe Order Parameters in the Unbalanced Holographic Superconductor*, *JHEP* **1306** (2013) 083, [1302.7205].

[83] V. Keranen, E. Keski-Vakkuri, S. Nowling, and K. Yogendran, *Solitons as Probes of the Structure of Holographic Superfluids*, *New J.Phys.* **13** (2011) 065003, [1012.0190].

[84] L. Landau and E. M. Lifshitz, *Course on Theoretical Physics; Vol 5*. Elsevier, 2008.

[85] D. Pines and P. Nozires, *The Theory of Quantum Liquids*. Advanced Book Classics. Perseus Books, 1999.

[86] D. Arean, P. Basu, and C. Krishnan, *The Many Phases of Holographic Superfluids*, *JHEP* **1010** (2010) 006, [1006.5165].

[87] D. Arean, M. Bertolini, J. Evslin, and T. Prochazka, *On Holographic Superconductors with DC Current*, *JHEP* **1007** (2010) 060, [1003.5661].

[88] M. G. Alford, S. K. Mallavarapu, A. Schmitt, and S. Stetina, *Role reversal in first and second sound in a relativistic superfluid*, *Phys.Rev.* **D89** (2014) 085005, [1310.5953].

[89] S. Nakamura, H. Ooguri, and C.-S. Park, *Gravity Dual of Spatially Modulated Phase*, *Phys.Rev.* **D81** (2010) 044018, [0911.0679].

[90] A. Donos and J. P. Gauntlett, *Holographic striped phases*, *JHEP* **1108** (2011) 140, [1106.2004].

[91] C. B. Bayona, K. Peeters, and M. Zamaklar, *A Non-homogeneous ground state of the low-temperature Sakai-Sugimoto model*, *JHEP* **1106** (2011) 092, [1104.2291].

[92] M. G. Alford, S. K. Mallavarapu, A. Schmitt, and S. Stetina, *From a complex scalar field to the two-fluid picture of superfluidity*, *Phys.Rev.* **D87** (2013), no. 6 065001, [1212.0670].

[93] Zhang, *A Unified Theory Based on SO(5) Symmetry of Superconductivity and Antiferromagnetism*, *Science* **275** (1997) 1089–1096.

[94] D. Vollhardt and P. Wolfle, *The Superfluid Phases of Helium 3*. Taylor and Francis, London, 1990.

[95] P. Goswami and B. Roy, *Axionic superconductivity in three dimensional doped narrow gap semiconductors*, 1307.3240.

[96] A. F. A. W. W. L. A. P. Schnyder, S. Ryu, *Classification of topological insulators and superconductors in three spatial dimensions*, *Phys. Rev. B* **78** (2008) 195125.

[97] L. A. Pando Zayas and D. Reichmann, *A Holographic Chiral $p_x + ip_y$ Superconductor*, *Phys.Rev.* **D85** (2012) 106012, [1108.4022].

[98] A. S. Y.-i. Shin, C. H. Schunck and W. Ketterle, *Phase diagram of a two-component Fermi gas with resonant interactions*, *Nature* **451** (2008) 689693.

[99] M. Chernodub and A. Nedelin, *Phase diagram of chirally imbalanced QCD matter*, *Phys.Rev.* **D83** (2011) 105008, [1102.0188].

[100] J. Erdmenger, V. Grass, P. Kerner, and T. H. Ngo, *Holographic Superfluidity in Imbalanced Mixtures*, *JHEP* **1108** (2011) 037, [1103.4145].

[101] M. Ammon, J. Erdmenger, M. Kaminski, and P. Kerner, *Superconductivity from gauge/gravity duality with flavor*, *Phys.Lett.* **B680** (2009) 516–520, [0810.2316].

[102] A. Krikun, V. Kirilin, and A. Sadofyev, *Holographic model of the $S^{\pm}$ multiband superconductor*, *JHEP* **1307** (2013) 136, [1210.6074].

[103] M. Ammon, J. Erdmenger, V. Grass, P. Kerner, and A. O'Bannon, *On Holographic p-wave Superfluids with Back-reaction*, *Phys.Lett.* **B686** (2010) 192–198, [0912.3515].

[104] R. E. Arias and I. S. Landea, *Backreacting p-wave Superconductors*, *JHEP* **1301** (2013) 157, [1210.6823].

[105] M. Henningson and K. Skenderis, *The Holographic Weyl anomaly*, *JHEP* **9807** (1998) 023, [hep-th/9806087].

[106] I. R. Klebanov, P. Ouyang, and E. Witten, *A Gravity dual of the chiral anomaly*, *Phys.Rev.* **D65** (2002) 105007, [hep-th/0202056].

[107] D.-F. Hou, H. Liu, and H.-c. Ren, *A Possible Higher Order Correction to the Vortical Conductivity in a Gauge Field Plasma*, *Phys.Rev.* **D86** (2012) 121703, [1210.0969].

[108] S. Golkar and D. T. Son, *Non-Renormalization of the Chiral Vortical Effect Coefficient*, 1207.5806.

[109] K. Jensen, P. Kovtun, and A. Ritz, *Chiral conductivities and effective field theory*, *JHEP* **1310** (2013) 186, [1307.3234].

[110] G. 't Hooft, *How Instantons Solve the U(1) Problem*, *Phys.Rept.* **142** (1986) 357–387.

[111] S. L. Adler, *Anomalies to all orders*, hep-th/0405040.

[112] B. Ioffe, *Axial anomaly: The Modern status*, *Int.J.Mod.Phys.* **A21** (2006) 6249–6266, [hep-ph/0611026].

[113] U. Gursoy and A. Jansen, *(Non)renormalization of Anomalous Conductivities and Holography*, 1407.3282.

[114] R. Casero, E. Kiritsis, and A. Paredes, *Chiral symmetry breaking as open string tachyon condensation*, *Nucl.Phys.* **B787** (2007) 98–134, [hep-th/0702155].

[115] E. Witten, *SL(2,Z) action on three-dimensional conformal field theories with Abelian symmetry*, hep-th/0307041.

[116] O. Domenech, M. Montull, A. Pomarol, A. Salvio, and P. J. Silva, *Emergent Gauge Fields in Holographic Superconductors*, *JHEP* **1008** (2010) 033, [1005.1776].

[117] S. Franco, A. Garcia-Garcia, and D. Rodriguez-Gomez, *A General class of holographic superconductors*, *JHEP* **1004** (2010) 092, [0906.1214].

[118] K. Landsteiner, E. Megias, L. Melgar, and F. Pena-Benitez, *Gravitational Anomaly and Hydrodynamics*, *J.Phys.Conf.Ser.* **343** (2012) 012073, [1111.2823].

[119] I. Amado, K. Landsteiner, and F. Pena-Benitez, *Anomalous transport coefficients from Kubo formulas in Holography*, *JHEP* **1105** (2011) 081, [1102.4577].

[120] E. Gorbar, V. Miransky, and I. Shovkovy, *Normal ground state of dense relativistic matter in a magnetic field*, *Phys.Rev.* **D83** (2011) 085003, [1101.4954].

[121] H. B. Nielsen and M. Ninomiya, *ADLER-BELL-JACKIW ANOMALY AND WEYL FERMIONS IN CRYSTAL*, *Phys.Lett.* **B130** (1983) 389.

[122] E. Gorbar, V. Miransky, and I. Shovkovy, *Chiral anomaly, dimensional reduction, and magnetoresistivity of Weyl and Dirac semimetals*, *Phys.Rev.* **B89** (2014) 085126, [1312.0027].

[123] D. Son and B. Spivak, *Chiral Anomaly and Classical Negative Magnetoresistance of Weyl Metals*, *Phys.Rev.* **B88** (2013) 104412, [1206.1627].

[124] S. Bhattacharyya, V. E. Hubeny, S. Minwalla, and M. Rangamani, *Nonlinear Fluid Dynamics from Gravity*, *JHEP* **0802** (2008) 045, [0712.2456].

[125] M. A. Metlitski and A. R. Zhitnitsky, *Anomalous axion interactions and topological currents in dense matter*, *Phys. Rev.* **D72** (2005) 045011, [hep-ph/0505072].

[126] D. T. Son and A. R. Zhitnitsky, *Quantum anomalies in dense matter*, *Phys. Rev.* **D70** (2004) 074018, [hep-ph/0405216].

[127] M. Lublinsky and I. Zahed, *Anomalous Chiral Superfluidity*, *Phys.Lett.* **B684** (2010) 119–122, [0910.1373].

[128] S. Lin, *An anomalous hydrodynamics for chiral superfluid*, *Phys.Rev.* **D85** (2012) 045015, [1112.3215].

[129] S. Lin, *On the anomalous superfluid hydrodynamics*, 1104.5245.

[130] Y. Neiman and Y. Oz, *Anomalies in Superfluids and a Chiral Electric Effect*, 1106.3576.

[131] S. Bhattacharyya, S. Jain, S. Minwalla, and T. Sharma, *Constraints on Superfluid Hydrodynamics from Equilibrium Partition Functions*, *JHEP* **1301** (2013) 040, [1206.6106].

[132] J. Bhattacharya, S. Bhattacharyya, S. Minwalla, and A. Yarom, *A Theory of first order dissipative superfluid dynamics*, *JHEP* **1405** (2014) 147, [1105.3733].

[133] S. Chapman, C. Hoyos, and Y. Oz, *Superfluid Kubo Formulas from Partition Function*, 1310.2247.

[134] T. Kalaydzhyan, *Chiral superfluidity of the quark-gluon plasma*, *Nucl.Phys.* **A913** (2013) 243–263, [1208.0012].

[135] G. M. Newman and D. T. Son, *Response of strongly-interacting matter to magnetic field: Some exact results*, *Phys. Rev.* **D73** (2006) 045006, [hep-ph/0510049].

[136] K. Landsteiner and L. Melgar, *Holographic Flow of Anomalous Transport Coefficients*, *JHEP* **1210** (2012) 131, [1206.4440].

[137] M. Stephanov and Y. Yin, *Conductivity and quasinormal modes in holographic theories*, *JHEP* **1202** (2012) 017, [1111.5303].